Combustion of alternative and low-grade biomass fuels on small-scale systems:

Potential and optimisation through pre-treatment

David Paul Maxwell

Submitted in accordance with the requirements for the degree of Doctor of Philosophy as part of the integrated PhD with MSc in Bioenergy

The University of Leeds

Centre for Doctoral Training in Bioenergy

School of Chemical and Process Engineering

Faculty of Engineering

March 2021

Declaration of Authorship

The candidate confirms that the work is his own, except where work which has been formed as part of jointly-authored publications has been included. The contribution of the candidate and the other authors to this work has been explicitly indicated below. The candidate confirms that appropriate credit has been given within the thesis where reference has been made to the work of others.

The work in Chapter 4 is based on the following publication:

Maxwell, D, Gudka, B.A, Jones, J.M, and Williams, A. 2020. Emissions from the combustion of torrefied and raw biomass fuels in a domestic heating stove. *Fuel Processing Technology*. **199**, p.106266.

I carried out all experimental work with the exception of the EC/OC analysis which was carried out by Sunset Labs Ltd. Dr Bijal Gudka helped with coordinating the experiments and fuels were provided through the Supergen Hub. The remaining authors provided supervision, guidance and corrections to the manuscript.

Part of the work in Chapter 6 is based on the following publication:

Mitchell, E.J.S, Gudka, B, Whittaker, C, Shield, I, Price-Allison, A, Maxwell, D, Jones, J.M, and Williams, A. 2020. The use of agricultural residues, wood briquettes and logs for small-scale domestic heating. *Fuel Processing Technology*. **210**, p.106552.

I carried out experimental work including composition analysis and combustion tests, as well as carrying out the majority of the results processing for the emissions data.

Acknowledgements

On a personal level for their support, I would like to thank my friends for always supporting me and encouraging me to keep pushing myself: *Miss Laura Bond; Miss Eve Doughty; Mrs Kirsten Cameron; Mr Adam Ruckwood OLY.; Miss Alex Trzcionkowska; Miss Amy Williams; Miss Paris Kiernan; Miss Jana Harris; Miss Rebekah Brown.*

My Thanks to my family for their love and encouragement: *Mrs Rebecca Maxwell Grainger; Miss Katrina Maxwell; Mr Sam Maxwell Grainger; Mr Philip Stone; Mrs Sarah Stone; Mr Robert Stone; Ms Diana Siniawski; Mrs Ilaina Siniawski; Mr Justin Dobson; Mr Alex Siniawski; Mrs Claire Siniawski; Miss Kathryn Siniawski.*

My Beautiful Dogs Cassie and Daisy, who sat with me the entire time I wrote this thesis, our visiting guest Bruno at times.

A special mention to my grandad and dad for creating my interest in engineering and encouraging my pursuit of further knowledge: *Mr Frank Maxwell; Mr Adrian Maxwell*

A very special acknowledgement to my mum, *Mrs Marion Maxwell*, this thesis represents so much to the both of us. It is the light at the end of a very dark time and is both symbolically and metaphorically the end of a chapter. You have always believed in me and taught me about what kind of person I want to be. I am forever thankful.

Finally, to my partner in life, *Matthew*. Your tireless support can never be repaid. You have seen my hardship throughout my PhD and without you this would have been impossible to achieve. You will forever inspire my future.

I would like to dedicate this work to my nan, Philomena Antoinette Harding. She was a blessing to us all, teaching me how to love and think of others. This has been a lot harder without you. I know how proud you would be. You are always with me.

Abstract

As the earth transitions to a low carbon sustainable future, the diversity of biomass fuels must be expanded to accommodate the growing energy demands. This can have advantages such as encouraging the use of waste feedstocks to capitalise on economic gains as well as disadvantages such as the associated environmental and operational problems from biomass high in inorganics and minerals. Globally the heating sector is the largest sector of the energy industry accounting for 50% of energy consumption [IRENA, 2018]. Of this 14% comes from traditional biomass used in heating stoves. This an area of increasing interest since these systems are having a detrimental effect to air quality from high emissions of NOx, SO_2, unburnt hydrocarbons and particulate matter.

In this thesis the aim was to understand the relationship between the fuel properties and emissions from combustion on a domestic stove. This included analysing the impacts of pre-treatment on the performance and emissions. Traditional wood fuels, willow and spruce logs, were used as benchmarks and compared to their torrefied counterparts. The results showed that torrefied fuels increased the emissions of CO_2 (spruce 65-90 and willow 67 to 78 kg GJ^{-1}) but reduced the emissions of CH_4 (spruce 0.37 to 0.18 and willow 0.18 to 0.04 kg GJ^{-1}). Reductions in NOx from torrefied fuels was the result of a shift in N partitioning and retaining more fuel-N in the char which was released as N_2 from reducing conditions during char burnout. Similarly, sulphur retention in the ash increased because of the increased Ca/S ratio of torrefied fuels, thereby reducing SO_2 emissions. Particulate matter emissions were also reduced from using torrefied fuels. The torrefaction process reduced the emissions of soot forming volatiles such as eugenol and vanillin which can contribute to soot formation by both the hydrogen abstraction carbon addition and cyclopentadiene methods.

Waste spent coffee grounds, bracken and agricultural residues were analysed in comparison to wood logs and briquettes as potential novel fuels for the domestic market. The very fine particle size and high calorific value (21.1 MJ kg^{-1}) of the spent coffee resulted in high flue gas temperatures (peak temperature 600°C). However, the high fuel-N content (1.84 wt.% db) resulted in excessive emissions of NOx (190 g GJ^{-1}) which was more analogous with coal and peat than biomass. Bracken is currently a

large management problem globally as it is so dominant and fast growing, the most used management technique involves harvesting and burning it in large open fires. Commercial bracken briquettes when combusted were difficult to ignite because of the density of the briquettes (1250 kg m^{-3}). These were broken down into four evenly sized segments and it was apparent the size, shape and density of the briquettes was preventing efficient combustion (mass conversion increased by 20%). By reducing the size of the briquettes, and increasing the surface area to volume ratio, the emissions of CO decreased from 180 to 140 g kg^{-1} of fuel and the total organic carbon emissions from 1.3 to 0.8 g kg^{-1} of fuel. The SO$_2$ (1.7 g kg^{-1}) and HCl (0.6 g kg^{-1}) emissions from bracken briquettes were much higher than compared to barley straw (0.8 and 0.3 g kg^{-1}), wheat straw (0.5 and 0.2 g kg^{-1}), miscanthus (0.8 and 0.3 g kg^{-1}) and wood briquettes (0.3 and 0.06 g kg^{-1}). This was because of the high S (0.2 wt.% db) and Cl (0.14 wt.% db) contents of the fuel.

Because of the strong correlation between the fuel mineral contents and the emissions, SRC willow grown on contaminated land was pre-treated by washing to investigate the removal efficiency of problematic species and the impacts on the emissions. The ash content of the pre-treated willow reduced by 27%; this was lower than seen in previous work, however the method used was more applicable to industry methods of pre-treatment. High removal efficiencies of Pb (69%), S (55%) and Cu (47.5%) were observed and this came from a combination of solid mineral removal from soil and bark as well as some leaching. When combusted the washed willow had reduced emissions of CO (5.2 reduced to 2.45 kg GJ^{-1}), THC (0.22 reduced to 0.125 kg GJ^{-1}) and PM (0.12 reduced to 0.063 kg GJ^{-1}). However even though the fuel-N content decreased, the NOx emissions were 25% higher for the washed willow, this was mostly likely due to the reduced Na content which has been shown to catalyse NOx reduction reactions during char combustion.

The overall outcome of this thesis is a stronger understanding of the chemical and physical properties of fuels that influence the emissions from combustion on stove systems. Several useful correlations have been identified between the composition analysis and the emissions data that include the majority of fuels used in this thesis. These correlations are useful in identifying the suitability of novel fuels and also in identifying the advantages of pre-treatment for industry and the potential expansion of their fuel inventories.

Contents Page

Table of Tables

Table of Figures

Nomenclature

Abbreviations

AFT- Ash Fusion Test

AI- Alkali Index

AQMA- Air Quality Management Areas (UK)

ATP- Adenosine Triphosphate

BMRB- Brewed Mexican Robusta Bean

CCC- Committee on Climate Change (UK)

CDC- Centre for Disease Control (US)

CF- Chemical Fractionation

CHP- Combined Heat and Power

CIS- Commonwealth of Independent States

CPD- Cyclopentadiene

DEFRA- Department for Environment, Food and Rural Affairs (UK)

DTG- Derivative Thermogravimetric

EC- Elemental Carbon

EDX- Energy Dispersive Spectroscopy (x-rays)

EfW- Energy from Waste

EIA- Energy Information Agency (US)

FC- Fixed Carbon

FT- Flow Temperature

FTIR- Fourier Transform Infrared spectroscopy

GCV- Gross Calorific Value

GG- Greenhouse Gases

GWP- Global Warming Potential

HACA- Hydrogen Abstraction Carbon Addition

HGV- Heavy Goods Vehicle

HHV- Higher Heating Value

HT- Hemisphere Temperature

IC- Ion Chromatography

ICE- Internal Combustion Engine

ICP-MS- Inductively Coupled Plasma Mass Spectrometry

ICP-OES- Inductively Coupled Plasma Optical Emission Spectrometry

IDT- Initial Deformation Temperature

IEA- International Energy Agency

IRENA- International Renewable Energy Agency

ISO- International Organisation for Standardisation

LHV- Lower Heating Value

MCE- Modified Combustion Efficiency

MRB- Mexican Robusta Bean

NAAQS- National Ambient Air Quality Standards (US)

NAQS- National Air Quality Standards (UK)

NCV- Net Calorific Value

OC- Organic Carbon

OLS- Ordinary Least Squares regression model

PAH- Polycyclic Aromatic Hydrocarbon

PCB- Polychlorobiphenyls

PLS- Partial Least Squares regression model

PV- Photovoltaics

SDGFV- Specific Dry Flue Gas Volume

SEM- Scanning Electron Microscopy

SIR- System Integration of Renewables

ST- Softening Temperature

SVI- Slagging Viscosity Index

TDS- Total Dissolved Solids

TOC- Total Organic Carbon

TOMPS- Toxic Organic Micro-Pollutants

UNFCCC- United Nations Framework Convention on Climate Change

VM- Volatile Matter

VOC- Volatile Organic Compound

VRE- Variable Renewable Energy

WEO- World Energy Outlook

Units & Symbols

A- Pre-exponential Factor (used in kinetics calculations)

C_i- Concentration of species i

daf- dry ash-free basis

db- dry basis

E_a- Activation Energy

g- grams

g kg^{-1}- grams per kilogram of fuel (emission factor)

k- Reaction Rate Constant

kg GJ^{-1}- kilograms per giga-joule (emission factor on an energy basis)

kJ mol^{-1}- Kilo-Joule per mol

kW- kilo-watts

kWh- kilo-Watt-hours

MJ kg^{-1}- Mega-Joules per kilogram (energy content of a fuel)

MPa- Mega-pascals

Mt- Mega-tonnes

m^3 h^{-1}- meters cubed per hour (flow rate)

m_{mol}- Molecular Mass

mtoe- million tonnes of oil equivalent

$O_{2,\ 13\%}$- 13% oxygen Content (standard in emissions reporting)

P_A- Atmospheric Pressure (1013 kPa)

P_{abs}- Absolute Pressure

ppb- parts per billion

ppt- parts per trillion

R- Ideal Gas Constant (8.3145 J mol^{-1} K^{-1})

$R_{b/a}$ − Base to Acid Ratio

S^{-1}- per second

STP- Standard Temperature and Pressure

T- Absolute temperature, measured in kelvin (K)

TWh- Tera-Watt hours

THz- Tera-Hertz

V$_{m,s}$- Molar Volume (22.4 L mol$_{gas}^{-1}$)

Wt.%- weight percent (concentration)

μg Nm^{-3}- micro grams per normalised meter cubed (emissions measurements)

ρ$_{Wet\ Flue\ Gas}$- Density of Wet Flue Gas (~1 kg m^{-3})

Chapter 1. Introduction

Humans need energy to survive, this includes activities such as heating, cooking, processing and transportation. However, obtaining and using energy comes at the expense of the environment. Historic irresponsible industrial activities including the energy sector have caused irreversible damage to the planet. International efforts are focused on changing the fuels used, improving the efficiency of current technologies, the implementation of new technologies and abatement technology. Renewables are a key part of this strategy.

1.1 Energy, The Environment and Renewables

1.1.1 Overview of Global Energy Usage

Energy demand increased by 0.9% in 2019 according to the IEA Global Energy Review [2020]. The BP Statistical Review from 2019 [2020] measured a slightly higher level of primary fuel consumption at 1.3%. One of the main reasons global energy demand is increasing is because of population growth however based on Fig. 1.1 from Karpov [2019] average person energy consumption is also increasing; this is largely an effect of economic development in non-OECD countries. In Fig. 1.1 sections I and II define to s-shaped trends when global energy consumption accelerated for a period and then returned to its standard rate of increase.
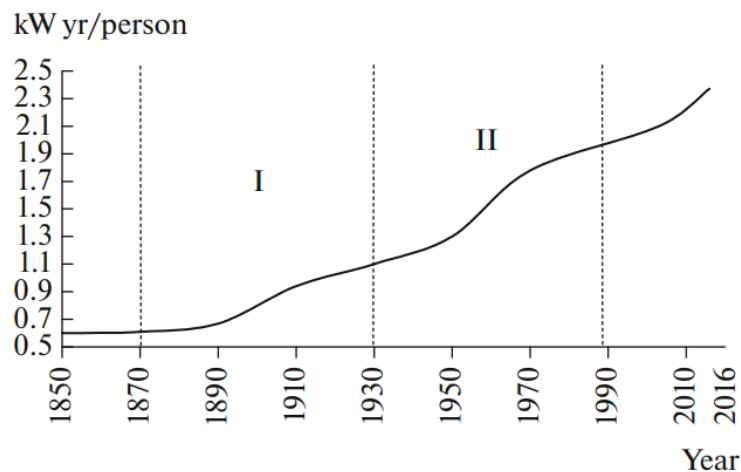
Figure 1.1: Average global energy consumption per person [Karpov, 2019]

Global energy consumption is not a comprehensive assessment of the energy sector. Table 1.1 uses data from the BP Statistical Review from 2018 [2019] and shows

the global divide of primary energy consumption. From Table 1.1 it is clear that the Asia Pacific region is the largest consumer, consuming more than North America and Europe combined which are the second and third biggest consumers respectively. This region includes China and India which are rapidly growing economies.

Table 1.1: Primary fuel consumption from 2010 to 2018 [BP, 2019]

	Primary Energy Consumption (Mtoe)					Growth Since 2008 (%)			
	2010	2012	2014	2016	2018	2012	2014	2016	2018
Global	12099.9	12575.5	12939.8	13228.6	13864.9	3.9	6.9	9.3	14.6
North America	2709.8	2657.4	2758.9	2737.2	2832	-1.9	1.8	1.0	4.5
South & Central America	627.1	670.9	692.9	691.1	702	7.0	10.5	10.2	11.9
Europe	2124.6	2072.3	1978.3	2027.5	2050.7	-2.5	-6.9	-4.6	-3.5
CIS	843.2	886.7	880.3	881.5	930.5	5.2	4.4	4.5	10.4
Middle East	709.8	767.3	817.2	864.9	902.3	8.1	15.1	21.9	27.1
Africa	383.8	399.2	422.6	439.4	461.5	4.0	10.1	14.5	20.2
Asia Pacific	4701.5	5121.6	5389.6	5587	5985.8	8.9	14.6	18.8	27.3

Europe is the only region in Table 1.1 that has reduced primary fuel consumption since 2008 and maintained primary fuel consumption below 2010 levels. As previously mentioned, energy consumption is mainly increasing in developing regions which are The Middle East and Africa, and in particular Asia Pacific where fuel consumption increased by nearly 10% between 2016 and 2018.

Unfortunately, current fuel usage is still dominated by fossil fuels as shown in Fig. 1.2, created using data from the BP statistical review from 2018 [2019]. It is apparent that Europe and South America have started to shift primary energy consumption to net carbon-zero sources (this includes nuclear, wind, solar, hydro, tidal and biomass). In Europe this has mainly been achieved through policy which has been linked to large-scale power generation however, this has also been aided by advances in localised systems such as combined heat and power (CHP) and energy from waste. In South America, advances in bioethanol production and hydro power have driven changes.

A large challenge in estimating values of energy demand and consumption is that a large part of the world still relies on systems such as cookstoves and localised heating and power generation. These are often powered by wood, local biomass, faeces

and waste which are not included in most outlook reviews but can have a large impact on the environment.
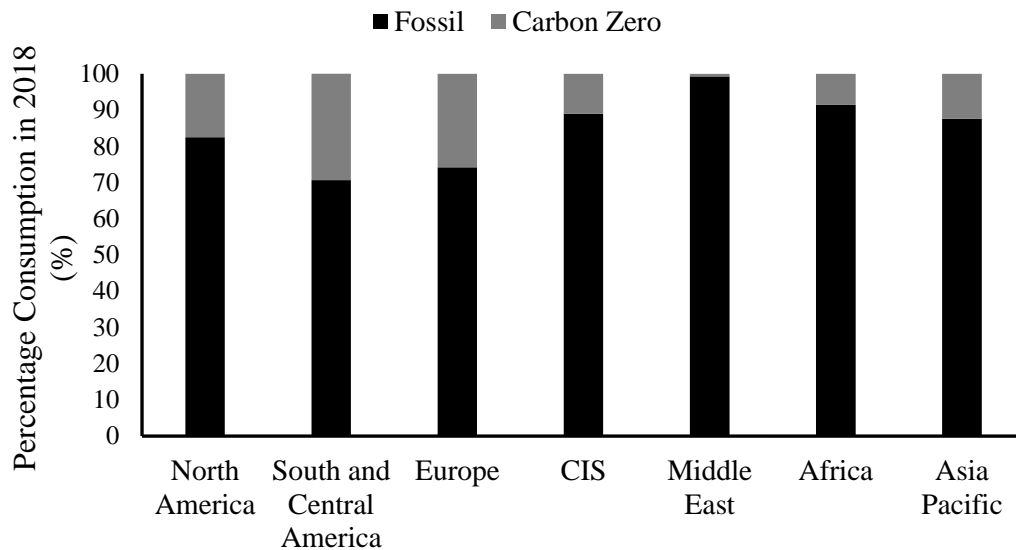
Figure 1.2: Percentage comparison of fossil versus carbon zero fuel consumption in different global regions. [BP, 2019]

1.1.2 Environmental Concerns

Environmental concerns can be related directly to emissions from conversion processes and from the activities in obtaining fuels. Climate change and environmental concerns are currently key topics of global politics, these include:

1.1.2.1 Global Warming

Global warming continues to challenge society as changes from the damage caused are becoming more apparent, such as extreme record high temperatures and rising sea levels. A special report by the International Panel on Climate Change (IPCC) [Matthews, 2018] states that the average global temperature has increased by 1.5°C since pre-industrial levels. This is being caused by greenhouse gases which are at their highest levels for 800,000 years [Nunez, 2019].

Greenhouse gases trap radiation from the sun in the atmosphere by absorbing infrared radiation energy and readmitting it back into the atmosphere. Various greenhouse gases have different potentials to cause the greenhouse effect, this is based on both their ability to absorb radiation and their lifetime in the atmosphere. These two parameters are described by the Global Warming Potential (GWP), this is quantitative assessment of the impact of a gaseous specie on the atmosphere within a

3

100-year time period compared to that of CO_2, for this reason CO_2 is given a reference level of 1. Table 1.2 compares some of the most common greenhouse gases and their GWP factors from the 2007 IPCC report on the Physical Science of Climate Change [Solomon et al., 2007]. Within this report a special focus on the impact variability with time was discussed which resulted in a GWP 20-year horizon factor being determined. GWP is a useful assessment since it helps to evaluate the global trajectory on climate change, for example NF_3 is emitted from the production of semiconductors for the electronics industry, these semiconductors are used to manufacture photovoltaic (PV) cells, this is an important consideration when choosing to increase solar energy generation [Arnold et al., 2013].

Table 1.2: Global warming potential of various greenhouse gases [Solomon et al., 2007]

Greenhouse Gas	Chemical Formula	Global Warming Potential		Atmospheric Lifetime (Years)
		GWP- 100-year horizon	GWP- 20-year horizon	
Carbon Dioxide	CO_2	1	1	100
Methane	CH_4	25	56	12
Nitrous Oxide	N_2O	298	280	114
Ozone	O_3	1000	65	<1
Chlorofluorocarbon-12 (CFC-12)	CCl_2F_2	10,900	11,000	100
Nitrogen Trifluoride	NF_3	17,200	12,300	740

1.1.2.2 Atmospheric Pollution

Atmospheric pollution and the greenhouse effect are often confused. Greenhouse gases are gases capable of causing global warming, described in the preceding section. Air pollution refers to the emission of any pollutant (gas, liquid or solid) that can cause damage to the ecosystem or human health. A greenhouse gas can also be a pollutant.

An article from the New South Wales Government Office for Environmental Health [2013] identifies the most common air pollutants to be: particulate matter 10-2.5 (PM), ground-level ozone, nitrogen dioxide, carbon monoxide and sulphur dioxide. The U.S centre for Disease Control and Prevention (CDC) [2019] expands this to include lead (Pb) and the UK Department for Food, Environment and Rural Affairs (DEFRA) [No date] also includes PM_1, volatile organic compounds (VOCs),

Toxic Organic Micro-Pollutants (TOMPS), Benzene, 1,3-Butadiene and selective heavy metals (Ar, Cd, Hg and Zn). This shows how variable the international interpretation and importance of air pollutants currently is. Table 1.3 describes more comprehensively some of the common air pollutants.

Table 1.3: Internationally recognised air pollutants of greatest concern

Pollutant	Chemical Symbol	Description	Source
Carbon Monoxide	CO	A colourless and odourless gas that can displace oxygen in blood and bind to haemoglobin. [a] [b]	Incomplete combustion including in vehicle engines, power stations and household stoves. [a] [b]
Sulphur Dioxide	SO_2	SO_2 causes acid rain when it solubilises in the atmosphere, this process causes haze and reduces the air visibility. It also increases breathing difficulty when in high concentrations. [a] [c]	Coal combustion and combustion of fuels high in sulphur. [a] [c]
Oxides of Nitrogen	NOx	Highly reactive nitrogen species which react in the atmosphere to form a variety of compounds including non-nitrogen containing species such as ozone. NOx contributes to acid rain and haze. Additionally, NOx causes nitrification of coastal waters and land which creates nutrient pollution. NOx can aggravate the respiratory system. [a] [c]	Combustion of most fuels including in power stations, internal combustion engines (ICE's), and domestic applications. [a] [c]
Particulate Matter	n/a	This is a general term used for solid particles and liquid droplets suspended in the air which can vary in size but the most concerning sizes range from 1-10μm. Some particles are emitted direct from source these are usually called dust particles. PM from the energy sector is usually called soot when it is high in carbonaceous species and forms PM by a series of complex reactions and sublimation and condensation of various inorganic species. PM can have a global warming effect as well as reducing visibility. The greatest concern is the respiration of these species at PM_1 size as these can penetrate deep into lung tissue and cause long term health effects including cancer. [a] [c]	PM can be directly from industrial activity. This includes dust particles from processing of materials and minerals and civil activities such as installing insulation in buildings and laying tarmac for roads. PM from combustion can be formed from any fuel in any conversion technology. Soot is primarily formed from diffusion flames and incomplete combustion. ICE's form very small PM from incomplete combustion and rapid cooling in exhaust gases. [a] [c]

Table 1.3 Cont.: Internationally recognised air pollutants of greatest concern

Pollutant	Chemical Symbol	Description	Source
Ozone	O_3	Ozone in the upper atmosphere is critical to protecting the planet from intense radiation from the sun. However, ground-level ozone can cause lung irritation, airway inflammation and reduce lung function. [a]	Ground-level ozone is formed from the reaction of NOx and volatile organic compounds (VOC's). Sunlight and heat are required for the reaction so ozone levels are higher on hot sunny days. [a]
VOC	n/a	These are gaseous organic compounds that have a high vapour pressure and low solubility. They include industrial solvents such as trichloroethylene, and chlorinates from water treatment like chloroform. Health effects are variable and include short-term and long-term effects. Lower concentrations lead to nausea, irritation, dizziness and breathing difficulties. Higher concentrations can lead to more devastating damage such as damage to the central nervous system, kidney and liver toxicity and cancer. [d] [e]	VOCs are formed from anthropogenic processes and are used in many commercial products such paints, inks, cleaning products, adhesives and building materials. Combustion of fuels produce VOCs from incomplete combustion in fuel-rich processes. [d] [e]
Benzene	C_6H_6	Benzene is similar to VOCs however exists primarily in the vapour phase. It is commonly used in many commercial products such as glues, dyes and detergents. Benzene is a carcinogen and can reduce red blood cell production and the effectiveness of the immune system. Benzene can react to form photochemical smog which can then be deposited in water bodies and soil through rain or snow. [f] [g]	Benzene is used in many products for cleaning and treatment purposes. It is a highly manufactured chemical, one of the top 20 in the U.S, and its release mainly comes from industrial processes such as burning of coal and oil (less from gas). Vehicle ICE's cause approximately 20% of benzene emissions and tobacco smoke is the most common source of indoor benzene. [f] [g]
Polycyclic Aromatic Hydrocarbons (PAHs)	n/a	PAHs contain at least two aromatics rings and are formed at high temperatures. Low molecular weight PAHs are usually present as vapour, as they increase in size and molecular weight they form more as solid particles. Their degree of carcinogenicity is variable however they are all described as toxic to human health. [h] [i]	PAHs are only formed from combustion and pyrolysis processes. This is mainly from transport emissions in outdoor air and mainly from solid fuel combustion in indoor air. Cooking on a fuel-fired stove can cause elevated concentrations of PAHs. [h] [i]

Table 1.3 Cont.: Internationally recognised air pollutants of greatest concern

Pollutant	Chemical Symbol	Description	Source
Toxic Organic Micro Pollutants (TOMPS)	n/a	TOMPS is a group of species that cause devastating health effects including cancer, reduced immunity, central nervous disorders, child development and pregnancy problems. At very high concentrations death is a possible outcome from inhalation. The group includes PAHs, polychlorinated biphenyls (PCB's) and dioxins. [j]	All TOMPS in the atmosphere are from combustion of fuels including gas, oil, coal and biomass. [j]
Lead	Pb	Heavy metals in the atmosphere at low concentrations can be deposited into soil and water bodies. Their volatility is variable which means they can be released and deposited readily. Bioaccumulation in the ecosystem is of great concern since it can occur quickly. Heavy metals can cause a range of health problems including kidney and bone damage, cancer, neurobehavioral disorders and increased blood pressure. [k]	Heavy metals in the atmosphere can be present as vapour or solid particles. Their emission is from their presence in fuels which are combusted. [k]
Zinc	Zn		
Mercury	Hg		
Cadmium	Cd		
Chromium	Cr		
Arsenic	Ar		

Table references: [a] United States Environment Protection Agency [2019], [b] Townsend and Maynard [2002], [c] WHO [2005], [d] Government of Canada [2019], [e] HealthLink British Colombia [2018], [f] Agency for Toxic Substances and Diseases Registry [2007], [g] Duarte-Davidson et al. [2001], [h] Lee [2010], [i] Choi et al. [2010], [j] Envirotrain [2018], and [k] WHO [2007].

1.1.2.3 Monitoring and Control of Air Pollution

Most air pollutants from Table 1.3 are of concern when they are in high concentrations, therefore localised monitoring is required to control the impact they have. Emissions are measured over a time period or online (real time) both of which are variable depending on the time of day and the activities taking place. For example, during the morning and evening rush hour travel when people commute to and from work emissions are higher. Therefore, it is important that both the average emission levels and the time period of peak emissions are monitored.

In the UK, National Air Quality Standards (NAQS) are used to monitor and control air pollution. The United States and China are the largest energy consumers, this is largely due to industry and population requirements. In order to monitor and control their air quality they have their own set of air quality measures and objectives-U.S National Ambient Air Quality Standards (NAAQS) and China's Ambient Air Quality Standards. The Chinese standard is used to describe the quality of air by using

categories, i.e., the air quality in a class 1 area is better than a class 2. Table 1.4 compares the UK Air Quality Objectives, NAAQS (US), China's Ambient Air Quality Standards and the Air Quality Guidelines from the World Health Organisation (WHO).

In Table 1.4 the major air pollutants are listed. Additional pollutants have been added into national objective criteria such as ammonia, mercury, benzene, polycyclic aromatic hydrocarbons (PAHs) and dust however these are not ubiquitous and are usually only specified in relation to certain industrial activities.

Table 1.4: Comparison of air quality control targets in ambient air from the UK [DEFRA, 2007], US [EPA, 2016], China [Li et al., 2018] and the World Health Organisation (WHO) [2005].

Pollutant	UK		U.S.		China Class 1	China Class 2	Time Period	WHO	
	Limit	Time Period	Limit	Time Period	Limit	Limit		Limit	Time Period
CO ($\mu g.m^{-3}$)	10	8 hours	10.35	8 hours	4	4	Daily	n/a	
Pb	0.25	Annual	0.15	Quarterly Average	n/a				
NO₂	30	Annual	99.64	Annual	40	40	Annual	40	Annual
PM₁₀	40	Annual	150	24 hours	40	70	Annual	50	24 hours
								20	Annual
PM₂.₅	25	Annual	35	24 hours	n/a			25	24 hours
								10	Annual
O₃	100	8 hours	137	8 hours				100	8 hours
SO₂	350	1 hour	196.5	1 hour	20	60	Annual	20	24 hours

Table 1.4 demonstrates the variability in the international standards. China has the strictest standard in relation to CO from initial observation however the averaging time period is three times longer than for the UK and U.S, this would therefore include night time emissions which are low because of reduced activity. Nitrogen dioxide emissions are the only monitored emissions where all the standards use the same averaging time period. The UK has the lowest target and recently introduced emission control zones in major cities to reduce these emissions further [CCC, 2019]. The target emission level is below the WHO target which is based on the long-term impact of emissions to human health, China has used this level as their own guideline as well. The U.S level is over two times the WHO limit and over three times the UK limit. Limits on emissions of PM₁₀ and PM₂.₅ are all significantly above the recommended limits by the WHO, it is important to recognise that the WHO limits were designed

based upon statistics collected in 2005, this is concerning when more current targets still have yet to coincide with limits that were devised over a decade ago.
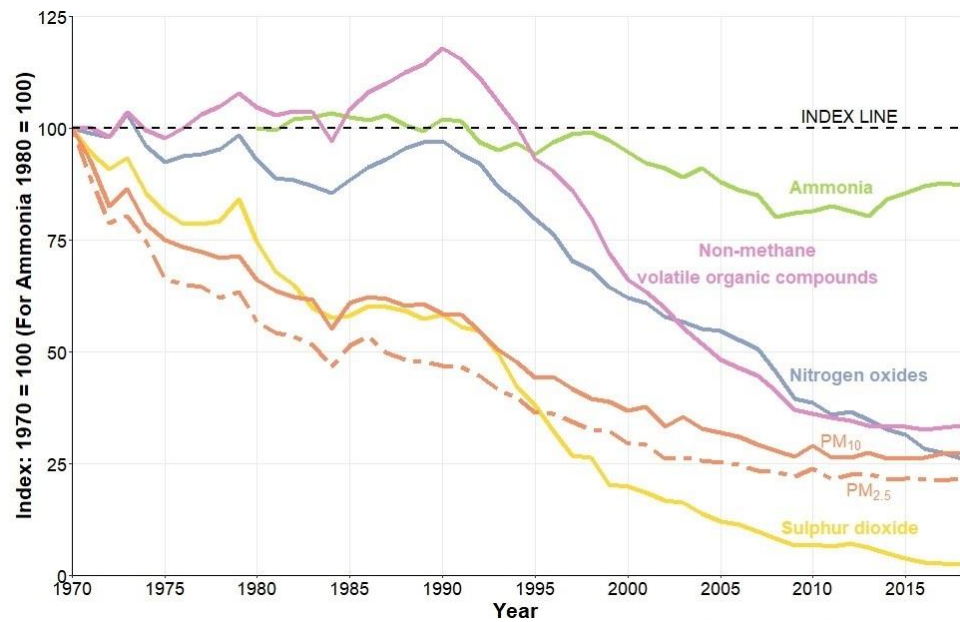
Figure 1.3: Annual trends in emissions in the UK of certain air pollutants from 1970-2018 [DEFRA, 2020]
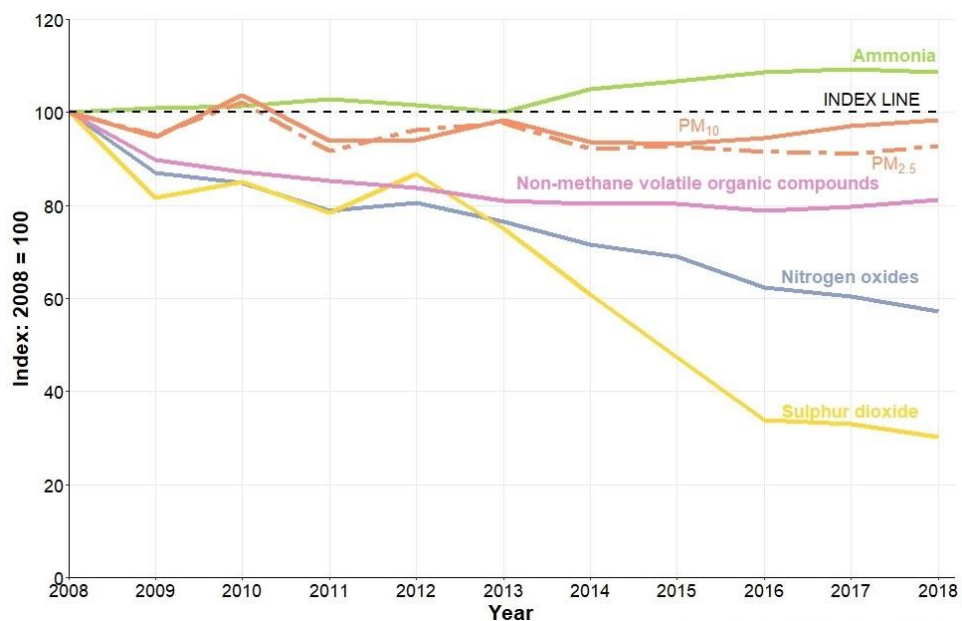
Figure 1.4: Annual trends in emissions in the UK from 2008-2018 [DEFRA, 2020]

As air pollution has developed as a political subject, the more rigorous and comprehensive recording and monitoring has become. Fig. 1.3 is from DEFRA [2020] and demonstrates the relative reduction in emissions. With the exception of ammonia, the emissions of all the pollutants have decreased to levels below 40% of the nominal

1970 levels. The main factor has been the reduced use of coal in power generation, the increased use of abatement technology across the energy use sector (transport and power generation) and the increase in renewables [CCC, 2019]. More recently, since the 2007 limits were introduced, emissions have plateaued, with the exceptions on NOx and SO_2, Fig. 1.4. NOx and SO_2 have continued to decrease again from the reduced use of coal but also by targeting technology and legislation changes. In particular, in the transport sector by the aforementioned emission zones and the addition of NOx reduction technology on diesel cars [CCC, 2019]. Ammonia emissions in the UK are mostly related to the farming and agricultural sector [DEFRA, 2020].

1.1.3 The Renewables Sector

Renewable energy is a key part of the immediate strategy to reduce pollution levels and prevent further climate temperature rises. This is particularly challenging since it is expected that global energy consumption will increase by 56% by 2040 based on 2010 levels [EIA, 2013]. The World Energy Outlook (WEO) report from the IEA [2020] shows that the immediate capacity in the renewables sector is much greater than in any other sector and estimates that this capacity will increase with time for solar and wind, Fig. 1.5.
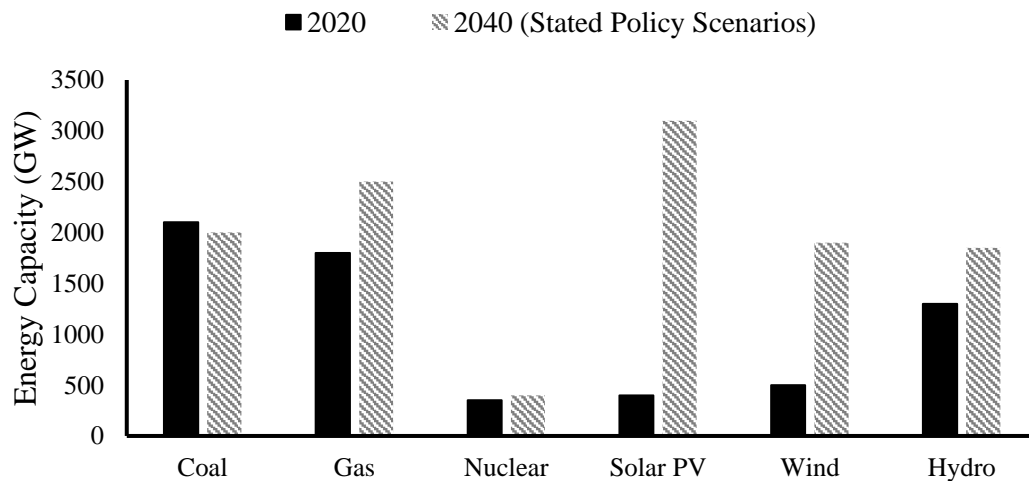
Figure 1.5: Primary energy capacity by energy source for current and projected global energy consumption [IEA, 2020]

Fig. 1.6 from the EIA shows the projected global energy demand by fuel and scenario [2020]. Based on stated policies and the delayed recovery scenario (based on changes from the Covid-19 pandemic) the global trend suggests that there will be an

increase in the use of oil, gas, nuclear and renewables. In the ideological scenarios, sustainable development scenario and net-zero emissions case, a significant decrease in oil and a small decrease in gas will be required to achieve environmental targets.
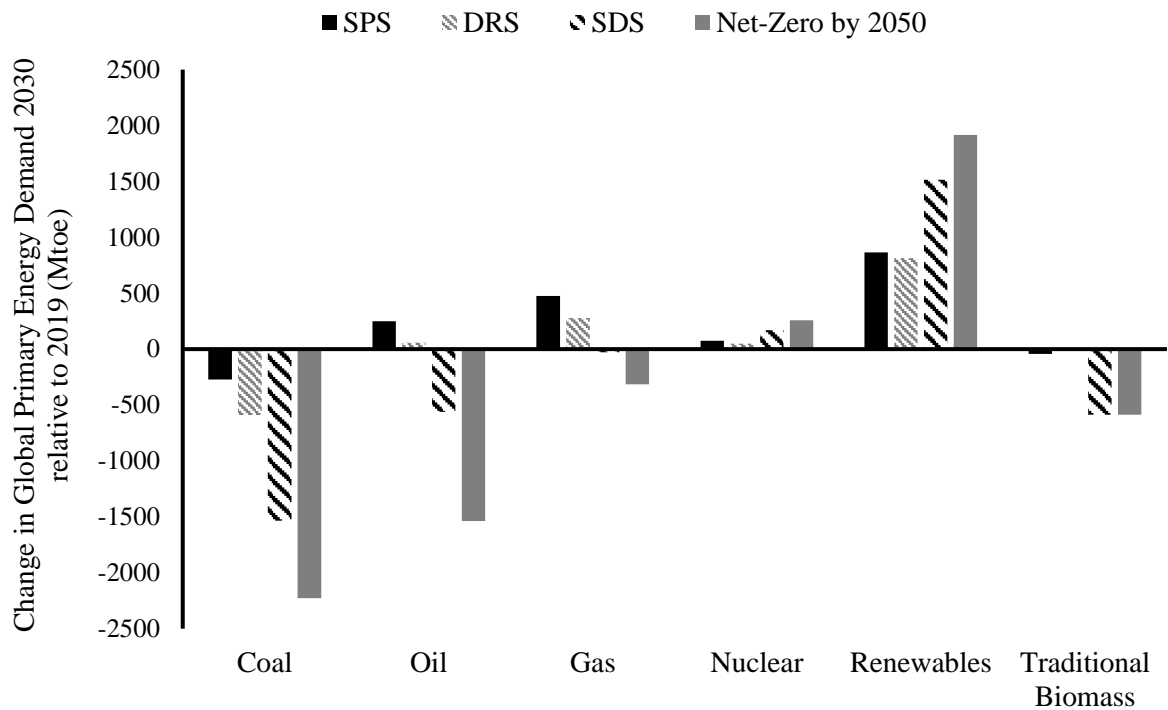
Figure 1.6: Projected change in global primary energy demand to 2030 based on 2019 for four key scenarios. Stated policies scenario (SPS), delayed recovery scenario (DRS), sustainable development scenario (SDS) and net-zero emissions by 2050 [EIA, 2020]
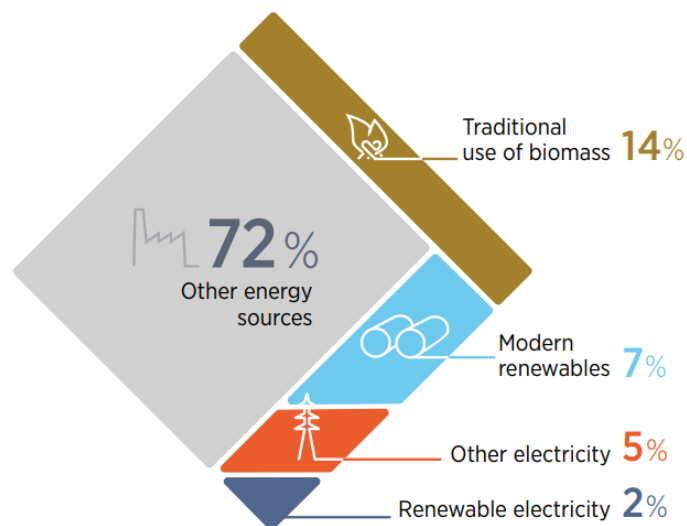
Figure 1.7: Division of global energy sources for heating and cooling end-use [IRENA, 2018]

According to a report for the International Renewable Energy Agency (IRENA) [2018] in order to analyse the role of renewables in the future, four sectors should be considered individually, these are: Heating and Cooling, Transport, Power Generation and System Integration. Heating is the largest end-use energy sector accounting for 50% of energy consumption, the majority of which is supplied by fossil fuels (~70% in 2015) [IRENA, 2018]. The main renewable source in this sector is from traditional biomass as shown in Fig. 1.7 from the IRENA 2018 Report [2018], this is from the combustion of wood logs in domestic appliances.

Modern bioenergy is a rapidly growing sector which includes injections of biomethane and biohydrogen into natural gas systems, solid fuel boilers, co-generation and district heating schemes. Although, the contribution of renewables in this sector is relatively low, this number is highly variable across the earth, for example in Sub-Sahara Africa 70-90% of primary energy supply (mainly heating and cooking) comes from biomass [Eleri and Eleri, 2009] and in South-East Asia approximately 45 million people are still dependent on traditional biomass for primary energy [IEA, 2019].
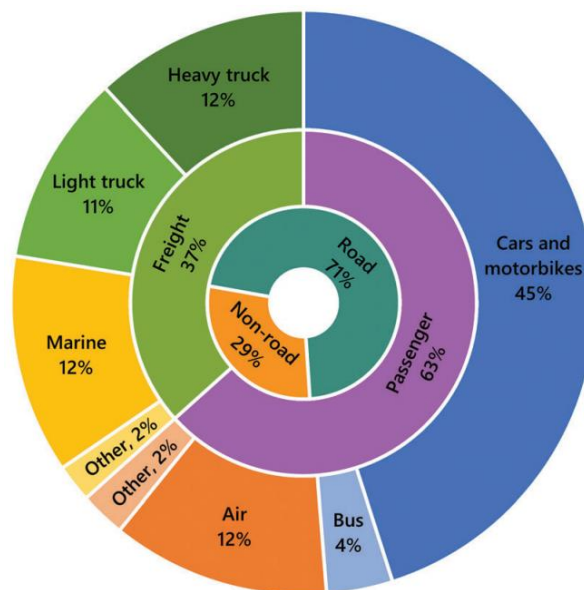
Figure 1.8: Breakdown of the global transport sector in 2015 [Staffell et al., 2019]

The transport sector is the second largest energy consumer accounting for 25% of global consumption [EIA, 2015], 96% of which comes from petroleum products [IRENA, 2018]. The outlook of renewable energy in this sector is facing many challenges, mainly the implementation of an infrastructure which can support the use of biofuels. Instead, many countries are choosing to focus on electric vehicles, with

the potential addition of hydrogen vehicles in the future [Staffell et al., 2019]. Fig. 1.8 shows the breakdown of the transport sector in 2015, the inner circles show the mode and function of transportation respectively whilst the outer circle shows the individual transport methods [Staffell et al., 2019]. As can be seen in Fig. 1.8 personal daily transportation methods are the greatest consumers. Bioethanol has made some small changes to transport fuels by blending with petrol (gasoline). Across Europe 5% is blended and in Brazil all gasoline has a 27% blend of bioethanol [Mączyńska et al., 2019]. In the UK a new 10% blend will reduce CO_2 emissions by 790,000 tonnes from the transport sector [Department of Transport, 2021]. Other progress has been in the Heavy Goods Vehicles (HGV) market by using straight used cooking oil or converting the oil to biodiesel [Li et al., 2014].
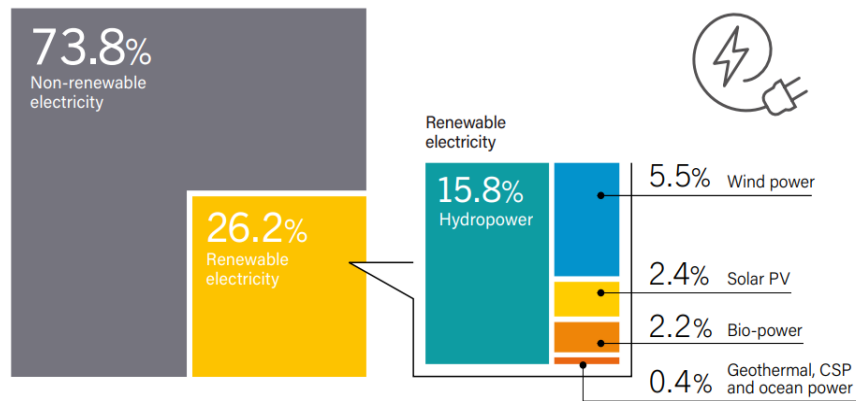
Figure 1.9: Breakdown of global electricity generation by fuel source [Ren21, 2019]

Consumption in the power generation sector is highly variable. Globally it represents about 20% of consumption however in more developed countries this increases [IRENA, 2018]. Renewable energy has made consistent and substantial progress within this sector and in 2018 made-up 26.6% of global electricity generation [Ren21, 2019]. Hydropower has the largest share of this sector (15.8%) followed by wind (5.5%), solar (2.4%), biomass (2.2%) and geothermal (0.4%), as shown in Fig. 1.9 [Centre for Climate and Energy Solutions (C2ES), No Date] [Ren21, 2019]. Consistent growth from hydropower is from the setup of small hydropower units. Lower capital costs and environmental impact has increased favourability of such units over large dams. New technology is driving the increase in wind and solar usage, in the case of the latter it is the fastest growing industry within the electricity generation sector. Geothermal projects remain small and sparse, the focus is more on using geothermal to supply heat. Biomass is being used to make large increases in

renewable electricity generation, in the UK an increase in 30% capacity and 11% generation in 2018 was achieved through conversion of coal power stations to biomass, a relatively low capital investment [Ren21, 2018]. Other large increases in generation were seen in South Korea (50%), Thailand (39%) and China (14%) [Ren21, 2019].

The final sector is system integration which overarches the power generation sector. Without sufficient flexibility in the power generation sector renewable technology is not feasible [IEA, 2020]. The rain doesn't always fall, the wind doesn't always blow and the sun isn't always out, although there is huge capacity in all three of these areas, they are all inconsistent forms of power generation and do not have the versatility of providing an increased demand or reducing when demand is low. This is termed Variable Renewable Energy (VRE) and it has to be combined with System Integration of Renewables (SIR) to maintain grid electricity supply [IEA, 2020]. SIR strategies are becoming more important as the VRE share increases. Additionally, as the heat, transport and power generation sectors merge, electric vehicles and CHP, this will also increase the need for effective SIR strategies [IRENA, 2018] [IEA, 2020]. In certain countries where renewables already operate a large share of the market SIR is the main focus to improve energy demands. An example of this is in Norway where water storage capacity is used to control electricity demand, this is a particularly low-cost strategy being deployed effectively [Norwegian Ministry of Petroleum and Energy, 2019].

Geothermal and nuclear both have the advantage of being independent of weather and time of day, however they are not versatile enough to be used when there are surges in electricity demand. Biomass however offers the versatility and robustness to be fired according to demand. Additionally, biomass is the only source which can be used directly as a fuel to supply energy in all of the sectors. Therefore, biomass is an instrumental part of the future energy strategy.

1.1.4 The Role of Renewables in the UK Energy Sector

In the UK ambitious targets to have a net-zero economy by 2050 has driven significant changes in the energy landscape. Of these changes, the greatest impact has been in the power generation sector, between June 2013-2016 emissions from electricity generation have fallen by 46% [Staffell, 2017]. This has been from the

displacement of coal with gas and a dramatic increase in the uptake of solar, wind and biomass which contributes up to 45% of energy demand [Staffell, 2017]. This replacement of coal has mainly been driven by policy from the UK government which has limited the use of coal with all permits ending in 2024 [BEIS, 2020]. Additionally, the introduction of Renewable Obligation Certificates (ROCs) in 2002 has steadily encouraged the increased use of renewable sources of power generation, this is done by claiming ROCs which can be sold at premium. Investment in energy from waste (EfW), hydrogen and continued investment in offshore wind power in the North Sea aims to continue this progress [BEIS, 2020].

Additionally, recent announcements from the UK government to convert all petrol supplies to an E10 blend by September 2021 are driving change in the transportation sector. This is targeted at reducing transport CO_2 emissions by 750 000 tonnes per year [Department for Transport, 2021]. This has been accompanied by a £15 million investment to replace aviation fuel with fuel manufactured from household waste [Department for Transport, 2021].

The space heating sector, which accounts for 37% of the UK energy sector, has had less success at converting to renewables [Energy Catapult, 2020]. The UK is the second highest user of natural gas for heating systems in Europe [BEIS, 2018]. Recent trial projects injecting hydrogen into the natural gas network are underway but this is still in the development phase [ITM Power, 2020]. Alternative options include small-scale heating systems (localised pellet boilers and CHP systems) or domestic stoves. Renewable Heat Incentives (RHIs), introduced in 2014, has encouraged the decarbonisation of space heating by paying system operators a quarterly payment for every kWh of renewable heat produced [BEIS, 2020]. However, this system has received a lot of criticism in Northern Ireland as the scheme was not properly regulated resulting in the price per kWh exceeding the cost of the fuel and thus people were profiting from heating their homes at the cost of the tax payer [BBC, 2019]. The use of traditional biomass on domestic stoves is an attractive prospect of replacing fossil-derived CO_2 emissions with renewable emissions however, as current data shows this action of decarbonising heat is causing devasting effects on air quality. 38% of particulate matter below 2.5μm ($PM_{2.5}$) comes from combustion on household stoves (closed systems) and open fires [Mitchell et al., 2019]. In December 2020 a UK court ruled that the cause of death from a young asthma sufferer was from breaches of PM

ambient air quality limits [Noor, 2020]. Use of such systems tends to be driven by aesthetic and financial reasons and to tackle the irresponsible use of such systems the UK government has banned the use of coal and wet fuels on such systems [DEFRA, 2020]. Alternative fuels such as agricultural and food processing wastes are of increasing interest because of the more favourable circular economy of these products, however more data and information are required to understand the emissions from these fuels [DEFRA, 2020]. This information is critical in the development of a strategy for the future of these systems which resolves the tension between decarbonising heat and preventing a decline in ambient air quality.

1.2 Biomass

1.2.1 What is Biomass?

According to the Oxford English Dictionary the natural definition of biomass is the volume or weight of organisms in a given area. In terms of energy, it is defined as organic matter used as a fuel. Although this definition does not explicitly say that it is renewable, it implies that the organic matter comes from a living source which is dependent on sunlight and not from organic matter buried in the earth's crust.

Biomass is a term that covers a variety of living organisms. It can be broken down into categories which often vary but are usually woods, herbaceous and agricultural biomass, aquatic biomass, fruit bearing biomass, animal residue and waste [British Standards Institute, 2014] [U.S. Department of Energy, no date]. This is discussed more in section 2.1. Waste is a more complex area because of the variability of material sources. Sectors such as industrial wood waste from lumber mills is a consistent material so can be considered as biomass, often included as wood, however household waste (municipal solid waste) is a mix of biogenic and fossil material [IEA, 2003]. Therefore, is usually only determined as biomass if more than 50% of its content is from a biogenic source [IEA, 2003]. Food processing wastes are an attractive source of biomass because of their increasing availability, superior economic aspects (circular economy) and lower carbon investment from cultivation, treatment and transportation. Conservation biomass generated from land management to improve the local ecosystems is a current area of interest and is often burned in open fires outdoors. Utilising this biomass as fuel in local heating systems would harness

both the energy content and control emissions with improved conversion techniques or pre-treatment.

1.2.2 The Structure of Biomass

The biological composition of biomass is made up a series of polymers in various forms including cellulose, hemicellulose, lignin, starch, triglycerides and fatty acids. The former three make up the majority of the structure and are termed lignocellulose, Fig. 1.10 [Hasanov, Raud and Kikas, 2020]. When the structure in Fig. 1.10 is broken down the components can be used to make chemicals or converted to energy by completely breaking down the polymer chains. Although there is some variation between species the typical content is 40% cellulose, 25% hemicellulose, 15-25% lignin and up to 10% other elements [Brandt-Talbot et al., 2017].
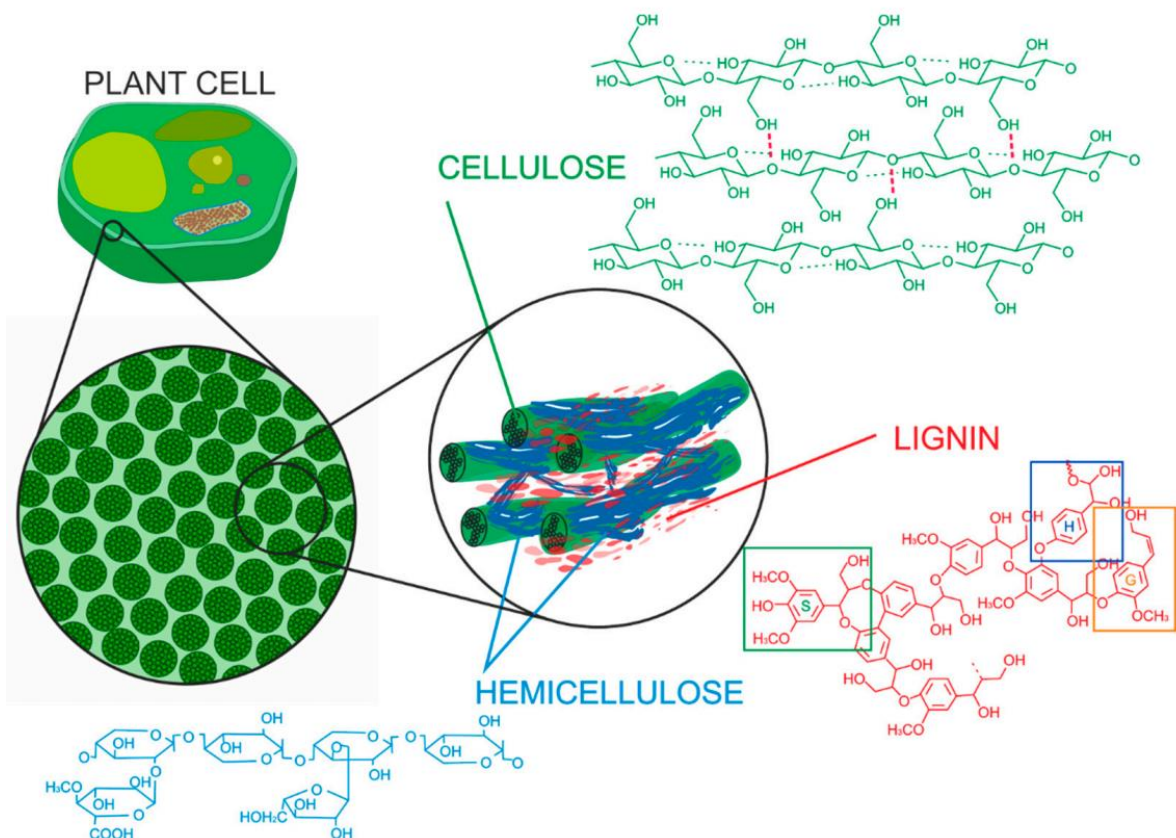
Figure 1.10: Structure of lignocellulosic biomass [Hasanov, Raud and Kikas, 2020]. Labels S, H and G are primary lignin monomers described in Fig. 1.11.

Cellulose is an insoluble polysaccharide formed from the monomer D-glucose. D-glucose monomers are bonded together by glycosidic bonds to form repeating units consisting of two monomers called cellobiose [Bai, Yang and Ho, 2019]. Long chains

of repeating units are called glucans, each glucan can consist of 10,000 glucose monomers. Hydrogen bonds form inter- and intramolecularly as shown in Fig. 1.10. The crosslinking of parallel polymer chains is by intermolecular hydrogen bonds and Van der Waals forces forms microfibrils [Bai, Yang and Ho, 2019]. The packing density of microfibrils can result in the structure being crystalline (tight) or amorphous (loose) [Gudka et al., 2008].

Hemicellulose is a heteropolymer made up of small linear and branched polymer chains (up to 500 units), monosaccharides, these include hexoses (D-galactose, D-glucose and D-mannose), pentoses (D-arabinoses and D-xyloses), deoxy-hexoses (galactose) and related sugar acids [Hasanov, Raud and Kikas, 2020]. Hemicellulose polymers are soluble in dilute alkali [Gregory and Bolwell, 1999]. The variety of hemicelluloses vary between biomasses, for example hardwood is mainly composed of xylans, whilst softwood is composed more of mannose and galactose [Asif, 2009]. Hemicellulose is an amorphous structure which can be classified as either water-soluble low hydration polysaccharides or hydrocolloids [Brunner, 2014]. The former stabilises the cell wall by hydrogen bonds with cellulose and covalent bonds with lignin and acts as a glue between the polymers. Hydrocolloids act as storage pockets for energy and water [Brunner, 2014].
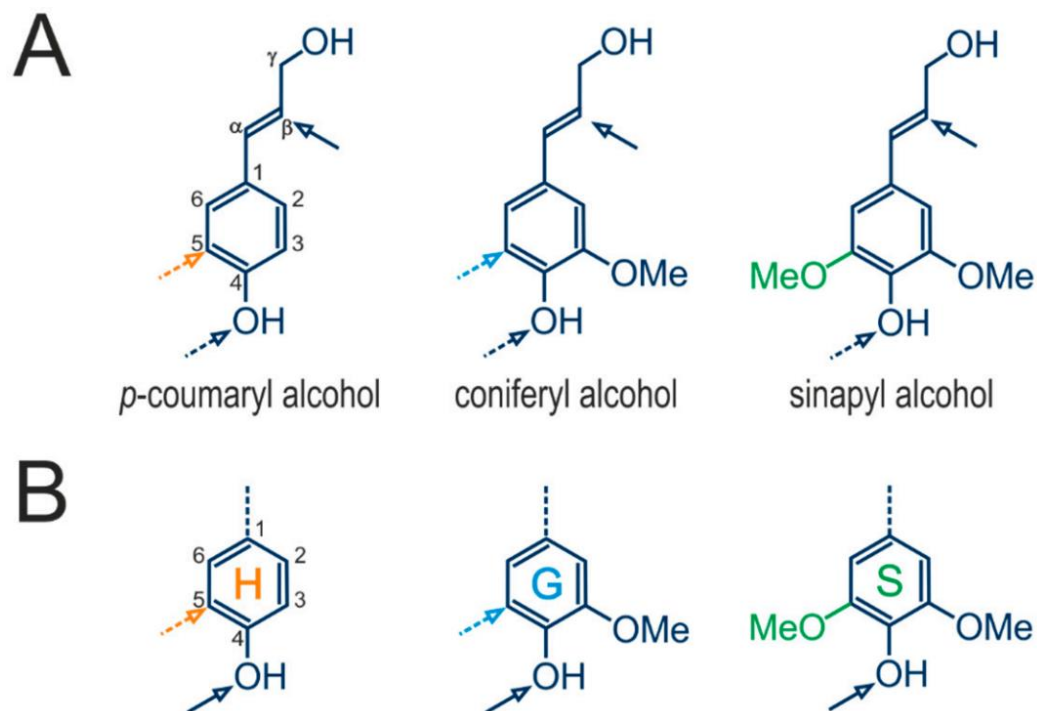
Figure 1.11: Main lignin constituents: (A) monolignols and (B) monomers. Arrows indicate more reactive sites and dashed lines less reactive sites [Hasano, Raud and Kikas, 2020]

Lignin is an aromatic polymer, phenylpropane, comprising of monomers coniferyl alcohol, sinapyl alcohol and coumaryl alcohol [Vanholme et al., 2010]. It is key to plants as it gives the plant strength, structure to the vascular system in xylem and prevents degradation from enzymic activity [Yoo et al., 2017]. The degree of polymerisation is unknown because lignin is heterogeneous and doesn't have a defined primary structure. It contains many cross-linkages from functional groups such as aliphatic hydroxyl, phenolic hydroxyl and methoxy groups [Chio et al., 2019]. The make-up of lignin in hardwood (mostly synapyl alcohol units) differs from softwood (mostly coniferyl alcohol units) [Li, Carlon and Lacis, 2014]. Fig. 1.11 shows the monolignols and their monomers which contribute to lignin structures [Hasanov, Raud and Kikas, 2020].

As well as the organic components (C, H and O) N is a key nutrient in biomass. Uptake, assimilation, storage and transportation of N is critical to biomass growth and development and is therefore often applied as a fertiliser. Accumulation of N in trees has been shown to be dependent on the biosynthesis of glutamine and is associated with the formation of vascular systems in stems and roots and chloroplasts in leaves. Other inorganics (S and Cl) and ash components (K, P, Na, Ca, Mg, Al, Mn and Si) are also taken up by biomass some of which are key to plant metabolism and growth or can be detrimental in large quantities, this is discussed more in section 2.2.3.

During conversion degradation of the biomass structure results in the reaction of various components and in some cases their undesirable emission. The concentration of various species, the conversion method and parameters influence their release, this is discussed more in relation to combustion in section 2.3. Pre-treatment of biomass can prevent the release the of these species by removing them or binding them into the char/ash matrix, section 1.3.1 and 2.4.

1.2.3 Why Use Biomass?

As discussed in section 1.1.3, biomass is fundamental to the future of energy sustainability because it is the only renewable energy source that can consistently provide energy and be used when surplus energy is required. However, there are other factors that support the use of biomass.

The main advantage of using biomass is that it is considered to be carbon neutral. The carbon emitted through combustion, which forms CO_2, is taken in during

photosynthesis and returned to the plant structure. This cycle results in no net carbon being emitted to the atmosphere preventing global warming effects. Carbon emissions from the processing and transportation of biomass can have a heavy influence on the neutrality of this process and have to be considered through LCA to determine if a feedstock is net-carbon neutral (carbon emitted through the lifecycle of the feedstock is less than or equal to the carbon drawn in through its growth). In addition, sulphur emissions are usually lower for biomass compared to coal which reduces problems with acid rain and photochemical smog. The Industrial Emissions Directive has recently reduced the emissions limit to 150 mg Nm^{-3} for NOx which is unattainable with the use of coal but possible with low-N biomass [Birley et al., 2019].

Another advantage is that biomass can be sustainable, it can be regrown, as long as strict harvesting practices are implemented to prevent land-use change and ecosystem damage. This is extremely important as the concept of sustainability includes both energy and material factors. In terms of energy, although feedstock resources can vary, biomass grows fast which can overcome these issues. Additionally, agricultural waste and biogenic municipal waste can reduce the need for landfill which is more harmful to the environment. In terms of materials biomass has some advantages compared to other renewables; for example, expensive extraction of rare minerals which are required to manufacture solar cells, fuel cells, and batteries are in low supply and can cause more environmental damage through mining [Vandepaer et al., 2019].

Traditional systems designed for use with coal, oil and gas can be converted with lower capital investments to be run on biomass or biofuels. Examples of this include conversion of coal power station boilers to use biomass, combustion of oil, biofuel or biogas in ICE's for transport or power generation [Caposciutti et al., 2020] and injecting biogas into existing turbine systems [Moliere, 2005].

Globally traditional use of biomass for cooking and heating is still a necessity for many, especially in developing countries. Although current schemes are trying to promote the use of LPG and modern biomass systems, cost and technical problems are preventing effective implementation and instead many communities are reverting back to the use of traditional biomass [Núñez et al., 2020]. Even in the more developed

world, biomass is still being used as an essential means to heat spaces in more rural communities that cannot access nationalised gas and electricity networks.

Biomass can also be used advantageously to remediate contaminated land and irrigate process effluents which would otherwise contaminate water sources. This is done through the process of phytoextraction (also called phytoremediation) [Pulford and Watson, 2003]. This can prevent the need for mechanical land aeration or soil replacement techniques that would require significant energy input [Pulford and Watson, 2003].

The sustainability of biomass is a current important question and is typically assessed using life cycle analysis (LCA). Kadiyala, Kommalapati and Huque [2016] showed that GHG emissions per unit of energy over the lifetime of a fuel including cultivation, harvesting, transportation, the formation of pellets and then conversion to form energy was lowest for industrial residues such as sawdust pellets 45.93 gCO_2e kWh^{-1}. Compared to dedicated energy crops, 208.41 gCO_2e kWh^{-1}, this is a 75% saving in GHG emissions [Kadiyala, Kommalapati and Huque, 2016]. Conservation biomass is also an area of interest however there is insufficient data on practices and emissions to assess these in comparison to other traditional fuels.

Residues and wastes are a particular area of interest because they will often be either incinerated in open fires for disposal or sent to controlled incineration/land fill. In both cases the uncontrolled formation of GHG is an important consideration in the carbon balance and harnessing the energy from these materials. A LCA from cradle-to-gate study by Pfadt-Trilling, Volk and Fortier [2021] on an EfW facility diverting material from land fill showed that on electricity generation only the GHG emissions were 775 gCO_2e kWh^{-1}, this is significantly higher than industrial residues or energy crops discussed earlier. However, when the GHG savings are included from diverting from landfill the net GHG emissions were calculated at 84.5 gCO_2e kWh^{-1} and this could be reduced further, 63 gCO_2e kWh^{-1}, when ferrous metals were separated out for recycling [Pfadt-Trilling, Volk and Fortier, 2021]. This only assesses the GHG emissions but additional environmental gains include preventing contamination of land and water systems from landfill leachate and long-term ecosystem damage from mechanical activities. These fuel sources do have their problems as well- these are discussed in section 1.4.

1.3 Biomass Conversion Processes

There are many different process options to convert biomass to energy. Primary stages of processing convert the raw biomass to a more useable fuel by improving the chemical and physical properties. Following this the fuel is converted by thermochemical processes to release biogas, bio-oil and heat. Thermal pre-treatment processes are also thermochemical processes but in the context of this work, pre-treatment refers to the production of a solid combustible fuel product instead of production of a gas or liquid.

1.3.1 Pre-Treatment

1.3.1.1 Drying

After biomass is harvested, it is very high in moisture, this can range from 15% in cereal straws to 90% in algae. Moisture is problematic since it gives the biomass more elastic mechanical properties and can cause self-heating during storage or in milling processes. It is also less efficient and profitable to move biomass that is high in moisture and also cause poor combustion efficiency and ignition [Price-Allison et al., 2019]. Therefore, the biomass goes through various drying processes depending on its end product. Ambient drying will reduce the moisture down to an equilibrium with its local environment however this takes long residence times and will still require further drying.

The most common process is to use a conveyor drying system where hot air is drafted in either a co-current, cross-current or counter-current direction to the biomass being carried on the conveyor. This system uses forced convention to remove moisture which is a faster and more thermodynamically efficient process. Because of the shorter residence time in the drying zone, this process is only suitable to biomass with a high surface area to volume such as wood chips, brash, straws, processing residue (sawdust, olive cake and rice husks), grasses and shrubs.

For larger fuel products such as wood logs, where the surface area to volume is much lower, continuous process systems are not suitable. Drying of these products requires long residence times to allow heat, air and moisture to transfer and diffuse through the body of the wood log. Wood logs for use in residential and local solid fuel appliances are described as either fresh-cut, seasoned or kiln dried, the name is given based on the treatment of the wood. According to Price-Allison et al. [2019], fresh-cut

logs have a moisture content of more than 40 wt.%, seasoned (dried in ambient conditions) between 25-35% and kiln dried <20% (dried at above 60°C).

Very wet biomass (>45 wt.%) is usually not dried because of the high energy requirements/costs (approximately £100000 per year to dry biomass from 60 wt.% to 24 wt.%) [Han, Choi and Kim, 2020] and instead used in thermal hydrolysis processes to produce biogas (biomethane or biohydrogen) and hydrochar. Hydrochar is discussed in more detail in section 1.3.1.3.

1.3.1.2 Densification and Size Reduction

Densification increases the bulk density and thus improves the energy content, the transportation efficiency and the storage/handling capacity. There are three main mechanisms for densifying biomass: extruding, pelleting and briquetting. In each case the biomass is first reduced in size by shredding, chopping and/or milling. Extrusion uses a screw mechanism to compress the biomass particles together. Pelleting pushes biomass material through open ended die holes and briquetting uses either a hydraulic press or rollers to compact the material into briquette moulds or dies.

For a briquette or pellet to hold its' shape it requires the use of a binder. The binder can be a chemical that is added which helps the densified biomass to set such as phenolic resin, or it can be from natural mechanisms within the biomass. Lignin is a natural binder in biomass that when mildly heated (100-200°C) softens to bind the biomass together by interlocking particles. Moisture is also a binder by increasing chemical bonding between particles through hydrogen bonds and van der Waals forces [Kaliyan and Morey, 2009]. Depending on how durable the pellets/briquettes need to be, remembering that sometimes they have to be broken apart again after transporting, will dictate how they are bound together.

The particle size also influences the mechanical strength and durability of the pellets/briquettes. Small and flat particles reduce the number and size of space voids that can form during densification [Kaliyan and Morey, 2009]. Typically, biomass is broken down to particles less than 5mm in dimension before being pelleted or briquetted. This can be done using cutting mills (shredders) or ball mills, the latter of which forms smaller particles.

23

1.3.1.3 Thermal Pre-Treatment

Thermal pre-treatment goes beyond drying and the removal of excess moisture to cause irreversible chemical and physical changes. As mentioned before these are described in relation to the formation of solid fuel products. A Van Krevelen diagram shown in Fig. 1.12 describes the process of coalification, the natural process of coal production by pressure and heat in the earth's crust, where fuels become more carbon rich through dehydration and decarboxylation [Guo et al., 2017]. Depending on the severity of thermal pre-treatment conditions, raw biomass can be transformed to perform more like coal.

Torrefaction is a mild pyrolysis process. Temperatures between 200-300°C in either reducing (more common) or oxidising environments are used to dehydrate and thermally decompose all the hemicellulose and approximately 70% of the cellulose. This process releases low calorific value volatiles as either tars or vapours but concentrates the carbon and energy content of the biomass producing a dark solid residue. The severity of torrefaction is controlled by the peak temperature and residence time [Bridgeman et al., 2008]. The benefits of torrefaction are increased energy density and thermal stability. Torrefied fuels are hydrophobic so are easier to store and less at risk of self-heating, as well as having improved mechanical properties, more plastic and brittle, for milling and size reduction [Akinrinola, 2014].

Biochar production is a similar process to torrefaction but uses increased temperatures (300-650°C) and longer residence times to remove all the volatiles. It must be performed in an inert environment. This increases the carbon content and aromaticity of the fuel, and also improves the grindability, porosity and energy content [Wang et al., 2019]. Biochar can be fired into combustion systems but is also regularly used as soil conditioners for carbon sequestration. The ash concentration is significantly increased in biochar and can lead to high emissions of particulate matter in combustion systems [Wang et al., 2019].

Hydrothermal Carbonisation (HTC) submerges biomass into water which is pressurised (2-6 MPa) and heated (180-280°C) for 5-240 minutes [Arellano et al., 2016]. The process can produce oils by liquefaction and the process waters can be used in anaerobic digestion to produce biomethane or biohydrogen. The hydrochar produced has an increased energy content and has a decreased content of alkali and

alkaline earth metals (AAEMs) [Kambo and Dutta, 2015]. The main issue is that HTC has to happen in a closed system because of the pressure effects when trying to load fresh material into the reactor [Abelha et al., 2019]. Additionally, the hydrochar produced in HTC is removed as a slurry which requires dewatering and then thermal drying. In the most severe conditions, high temperature and pressure and long residence times, a solid product similar to bituminous coal is formed.
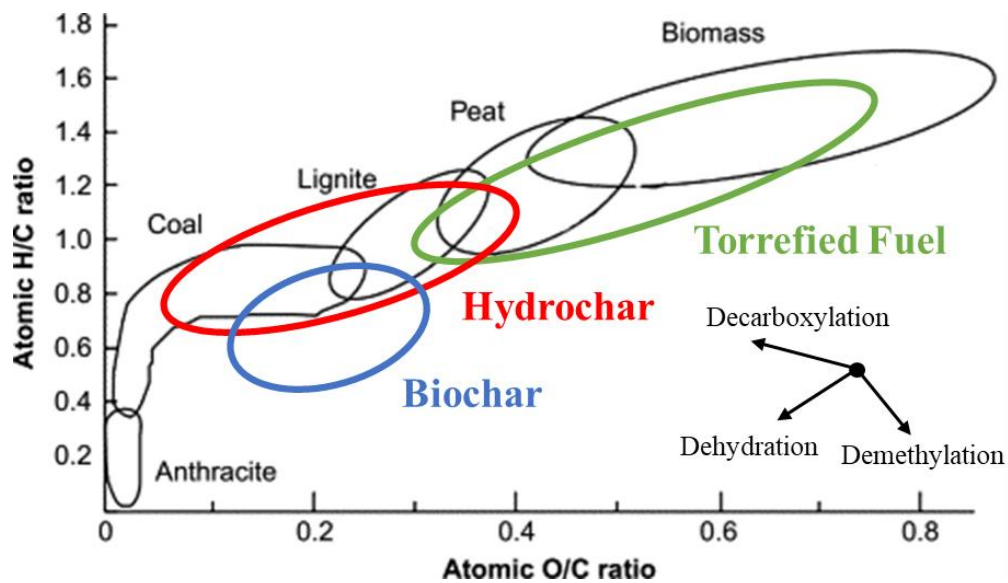
Figure 1.12: Van Krevelen from Ronsse, Nachenius and Prins [2015] modified to show position of torrefied fuels, biochar and hydrochar

Fig. 1.12, which is modified from Ronsse, Nachenius and Prins [2015], shows where the three types of thermally treated fuels fit on a Van Krevelen diagram compared to coal. Biochar is resemblant of coal (in terms of composition), hydrochar is most like lignite and bituminous coal under extreme conditions whilst torrefied fuel is similar to peat and lignite (severe torrefaction).

1.3.1.4 Washing

Biomass washing is focused on removing ash by surface washing and leaching. Alkali and alkaline earth metals, Cl, S and N levels are reduced using water or an alkali or acid medium [Carillo, Staggenborg and Pineda, 2014]. Removal efficiencies can be improved by using, acids and hot water [Carillo, Staggenborg and Pineda, 2014]. Washing has been used on agricultural biomass such as straws and grasses but more recently fast-growing woods such as short rotation coppice willow [Yu et al., 2014]. Biomass grown on contaminated land and waste woods from industry, which are higher in heavy metals, have also benefitted from washing making them more useable

[Abelha et al., 2019]. Emissions from washed biomass can be improved by removal of Cl, S and K which are key to fly ash formation, this reduces PM emissions and can reduce the slagging and fouling effects [Gudka et al., 2016].

1.3.2 Thermochemical Conversion

1.3.2.1 Combustion

Combustion is the reaction of carbon and hydrogen in fuel with oxygen to release energy. Combustion can be done with solid fuels, oils or gases, the former is the focus of this work. Co-firing of fuels is common in power generation but less so in smaller systems such as pellet boilers and stoves. The main products of combustion are CO_2, H_2O, CO and smaller amounts of CH_4, NOx, SO_2, unburnt hydrocarbons and particulate matter [Williams et al., 2012]. The concentrations of these emissions are dependent on the combustion system and the fuel.

Large scale systems in power stations such as fluidised beds, fixed beds, moving grates and pulverised fuel boilers fire the fuel into the combustion zone where it rapidly heats up and reacts [Williams et al., 2012]. The hot flue gases heat water in a heat exchanger known as a super heater which produces steam to turn the turbine by thermal expansion. The flue gases are emitted to the atmosphere after a series of gas cleaning stages such as catalytic reduction, electrostatic precipitation and desulphurisation [Ndiema, Mpendaoe and Williams, 1998]. Bottom ash is removed from the furnace and used as a material in the construction industry or sent to land fill. The main obstacle in large scale systems is to increase the rate of heat transfer and mixing to increase the efficiency of combustion whilst a continuous feed of fuel is being added [Mason, 2016].

Smaller localised systems which are designed to supply heat and power to communities in areas without access to national utilities also use steam generators and boilers. However, the system is much smaller and there are no mills which can reduce the fuel particle size, so pellets, chips and coarse fuel particles are directly loaded into the boiler by a conveyor system [Nosek et al., 2020]. The boilers are fixed bed systems to increase the residence time and improve the conversion efficiency [Limousy et al., 2013]. Bottom ash often has to be manually removed from the boiler. Because of the size restrictions, flue gas abatement technology is usually reduced to a single electrostatic precipitator for PM and fly ash, in a few systems flue gas recirculation is

used to reduce NOx emissions [Limousy et al., 2013]. Pre-treated fuels are particularly useful in these systems to prevent large emissions of NOx and SO_2 [Nosek et al., 2020].

The smallest combustion systems are domestic stoves. These are used in households more commonly for heating but in the developing world they are important for cooking [Ozgen et al., 2014]. This includes open fire systems where fuel is placed on a slab and combusted with no barrier between the user and the flame. In Europe there are over 70 million solid fuel appliances most of which are outdated [Clean Heat, 2016]. Batches of fuel are loaded into a combustion zone and left to combust until the temperature drops when more fuel is added or left until combustion ends. Because the system combusts in cycles with a hot flaming phase followed by a smouldering phase when the stove cools, emissions do not stabilise and instead peak at different stages depending on the radiative forces, temperatures, particle sizes (surface area to volume and porosity) and stoichiometry [Roy and Corscadden, 2012]. Commonly, these systems have no abatement technology and all combustion is through diffusion which means there is more incomplete combustion and emissions can be more varied. Fuel composition is critical in such systems to reduce emissions and improve combustion performance [Roy and Corscadden, 2012].

1.3.2.2 Pyrolysis

During pyrolysis, fuel is heated in an inert environment (absence of oxygen) to produce a mix of char, oil or gas, the relative amounts depending on the temperature, heating rate or residence times [Mohan, Pittman Jr. and Steele, 2006]. Table 1.5 summarises the different operation methods to produce the various products. The oil can be used in reciprocating generator engines or converted to produce biofuel such as biodiesel, bioethanol or aliphatic fuel oil. The gas produced contains CH_4, CO, H_2, H_2O and CO_2, there is also a lot of tar and more complex hydrocarbons produced which, based on recent research, can be cracked and reformed using plasmas to upgrade the syngas [Blanquet, Nahil and Williams, 2019].

Table 1.5: Products of various pyrolysis processes [Mohan, Pittman Jr. and Steele, 2006]

Pyrolysis Technology	Residence Time	Heating Rate	Temperature (°C)	Products
Carbonisation	days	Very Low	400	Charcoal
Conventional	5-30 mins	Low	600	Oil, Gas, Char
Fast	0.5-5s	Very High	650	Bio-Oil
Flash-Liquid	<1s	High	<650	Bio-Oil
Flash-Gas	<1s	High	<650	Chemicals, Gas
Ultra	<0.5s	Very High	1000	Chemicals, Gas
Vacuum	2-30s	Medium	400	Bio-Oil
Hydro-Pyrolysis	<10s	High	<500	Bio-Oil
Methano-Pyrolysis	<10s	High	>700	Chemicals

1.4 The Problems with Biomass

Biomass is an important part of the transition from fossil fuels to renewables. It is widely accepted that biomass will play a vital role in this transition which includes using biomass for heat, transport fuels and in power generation. However, there are some problems and obstacles with the use of biomass. From a social point of view land use change is a great concern. In OECD countries this is changing land use from food production to growing energy crops whilst in South-East Asia and South America the land use change is from rainforest to energy crop farms [Matthews and Tan, 2009]. Legislation in Europe has been introduced to try and prevent the use of energy crops grown unsustainably or with a net negative environmental impact, which has increased the use of waste and residues [Matthews and Tan, 2009]. Additionally, the felling of trees and preventing carbon sequestration in soils is also reducing the sustainability credentials of biomass [Spracklen and Righelato, 2016]. Therefore, the implementation of biomass requires the use of fuels with better sustainability prospects to prevent land use change and minimise the use of trees which act as large carbon sinks.

As discussed in section 1.2.3, residues and wastes offer an alternative with a better sustainability outlook which will help decarbonise the energy sector. However, the high variability of biomass is creating air quality concerns particularly from their combustion in small scale biomass systems and closed and open stoves. Biomass,

compared to coal, has a higher concentration of moisture and volatile matter which increases the amount of incomplete combustion and the formation of particulate matter [Mitchell et al., 2016] [Price-Allison et al., 2019]. The ash content is also highly variable and can often contain high concentrations of volatile metals and inorganics such as K, Cl, S, Na and Zn which can increase particulate matter formation [Williams et al., 2012]. The use of residues and wastes exacerbate this issue as they can often be contaminated with volatile heavy metals such has Cd, Cr, Hg, Pb and Cu. These metals are a major health concern risk especially in domestic heating systems where users are positioned close to the stove [Valvanidis, Fiotakis and Vlachogianni, 2008].

The Department for Environment, Food and Rural Affairs have identified that coal and wet wood are responsible the high concentrations of $PM_{2.5}$ in urban areas (more than industrial combustion and transport combined) and have targeted this reduction by banning the use coal and all wood must have a moisture content below 20 wt.% [Mitchell et al., 2019]. In addition to these laws, DEFRA have created an approved fuels list which must be adhered to in smoke control zones. There are many fuels on the UK market that are not approved on the list including agricultural, industrial and food processing residues and conservation biomass because more research is required to understand their combustion performance and emissions in stove systems. With more research any concerns with the use of these fuels could potentially be addressed with either pre-treatment or changes in the physical properties of fuels. This will increase the inventory of approved fuels and introduce more sustainable fuel sources.

Pre-treatment of biomass is an area of research with increasing interest. Moisture and ash in biomass are undesirable since it reduces the efficiency of operations such as transportation and can make storage, handling and combustion more difficult. These issues often mean in LCA large amounts of energy are used in the preparation (in particular milling) and transportation of biomass [Pfadt-Trilling, Volk and Fortier, 2021]. Targeted pre-treatment could resolve these issues improving the sustainability credentials and emissions from combustion. Pre-treatment could also increase the inventory of fuels available by allowing the use of fuels grown on contaminated land (land unsuitable for growing food and in need of remediation).

It is clear from current policies and research that there are large holes in the effective implementation of biomass in particular in the space heating sector. Whilst the UK is a nation that predominantly uses natural gas, there are greater concerns to the environment and human health from combustion of solid fuels [BEIS, 2018] [Mitchell et al., 2019]. In order to address some of these gaps it is important to assess the use of fuels that prevent land use change and deforestation. Additionally, by combining the energy sector and other industrial sectors creating biogenic waste, new practices and infrastructures can be made to reduce waste and improve the carbon-balance across the energy and industrial sectors. This also includes biogenic material created from conservation and agricultural practices. However, all of this is dependent on understanding the performance and emissions of these materials in their end-use system, and without this information all of these potential new routes to decarbonising the economy are redundant.

1.5 Thesis Aims and Objectives

As energy consumption transitions to renewable fuels, the use of biomass will increase. The only way to fulfil this demand is by using a variety of biomass including the use of agricultural and commercial wastes. Biomass for supplementary heat has seen a resurgence in the UK in recent years with drivers including decarbonisation, economics and aesthetics. However, much of the biomass use has been in open fires or poorly controlled, simple stoves, which areVassi impacting air quality particularly in urban areas. This has prompted the emergence of novel fuels into the market alongside traditional logs and charcoal. This thesis seeks to understand how cleaner fuels might be developed particularly from novel sources including food processing residues and wastes. Therefore, the aims are:

1. To study the emissions from combustion of various biomass on a domestic stove.
2. To investigate the impacts of pre-treatment, by torrefaction and washing, on the fuel quality.
3. To assess the suitability of unconventional novel biomass for combustion applications.
4. To evaluate the impact of chemical composition on the emissions and performance of various biomass combusted on a domestic stove.

To achieve these aims, the objectives are:

- To measure the chemical composition of common biomass fuels (willow wood logs, short rotation coppice willow, spruce and olive stone), torrefied biomass (torrefied willow, torrefied spruce and torrefied olive), washed biomass (washed SRC willow) and biomass wastes (spent coffee grounds and bracken) by using proximate, ultimate (CHNS) and metal analysis (ICP and IC).
- To classify the biomass being investigated by comparing to existing data and data in standards.
- To measure the combustion properties (kinetics, burning rate, time length of combustion phases and heat release) using thermogravimetric, single particle combustion and stove combustion experiments.

- To investigate the gaseous and particulate emissions from combustion of all the fuels on a domestic stove and to produce a table of emission factors that will compare them to current standards.
- To summarise the fuel properties, chemical and physical, which have the greatest influence on the emissions.

1.6 Thesis Outline

Chapter 1- This chapter gives an overview of the energy sector and how biomass fits into our energy futures. It introduces current problems such as global warming and air pollution, what biomass is, why it is important and some of the associated problems and current technologies. This demonstrates why the research in this thesis is important and relevant to the successful use of bioenergy.

Chapter 2- Contains a literature review of fuel properties, characterisation, pre-treatment, combustion on domestic stoves and emissions.

Chapter 3- Outlines the biomass materials studied and experimental techniques used in both fuel preparation and analysis.

Chapter 4- Compares the composition and combustion of untreated spruce, willow and olive residue and their torrefied counterparts. Differences in the chemical and physical properties are used to explain the differences in emissions.

Chapter 5- Presents data from an investigation into the use of spent coffee grounds in domestic combustion applications. Composition and emissions from stove combustion are used to identify if spent coffee grounds are suitable for domestic use.

Chapter 6- Examines the agronomy of bracken collected over an annual cycle and how it compares to other agricultural residues and traditional biomass. Their potential for use in various combustion systems has been analysed.

Chapter 7- Analyses the changes in composition from pre-treating SRC willow grown on contaminated land by washing and torrefaction and their application in domestic systems.

Chapter 8- Concludes the overall finding and discusses their relation to current policy. Future work suggestions are recommended.

Chapter 2. Literature Review

In this thesis the composition and combustion properties of traditional, waste (spent coffee grounds and bracken) and pre-treated (torrefied and washed) biomass are investigated. The chemical composition of biomass is highly variable and dependent on a number of factors including harvesting period, growing conditions, the part of the plant and plant genetics. Combustion of biomass is seen as a carbon-neutral replacement for coal; however, biomass has a higher moisture content and lower calorific value meaning to achieve the same energy production more biomass has to be used [Darvell et al., 2010]. Additionally, biomass is often high in alkali metals meaning its tendency to form metal aerosols is high. This chapter summarises the characteristics of biomass and their combustion properties. Later in this chapter, there is an overview of pre-treatment technology and discussion on some of the current work on combustion of pre-treated fuels.

2.1 Characterisation of Biomass

To effectively use biomass, characterisation is instrumental. This is a complex subject because biomass is so variable, therefore it is constantly under review and an area of research interest. Biomass is most commonly defined by its feedstock. The International Organisation for Standardisation (ISO) defines five categories in ISO 17225-1 [2014], which are woody biomass, herbaceous biomass, fruit biomass (fruit bearing), aquatic biomass and blends and mixtures. Within the former three categories, sub-categories based on whether the biomass is sourced directly from the harvest, a by-product, or is a blended product are used to distinguish between biomass of the same type but of different qualities. Similarly, Vassilev et al. [2010] collated data from many sources for various biomass and instead came to the conclusion that there were six categories of biomass which included woody biomass, herbaceous and agricultural biomass, aquatic biomass, animal and human biomass wastes (faeces), contaminated biomass, and industrial wastes and biomass mixtures. The two key differences between the categories defined by the ISO standards and those described by Vassilev et al. [2010] are that fruit biomass is included in the herbaceous category and the inclusion of biomass derived from industrial wastes such as chipboard, municipal solid waste and paper-pulp. The inclusion of wastes that can be used to make solid recovered

fuel (SRF) has its own standard, BS EN 15359:2011, which includes a very strict set of specifications, classifications and rules for use of such materials.

The classification of biomass is of greatest importance when trading solid biomass fuels, ISO standards 17225 parts 2-7 [2014]. Low grade fuels with high moisture, ash, nitrogen, chlorine and sulphur contents have greater potential for emissions of NOx, SO_2, HCl and PM as well as a greater tendency of slagging, fouling and corrosion, and hence retail at lower prices. Within the solid biofuel trading standards, physical properties are also specified. The form in which the biomass is supplied is a primary defining feature e.g., briquettes, pellets, chips or logs. Secondary to the supplied form, the dimensions, density, particle size, mass of fine material and mechanical durability are considered. These features are not only for woody biomass but apply to all five categories described earlier. Concentrations of heavy metals (As, Cd, Cr, Cu, Pb, Hg, Ni and Zn) are also specified. These are both guides for the quality of the biomass as well as regulating limits. These limits are particularly important for determining if a biomass is contaminated.

Thermally treated biomass, such as torrefied fuels and charcoal, have a separate specification [BE EN ISO 17225-8, 2016] which recognises the increased energy and ash content. Within this standard, there are two tables which relate to woody biomass and the herbaceous, fruit and aquatic respectively. The physical properties are not considered within this standard.

2.2 Composition of Biomass

The chemical composition is fundamental to understanding and predicting the performance of solid biofuels. The chemical composition of biomass is highly variable since it is a function of both natural (authigenic and detrital) and anthropogenic (man-made) processes. Biomass composition is 'commonly' defined by three analyses: proximate, ultimate and mineral analysis discussed in the following sections.

2.2.1 Proximate Analysis

Proximate analysis measures the moisture, volatile matter and ash contents of biomass, the fixed carbon is calculated by the difference, Eq. 2.1, see section 4.3.1 for more details. The moisture content of biomass is an important factor as it reduces the

energy content and prevents efficient handling, transportation and combustion. Moisture can be measured on an as received, air-dried or oven-dried basis, air-dried being the most common, and is typically in the range of 3-63 wt.% depending on the type of biomass. In some exceptional cases of fresh cut biomass, the moisture content can be as high as 80 wt.%. The moisture in plants comes from the living cells and is important for the transportation of minerals and glucose [Vassilev et al., 2010].

$$FC\ (\%) = 100 - VM\ (\%) - Ash\ (\%) - Moisture\ (\%)\ (2.1)$$

Volatile matter is typically 2.7 times higher in biomass than in coal, ranging from 48-86 wt.% db [Vassilev et al., 2010]. Volatiles are the gases and vapours released during thermal decomposition, termed devolatilisation or pyrolysis depending on the environment. These include carbonaceous species such as CO, CH_4, unburnt hydrocarbons, PAHs and soot as well as inorganic aerosols and pollutants (NOx, SO_2 and HCl) [Williams et al., 2012]. Volatiles react in the gas phase through homogeneous reactions with oxygen, these reactions occur very quickly and are responsible for between 40-70% of the energy released [Williams et al., 2012]. Combustion of volatiles produces a luminous flame; the colour of this flame depends on the mixing and oxygen availability. Premixing the fuel with pure oxygen produces a blue flame (more complete combustion) whereas post-mixing with air produces a yellow diffusion flame. Because the reaction in the gas phase is so rapid, the process is dependent on the rate at which volatiles diffuse from the biomass and the subsequent convection to the combustion zone above the fuel particle surface [Jenkins et al., 1998]. This is dependent on many factors including the fuel particle size, moisture content, residence time, heating rate and temperature [Douglas Smoot and Baxter, 2003].

The ash content in biomass varies between 0.1-46 wt.% db, however it is typically below 20 wt.% db for herbaceous biomass and agricultural residue, and below 10 wt.% for woody biomass. Contaminated biomass by the definition of Vassilev et al. [2010], which includes demolition wood, industrial sludge and furniture waste, is much higher in ash because of paints, resins and treatment processes which use minerals to enhance the mechanical properties and production processes. Ash is a generic term used to describe the remaining mass after a fuel is combusted and is often confused with the inorganic matter. Although the ash content is a useful tool for

measuring and predicting the inorganic and mineral content in biomass it is subjective to the combustion process. For example, ash yield produced at above 1000°C is between 20-70% lower than that produced in biomass ash tests at 550°C (based on the British Standard) [Vassilev et al., 2010]. This is because of the increased phase transformations and volatilisation of inorganic species that do not occur at lower temperatures. Therefore, it is important to analyse the composition of the ash as well as the quantity [Vassilev et al., 2010].

Fixed Carbon (FC) is the carbon that forms char after devolatilisation. This carbon reacts heterogeneously with air during the char combustion (smouldering) stage and makes the char glow due to its exothermicity. There is between 1-38 wt.% db of FC in biomass which is a narrower range than compared with coals (between 20-72 wt.%) [Vassilev et al., 2010]. Because char combustion is a slower process, often in smaller combustion systems residual FC is left in the ash, because of reduced conversion efficiency.

2.2.2 Ultimate Analysis

Ultimate analysis measures the concentration of five key elements: carbon (C), hydrogen (H), nitrogen (N), sulphur (S) and oxygen (O), O is calculated by difference, Eq. 2.2. The variation in moisture and ash content has a heavy influence on the composition of the five elements, therefore comparisons are usually made on a dry ash-free basis (daf). Chlorine (Cl) can be included in elemental analysis; however it is measured by a different method and can often be in very low concentrations.

$$\% \, O = \, 100 - \%C - \%H - \%N - \%S - \%ash - \%moisture \ (Eq. 2.2)$$

A high C content fuel also has a high energy content, a 1 wt.% increase in the carbon content can increase the calorific value by approximately 0.39 MJ kg^{-1} [Jenkins et al., 1998]. The carbon content in biomass (40-60 wt.% daf) is usually lower than in coal (60-80 wt.% daf) [Vassilev et al., 2010], however carbon densification can be achieved through various pyrolysis processes, discussed in more detail in section 2.4.

The concentration of O is the second most abundant in biomass (30-50 wt.% daf) but is in lower concentrations in faecal biomass from animals (20-30 wt.% daf) and coal (10-30 wt.% daf); in bituminous coals it is below 10 wt.% daf. The O content is higher in living biomass because of photosynthesis, O in glucose is used in the

make-up of functional groups of cellulose, hemicellulose and lignin [Jenkins et al., 1998].

The H content increases the energy content of a fuel but is present in much lower concentrations in both biomass (6-8 wt.% daf) and coal (3-6 wt.% daf) [Vassilev et al., [2010]. Similar to O, H is used from glucose to form structural and non-structural cellulose, hemicellulose and smaller carbohydrate chains, it is for this reason that there is usually a direct correlation between the carbon and hydrogen contents [Jenkins et al., 1998].

The concentration of N, S and Cl are all typically below 1 wt.% daf in biomass but can be higher in certain types of biomass, for example in pepper plants the N content is above 3 wt.% and in straws the Cl content is between 0.5-1 wt.% daf [Vassilev et al., 2010]. Fuels high in these elements emit NOx, SO_2 and HCl. S and Cl can be critical in the formation of PM and in slagging and fouling, discussed in sections 2.3.2.6 and 2.3.3 respectively. All of these elements are key macronutrients in plants, they are critical in the formation of chlorophyll, enzymes, proteins and vitamins which regulate a plants system such as the uptake of water, expulsion of oxygen and protecting against disease [Jenkins et al., 1998] [Williams et al., 2012] [Chen et al., 2010].

Fig. 2.1 is a ternary diagram from Vassilev et al. [2010] and demonstrates how coals and different biomass elemental compositions vary. As mentioned earlier biomass is typically higher in H and O but lower in C, this reduces the aromaticity of the fuel and consequently it decomposes more at lower temperatures during devolatilisation. As the atomic ratio of H:C and O:C increases, as shown in Van Krevelen diagrams for coalification, Fig. 2.2 [Baxter, 1993], the energy content decreases. This is why biomass is positioned in the upper right corner of the diagram. However, through pre-treatment biomass can move across the diagram towards the bottom left corner, this is discussed more in section 2.4.
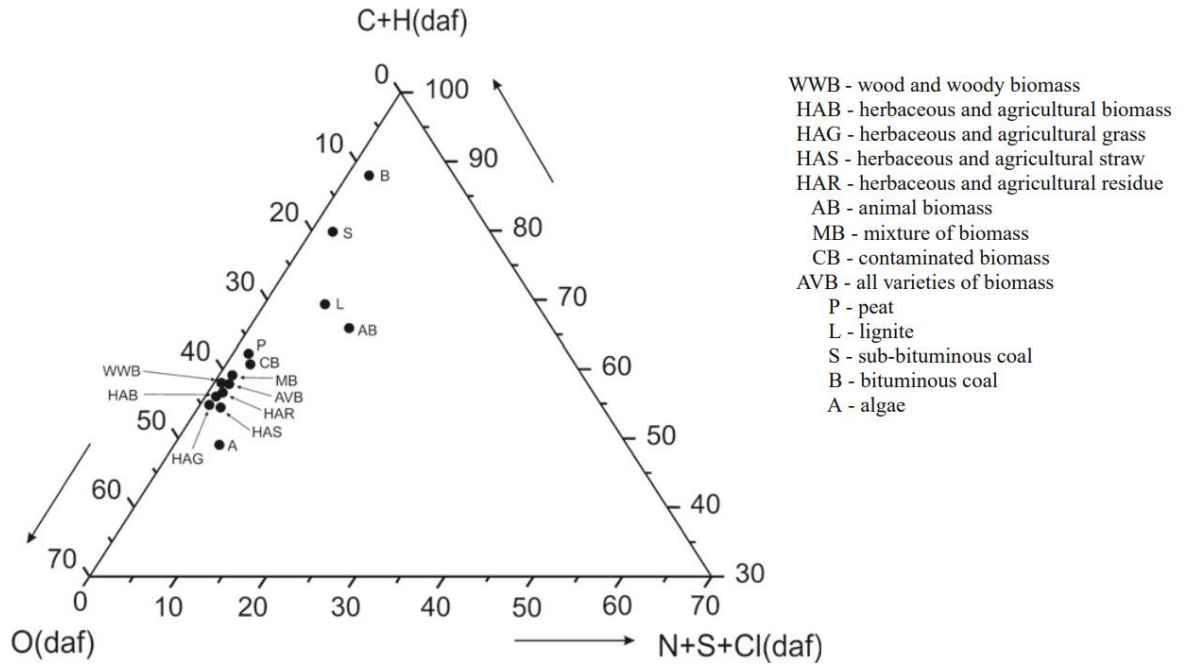
Figure 2.1: Ternary diagram demonstrating the normalised wt.% compositions of various biomass and coals from Vassilev et al. [2010]
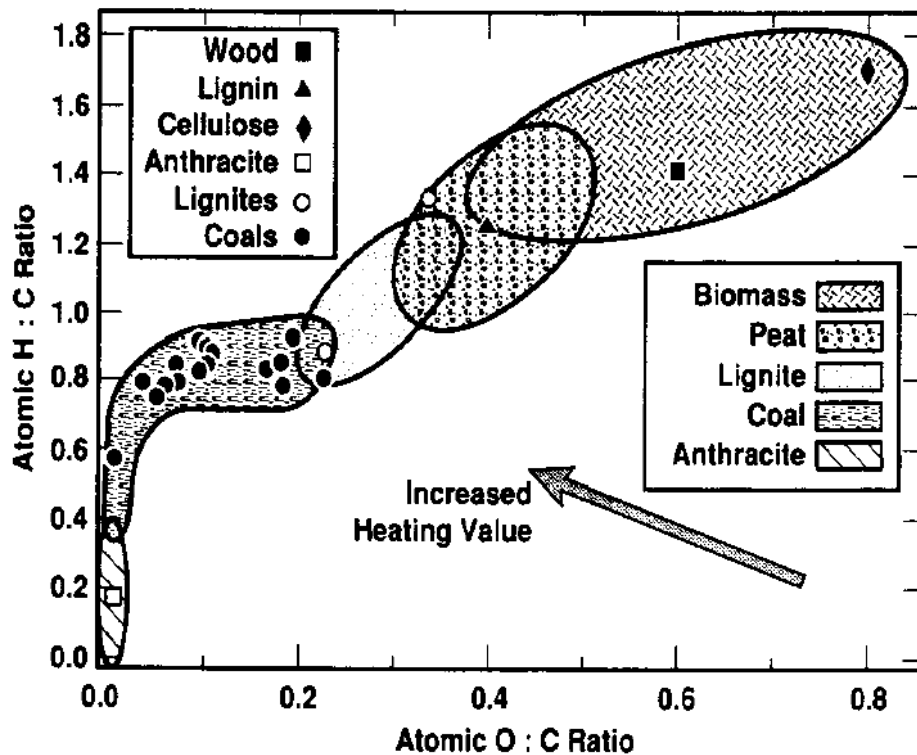
Figure 2.2: Van Krevelen diagram showing the coalification process of biomass to coal from Baxter [1993]

2.2.3 Inorganics

Extensive ongoing research into biomass ash has identified multiple technological and environmental problems during utilisation as well as some advantages. The main complexity is in its composition which is highly variable and dependent on many factors including the genetics and age of the plant, the localised growing conditions, extraneous material from harvesting and processing and changes during storage and pre-treatment (e.g. leaching) [Vassilev et al., 2017]. The main components of biomass are C, O and H, the remaining mass is made of inorganic constituents. Species N, S and Cl have already been discussed in the preceding section however they commonly constitute the next most common elements and the major inorganic elements. Other inorganic elements that are present in biomass include Si, Ca, Mg, K, P, Na, Al, Fe, Mn, Ti, Cu, Zn, Co, Mo, As, Ni, Cr, Pb, Cd, V and Hg [Boström et al., 2012].

Before discussing these individual elements and their role, it is important to first review what forms inorganic elements can be present as. Within biomass there is a heterogeneous mixture of solid structures (crystalline, non-crystalline and amorphous) and fluid (moisture and gases/liquids involved in mineral transportation and biochemical reactions) [Bradl, 2005] [Boström et al., 2012]. Based on this knowledge, Doshi et al. [2009] defined the speciation of inorganics in biomass into three groups: (i) salts that are ionically bound (ii) inorganics that are organically bound to carbonaceous material (iii) minerals that occur naturally and extraneous minerals such as clays and soils usually associated with harvesting. Some inorganic elements such as Ca and P can be present as all three where as others such as Al are only found as one species. The form in which an inorganic element is present as well as its concentration can be used to predict its transformation during combustion, section 2.3.3.

Chemical Fractionation (CF) is an established method for determining the presence of inorganic elements. CF uses a sequential series of leaching experiments to determine the solubility of elements in solvents of increasing strength. The main advantage of CF is that it can effectively distinguish between elements that are highly volatile versus those that remain stable [Baxter et al., 1996]. The main problem with CF is that typically only three leaching solutions are used, which can often become acidified from organic acids within the biomass, meaning that analysis is broad and

lacks the sensitivity for effective composition and bonding determination. Additionally, equilibrium effects are often not considered which can have a large influence on the result. Doshi et al. [2009] recommends the CEN method for waste leaching behaviour as this uses multiple leaching experiments in the fixed pH range between 2-12. This provides enough range to ensure maximum leaching of the main inorganic elements. Although this method is effective at determining the nature of inorganics within biomass, for the analysis in this work in low temperature combustion systems, determination and quantification of inorganics from biomass and biomass ash is sufficient.

The composition of inorganics in biomass is different to in biomass ash. When a fuel combusts, the inorganic elements undergo transformations based on their volatility, reactivity, structural presence and quantity- these ash transformations are discussed more in section 2.3.3 [Boström et al., 2012]. Therefore, it is difficult to universally define whether an element is a major or minor inorganic specie, as is the case in literature [Vassilev et al., 2017] [Boström et al., 2012]. In this work a flexible approach was used, defining each element based on its relative concentration to the total inorganic composition. It is important to note that inorganic elements in biomass ash are present mostly as oxides as well as small amounts of carbonates, sulphates, silicates and phosphates [Williams et al., 2012]. Table 2.1 lists some of the common inorganic elements and describes some of the features.

In addition to the elements in Table 2.1, various trace metals are also present in plants, these include Cu, Zn, Co, Mo, As, Ni, Cr, Pb, Cd, V and Hg. Some of these elements (Cu, Zn, Co, Mo, Ni and V) are micronutrients and are important in enzyme activity, however too much of these elements normally indicates contamination and can be toxic. The other elements are more toxic elements which in small concentrations reduce the plants growth [Bradl, 2005].

Table 2.1: Inorganic elements in biomass

Element	Description
Si	• Both organic and inorganic associations. [a] [b] • Take up as silicic acid and precipitates in mostly amorphous forms. [c] • Some crystalline structures form especially if Al is present to co-precipitate. [a] • It boosts a plants immunity to fungal pathogens and insects. [d] • More enriched in herbaceous biomass. [a]
Ca	• Both organic (e.g. carbohydrates, functional groups of carboxylic acids and oxalates) and inorganic (e.g. carbonates, silicates and hydroxides) associations. [a] [e] • Concentrated in bark and foliage as it co-precipitates with Mn to form oxalates. [d] [e] • An essential plant nutrient, present as Ca^{2+} ions to give cell walls and membranes structure. [d] • Higher concentrations in woody biomass. [a]
K	• Both organic and inorganic associations (similar to Ca). [b] [e] • Present as free K^+ ions to form ionic salts such as KCl and KNO_3. [a] • Essential in plant regulation systems e.g. transportation of nutrients and water, and control of the stomata for intake of CO_2 during photosynthesis. [d] [f] • Commonly applied as fertilisers. [c]
P	• Present as both organic (e.g. phytates and nucleic acid) and inorganic (phosphates, phosphoric acid and water solutions) associations. [a] [e] • Free P ions are essential in the production of ATP which provides energy to cells. [d] • Commonly applied as a fertiliser. [c] • As with Ca, species of P can be as ionic salts, organically bound inorganics and in authigenic minerals. [e]
Mg	• Both organic (e.g. chlorophyll, carbohydrates and phytates) and inorganic (e.g. crystalline structures as silicates and oxyhydroxides and water soluble ions) associations. [a] • Mg is the central atom of chlorophyll molecules and vital for plant survival (organically bound). [d] • Ionic salts include nitrates, phosphates and chlorides. [a]
Na	• Na concentration is very variable in biomass and is heavily influenced by localised conditions. [a] [f] • Na occurs in biomass in the same associations as K, however these can occur from detrital origin as well as authigenic. [a] [g] • Na is not essential in plants but can help metabolise chlorophyll. [d] • Too much Na is toxic to plants. [d] • Typically, only occurs as ionic salts. [e]

Al	• Most Al measured in biomass comes from extraneous sources, mainly soils and clays as aluminosilicates (kaolinite). [a]
	• In acidic soil, moisture in soil causes hydrolysis of stable Al ligand complexes to form the Al^{3+} ion which dominates. [h]
	• This is taken in by the plant through the roots and can form organic (organic acids and lipids) and inorganic (phosphates, sulphates and fluorides) associations. [b]
	• Al is toxic to plants at low concentrations; however, it is rare that free ions dissociate from the stable structures present in the soil. [h]
S	• Both organic and inorganic associations. [a]
	• Inorganic S is mainly present as sulphates. [c]
	• It is mainly taken up through the roots as sulphates (this can occur naturally but also from the addition of fertilisers). Small amounts can be obtained from assimilation of SO_2 in the air. [c]
	• It is essential in chlorophyll, proteins, enzymes and vitamins. [d]
Fe	• Organic (e.g. organo-metallic complexes, phytoferritin and chelates) and inorganic associations (crystalline silicates and oxyhydroxides) associations. The latter mostly come from detrital origin. [a] [e]
	• It is an essential micronutrient in the structure of all living organism's DNA, as well as chelates which transport nutrients and is fundamental in the structure and function of chloroplasts. [d]
Cl	• Cl is a highly mobile element used as a charge balance compensator and regulates osmotic pressure. It is taken up by the roots as Cl^-. [a] [i]
	• A lot of chlorine is taken up by plants from anthropogenic activities. An example of this is Cl from de-icer salts which run off roads and tarmacked areas into agricultural land. [i]
	• Cl is mainly present as Cl^- ions in plants. [i]
Mn	• The concentration of Mn can be highly variable depending on the plant species. Plants which go through an annual cycle with a senescence phase can change colour going a dark orange/brown colour from high concentrations of Mn. [j]
	• It can be in both organic and inorganic associations. [a]
	• Mn is an essential micronutrient in plant cell metabolism in various cells. It is very important in oxygen-evolving complexes in photosynthesis cells. [j]

Table references: [a] Vassilev et al, [2017], [b] Boström et al, [2012], [c] Williams et al. [2012], [d] Marschener [1995] [e] Doshi et al. [2009], [f] Jenkins et al. [1998], [g] Bryers [1996], [h] Baxter et al. [1996], [i] Chen et al. [2010], and [j] Bradl [2005].

2.3 Combustion

Since this thesis is focused on utilising fuels in domestic stoves and small biomass systems and the associated emissions, this section reviews the properties which are generic to combustion but discusses them in relation to such systems.

2.3.1 Stages of Combustion

Defining the stages (phases) of combustion is a challenging task because there is no definitive point when combustion moves from one stage to the next. Even on a particle level in very fast heating rates one side of a particle could still be drying whilst another part has started to release volatiles or turned to char [Trubetskaya et al., 2017] [Mason, 2016]. It is universally accepted that there are four stages of particle combustion: drying/heating up, devolatilisation (pyrolysis), flaming combustion and char burnout. There has been some debate over the presence of more phases, in some cases up to seven, however most of these additional stages are often sub-stages of the four mentioned previously [Mitchell et al., 2016] [Ozgen et al., 2014]. Fig. 2.3 is a very descriptive schematic from Brown [2003] and Jones et al. [2007] based on the combustion of small particles in fast heating rate environments.
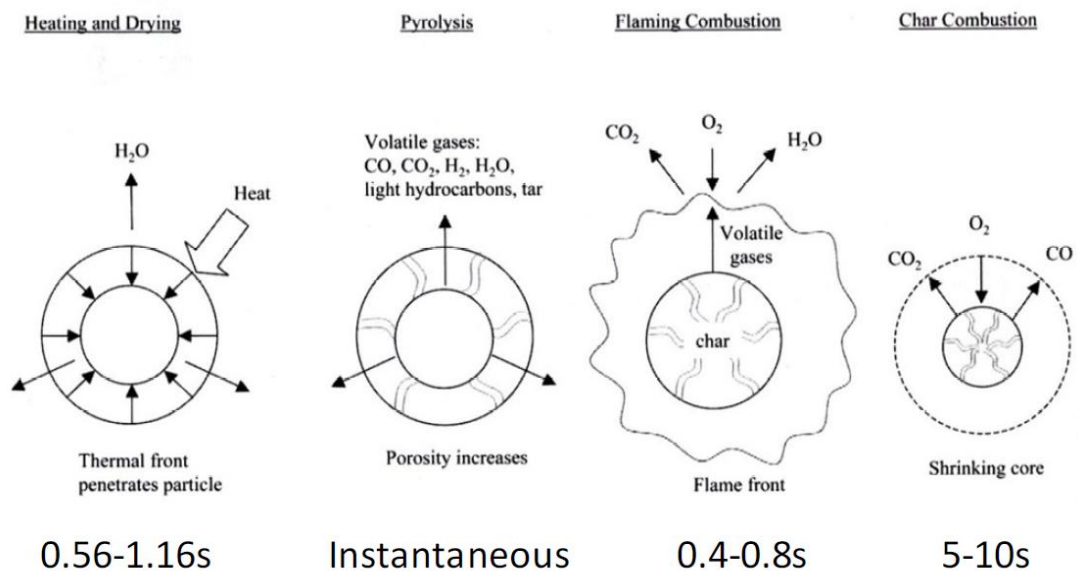
Figure 2.3: Stages of combustion for biomass particles between 0.05-4mm in fast heating rate environments [Brown, 2003] [Jones et al., 2007]

In stove systems, because the particle sizes are usually much bigger, the heating rate is much slower and there is less turbulence, these time periods are much longer. Therefore, when low CV value and high moisture content fuel is combusted in

such systems, sometimes all four stages can occur at the same time. It is for this reason, the stages of combustion are commonly reduced to three principal stages in stoves, ignition, flaming and smouldering, based on the macroscale observation [Ozgen et al., 2014] [Orasche et al., 2012]. This is helpful in the analysis of the conversion, heat release and emissions.

2.3.1.1 Drying and Heating Up

As discussed earlier, the moisture content of biomass is substantially higher than in coal, this can increase the ignition delay time and reduce the thermal output. The high porosity of biomass allows for moisture to be released from biomass particles within seconds in high heating rate environments. Whilst the particle is drying, energy is consumed by the vaporisation of water, this prevents the particle from heating up until it is sufficiently dry [Riaza et al., 2017]. This process occurs between 100-200ºC, however from literature on the storage properties of biomass it is accepted that excess moisture will start to be removed at lower temperatures [Jirjis, 1995].

The moisture in briquettes can be assumed to be uniform as it is a function of the individual particles within the volume of the briquette. Some work has suggested that moisture within the centre of a briquette is higher because of temperature and pressure gradients during briquetting, however these differences are so small, <1%, they can be considered negligible [Tanger et al., 2013] [Singh, 2004]. This means that the main factors affecting the drying and heating up stage of combustion for briquettes are the porosity and density of the briquette.

Wood logs usually have a large moisture gradient, driest at the outer surface, this can be reduced by seasoning and kiln drying before use. The moisture gradient can prevent smooth ignition since the temperature is inconsistent across the log. It also creates at overlap between the drying and devolatilisation stages, reducing the combustion efficiency and increasing the formation of more problematic pollutants [Tanger et al., 2013] [Price-Allison et al., 2019]. Smaller logs to increase the surface area to volume is the most effective method to improve the rate of drying and decrease the ignition delay time.

2.3.1.2 Devolatilisation

As a biomass fuel thermally decomposes a mixture of volatile organic (CO, CH_4, CO_2, and longer chain and aromatic hydrocarbons) and inorganic compounds (K, P, N, S and Cl) elude from the solid particle, this process is called devolatilisation. The temperature, particle size, heating rate, moisture and ash content all influence the rate of devolatilisation. The flow of gases and vapours from the particle surface creates a pressure gradient preventing oxygen and air from reaching the particle surface so oxidation reactions do not occur close to the particle during devolatilisation. Pyrolysis is the same process but in completely inert environments [Lu et al., 2008].

As discussed in section 1.2.2, biomass is made up of cellulose, hemicellulose and lignin. The former two are bonded by C-O bonds whilst lignin has lots of linkages with O functional groups and C in the aromatic rings. During devolatilisation, many of these bonds and linkages break and rearrange forming carbon rich gas molecules which escape through pores or by a build-up of partial pressure and forcing their way out (more common in coal). At the same time more stable fragments rearrange to form new stronger interactions with neighbouring structures, these stronger interactions build up to form char particles. Hence, there is competition between solid decomposition and char forming reactions which are dependent on the activation energy and reaction kinetics of all the competing processes. For biomass the majority of the particle mass is lost during devolatilisation [Glassman, Yetter and Glumac, 2015].

2.3.1.3 Flaming Combustion

Flaming combustion is the rapid oxidation of volatile species after they have been released from the fuel particle. Its name comes from the luminous flame that is produced from the energy released during the reactions. There is a significant amount of overlap between devolatilisation and flaming combustion, mainly because of how fast the volatiles oxidise after release. Therefore, it is often easier to use the identification of a flame as the start of devolatilisation (ignition) in experimental methodology [Riaza et al., 2017].

During flaming combustion, the conversion of carbonaceous species is mostly by complete combustion, since the temperature, turbulence and thermodynamics favour this reaction mechanism. Thus, the main products of flaming combustion are

CO_2 and H_2O. However, there is some incomplete combustion resulting in emissions of CO, CH_4, unburnt hydrocarbons, PAHs and PM. Emissions of NO, SO_2 and HCl are also at their greatest during flaming combustion because of their volatility when bound to organic structures or present as salts, see Table 2.1 [Mitchell et al., 2016] [Williams et al., 2012].

In stove systems, because the system is closed and the fuel bed is fixed, as is the case with particle burning experiments, flaming combustion peaks (and burning rate) after ignition and then transitions to more char combustion as time progresses. This is also accompanied by a change in the emissions, a decrease in CO_2 but an increase in CO. The main factors which can influence this process are the moisture content, the volatile content, the fuel geometry, the physical properties of the fuel and the composition of the ash [Ozgen et al., 2014] [Ndiema, Mpendazoe and Williams, 1998].

2.3.1.4 Smouldering Combustion (Char Burnout)

Char combustion is the slowest of the combustion stages because it is a heterogeneous reaction on the char particle surface. This requires oxidising gases to pass through the particle boundary layer, adsorb onto the particle surface, react, desorb from the particle and diffuse into the bulk gas phase. The main products of char combustion are CO_2 and CO, Eq. 2.3. On a particle level, if the particle is thermally thin, char combustion is mostly a discrete phase but can have a small overlap with flaming combustion. Particles with a larger diameter, and a greater distance from the particle surface to the core, undergo flaming and char combustion simultaneously. This is because heat has to transfer from the outer surface to the centre which results in the outer surface turning to char whilst the centre devolatilises. This is an important phenomenon since it can influence the emissions [Williams et al., 2012].

As mentioned previously biomass particles are naturally more porous, this means the oxidising gases can flow through the char structure. Therefore, if the char on the surface reacts first then the particle starts to shrink, conversely if reactions happen at the centre first the particle becomes more porous and depending on the partial pressure of the combustion gases can either look the same size or swell slightly [Mason, 2016] [Riaza et al., 2017].

During char combustion multiple inorganic ash transformations occur such as vaporisation (K, Na and P), surface migration, coalescence and metal incorporation into silicate (glass) structures. Many of these transformations rely on the temperature as they require phase transformations [Wornat et al., 1995]. The main factors which influence char combustion are the char structure, surface area, particle size, pore structure, composition of the ash and the active site concentration [Dooley, 2017].

$$Char + \frac{1}{\varphi}O_2 \rightarrow \left(2 - \frac{2}{\varphi}\right)CO + \left(\frac{2}{\varphi} - 1\right)CO_2 \quad (2.3)$$
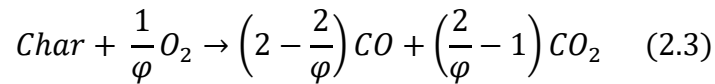
2.3.2 Pollutants

There are multiple pollutants formed during biomass combustion. They all originate from the fuel however combustion temperatures, moisture, stoichiometry and other elements or compounds can influence the formation mechanisms.

2.3.2.1 Carbon Monoxide

Carbon Monoxide (CO) is a highly toxic gas with a large global warming impact. It is mainly formed from incomplete combustion of volatile species after devolatilisation and from heterogeneous char combustion reactions, Eq. 2.3. During devolatilisation volatile products are released because of the depolymerisation of cellulose (300-400°C), hemicellulose (250-350°C) and lignin (200-600°C) [Srifa et al., 2019]. The pyrolytic products are a mixture of gaseous volatiles and tars. Depending on the factors mentioned earlier in this section, these products can undergo cracking, gasification and oxidation reactions forming a variety of gaseous organic products, CO is one of the major products of these reactions [Khasraw et al., 2021].

In char combustion, CO is primarily formed by the oxidation of carbon as shown in Eq. 2.4. The CO produced can then be converted to CO_2 by secondary oxidation, Eq. 2.5. This latter reaction is much slower and requires longer residence times and higher temperatures. CO can be produced from CO_2 by the Boudouard reaction, Eq.2.6, this is a redox reaction caused by low O_2 concentrations within the fuel bed [Dell'Antonia et al., 2012].

$$C + \frac{1}{2}O_2 \rightarrow CO \quad (2.4)$$

$$CO + \frac{1}{2}O_2 \rightarrow CO_2 \quad (2.5)$$

$$CO_2 + C \rightarrow 2CO \quad (2.6)$$
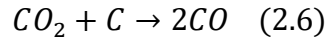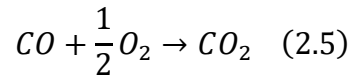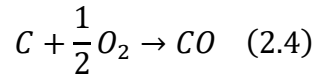
In stove systems CO emissions are highest during smouldering combustion. Often, they are used to identify the transition from flaming to smouldering combustion [Mitchell et al., 2016]. During smouldering combustion low temperatures, poor mixing and short residence times prevent secondary reactions, such as the oxidation of CO to CO_2. High moisture fuels prevent these secondary reactions because of the lower temperatures from vaporised water as well as fuel-rich combustion from poor air-flow [Roy and Corscadden, 2012].

2.3.2.2 Methane

The origin of Methane (CH_4) emissions is a disputed subject. After the volatiles are released from biomass, the lighter hydrocarbons (both gases and tars) are unstable and further decomposition (decarboxylation of acids and aldehydes) or gasification (hydrogenation of CO) can result in the production of methane [Ranzi et al., 2008] [Ndiema, Mpendazoe and Williams, 1997]. Therefore, it is difficult to determine if CH_4 is produced directly from devolatilisation of lignocellulose or if it is the product of secondary reactions. In stove systems methane emissions can peak because of fuel-rich combustion (fuel overloading) or low reaction temperatures [Ranzi et al., 2008] [Ozgen and Caserini, 2018].

2.3.2.3 Unburnt Hydrocarbons

Unburnt hydrocarbons are simply the products of devolatilisation that escape by fuel-rich, moist or low temperature pockets in the combustion zone. In stove systems high amounts of smouldering combustion and low mixing results in higher concentrations of these species being emitted to the environment. Some of these unburnt hydrocarbons react in hotter zones to form soot through chemical and physical reactions (condensation and coalescence) [Williams et al., 2012] [Ranzi et al., 2008]. These combined with inorganic fly ash and char fragments make up particulate matter discussed latter in section 2.3.2.6.

2.3.2.4 NOx

Oxides of nitrogen (NOx) primarily consists of nitric oxide (NO) and nitrogen dioxide (NO_2). They are formed by three mechanisms:

- Prompt NOx- N_2 in the air reacts with hydrocarbon radicals to form NCN at high temperatures (>1300°C) and a fuel-rich environment. NCN is then oxidised to form NO [Williams et al., 2012].

- Thermal NOx- Produced at above 1500°C, usually in the flame, from the reaction of oxygen radicals with molecular nitrogen in the air. The extended Zeldovich mechanism, Eq. 2.7-2.9, explains the mechanism for the formation of thermal NOx, the main reaction route is dependent on the temperature and percentage of excess air.

$$O + N_2 \leftrightarrow N + NO \quad (2.7)$$

$$N + O_2 \leftrightarrow NO + O \quad (2.8)$$

$$N + OH \leftrightarrow NO + H \quad (2.9)$$
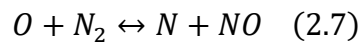
- Fuel NOx- This is the oxidation of N bound in the fuel.

During combustion the majority of emissions are from fuel NOx with a variable contribution of thermal NOx depending on the combustion system [Riaza et al., 2019]. The contribution from prompt NOx is unclear since previous results in literature are inconsistent, however the general conclusion is that the contribution is small [Houshfar et al., 2012]. In stove systems NOx emissions are entirely from fuel NOx because of the low combustion temperatures and short residence times. Additionally, the majority of emissions are in the form of NO (rather than NO_2) because of the high amount of excess air [Dell'Antonia et al., 2012].

Formation of fuel NOx has been extensively described by Williams et al. [2012], Fig. 2.4. N in biomass is present in many forms, mostly as proteins as a mixture of linear and aromatic molecules. During combustion nitrogen is partitioned between volatile products (as NH_3 and HCN), tars and char, this is dependent on the environment, temperature and heating rate. For biomass, most of the nitrogen is released as volatiles [Riaza et al., 2019].
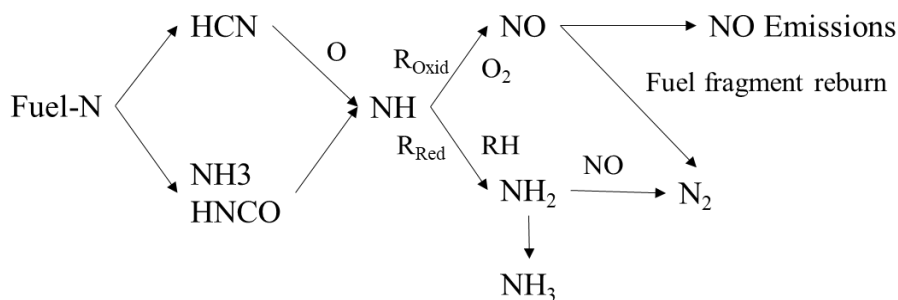
Figure 2.4: Mechanisms for NOx formation from fuel N [Williams et al., 2012]

During devolatilisation, decomposition of linear molecules tends to form NH_3 and HNCO whilst aromatic molecules decompose to HCN [Ren et al., 2011]. However, this is also dependent on the temperature, particle size and presence of minerals (especially K). These precursors react through multiple mechanisms to form NOx species depending on the stoichiometry [Williams et al., 2012].

Char N in biomass is more complex and less understood, however it is believed to be similar to char N in coal. Although some research has suggested that HCN precursors are formed during char combustion, direct oxidation of N at active sites to NO is the more widely accepted mechanism for biomass [Molina et al., 2009] [Backreedy et al., 2003]. NO formed in the pores of the char can be reduced to N_2 by carbon atoms because of the long residence time to diffuse from the char structure [Wang et al., 2016]. This process is suspected to be catalysed by the presence of minerals (mainly Na) [Wang et al., 2016].

2.3.2.5 Sulphur Dioxide

Sulphur Dioxide (SO_2) is formed from the oxidation of S. S is present in biomass in both organic, such as cysteine and methionine, and inorganic forms [Knudsen et al., 2004]. Fig. 2.5 from Johansen et al. [2011] shows the mechanisms for organic and inorganic S release from biomass. During devolatilisation, high temperatures increase the S released because of the reduced mass of char produced. Inorganic elements Ca and K have a high affinity for S at low temperatures (<800°C) and efficiently form metal sulphates which retain the S in the ash. If the Si concentration is high, as the temperature increases (>800°C), Ca and K have a higher affinity to form silicates which results in the S being released from the ash. Char destruction can also cause S to be released however this S has not reacted to form metal sulphates [Johansen et al., 2011] [Han, Gao and Qui, 2019]. Some of the SO_2

can react with KCl in slags formed in superheater systems creating a highly corrosive eutectic which releases Cl_2 (g) or HCl (g) [Van Lith et al., 2009]. In stove systems, low temperatures and inconsistent combustion across the fuel bed means that only a small percentage of the S in the fuel is converted [Roy and Corscadden, 2012].
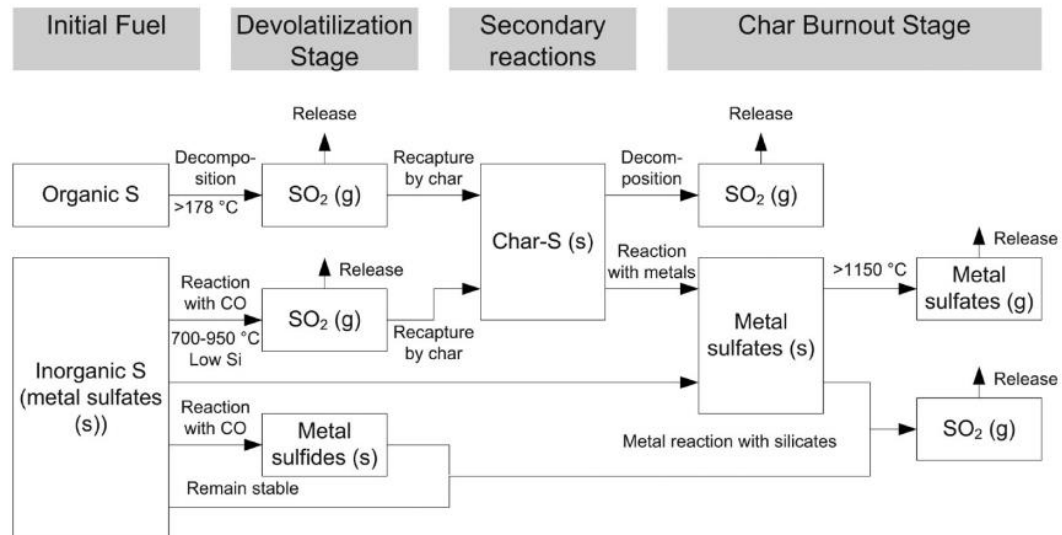
Figure 2.5: Formation routes for SO₂ in biomass combustion [Johansen et al., 2011]

2.3.2.6 Particulate Matter

Particulate Matter (PM) is the solid matter that is entrained in the flue gas. It can consist of soot, tar, char fragments, fly ash and condensed volatile heavy metals. Soot is formed by a series of complex reactions from unburnt hydrocarbons starting in the flame. The species and nature of soot formed is dependent on the flight path from the combustion zone to being emitted into the environment and its continued path in the atmosphere. The two most common soot forming mechanisms are the HACA (hydrogen abstraction, C_2H_2 addition) and CPD (cyclopentadiene) routes [Fitzpatrick et al., 2008]. In the former, light hydrocarbons from the pyrolysis of cellulose are not combusted and through pyrosynthesis reactions form acetylene (C_2H_2) molecules, these molecules form benzene which grows by successive additions of C_2H_2 into polycyclic aromatic hydrocarbons (PAHs). The CPD route originates from the pyrolysis of lignin which produces larger aromatic molecules from lignin monomers, in particular phenols. These lignin monomers undergo cracking and decomposition reactions to form cyclopentadiene (CPD) and CO [Fitzpatrick et al., 2008]. CPD is highly reactive, much more so than its parent phenol, so it quickly reacts

to form one ring or two ring compounds such as benzene, toluene, indene or naphthalene. These species then can grow by either the HACA method or addition of other hydrocarbon radicals [Fitzpatrick et al., 2008]. In biomass combustion because the oxygen content of the fuel is so much higher, oxygenated PAHs can also form [Fitzpatrick et al., 2007] [Williams et al., 2012]. Confined PAH growth results in condensation and agglomeration of fine spherical carbon-rich particles- i.e. soot (black carbon).

The soot species formed from the combustion zone can have adsorbed VOCs forming hydrophilic surfaces which are very effective sites for condensation of organic compounds such as tars. As the tar condenses onto the particle surface it can either coalesce and form an even sticky coating around the particle surface or agglomerate where it sticks to a point on the soot particle. These processes depend on the viscosity of the condensing tar which is a function of the temperature when it condenses and the length/interactions making up the tar [Lea-Langton et al., 2015] [Jones et al., 2018]. This carbonaceous PM from stove combustion consists of both black and organic carbon.

The biochar produced after devolatilisation of biomass has a very porous structure. Char is very brittle and with the porous nature of biochar it can fracture easily. These fragments can be entrained into the flue gas and if the path is through fuel-rich pockets in the combustion system they can avoid being combusted and instead emitted as char fragments. Depending on the temperature and flight path these fragments can agglomerate with sticky tar and condensed inorganic surfaces increasing the particle size [Fine, Cass and Simoneit, 2002] [Freeman and Cattell, 1990] [Fitzpatrick et al., 2008] [Williams et al., 2012].

Inorganic contributions to particulate matter are highly variable depending on the combustion system. Inorganic elements (particularly K, S, Cl, Si, Na, Al, Ca and P) can nucleate new particles or aid in the growth of existing particles. Heavy metals species such as Zn, that are volatile, can also be significant contributors to PM. These routes are discussed in more detail in section 2.3.3 [Sippula et al., 2009].

Particulate matter from stove combustion is an important area of research since small combustion devices are less likely to have abatement technology and the majority of PM is sub-micron size. Poor mixing and lack of control (heating rate, air

flow and temperature) in stoves means that PM emissions are much higher than in larger systems. Additionally, fuel properties such as moisture, mineral content, particle size and the composition of volatile products can increase the PM emissions [Williams et al., 2012] [Mitchell et al., 2016].

2.3.3 Entrained Metal Aerosol Emissions

Metals in the ash of biomass can be entrained into the flue gas by vaporisation and condensation or through convective turbulence of particles in the ash. The former is the more prominent method for aerosol formation where volatile species are vaporised during flaming combustion and carried out by the hot flue gas [Williams et al., 2012]. As the flue gas cools it becomes supersaturated and, depending on the volatility of the species, aerosols form from homogeneous nucleation and heterogeneous condensation [Doshi et al., 2009]. These processes form very fine particles which can grow from surface reactions, agglomeration and coagulation [Sippula et al., 2009].

Coarser inorganic particles can form from reactions in the bottom ash. Species in the bottom ash are present in varying amounts and as various complexes depending on the composition in the original biomass and what has been removed in the early stages of combustion. The mixture of these compounds forms a unique structure where the phase transformation point is at a lower temperature than any of the phase transition points of the individual compounds. This means stable elements, such as silicon and calcium, can be vaporised at lower temperatures [Boström et al., 2012] [Roberts et al., 2019] [Doshi et al., 2019].

Although fly ash is typically used to described large ash particles which are entrained into the flue gases, more common in large scale utilities, in this work the term is used to described inorganic particulates.

The volatility of inorganic elements is one of the most important factors in determining ash transformation reactions. At low temperatures K, Cl, S, Na and P all vaporise, they also constitute a large proportion of the inorganic composition of biomass and thus the fly ash. Finney et al. [2018] reported that K aerosols were on average 6.5 times higher from biomass combustion than coal. Mason [2016] combusted single particles of biomass and coal and monitored the potassium release throughout, the results showed that the higher volatile content of biomass caused a

spike in the K released during devotalisation. A smaller peak is observed during char combustion but the intensity is much lower.

The Cl in biomass is very soluble and entirely removed in water leaching, this means it is very mobile. Cl and K are particularly reactive and are usually the most dominant alkali species in the PM formed during stove combustion because of the lower combustion temperatures [Boman et al., 2004] [Jöller, Brunner and Obernberger, 2005]. Cl also reacts with more stable metals reducing the temperature at which they condense such as Cr, Mn, Ni, Cu, Pb and Zn [Zając, Szyszlak-Bargłowicz and Szczepanik, 2019]. During combustion organically bound S reacts to form SO_2 at low temperatures, this SO_2 plays an important role thermodynamically in the mobility of metal species. Jiménez, Pérez and Ballester [2008] show that as the SO_2 concentration increases, Mn and Fe are fixed more into the bottom ash however later work by Zając, Szyszlak-Bargłowicz and Szczepanik [2019] show that this correlation only applies to Fe.
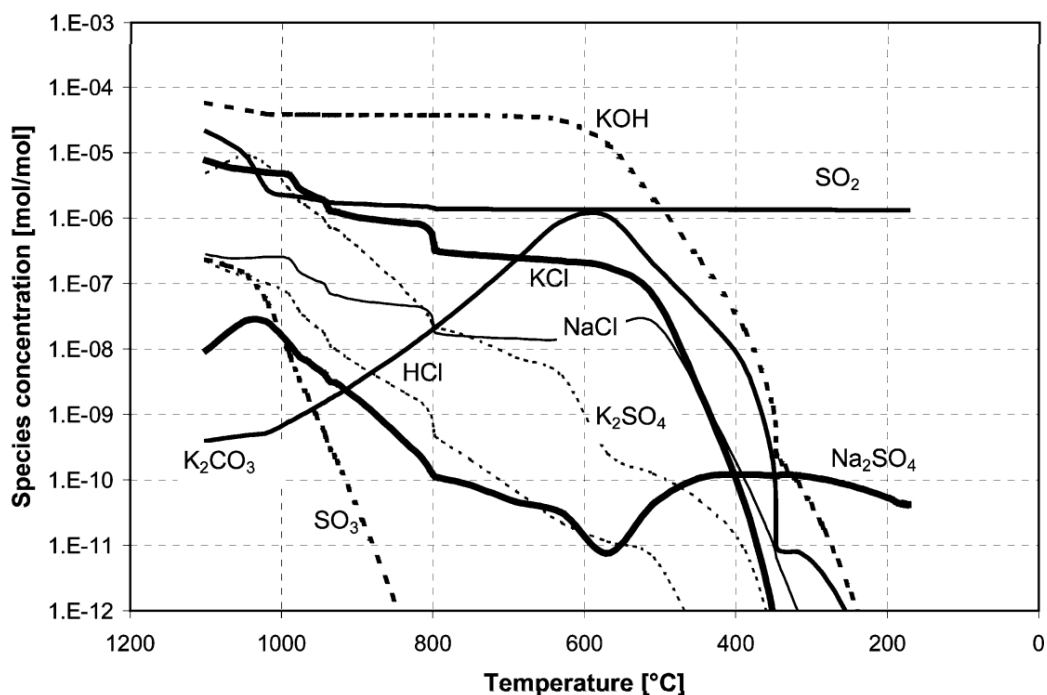
Figure 2.6: Gas phase equilibrium of the most common fly ash forming species [Jöller, Brunner and Oberberger, 2005].

Temperature has been shown to have the greatest influence on the formation of alkali salts during combustion. Fig. 2.6 from Jöller, Brunner and Obernberger [2005] shows the equilibrium gas phase specie formation of the most common inorganic aerosols. Between 750-900°C chlorides are sulphated and condense; this

means fly ash is dominated by K_2SO_4. At lower temperatures chlorides are largely present (KCl and NaCl) however depending on the oxygen content the formation of carbonates and oxides are also prevalent.
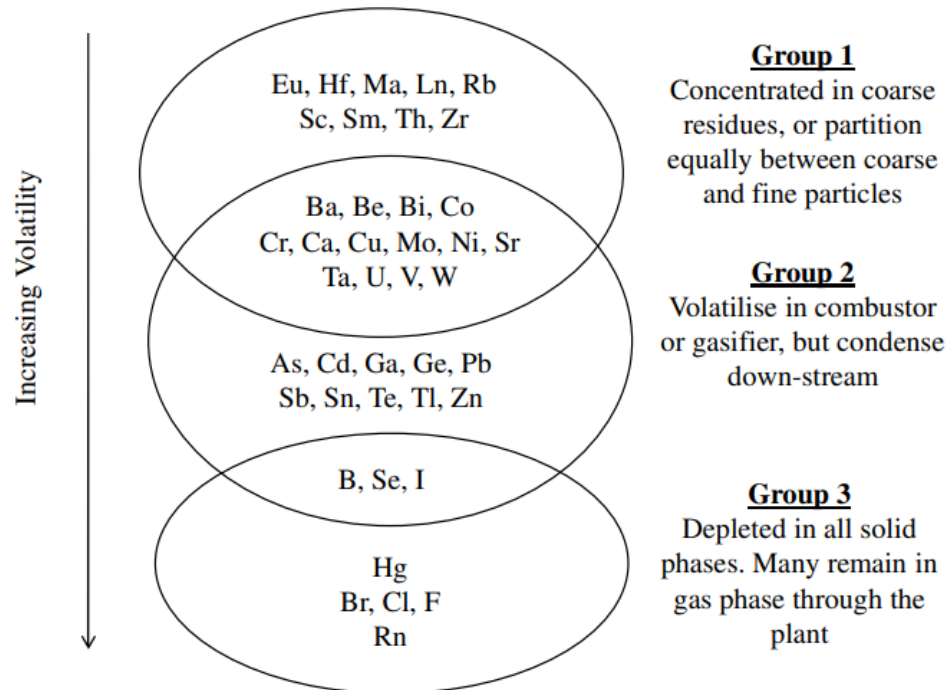
Figure 2.7: Relative volatility of heavy metals [Gudka et al., 2016]

Trace elements such as heavy metals are a current area of high interest since they can be very volatile and, without removal technology, their emission is a serious threat to public health. Fig. 2.7 from Gudka et al. [2016] shows the relative volatility of heavy metals. Zn is a prominent heavy metal in most biomass in much higher concentrations than other heavy metals. There is a lot of literature on the role of Zn in PM formation as it is a fairly mobile species. Torvela et al. [2014] used Transmittance Electron Microscopy (TEM) imaging coupled with Energy Dispersive X-ray analysis (EDX) to determine the size and composition of ultrafine PM collected from a 40kW boiler burning wood chips from different types of combustion (efficient, intermediate and smouldering). The conclusion from this analysis was that ZnO condensed first from the gas phase to form a nucleus that other inorganic species could condense onto. Earlier work from Boman et al. [2004] also concluded that Zn played a major role in the formation of fly ash in PM by analysing (SEM-EDX) PM collected on filters using gravimetric impactors from a 3kW boiler fired with various biomass pellets. Wiinikka, Grönberg and Boman [2013] also came to the same conclusion from sampled PM in

wood stoves. In more recent work there has been some contention over the nature of Zn in biomass and whether it is all in a mobile state based on its comparison with coal. Finney et al. [2018] using online measurements (ICP-OES) at a pilot scale pulverised fuel combustion plant analysed heavy metals produced from firing coal and biomass. Although the concentration of Zn in the biomass was considerably higher the emissions were the same. However, it is accepted that increases in temperature increase the vaporisation of Zn which could explain the measured differences [Zając, Szyszlak-Bargłowicz and Szczepanik, 2019] [Jiménez, Pérez and Ballester, 2008].

2.3.3.1 Slagging and Fouling

In large utility systems slagging and fouling from ash transformation reactions is a major problem as it reduces power station efficiency and in extreme cases can cause shutdown. To investigate the potential of a fuel to cause slagging and fouling there are various methods including ash fusion tests (AFT), slagging and fouling indices and sinter strength tests. The AFT is the British Standard method (BS EN ISO 21404:2020) which determines four characteristic temperatures, these are discussed more in section 3.4.6, of a cylindrical test piece made from ash which is heated at a constant rate. AFT are important because they determine the temperatures at which ash deposits transform into slags and therefore the suitability of fuels to various applications. The main disadvantage with AFT is that analysis of the results lacks accuracy and reproducibility because it is determined by the human eye. Advancements have been made to try and improve the reproducibility by using computational software models to monitor changes [Tambe et al., 2018]. However, there are still issues with these methods especially when applied to biomass because of swelling effects.

Slagging and fouling indices use chemical composition data to determine a numerical value which describes the probability of slagging occurring. Various models have been proposed including the base to acid ratio ($R_{b/a}$), the alkali index (AI) and the slagging viscosity index (SVI), Eq. 2.10-2.12. Slagging and fouling indices are useful as they can be tailored to assess certain parameters of the slagging and fouling process. Their disadvantage is they are often an oversimplification and don't consider the impacts of temperature, heating rate or other inorganic constituents which may also influence the formation of slags [Roberts et al., 2019].

$$R_{b/a} = \frac{(Fe_2O_3 + CaO + K_2O + Na_2O)}{(SiO_2 + TiO_2 + Al_2O_3 + P_2O_5)} \quad (2.10)$$

$$AI = \frac{x_f^a\left(x_a^{K_2O} + x_a^{Na_2O}\right)}{HHV} \quad (2.11)$$

$$SVI = 100 \times \left[\frac{SiO_2}{SiO_2 + Fe_2O_3 + CaO + MgO}\right] \quad (2.12)$$

For the base to acid ratio, Eq. 2.10, a value of <0.5 means the fuel has a low slagging probability, >1.0 means a high slagging probability and between the two there is a moderate probability. The $R_{b/a}$ is a simple model which considers the interactions of acidic and basic compounds. This model is based on the principle that alkali species are more volatile and therefore their increased concentration will increase the slagging propensity unless there are acidic species to react with which increases the temperature at which these species melt.

In Eq. 2.11, x is the mass fraction, a is ash and f is fuel. The AI represents the quantity of alkali oxide per unit energy of fuel (kg alkali GJ^{-1}). The upper threshold is 0.34 kg alkali GJ^{-1} (high probability of slagging) and the lower threshold is 0.17 kg alkali GJ^{-1} (low probabilty of slagging).

The slag viscosity index (Eq. 2.12) represents the percentage silica in the sum of the basic components in the ash excluding the alkali species. Although this is not directly a measurement of the viscosity of a slag, past work has shown that eutectic compounds low in silica form very hard ceramic slags- this is because the flow properties of low silica compounds are more isotropic [Garcia-Maraver, 2017] [Park and Min, 2016] [Pronobis, 2005]. The resultant number of the slag viscosity index is an indication of the difficulty to remove these compounds. Values greater than 72 have a low slagging propensity whilst values less than 65 have a high slagging propensity.

More recently the focus has shifted to not only understand the propensity of slagging and fouling but also to try and understand the physical properties of the slags formed. This is useful to power stations as it allows them to plan maintenance and also understand how effective some of their technology solutions are at removing slags such as soot blowers. For these reasons sinter strength tests are increasing in popularity. These tests form cylindrical pellets of ash which are gradually heated to

simulate the formation of a slag deposit. To determine the sinter strength, the pellets are compressed at a gradually increasing pressure. The point at which they fracture determines the strength of the slags formed [Roberts et al., 2019].

2.4 Stove Combustion

Current literature on stove combustion is sparse and further research is needed to understand how such systems operate and the relation between operation and emissions. This includes analysis of various fuels on such devices and the influence of fuel properties, both chemical and physical, on emissions. This section explores the current literature on this subject.

2.4.1 Stove Combustion Tests

Stove combustion tests are difficult to perform. This is mainly because of the large number of variables that have to be controlled in order to produce a reproducible result. For the results to be valid methods have to use various measurement techniques and measure multiple parameters including burning rate, temperature, flue gas flow rate and visual assessments of the combustion phase.

There is no uniform method for performing combustion tests and there is a large disparity between international standard tests and tests performed in research. The British Standard (BS EN 13240/PD 6434) sets the stove up within a trihedron from which the flue gas is sent up a stack and emissions can be measured by sampling directly through a suction pyrometer probe. The method uses a single batch of fuel that is loaded into the stove, ignited and then left until the fuel burns out, during this time the stove door is not opened and the fuel bed is left untouched. Emissions are measured over the time period when the stove is at its nominal thermal output. Repeat experiments are used to show the reproducibility of the results. The main advantage of this method is all the variables are controlled except for the fuel and the type of stove which means results can be reliably compared and are easier to reproduce. However, this assessment of stove performance and emissions is unrealistic, the main issue being it doesn't account for the potential operational differences or the transient periods such as heating up or char burnout, assessment is at a steady state.

An alternative method is the European-German Standard (DIN EN 13240), which uses the same experiment set-up however multiple fuel batches (at stove nominal heat output) can be used in the assessment of thermal performance and

emissions. This is defined by the running time which must exceed a certain length of time for the test to be valid. However, by again only considering the emissions at the nominal thermal output, the method still does not account for the transient phases.

Most commonly in current research hybrid methods are used. Ozgen et al. [2014] developed one of the first methods where a 'real-life' combustion cycle is defined. This method using a start-up batch of kindling which after 20 minutes is loaded with a nominal fuel load. After an hour a second batch is added and a third batch is loaded after another subsequent hour. The analysis is conducted over 45 minutes after the stove has stabilised in temperature from each fuel load. This method assesses more of the combustion time period and does consider more of the transient phases however it fails to assess the periods of low turbulence and non-homogeneous temperature variations when reloading.

Li et al. [2020] used a variation of this method by continually monitoring emissions for a 24-hour period. This included any reloading periods and accounts for all the transient effects. This method similar to the method by Ozgen et al. [2014] dilutes the flue gas sample before analysis. Klauser et al. [2018] demonstrated that the method of analysis can have a big influence on the results and therefore compared to the methods described in standards it is very difficult to compare emission factors from different experiments and from different researchers. It is therefore imperative that a method is developed around the objectives of the experiment.

2.4.2 Emissions from Stove Combustion

Although there has been some discussion related to this area in section 2.3.2, this section develops the areas of research interest and the conclusions that have been developed.

Assessment of the variables which influence emissions is a growing area of interest. Roy and Corscadden [2012] showed that thermal efficiency increased when using briquettes and this resulted in lower amounts of incomplete combustion. Peterson et al. [2011] also observed the same result when comparing pellets and logs. The main reason for the improved combustion performance for briquettes and logs is the increased surface area to volume ratio. However, this effect, particularly for the briquette and log comparison, is dependent on the rate at which the briquette disintegrates. This is an area that has not been addressed in current literature.

59

Following this point the rate at which a briquette disintegrates is influenced by the use of binders which can also influence the emissions. This was a result tested by Potip and Wongwuttanasatian [2018] for a crude glycerol binder and showed that the increased addition of the binder increased the rate of combustion and the temperature. A review by Olujbade, Ojo and Mohammed [2019] also states that the majority of binders increase the combustion rate and thus has an impact on emissions by increasing the amount of complete combustion. However, this review does suggest that the selection of binder has to be carefully considered as minerals in the binder can negatively influence the particulate emissions by increasing the volatility of metals.

Although other physical factors have a strong influence on the combustion performance such as air flow, fuel chemical factors are an area of high interest. Mitchell et al. [2016] demonstrated that most of the emissions are related to chemical fuel properties. These correlations include fuel-N to NOx, S to SO_2, volatiles, K and C/O to PM [Roy and Corscadden, 2012] [Orasche et al., 2012] [Ozgen and Caserini, 2014]. Previous work has demonstrated certain aspects of these correlations however a total assessment and comparison of these correlations has not been explored. Additionally, research into other correlations such as those related to CH_4, metals and soot are still sparse [Atiku et al., 2017] [Finney et al., 2018].

2.5 Pre-Treatment

Historically pre-treatment of biomass was focused on optimisation of chemical and physical properties and energy density to enhance the performance and improve the feasibility of using biofuels over fossil alternatives. However, because of more stringent regulations and pressing concerns over the state of the environment, pre-treatment has evolved to focus on producing the cleanest fuels, in terms of emissions, and increasing the diversity of fuels available.

2.5.1 Torrefaction

When a fuel is torrefied the mass loss from removal of moisture and low CV hydrocarbons, from decomposition of hemicellulose and cellulose, is greater than the energy lost from these species. Dhaundiyal et al. [2021] estimates the mass loss is approximately 30% and the energy loss is 10%, however, in reality, these losses are a function of the torrefaction process, the severity of torrefaction, the type of biomass and the ash composition, in particular K [Chen et al., 2021].

During torrefaction, depending on the severity, volatile products from low temperature pyrolysis are released, this reduces the reactivity of torrefied fuels. During combustion this shortens the devolatilisation period and increases the mass of char produced. The char produced is enriched in C but depleted in O, additionally it is less porous and has a reduced surface area [Li et al., 2015] [Lu et al., 2008] [Chen et al., 2017]. The conversion time for char combustion is dependent on the mass of char however the reactivity of char produced is disputed. Lu et al. [2017] observed no effect from torrefaction on the reactivity of wood char particles however, Chen et al. [2017] saw a reduction in the reactivity during gasification of straw char. Reduced reactivity may be observed because of reduced porosity or carbonisation both of which reduce the reaction surface area and thus the rate of external heat and mass transfer [Lu et al., 2016].

The impact of torrefaction on the formation of soot and PM is an area of high interest. Torrefaction can impact on the formation of soot by changing the volatile species released during devolatilisation and changing the partitioning of key ash species. Results from Akinrinola [2014] and Atiku et al. [2016] demonstrated that torrefaction lowers the amounts of key soot forming species during devolatilisation, such as eugenol and vanillin (which increase soot formation as they can form soot by both the HACA and CPD mechanisms) [Fitzpatrick et al., 2008]. Additionally, at lower temperatures, when combustion is less efficient, torrefied fuels produce less naphthalene and anthracene which are soot precursors [Atiku et al., 2016] [Fitzpatrick et al., 2008]. This was observed in stove combustion studies by Mitchell et al. [2016] where the PM emissions during flaming combustion were substantially lower for torrefied briquettes.

Inorganic elements discussed in section 2.3.3 are very influential on the formation of fly ash which is present in PM. During torrefaction the ash content is concentrated [Akinrinola, 2014] however the constituent ash species can vary depending on the peak temperature. At low temperature pyrolysis Cl and S can be vaporised [Williams et al., 2012] [Johansen et al., 2011] and K can be bound into carbon structures [Mason, 2014] [Lu et al., 2016]. This reduces the release of volatile inorganic species and increases the partition of some species into the char and ash [Atiku et al., 2016].

Nitrogen partitioning is also a consideration in torrefied fuels. Akinrinola [2014] found that N is lost monatomically with C, however the overall effect is that N is concentrated in torrefied biomass. Trubetskaya et al. [2019] found that the increased N content in torrefied olive partitioned more into the char during combustion and was released forming N_2 instead of NO. Conversely Meng et al. [2020] saw the opposite effect when combusting raw and torrefied distillery grains and rice husks, emissions of NO increased. Further work is needed to understand these partitioning properties and the impacts torrefaction can have.

2.5.2 Washing

Biomass rich in carbon but low in moisture and ash is desirable in combustion, however there is not a surplus in availability of high-quality biomass and social limitations prevent the overuse of agricultural land to grow energy crops [Harvey and Pilgrim, 2011]. Therefore, a more diverse source of biomass that is high in alkali metals, S and heavy metals must be considered to transition away from fossil fuels. Washing is one of two methods, hydrothermal processing being the other, that can reduce the ash content, removing undesirable inorganic species, and improve the conversion of biomass.

Inorganic species in biomass vary in mobility/solubility, as discussed in sections 2.2.3 and 2.3.3. Chemical fractionation experiments, section 2.2.3, have shown that water washing will only remove certain elements if they are present in forms that will leach into water. Carillo, Staggenborg and Pineda [2014] showed that 50-90% of alkali metals in biomass are in a water-soluble form. Runge, Wipperfurth and Zhang [2013] observed similar removal efficiencies (60-75%) but also a 25% increase in the energy density when using hot water washing of poplar wood, corn stover, switchgrass and miscanthus. Deng, Zhang and Che [2013] measured a removal efficiency of over 80% for K, S and Cl when water washing rice straw, wheat straw and cotton stalk agricultural residues which was consistent with results using the same method and fuels as Jenkins, Bakker and Wei [1996]. Therefore, there is good consistency in previous research that water washing can remove the most problematic inorganic species.

More recent work has focused on the factors that influence the removal efficiency and rate of removal [Abelha et al., 2019] [Schmidt et al., 2020] [Bandara,

Gamage and Gunarathne, 2020]. It was concluded that particle size has the greatest influence on the removal efficiency whilst the water temperature improves the water capacity. Abelha et al. [2020] combined washing and torrefaction, based on a comparison with hydrothermal carbonisation, to both reduce the ash but also to energy densify the fuel and mitigate any organic losses. The combination of the two techniques reduced PM emissions by more than 50% for straw, miscanthus and road-side grass combusted in a drop tube furnace. Wang et al. [2020] observed a similar trend for PM_1 emissions for rice straw, by hot water washing followed by torrefaction, because of the removal of K, Cl, S and Si during combustion in a high temperature drop tube furnace. However, if too much Si was removed emissions of PM_{1-10} started to increase from char fragmentation.

Some careful consideration must also be taken as to the organic losses since these can have the negative effective of reducing the energy content. Long, Deng and Che [2020] measured the organic content of the water leachate from washing various agricultural residues at increasing temperatures (30/60/90°C). The results show that at the hotter temperatures more aromatics and alkenes were present in the leachate which could influence the volatile yields in the early stages of combustion however the energy content was relatively unaffected.

Gudka et al. [2016] currently is the only review of existing literature on washing pre-treatment processes. Interestingly in waste wood pre-treatment high removal efficiencies of heavy metals species such as Cd, Cr, Pb and Zn were observed. In waste wood these elements are in high concentrations because of adhesives, additives, paints and resins used in their preparation. Some leaching of these elements was observed however intriguingly it was believed that the majority was removed as solid residue such as flakes of paint. Currently little research has investigated filtering off these solid fines and analysing them, the application of which could determine the feasibility of water pre-treatment processes because of the reduced environmental risks from disposing of the leachate.

Water pre-treatment of biomass is an important, current area of research and has shown large improvements in PM emissions from reduced concentrations of inorganic species. Further work is required to assess the removal efficiencies of heavy metals and to also analyse how this will impact their fate in combustion applications.

2.6 Conclusions

It is clear from previous research that more experiments are required to understand the performance and emissions from stove combustion. However, the approach needs to be targeted at specific objectives. In the case of this work the objective is focused on fuels and how fuel properties effect emissions. Currently most research has explored the use of wood fuels in stoves and compared them to traditional fuels such as coal and charcoal. However, there is little work on alternative fuels such as agricultural residues and biogenic wastes. Exploring these alternatives fuels is one of the objectives of this thesis.

As discussed in section 2.4.2, previous research as made correlations between certain fuel chemical properties and the emissions from combustion. Further testing of these correlations is important in order to effectively investigate the suitability of alternative fuels and to also aid the development of future fuels. Using other combustion and composition analytical methods the understanding of these correlations' can be developed further.

These objectives can also address some specific research gaps. Currently there is no study directly comparing the performance of raw and torrefied fuels on a domestic stove. This is a very sought-after study because it could address some of the air quality problems with stove systems by utilising existing technology. Furthermore, technologies such as washing which historically was used as a method to prevent acid rain could provide answers to the development of premium fuels which would help decarbonise heat and prevent air quality problems.

Finally, it should be noted based on section 2.4.1 that the definition of a combustion cycle has varied between research and standards. This is particularly challenging when trying to compare results and define appropriate fuels for fuel inventories. In this work it was important to consider the whole fuel cycle including the whole time period around reloading. This is so all the transient periods common in real life stove combustion are accounted for.

Chapter 3. Materials, Experimental Methods and Equipment

3.1 Introduction

This chapter summarises the fuels studied and the experimental methods used in the analysis. The following sections are split to discuss the fuels investigated (section 3.2), the sample preparation (section 3.3), characterisation analysis (section 3.4), combustion experiments (section 3.5) and pre-treatment methods (section 3.6), in that order. The fuels investigated are discussed based on the chapter in which they are studied. Although this thesis is focused on the application of these fuels in stove systems, additional combustion experiments are used to further define the attributes of the novel and pre-treated fuels. Only two forms of pre-treatment were studied, torrefaction and washing. These methods are discussed for the experimental work that was conducted at the University of Leeds. There is some discussion on errors throughout the following sections.

3.2 Fuel Samples and Descriptions

In this study various fuels have been sourced to compare their properties and suitability for combustion with a focus on their application in domestic stoves. The fuels used can be sourced in reasonable quantities in Europe. The fuels used in each chapter are explained in more detail in the following sections.

3.2.1 Fuels used in Chapter 4

The fuels in this chapter were selected based on a single criterion, their commercial availability to be combusted on domestic stoves. Spruce and willow are common woods used for logs on stoves and in biomass boilers. This is largely because of their fast growth and their potential to supply the increasing demand. Briquetted fuel is a rapidly growing market, most commonly this is briquetted sawdust and industry processing residues, however food and agricultural briquetted residues are taking an increasing market share. In 2017-18 there was 2,186,000 tonnes of olive oil manufactured in the E.U. [European Commission, 2019]. Solid waste products can make up 30% of the process output by volume [Fernández-Bolaños, 2006]. The high

production of olive waste presents an opportunity for economic gain by converting the waste to a product. Spruce, willow and olive stone, and their torrefied counterparts were sourced for comparative analysis, Fig. 3.1a-f. For the spruce and willow the torrefied form was sourced from a different supplier to the original wood, this is because of the few suppliers who can provide untreated and torrefied fuels. For the olive stone, the same source of olive stone was used to make the torrefied form. Details of all six fuels are listed in Table 3.1. The torrefaction processes for the torrefied fuels are: (a) torrefied spruce, heated up to 260°C for 30-40 minutes, (b) torrefied willow, heated up to 250-260°C for 90 minutes, (c) torrefied olive, heated up to 280°C for 100 minutes.
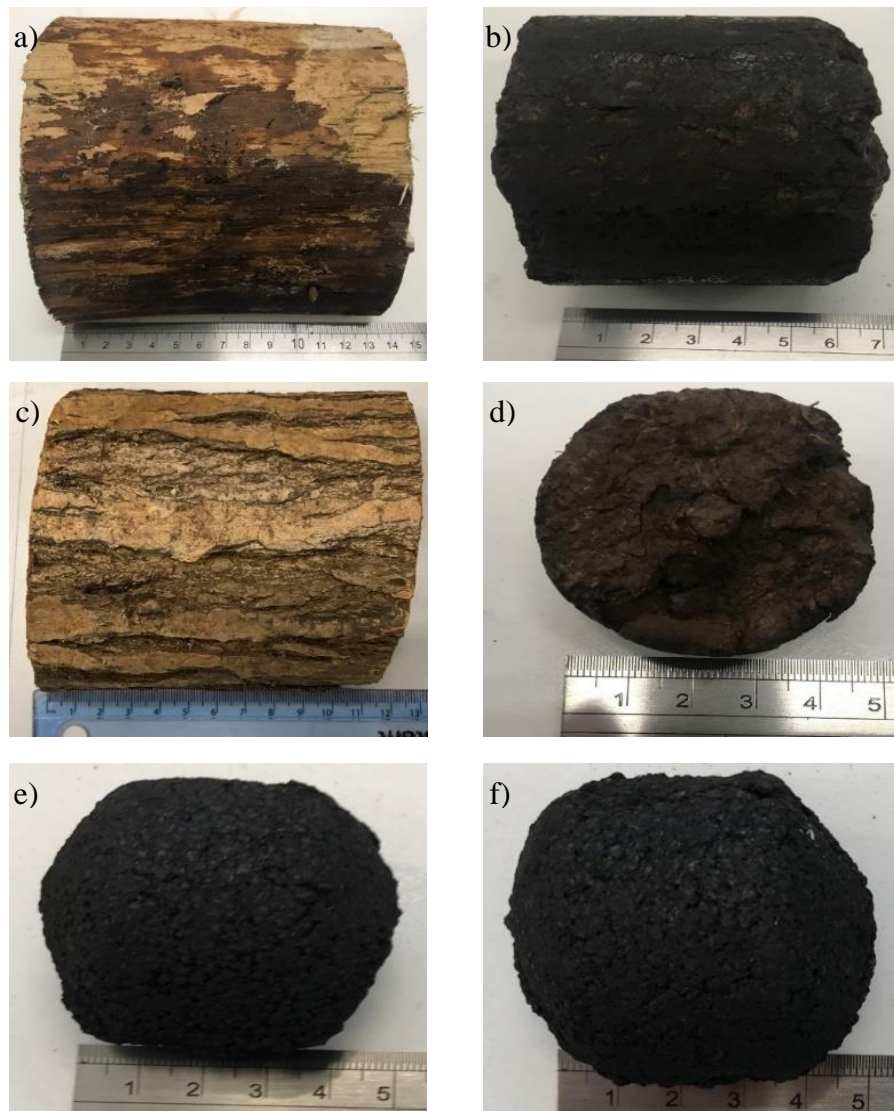
Figure 3.1: Fuels used in Chapter 4, (a) Aberdeenshire spruce wood (b) torrefied spruce wood (briq.) (c) white willow (d) torrefied willow (briq.) (e) olive stone briquettes (briq.) (f) torrefied olive stone briquettes (briq.)

Table 3.1: Description of fuels used in chapter 4.

Fuel	Form	Dimensions (mm)	Forming Process	Description	Density (kg m^{-3})	Source	Provided to Leeds by
Spruce	½ split logs w. bark	140x80x50	n/a	• Uniform shape and size • Not susceptible to splintering	550	Aberdeenshire, Scotland	D. Spracklen (University of Leeds)
Torrefied Spruce	Cylindrical briquettes	70x60(d)	High Pressure Extrusion	• Uniform • Vary hard, requires a lot of force to break a briquette • Smooth outer surface	1000	Andritz AG, Austria	Supergen Bioenergy Hub
Willow	½ split logs w. bark	130x90x50	n/a	• Uniform • Moderately susceptible to splintering	500	RSPB Idle Valley, Nottinghamshire	Supergen Bioenergy Hub
Torrefied Willow	Cylindrical briquettes	20x50(d)	High Pressure Extrusion	• Some irregularity to shape and size • Briquettes crumble and break easily	450	Rothamsted Research, produced by ECN and C.F Nielsen, Denmark	I. Shield (Rothamsted Research)
Olive	Stone shaped briquettes	50x35x25	Thermal Moulding	• Very uniform in shape and size • Briquettes are hard and durable • Highly porous structure	700	Arigna Fuels, Northern Ireland	R. Johnson (Arigna Fuels)
Torrefied Olive	Stone shaped briquettes	50x35x25	Thermal Moulding	• Very uniform in shape and size • Briquettes are hard and durable • Highly porous structure • Formed from 50% torrefied olive stone and 50% raw olive stone	700	Arigna Fuels, Northern Ireland	R. Johnson (Arigna Fuels)

3.2.2 Fuels used in Chapter 5

In this chapter the aim was to analyse the suitability of briquetted spent coffee in domestic stoves. Commercial briquetted spent coffee, termed coffee logs, is made from spent coffee grounds collected from various coffee shops across the UK, Fig. 3.2. The intention is to take the high mass yields after the coffee has been brewed and to use it in energy applications, this improves the circular economy. Along with the briquetted coffee, a small sample of spent ground coffee was also supplied for composition analysis.

Figure 3.2: Coffee Logs.

In order to assess the variability of coffee waste and to determine if the coffee logs were representative of ground coffee waste a control sample was used in the composition analysis. The control sample was from a Mexican Robusta Bean (MRB) which was grown on the west coast of Mexico in the mountain town of San Sebastian del Oeste at the La Quínta coffee farm. The coffee cherries were harvested and deshelled by hand. They were then torrefied at 220°C in air using a Solocafé small LPG coffee toaster. The coffee was ground at the farm and exported to the U.K. In the U.K the coffee was brewed to make single shot espresso coffee in a Fracino 2 group semi-automatic machine, water pressure 3 bar and temperature 80°C. The spent coffee was collected and dried before analysis, Fig. 3.3.

In order to compare the emissions produced from combustion of the coffee logs to those from a wood fuel, willow wood logs were also analysed (both composition and combustion). The willow wood logs were supplied from the same

supplier as the coffee logs as seasoned ½ split logs with the bark. Several of the logs were used cut and milled to create a sample for composition analysis, Fig. 3.4.

(a)

(b)

(c)

Figure 3.3a-c: Control sample of Mexican Robusta Beans (a) Torrefaction Equipment (b) Torrefied Coffee Beans (c) Torrefied Ground Coffee.

Figure 3.4: Seasoned willow wood logs.

3.2.3 Fuels used in Chapter 6

The objective of this study was to assess if bracken could be used as an energy crop in solid combustion applications. This required a comparison between bracken and other fuels; the other fuels were selected based on criteria that they are either a residue or have similar physical or growing properties to bracken. Eventually this led to the selection of an agricultural residue (straw), an energy crop (miscanthus) and an industrial residue (wood briquettes). Some composition comparisons were made with fuels in Chapter 4.

3.2.3.1 Bracken

Bracken (*Pteridium aquilinium*) is the UK's most common fern and grows globally except for in extreme climates. Fig. 3.5 is a schematic of a single bracken fern. The rhizome is what makes bracken so robust and dominant over an area of land. The rhizome is a central network from which the roots and fronds develop. This enables water, nutrients and energy to be stored and transported throughout the plant lifetime. The rhizome is usually close to the soil surface within a meter to 0.5m, however in well-draining, high sand concentration soils the rhizome can often be deeper than a meter. Fronds will emerge from the rhizome in early spring and will continue growing through spring, summer and to mid-autumn. A frond can range in size but they are typically larger than a meter up to 2.5m. The frond is split into two main sections: the stipe and the blade. The stipe is structural and when green has some small photosynthetic capabilities. The blade has three parts: the axis (*Rachis*), the leaflet (*Pinna*) and the leaf (*Pinnule*). The blade is responsible for both the production of energy and spores (reproduction). Common to most ferns, the spores will fall before fertilisation which is different to most plants which are fertilised first, this typically happens over the latter summer period.

Bracken has a C_4 photosynthetic perennial growth cycle, the growth cycle is described in Fig. 3.6. In spring and summer, the frond is green (chlorophyll), elastic and flexible. After the spores have dropped, into autumn, the frond turns yellow and then brown, the leaves wilt and some will drop from the leaflet. The frond becomes brittle and sharp. During this period minerals move from the frond into the rhizome, this causes some elements to become concentrated in the frond. As this mineral shift takes place, the lack of energy production causes the frond to collapse and lay down. With time this can form a mulch but the very slow decaying process often takes years

to break down a frond. This prevents an effective ecosystem forming and many animals from being able to nest and hibernate over the winter months.
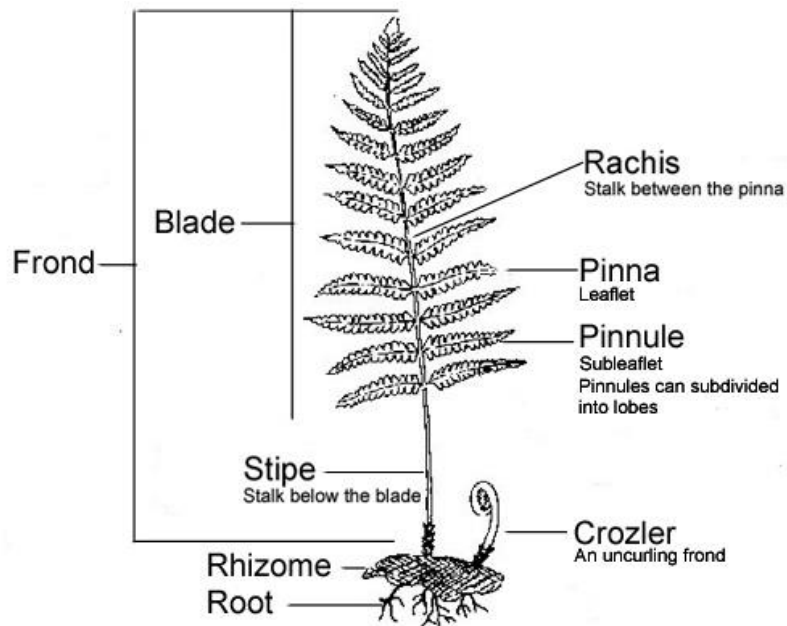
Figure 3.5: Single bracken fern [Bowe, no date]

Working in collaboration with the RSPB at Budby Moor lowland heath site in Sherwood Forest, Nottinghamshire, bracken was harvested between July - October 2018, Fig. 3.7. Discussions with the site managers meant that if the bracken was to be harvested as an energy crop, the machinery used would only harvest the frond from the bottom of the stipe, therefore only the frond was sampled. To analyse the changes over the growth cycle, four sampling points were set over the time period. Over August and the start of September the spores develop and drop, some past research has shown that the spores can be carcinogenic so harvesting of the bracken would not be feasible during this period from a health and safety point of view [Potter and Baird, 2000]. It was also important to assess the variation in the bracken composition across the site, so five sampling sites were selected and markers were used to ensure samples were consistently collected from the same sample area.
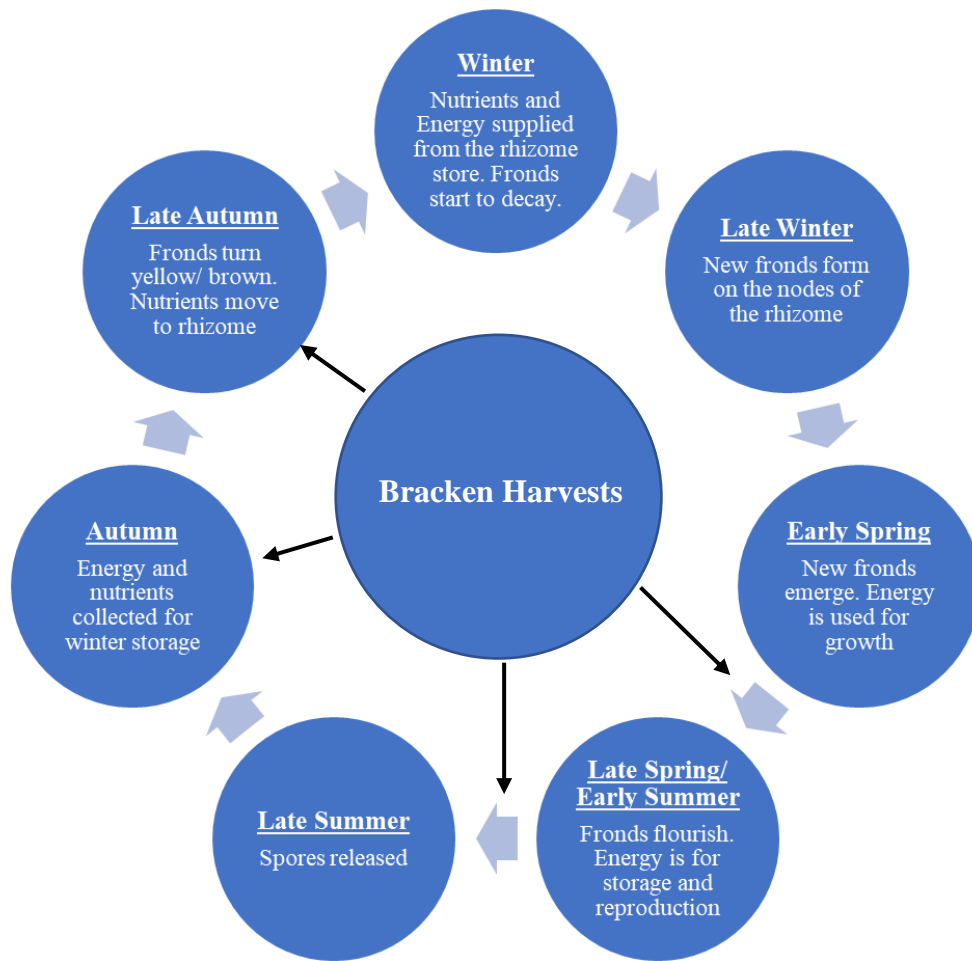
Figure 3.6: Annual growth cycle of bracken

3.2.3.2 Commercial Bracken Briquettes 'Brackettes'

Commercially manufactured briquettes (termed brackettes) made from bracken growing on land in the south-west of England was used in the stove combustion experiments. This was because of the lack of ability to briquette the harvested bracken at the University of Leeds. Although the brackettes were made from bracken from a different source, the bracken was harvested at the same time period in the growth cycle, late October. The briquettes were made without a binder using a high-pressure extrusion process, this resulted in circular dense briquettes (1250 kg m^{-3}) 150mm in length with a diameter of 70mm and smooth surface, Fig. 3.8. Analysis of these briquettes showed that the composition was within 5% on all measured variables (proximate, ultimate and metals) of the harvested bracken at site 2 harvest 4. It was therefore possible to assume that the performance of the brackettes on the stove would be representative of the harvested bracken. This is discussed more in Chapter 6.
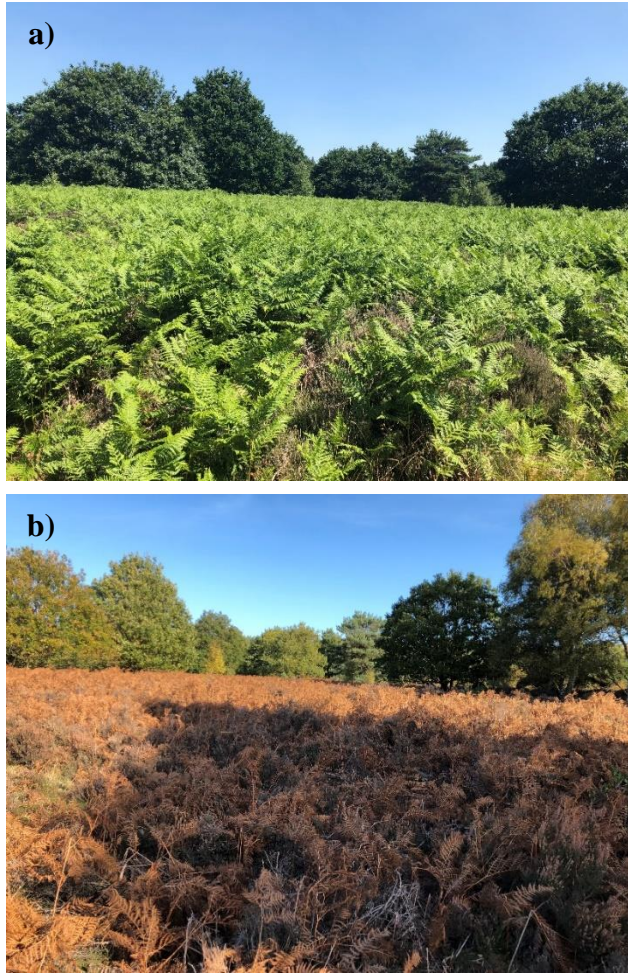
Figure 3.7: Change in bracken from a) late spring to b) late autumn

Figure 3.8: Bracken burn briquettes 'Brackettes'

3.2.3.3 Barley and Wheat Straw

Farming of cereal crops is a large industry in the UK; 2.7 million hectares was harvested in 2019, this accounts for 55% of all 'croppable' land area available [DEFRA, 2019]. Farming of wheat and barley produces a significant quantity of straw residue. Using the harvest index, a benchmark of 51% grain per crop harvest is targeted meaning on average 49% of a crop is residue (this includes the stem, leaves and chaf) [DEFRA, 2019]. Current farming practices use 50% of this residue as soil conditioner, and a proportion of the remaining percentage is often burnt in open fires [Glithero, Wilson and Ramsden, 2013]. Straw and bracken have many physical similarities in the latter stages of the year (colour, shape, size and texture) and are categorised as an agricultural residue.

The barley (BS 423) and wheat straw (WS 093) in this study came from Rothamsted Research, supplied by I. Shield and C. Whittaker, as part of an agronomy study. Both of the straws arrived at the University of Leeds milled and then were sent to be briquetted by an external company. Briquetting is discussed more in section 3.3, but it must be noted that straw has low amounts of natural binder (lignin) so a 10% solid pre-gelled wheat starch binder was used to briquette the straw at high pressure. This briquetting was not conducted at the University of Leeds but through an external service by Mr. R. Taylor. The briquettes were circular with a hole drilled through the centre (dimensions 60mm in length 75mm in diameter), Fig. 3.9. Even with the binder the briquettes were fragile and crumbly and would break easily, more binder could be added to improve the durability, however this would have distorted the stove combustion test results.

Figure 3.9: Straw briquette

3.2.3.4 Miscanthus

Miscanthus is a well-established energy crop in the UK. Approximately 40 thousand oven dried tonnes of miscanthus were used in 2018 [DEFRA, 2019]. Miscanthus has a C_4 photosynthetic perennial growth cycle and has a rhizome, the same as bracken. Therefore, comparative analysis between the two biomasses would be insightful. The miscanthus was supplied in briquetted form from Rothamsted Research as blocks of 60x40x40mm. The briquettes, Fig. 3.10, were more durable than the straw briquettes however they were still fragile and a small amount of force would cause them to break.

Figure 3.10: Miscanthus briquette

3.2.3.5 Wood Briquettes

Briquetting of sawdust and residual wood shavings from the timber industry is a growing market. This prevents the accumulation of waste and improves the economics of timber manufacturing. Sawdust briquettes are commonly sold in DIY stores in the UK. Sawdust is considered an industrial residue which once briquetted can significantly improve the specific density (loose density is approximately 250 kg m^{-3}, when briquetted 1200 kg m^{-3}) [Sánchez, 2014]. The wood briquettes used in this work were Eco-bright^{TM} wood briquettes which were formed using high pressure and mild heating (dimension 200x50x50mm with a central square hole 10x10mm through the length). The mild heating softens the lignin in the wood which acts as a natural binder. The briquettes were durable but with a rough surface. Rough surfaces have better heat transfer properties as there is an increased surface area.

3.2.4 Fuels used in Chapter 7

SRC willow is a fast-growing energy crop which is typically planted in dense mixed varieties of species all native to the UK. Energy plantations are usually harvested every 2-4 years with a lifetime of up to 30 years. The willow was supplied by Rothamsted Research who had been conducting experiments using SRC willow to remediate contaminated land. Use of biomass grown on contaminated land is limited by European and British Regulations which specify limits on concentrations of certain species (BS EN ISO 17225-1:2014) [British Standards, 2014]. Located in Derbyshire the land had been contaminated from historical coal mining activity, Renishaw colliery. The supplied SRC willow was after a three-year cycle of growth. The willow was chipped at source and consisted of only the wood, no leaves, with a particle size range from 3–45 mm, Fig. 3.11. This willow was pre-treated (washing and torrefaction), analysed, briquetted and combusted at the University of Leeds, details of this process are given in sections 3.3.5 (stove combustion) and 3.6 (pre-treatment).

Figure 3.11: Chipped SRC willow

3.3 Sample Preparation

For analysis samples need to be prepared by specific methods. Poor sampling and sample preparation can result in distorted results. Sampling and preparation followed standards where specified. More details on these methods are discussed in the following sections.

3.3.1 Drying and Sampling

For raw samples (wood chips, ground coffee and bracken) either collected directly after being harvested or samples that had been washed the biomass has to be dried first. To keep this initial drying process the same between samples a routine drying step was used. Samples were placed into an APEX 430 drying oven for 72 hours at 40°C. Every 24 hours the samples were mixed to ensure the whole sample dries and prevents moisture accumulating in the centre of the biomass pile. This process was repeated for the entire supply of biomass. This process reduces the biomass moisture content to less than 10 wt.%.

In order to ensure the samples used in characterisation and combustion analysis are representative of the bulk sample and not systematically bias, the coning and quartering method was used. This involved first passing the whole sample through the cutting mill to reduce the particle size to less than 4mm. This is not an accurate method of ensuring the particle size is consistently below 4mm therefore it was sieved further and particles above the size limit were separated out. The heap of separated particles is then flattened and split into four quarters. A small sample (~20g) is taken from each quarter, mixed and used for proximate analysis, single particle combustion and for ashing to be used in metals analysis. The remaining particles in the heap are combined, flattened and quartered, a smaller sample (~5g) is taken from each quarter and mixed; this sample is combined and cryomilled to a particle size of less than 100μm. This sample was coned and quartered again to select a sample to be used in ultimate analysis, py-GC-MS and TGA. Any remaining particles that have not been cryomilled are combined with the bulk sample to be used for briquetting. The cryomilled sample not used in analysis was kept separate for any additional analysis required.

3.3.2 Size Reduction/ Milling

For all analytical methods particle size is a key factor in ensuring sample presents as a homogeneous solid. To reduce the particle size to ≤4mm a Retsch SM300 cutting mill was used, Fig. 3.12. Biomass is fed by gravity from the top entry point to the cutting area. A central cutting rotor, at 1200 rpm, with three carbon steel blades shreds the biomass using centrifugal force, this is aided by three more blades (cutting bars) which are fixed to the walls of the milling chamber. The biomass falls to the bottom of the milling chamber where there is a mesh sieve with 4mm square holes.

Using a vacuum, the biomass is drawn through the sieve and into the sample collection pot.
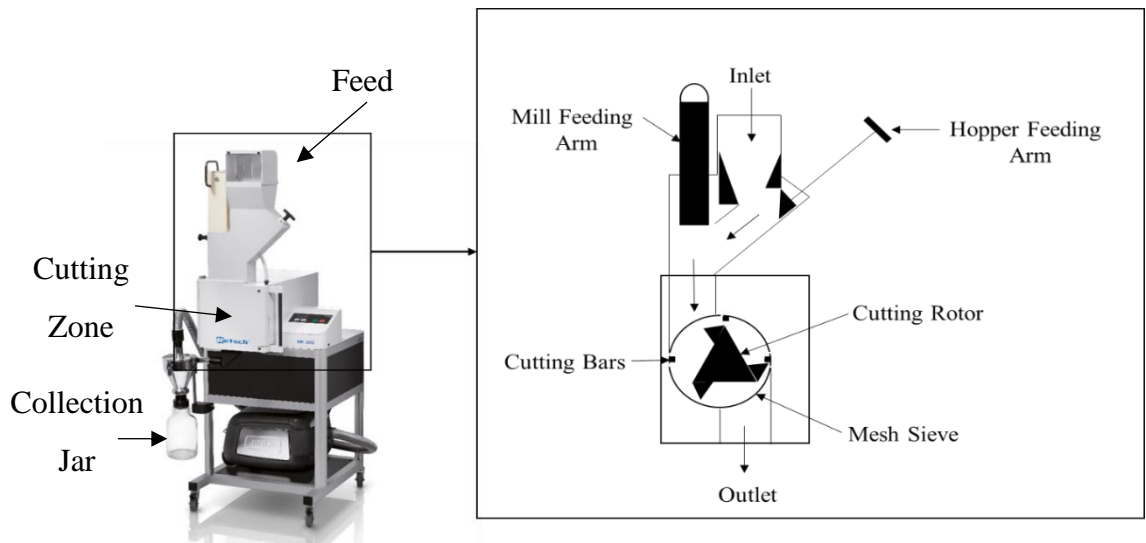
Figure 3.12: Labelled diagram of cutting mill (showing internal mechanism)

For some analysis smaller particle sizes of less than 1mm are required. This can be done using a cryomill. Although the ball mill has the advantage of being able to mill more sample in a single run, for the work in this thesis it was more important that the particle size distribution was in a narrow size range, this is to ensure the quality of the results. Therefore, only the cryomill, Fig. 3.13, was used to prepare smaller particle sizes.

Figure 3.13: Retsch cryogenic mill

The cryomill was a Retsch cryogenic mill and reduces the particle size to between 10-80μm. Approximately 3g of sample is loaded into a 100ml nitrile lined

grinding jar, a nitrile coated grinding ball is placed in with the sample. The jar is screwed into the cooling jacket and when the program is started liquid nitrogen flows from the dewar into the cooling jacket whilst the sample gently vibrates, 1Hz s^{-1}. This process first cools the sample to a set point before the vibration intensity increases. It is important that the sample is continuously moving to prevent moisture agglomeration of the sample or warm pressure zones forming within the grinding jar. Once the sample has pre-cooled the grinding frequency is increased to 5 Hz s^{-1} for 3 minutes. After which the sample is removed from the grinding jar in powder form.

3.3.3 Briquetting

For stove combustion tests the milled samples had to be briquetted using an MTI hydraulic press and a heating jacket, Fig. 3.14. When briquetting samples for stove combustion tests it is important not to use any binder if possible, this is because the binder will introduce different organic and inorganic compounds into the fuel mix which could influence the measurements. Briquetting biomass is mainly dependent on the quantity of lignin and moisture in the biomass. Lignin, when mildly heated (100-300°C), will soften and acts as a natural binder. Moisture similarly softens the biomass particles and improves intraparticle interactions which improves the durability of the briquettes.
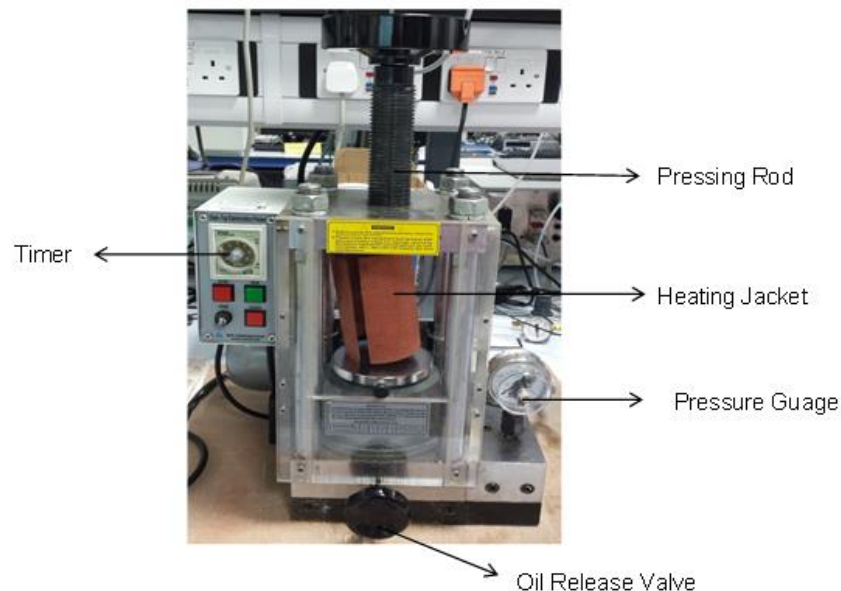
Figure 3.14: Hydraulic Press

Using a stainless-steel die with a diameter of 60mm, sample was loaded into the central column. The column was filled to half of its volume, ~30g of sample. A piston press is loaded on top and placed into the hydraulic press. The heating jacket

was placed around the die and set to 130°C. Using 25 MPa the sample was pressed for 30 seconds, during this time the pressure would fall because of the elasticity and porosity of the sample in the die, therefore the pressure was raised and then pressed for 2 minutes. This produced uniformly shaped briquettes.

3.3.4 Acid Digestion for Metals Analysis

As discussed in section 3.4.5, in order to analyse the metals in the solid sample, it must be digested into a liquid. Some digestions were carried out at the University of Leeds whilst others were sent for external analysis. The details of the digestion processes are explained in the sections below.

3.3.4.1 University of Leeds

Depending on the element of interest the sample may need to be ashed first, see section 3.4.1.5. The combustion temperature and heating rate can have varying impacts on the composition of the ash leading to residual unburnt carbon or loss of the more volatile metals (K) [Xing et al., 2016]. The fuels were ashed at 550°C for 3 hours, this reduces the C content to below 5 wt.%, and then during the digestion process HCl acid is added to remove any residual carbon. This method was chosen because it minimises any losses in volatile metals and is the same as the British Standard (BS EN ISO 18122:2015), see section 3.4.1.3.

0.4g of the ash was weighed into a polypropylene beaker and 10ml of hydrofluoric acid was added. This was left to reduce to dryness over a steam bath. Hydrofluoric acid is very good at breaking down silicate glass structures which are very common in biomass and organic matter. Once dry, 10ml of concentrated hydrochloric acid was added and the beaker was returned to the steam bath for 10 minutes. The HCl removes any carbonates released from silica structures and helps to dissolve some metal structures. After 10 minutes, 30ml of distilled water was added and the sample was left to cool.

After the sample had cooled, the contents of the beaker were transferred to a 400ml Pyrex beaker and placed on a hot plate at 80% heating capacity to completely dry. The dry sample is left to cool after which, 5ml of concentrated nitric acid and 3ml of 1:1 sulphuric acid is added, this is heated on the hot plate until white sulphuric flumes persist for at least 5 minutes- the sample must not be allowed to go dry. The mixture of HNO_3 and H_2SO_4 makes a strong oxidising agent meaning any remaining

inorganic elements should be solubilised. The sample was then removed from the heat and allowed to cool. The final step was to add 200ml of distilled water to the beaker and placed on the hot plate for 30 minutes, this is to ensure any elements which may have crystallised or precipitated can be dissolved into the solution. The solution was removed from the heat, transferred, and made up to 250ml in a volumetric flask. Dilution was always conducted to produce estimate concentrations in the parts per billion (ppb) range. For some of the samples in the final step only 50ml of distilled water was added and heated, and then when diluted only made up to 100ml. This was because the focus was on trace metal elements and over diluting the sample can mean a loss of sensitivity in the analytical instrument. This method was selected because biomass can often have high concentrations of silica. The combination of the acids used is very effective at extracting components from the glass structures and producing a high-quality solution for ICP analysis [Geana et al., 2011].

3.3.4.2 SOCOTEC Analysis

Some samples were sent to SOCOTEC UK Ltd (Bretby Business Park, Ashby Road, Burton upon Trent, DE15 0YZ) for analysis. This analysis was done by first ashing the sample according to the British Standard described in section 3.4.5. Then 0.25g of sample was dissolved in concentrated nitric acid for two hours using a whirl mixer. The solution was then placed in a heating block and incubator and left overnight. The following day 5ml of 25% HCl was added to the sample and heated to 80°C before transferring to a volumetric flask ready for analysis.

3.4 Experimental Methods for Characterisation of Fuels and Ash

This section focuses on the experimental methods used to determine chemical and physical properties of biomass. Samples were tested in duplicate or triplicate and the average of the results was used. The standard deviation was calculated to demonstrate the variability (error) across the sample.

3.4.1 Proximate Analysis

Proximate analysis is the characterisation of four fuel properties: moisture, volatile matter, ash content and fixed carbon. These are discussed in more detail in the following sections.

3.4.1.1 Moisture

Moisture analysis is to determine the as received (*ar*) moisture that can be removed from a fuel by oven drying, British Standard BS EN ISO 18134-3:2015. Using a milled sample with particle size of 1mm or less, ~1g of sample is weighed into a dish and dried in a Carbolite MFS oven at 105°C for a prolonged period of time, >3 hours. The sample is weighed after and the difference in mass is the loss of moisture, this is determined by Eq. 3.1.

$$M = \frac{m_b}{m_a} \times 100 \quad (3.1)$$

Where:

M- Moisture content

m_b- Difference in mass of sample before and after drying

m_a- Mass of sample before drying

3.4.1.2 Volatile Matter

Analysis of the volatile matter content is by British Standard BS EN ISO 18123:2015. Using ~1g of sub-1mm particle sized sample, the sample is weighed into a crucible and placed in a Carbolite OAF 101 furnace at 900°C (±10°C) for 7 minutes. The difference in mass before and after is due to the loss of volatiles from devolatilisation and moisture. The remaining sample is a combination of carbon-rich char and ash. The volatile content is determined by Eq. 3.2 on a dry basis (*db*).

$$VM_{db} = \frac{100 \times m_b}{m_a} - M \times \left(\frac{100}{100 - M}\right) \quad (3.2)$$

Where:

VM_{db}- Volatile matter content on a dry basis

m_b- Difference in mass of sample before and after devolatilisation

m_a- Mass of sample before devolatilisation

M- Moisture content

Volatile matter refers to the release of light hydrocarbons and tars into the gaseous phase from the thermal decomposition of a fuel. The release of volatile gases is termed devolatilisation.

3.4.1.3 Ash

The ash content is determined by British Standard BS EN ISO 18122:2015. Sample with a particle size of less than 1mm is weighed (~1g) into a crucible. The sample is placed into a Carbolite OAF 101 oven at room temperature. It is then heated to 250°C at a consistent heating rate over 30 to 50 minutes. When the oven reaches 250°C the sample is left to dwell for 60 minutes, this will remove moisture and volatiles. The temperature is then raised to 550°C (±10°C) at an even heating rate over a 30-minute period, the sample is left at this temperature for a minimum of 2 hours. The mass of sample remaining is the ash content calculated by Eq. 3.3 on a dry basis (*db*).

$$A_{db} = \frac{m_c}{m_a} \times 100 \times \left(\frac{100}{100 - M}\right) \quad (3.3)$$

Where:

A_{db}- Ash content on a dry basis

m_c- Mass of sample remaining after ashing

m_a- Mass of sample before ashing

M- Moisture content

3.4.1.4 Fixed Carbon

The fixed carbon content, FC_{db}, is calculated by difference, Eq. 3.4.

$$FC_{db} = 100 - VM_{db} - A_{db} \quad (3.4)$$

The fixed carbon refers to any material that is left after drying and devolatilisation but excluding the ash.

3.4.1.5 Analysis by Thermogravimetric Analysis (TGA)

For samples where there is only a small amount available or the particle size is very small (below 100μm), proximate analysis by TGA is a more suitable method. The greater sensitivity and online mass measurement will mean that the results will be more precise and identification of the end of each phase is more easily observed. Using a Mettler TGA/DSC 3+, Fig. 3.15, sample is weighed out into a crucible. The mass of sample is variable however it should not fill any more than 2/3rds of the crucible volume. The TGA is automated so will load the crucible onto the balance and into the furnace at room temperature. In nitrogen the temperature is raised to 105°C at

10°C/min and then held for 15 minutes. Still in nitrogen the temperature is raised to 600°C at a rate of 15°C/min and held for 30 minutes. The environment is then switched to air and heated to 610°C at 5°C/min and held for 30 minutes. Fig. 3.16 shows a typical plot from a TGA proximate experiment. Some methods will continuously heat the sample up to 900°C and hold the temperature for prolonged periods, however that is not necessary in the analysis of biomass since there is no observable change in mass above 600°C. Using the raw data from the TGA the amount of noise can be used to determine the error by standard deviation in the obtained values.

Figure 3.15: Mettler TGA instrument
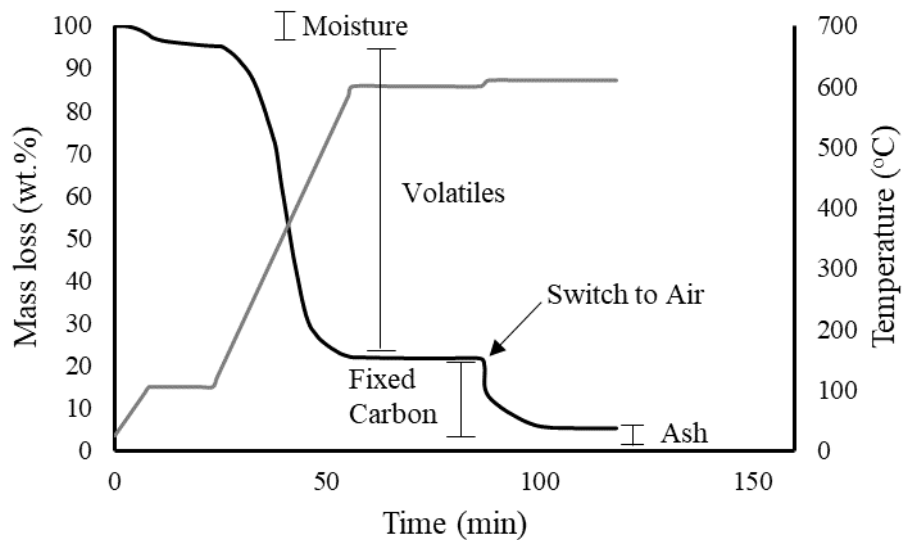
Figure 3.16: Typical TGA plot from proximate analysis

3.4.2 Ultimate Analysis

Ultimate analysis is used to determine the carbon, hydrogen, nitrogen, sulphur and oxygen concentrations of a biomass. The British Standard, BS EN ISO 16948:2015, only relates to the determination of carbon, hydrogen and nitrogen, this is because these are considered to be the most important input parameters when calculating parameters related to the combustion of solid biomass fuels. Using a Thermo CE Instruments CHNS Flash Elemental Analyser 1112 series the elemental contents of a sample are determined with oxygen being calculated by difference, Eq. 2.2. All the samples were run in duplicate or triplicate and the average and standard deviation (error) was calculated (errors are given within the results in the following Chapters). Since all the samples used were solid, tin capsules were used throughout, 2.5mg of sample was weighed into each crucible and sealed. The sample has to be cryomilled (particle size of less than 100μm) to ensure the complete combustion of the sample. The sample is loaded into a carousel along with a series of standards. The selection of standards is key to the reliability of the results. In this work the standards used were atropine, vanadium pentoxide, BBOT ($C_{26}H_{26}N_2O_2S$), oatmeal, methionine, sulphanilamide and cystine.

The CHNS works by injecting a sample into a combustion column at 900°C. The combustion column is filled with dry high purity oxygen- this is important to prevent the presence of undesired nitrogen and water which could impact on the result. As the sample combusts the carbon converts to carbon dioxide, the hydrogen to water, nitrogen to nitrogen gas or oxides of nitrogen and sulphur to sulphur dioxide. Chlorine in the fuel often reacts to produce hydrogen chloride but this is filtered out by absorbents. The ash in the sample falls to the bottom of the column.

The gases are then removed from the combustion chamber and carried by a flow of helium and passed over a high purity copper catalyst at 600°C. This removes any excess oxygen and reduces any nitrogen oxides to nitrogen gas. Combining this with the absorbent traps the remaining gas should be composed of carbon dioxide, water, nitrogen and sulphur dioxide. These gases are then separated by gas chromatography (GC) and quantified by thermal conductivity detectors. Quantification is only possible if the correct standards are used and the standards are of a high purity.

3.4.2.1 EC/OC Analysis

EC/OC analysis was conducted at Sunset Labs. This was done using the NIOSH 5040 method. This thermally desorbs the PM from the filter paper and this is carried by helium gas to an FID where it is analysed using a thermal optical technique to determine the representative quantities of EC and OC.

3.4.3 Chlorine Analysis

Chlorine analysis is more complicated since chlorine can be in both organic and inorganic forms. Cl can be determined by chemical fractionation using water, discussed in section 2.2.3, however this will only detect the water-soluble fraction. The British Standard method, BS EN 16994 [2016], uses a bomb calorimeter which dissolves the released gaseous Cl from combustion into deionised water by a gas washing bottle. The vessel and the ash are all rinsed out with deionised water which is combined with the water used to dissolve the gaseous Cl. The sample is analysed by ion chromatography (Dionex DX 100 Ion Chromatograph and LC20 Chromatography enclosure) with anion detection to determine the quantity of Cl in the sample.

Cl analysis was also conducted by SOCOTEC for some fuels. In this case the fuel was digested using hydrogen peroxide (H_2O_2) and made up to volume by deionised water. The sample was analysed by ICP-MS to determine the Cl contents.

3.4.4 Calculation of Calorific Value

Determining the calorific value used the wt.% C, H and N values on a db determined from methods in section 3.4.2. Friedl et al. [2005] presents two methods for calculating the higher heating value (HHV) of biomass based on the results of 122 different biomass samples. The two methods are based on developing a mathematical model which minimises the error between the predicted and measured HHV on a linear regression plot against the concentration of C, H and N. To perform this analysis, Friedl et al. [2005] uses an ordinary least square (OLS), Eq. 3.5, and partial least squares (PLS) method of analysis, Eq. 3.6.

$$HHV \ (OLS \ Model) = 1.87C^2 - 144C - 2820H + 63.8CH + 129N + 20147 \quad (3.5)$$

$$HHV \ (PLS \ Model) = 5.22C^2 - 319C - 1647H + 38.6CH + 133N + 21028 \quad (3.6)$$

The reason Friedl et al. [2005] uses two methods of analysis is to resolve problems of collinearity in multi-variable analysis. However, the results from both Eq.'s produce a similar result, therefore an average of two models is proposed, Eq. 3.7. Eq. 3.7 is used throughout this work and the HHV is on a dry basis in kJ kg^{-1}.

$$HHV\ (Averaged) = 3.55C^2 - 232C - 2230H + 51.2CH + 131N + 20600 \quad (3.7)$$

3.4.5 Metals Analysis

Metals analysis of solid samples, trace, minor and major metals (metals in ash), was determined by acid digestion of the samples, see section 3.3.4, and analysis by Inductively Coupled Plasma spectrometry (ICP). This included two types of ICP:

1. Inductively Coupled Plasma Mass Spectrometry (ICP-MS)- the sample is first atomised and dissociated into singularly charged individual ions within a plasma. The ions are passed through a quadrupole mass analyser where they are separated based on their mass to charge ratio. Quantification is by detectors which are calibrated against standards of known concentrations. The instrument used was a Thermo Scientific iCAPQc ICP-MS.

2. Inductively Coupled Plasma Optical Emission Spectrometry (ICP-OES)- the sample is aspirated and atomised and dissociated in a flame to produce atoms in an excited state then elements are determined by the energy released (emission of light) in electron deexcitation. The wavelength of light is characteristic of the element. Quantification is by detectors calibrated against standards of known concentrations. Instrument is a Thermo Scientific iCAP7400 Radical ICP-OES.

Both methods can analyse a large number of elements in a single run. However, ICP-MS detection is more sensitive, parts per trillion (ppt), where as in ICP-OES detection is only parts per billion (ppb). Conversely, the total dissolved solids (TDS) in ICP-OES can be up to 30% conc. Where as in ICP-MS this can only be up to 2%. These are two key factors when deciding the analysis method. During ICP analysis as well as the instrument calibration a small amount of each sample was separated and used to determine the precision of analysis. This was done by doping the sample with a known quantity of element being analysed.

3.4.6 Ash Fusion Tests

Ash fusion tests are used to determine the ash melting behaviour of samples by uniformly heating them from 500-1500°C and capturing a black and white image every 1°C increment. The images are then analysed by the analyst to determine 4 key characteristic temperatures at which deformation occurs. These key temperatures are termed: softening temperature (ST), initial deformation temperature (IDT), hemisphere temperature (HT) and flow temperature (FT). This is the method from British Standard BS EN ISO 21404:2020, Fig. 3.17.

Samples must first be ashed, method is in section 3.4.1.3, and enough ash must be collected to make a test piece. The ash was cryomilled to get a homogeneous particle size as variability in particle size can have a large impact on the results. The test pieces are made in duplicate using a stainless-steel mould. Moulds are cylindrical in shape with equal height and diameter (~3mm). The mould is coated in a thin layer of petroleum jelly to prevent the test pieces from sticking. In a beaker ash is blended with 2 or 3 drops of dextrin solution to form a thick paste. The mould is then filled entirely with the sample- any holes or unsmooth edges will make determination of the phases more difficult for the analyst. The sample is left to dry for 10 minutes, dry enough for it to be stable out of the mould. Once the sample is removed from the mould it is left to dry for at least 24 hours. The test piece should be a uniform cylinder with a flat top and defined sides.
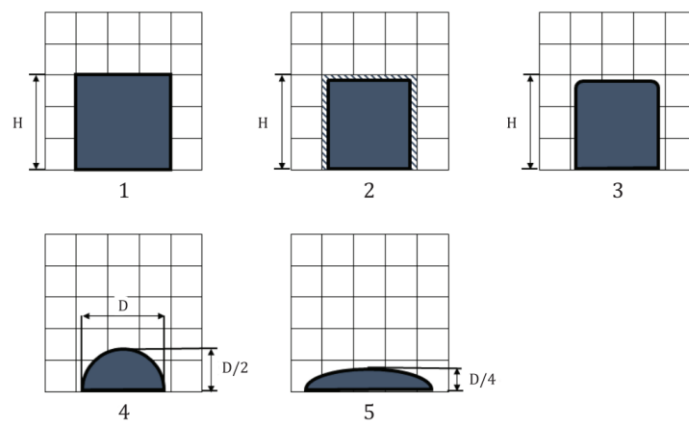
Figure 3.17: Ash melting behaviour determined in AFT 1) Initial test piece shape 2) Softening 3) Initial deformation 4) Hemisphere 5) Flow [British Standards, 2020]

Samples are loaded into the oven, a Carbolite digital ash fusion furnace, slowly to prevent thermal shock. The samples are heated at 10°C min^{-1} in air (oxidising environment) with a flow rate of 50 ml min^{-1}. The furnace is fitted with a camera and analysis of the samples is done by measuring the changes in height and aspects of the deformity of the test pieces. Fig. 3.17 shows the definitions of each characteristic temperature and how the temperature is determined [British Standards, 2020].

3.5 Experimental Methods for Combustion Analysis

3.5.1 Thermogravimetric Analysis (TGA) for Combustion and Pyrolysis Properties

Combustion and pyrolysis properties of fuels were analysed using a Shimadzu TGA-50. Up to 5mg of cryomilled sample was loaded into a crucible, no more than 2/3 of the crucible volume, and placed onto the microbalance. The microbalance positioned the crucible inside the furnace. The temperature was raised from room temperature to 900°C with a heating rate of 10°C min^{-1}. The mass of the sample is recorded throughout from which mass loss curves and derivative thermogravimetric (DTG) plots were obtained. For combustion analysis the furnace is filled with air at a flow rate of 50 ml min^{-1}. For pyrolysis the furnace is filled with nitrogen instead of air at the same flow rate. The heating rate, sample mass and flow rate were chosen to ensure a sequential process so that diffusion and heat transfer limitations have minimal influence on the results, this is particularly important when using the data to calculate kinetic parameters. The instrumentation is shown in Fig. 3.18. This type of TGA analysis is considered slow heating rate analysis. This is useful for defining individual stages of pyrolysis/combustion and analysing how a fuel will react within a temperature region.
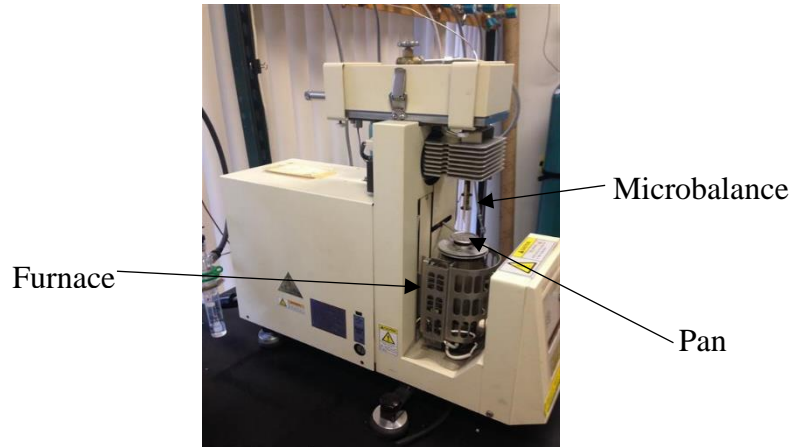
Figure 3.18: TGA used in combustion and pyrolysis analysis

3.5.2 Kinetics of Combustion and Pyrolysis

Analysis of the mass loss profiles can be used to determine kinetic parameters of the fuels. Assuming that the first order single step reaction model applies, the Arrhenius equation, Eq. 3.8, can be used to estimate the pre-exponential factor, A, for measured reaction rate constants, k, at different temperatures and the activation energy, E_a.

$$k = A exp\left(-\frac{E_a}{RT}\right) \quad (3.8)$$

In Eq. 3.8 R is the ideal gas constant and T is the temperature in K. The weight loss with time is assumed to be from one first-order reaction described by Eq. 3.9.

$$k_t = -\frac{1}{(m - m_\infty)}\frac{dm}{dt} \quad (3.9)$$

Where dm/dt is the tangent to the mass loss curve at time, t, m is the mass at time, t, and m_∞ is the terminal mass, selection of a terminal mass is highly influential on the value of k and the overall accuracy of the model. E_a and A can be evaluated graphically using Eq. 3.10.

$$\ln k = \ln A - \frac{E_a}{R}\frac{1}{T} \quad (3.10)$$

When using the constant reaction rate method, a boundary condition must be applied in both combustion and pyrolysis cases. The boundary condition means that the values of the kinetic parameters calculated are only applicable to the reaction rate constants within the temperature range. Calculation of the kinetic parameters uses a

linear regression method of analysis. Linear regression models calculate the best fit of the data to a line, this is usually evaluated by using the kinetic parameters calculated within the boundary to predict a reaction rate constant which is compared to the actual reaction rate constant. The difference between the two values is an observable level of error.

Minimising this error has been extensively researched with alternative methods proposed which estimate improved reaction kinetics. This includes proposed non-linear regression models which have improved accuracy and being non-linear can be applied to a greater range of data. Saddawi, Jones and Williams [2010] have compared results of the constant reaction rate method with bespoke methods proposed by other authors. The results showed that the apparent first order reaction rate constant method gives outstanding accuracy to predictions of kinetic parameters. Therefore because of its more simplistic method the constant reaction rate method is used throughout this work.

3.5.3 Pyrolysis- Gas Chromatography- Mass Spectrometry (Py-GC-MS)

Analysis of organic samples using GC-MS is highly efficient, accurate and sensitive. Pyrolysis of the sample, before being injected into the GC, breaks the biochemical components in biomass down into smaller fragments and volatilises them along with lipids already present in the biomass. These volatile components are separated based on their retention time within the GC column and are then identified using their mass to charge ratio (m/z) in the mass spectrometer. The whole technique allows the identification of a wide range of organic molecular components of biomass this is done by comparing peaks to the NIST database and literature. The decomposition source of resolved peaks (carbohydrate, lignin or fats) is determined by the time at which they are detected, earlier peaks are associated with carbohydrate sources, and their relative abundance is calculated by integrating the peak area. This is a semi-quantitative method and values are used comparatively- not as an absolute.

The pyrolysis of the fuels was performed in a CDS Pyroprobe Model 5000 at a rapid heating rate of 20°C ms^{-1} to a temperature of 600°C with a hold time of 60s. The sample was weighed (~2-3mg) into a 20mm silica glass tube between two plugs a quartz wool. It is important that the tube is cleaned sufficiently to remove any

residual ash and heat treated to remove any fats, grease or oils that can reside on the tube surface from handling and storage.

Once pyrolyzed the sample is fed into the GC column, Shimadzu GC-MS Model QP2010E, and mixed with a high purity helium carrier gas. The column was an RTX-1701 fused silica column, 60m in length with a 0.32mm internal diameter and 0.25μm film thickness. The volumetric flow rate in the column was 1.34mL min^{-1}. This type of column is a mid-polarity column which is typically used for separation of hydrocarbons, oxygenated, chlorinated, nitroaromatic and polychlorobiphenyls (PCBs). The GC oven started at 40°C for 2 minutes and then heated at 10°C min^{-1} to 180°C for a hold time of 2 minutes. The oven was then ramped again at 8°C min^{-1} to 280°C and held for 10 minutes.

The use of Py-GC-MS was to compare fingerprints and relative quantities of organics species from raw and pre-treated forms of biomass, pre-treatment was by torrefaction. Torrefaction is discussed in more detail in section 3.6.1, and is mostly concerned with removal of low volatile organics below 300°C. The column and oven temperatures/ heating rates used were to obtain the right sensitivity of separation for low-medium weight volatile compounds. The broader the analysis the less sensitivity of the separation and precision in identification. Therefore, careful consideration must be taken to selecting these conditions.

3.5.4 Single Particle Burning

Analysis of the combustion of biomass at higher heating rates can be performed using single particle combustion, this method is based on the one developed in Mason et al. [2016], Fig. 3.19a [Mason, 2016]. This is done by using a high-speed camera (Fujifilm Finepix HS10 digital camera) with a frame speed of 120 fps to capture the combustion profile. Using the images generated, demarcation of ignition, devolatilisation, char burnout and ash cooking is established, Figs. 3.19b-d.

Before combustion individual particles are sized and weighed, the typical size is approximately 2x1x5mm. The particle is suspended on a needle 25mm above a Mekér burner. The particle is then covered by a water-cooled sleeve which slides along two bearings and this is retracted and exposed to the flame at the start of each test.

This allows instantaneous exposure of the particle to the flame (<0.1s). The point at which the particle is exposed to the flame is t=0s.
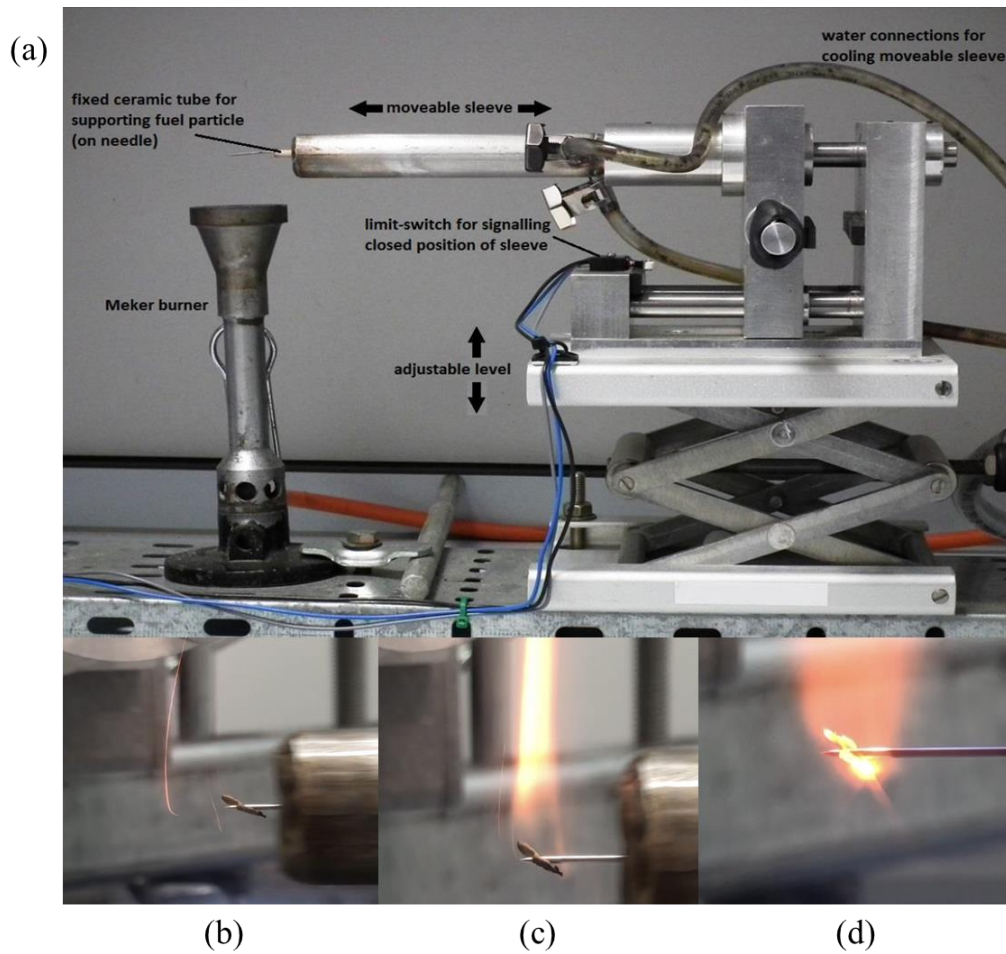
Figure 3.19: Single particle burning experiments (a) equipment setup [Mason, 2016] (b) particle heating up (c) flaming combustion (d) char combustion

The Mekér burner provides a methane-air mixed flame. The size of the Mekér burner (diameter of the base of the flame, 40mm) and the consistency of the environmental conditions surrounding the flame means that the flame can be assumed to be in a steady state. This includes the concentration of oxygen (21%), the temperature (1600K) and flow properties (3 ms^{-1}) in the combustion zone where the particle was suspended [Mason, 2016]. The camera was positioned 200mm from the particle in the same line of sight. The position of the camera and particle remained consistent between runs.

Identification of the combustion events was by the analyst using the video frame images collected. The events can be identified by the following criteria:

- Ignition- This is the point when the particle has dried and devolatilisation starts. Devolatilisation elutes a gas mixture which combusts above the particle surface which is recognised by a luminous flame. The time at which this flame appears is defined as the start of ignition/devolatilisation. The time between the first exposure of the particle to the flame and when the particle ignites is termed 'ignition delay'.

- End of volatile combustion/start of char burnout- For simplification in analysis it is assumed that char burnout starts at the point when volatile release ends, this is defined by when the luminous flame disappears. In reality this is not the case since the bottom surface of the particle is exposed directly to the flame which results in this surface heating at a faster rate. Therefore, when volatiles are being released from the top of the particle the bottom of the particle has turned to char and begins combusting.

- End of char combustion- This is the most difficult point to define. As char combustion proceeds the particle glows from the emission of CO and CO_2 from the particle surface. The intensity and brightness of the glow increases as char burnout progress until the particle begins to shrink. Whilst the particle shrinks the final carbon in the char combusts leaving residual ash. For this work the char combustion phase ends when the particle stops glowing. This covers the majority of the char combustion phase however by using an estimated 5% error margin should account for the missing time period.

The camera was run in conjunction with potassium release detection. Assuming that the flame temperature is stable for the duration of the observation, the intensity of spectral emission is directly proportional to the release of specific elements. Using a monochromator (Edmund Optics Techspec® band-pass interference filter) an emission wavelength of 766nm (bandwidth frequency of 5.11THz) is filtered out. This is focused onto a photodiode (Vishay BPW34) producing a current which is converted to a 0-5 volts output signal. The output signal is recorded and determines the relative intensity from potassium release. A second photo-detector system is set-up in parallel to the potassium measuring photo-detector but at a lower optical centre wavelength of 750nm (bandwidth frequency of 5.33THz). The second photo-detector

is used as a means to measure and correct for any background black-body radiation from soot particles and the flame. Further information is described in Mason [2016].

The photo-detector device has a high level of precision, estimated to be <1%. Volatilisation of potassium produces KCl and KOH both of which are volatile in the estimated flame temperature, however it is not possible to distinguish between the two. The photodiode is designed to have a linear response to photo-intensity and thus the concentration of potassium in the volatile phase. Gaydon and Wolfhard [1970] discussed the effects of self-absorption phenomena (absorption of the light emission from a potassium particle by another potassium particle) however as discussed by Mason [2016] this phenomenon can be assumed insignificant because of the low potassium concentration found in the biomass analysed.

3.5.5 Stove Combustion

Stove combustion tests were used to compare the emissions from various fuels in a real-life simulation. The stove used was a Waterford Stanley Oisin multifuel stove rated at 5.7kW and 79% thermal efficiency. This is a mid-range stove that is suitable for burning both coal and biomass. The stove was not changed throughout the experiments. The stove has internal dimensions of 250x270x190mm (*h*x*l*x*d)* and a single primary air supply point at the front on the stove door, as shown in Fig. 3.21. The air flow was controlled by keeping the orifice at a fixed opening, this was set to supply 150% excess air to the stove as recommended by the manufacturer for biomass fuels. The stove dimensions, fixtures and parameters were kept identical throughout. The whole stove assembly sits on a KERN balance for measuring the burning rates of each batch of fuel.

Operating conditions were chosen to simulate a real-life scenario. The method used was kept as consistent as possible throughout because small variations can have a significant impact on the performance and associated emissions. Ignition can be especially problematic with certain types of biomasses and therefore the procedure for lighting the stove varied. For this reason through all this work, combustion of the first batch of fuel was annulled and left out from the determination of average burning rates and emission factors. From the second batch onwards, all data was included until combustion was determined to have ended. Each batch of fuel that was loaded into the stove was kept consistent by weight (~1-1.5kg). Once the fuel was loaded the stove

door was closed until the majority of the mass of that batch had been consumed- this varied between fuels because of the energy required for the fuel to combust and the rate at which the fuel degrades. Multiple reloads were performed from 1 to 4 batches, this was to evaluate if the emissions were a reproducible result and to calculate average emission factors across the whole combustion run.

Using the extraction system of the lab, an extraction draught was used to draw the flue gas up through the stack and into the dilution tunnel. The draught was kept continuously at a static pressure of 12 Pa which is a flow rate of approximately 1.2 m^3 h^{-1}. The flue gas was mixed with room temperature air in the lab at the entrance to the dilution tunnel. Analytical equipment sampled from both the flue stack and the dilution tunnel; these can be seen Fig. 3.22.

Developing a method for stove combustion tests is a complex subject, as discussed in section 2.4. For the work in this thesis a hybrid method has been developed based on the objectives in section 1.5. As mentioned in section 2.4 by using a hybrid method it is important to ensure the results are reproducible. Therefore, the method is first tested by conducting the experiment with uniform wood briquettes, this is repeated three times. The results are shown in Figs 3.20a-c, all the results are within a 10% experimental margin of error which is acceptable.
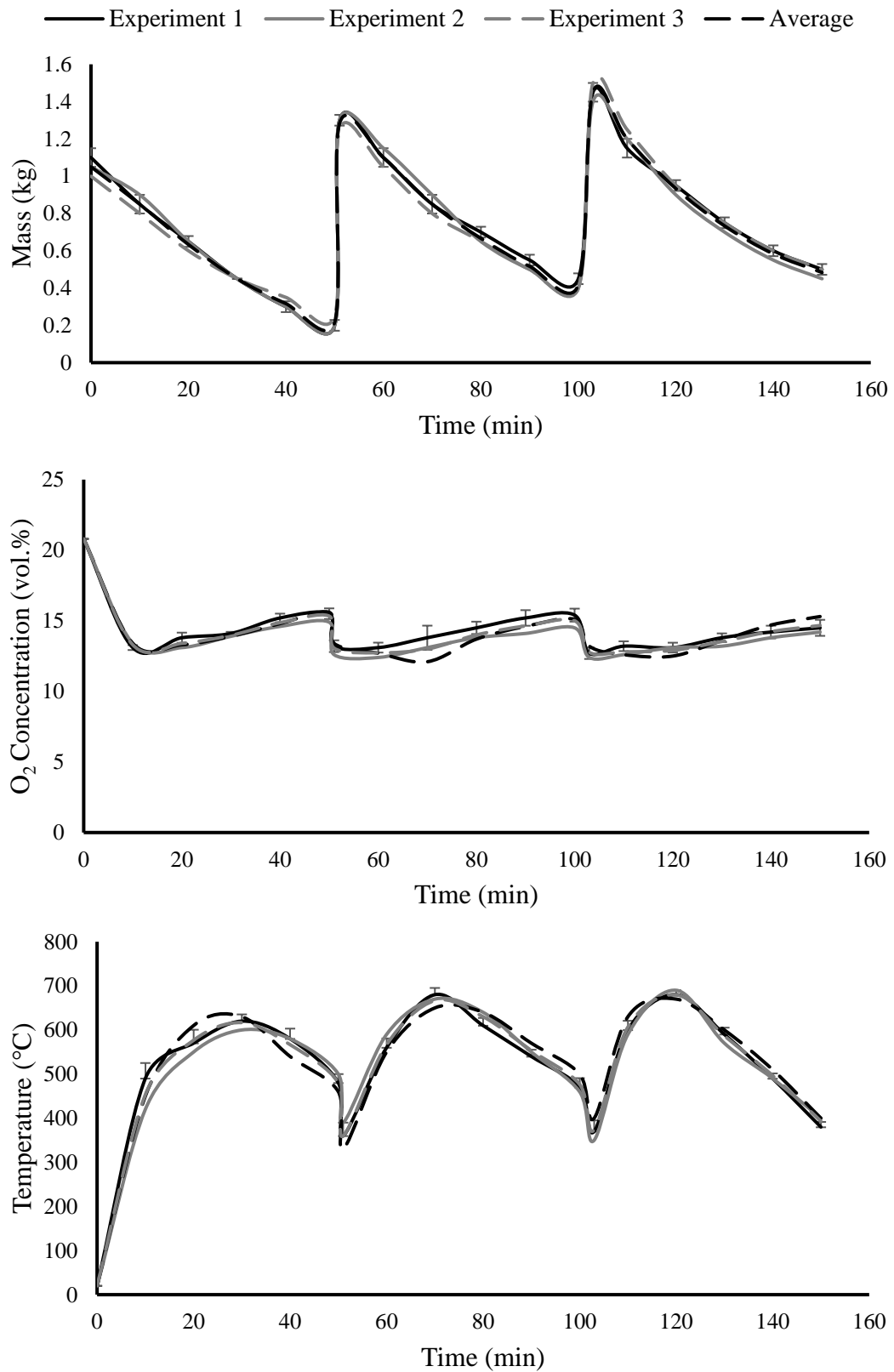
Figure 3.20: Test for reproducibility (a) Mass (b) O₂ Concentration (c) Temperature

97
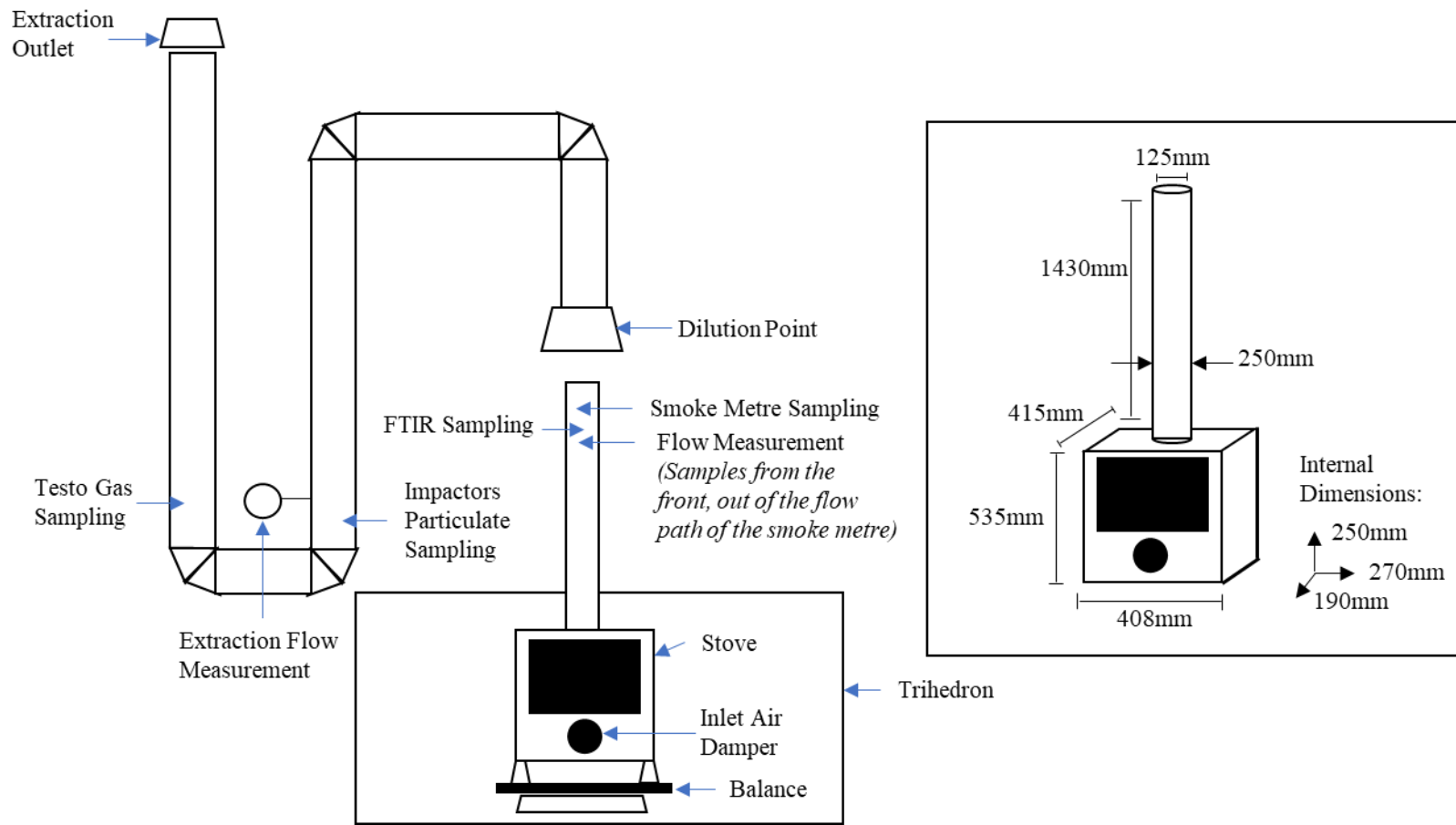
Figure 3.21: Schematic of stove combustion lab setup

Figure 3.22: Stove combustion lab setup

3.5.5.1 Gaseous Emissions

Measurements of gaseous emissions was by two instruments. The majority of emissions measurements was by a GASMET DX4000 Fourier Transform Infrared (FTIR) Analyser which sampled directly from the flue stack 1430mm above the stove, Fig. 3.23. A sampling unit draws the flue gas through a heated probe at 180°C which contained a 0.1μm sintered steel filter and then through a Teflon coated heated line (180°C) and a glass fibre filter. Within the sampling unit the oxygen concentration is measured by a Zirconia sensor (for calibration purposes) and then determination of the gaseous, and vapour- phases was analysed in the FTIR.

FTIR analyses the flue gas by exposing it to infrared radiation at various wavelengths and measuring the energy absorbed. The energy is absorbed by the chemical bonds within molecules. The interferometer produces an optical signal containing all the infrared frequencies and the energy absorbed in detected. The signal is read and decoded using Fourier transformations which produces a spectrum that is compared to a database library giving the identity and concentration of individual species.

The main advantage of analysing the flue gas using this technique is that it is an online measurement that can determine the identity and quantity of multiple gaseous species. Quantification can be in the ppb to 99.9 vol% range for some species, but the ppm level is more usual. This can be done with minimal sample and at short intervals. Additionally, the precision, accuracy and reproducibility of FTIR is exceptional, this is mainly because the interferometer uses a reference laser beam which is highly tuned to optimise performance. There are some limitations of FTIR the main concerns being that interference and overlap of signals can mean detection of certain species is less sensitive or lost (e.g. NO_2 and certain hydrocarbons) and the calibration of the instrument is essential to the results. Associated errors for 12 gaseous species are shown in Table 3.2.
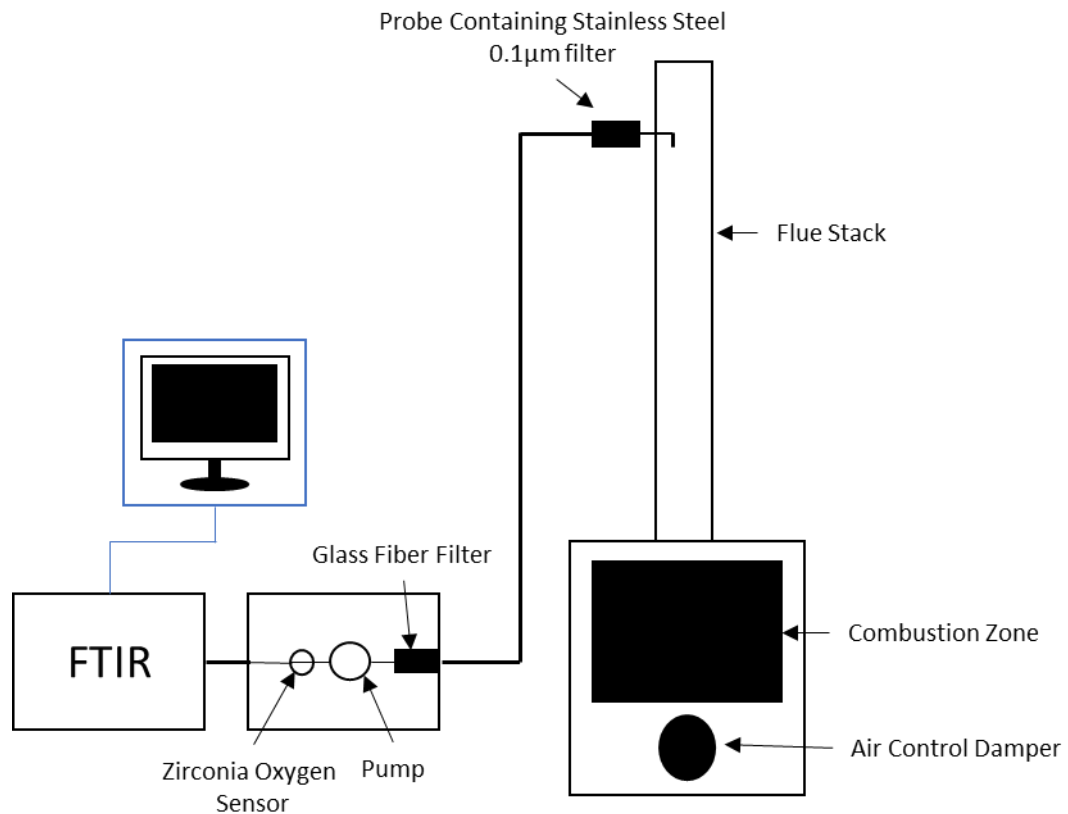
Figure 3.23: Schematic of FTIR set-up

Table 3.2: Uncertainty in measurements for FTIR DX 4000 [MCERTS, 2016]

Gaseous Species	Error (%)	Gaseous Species	Error (%)
O_2*	2.4	HCl	11.3
CO	6.5	NH_3	9.3
NO	5.6	CO_2	5.0
NO_2	6.7	H_2O	6.0
SO_2	9.2	HF	19.4
CH_3OH	4.0	CH_4	6.1

Zirconia sensor

The other method of gas analysis was with a Testo 340 Analyser which samples from the dilution tunnel. The Testo can only analyse concentrations of O_2, CO, CO_2, NO, NO_2 and NOx. It measures concentrations of these species using electrochemical sensors which use oxidation and reduction reactions to generate a current proportional to the concentration. It is an online measurement technique which offers great sensitivity and accuracy, however the sensors can become overloaded easily if the concentration (usually CO_2) and temperature of the sample is too high, for

this reason it must be placed in the dilution tunnel. Operational measurement errors are shown in Table 3.3. The dilution factor can be calculated by the ratio of $[CO_{FTIR}]/[CO_{Testo}]$, this is important for calculating the emissions of particulates.

Table 3.3: Uncertainty in measurements for Testo 340 Analyser [Testo, no date]

Gaseous Species	Error (%)
O_2	0.2
CO_2	0.2
CO	10
NO	5.0
NO_2	5.0
NOx	5.0

3.5.5.2 Particulate Measurements

Particulate sampling and measurement techniques used filter papers and foils to collect PM. Then by measuring the difference in mass over the sampled volume of flue gas the emissions can be calculated (gravimetric analysis). This is a discrete method that cannot be used to give real-time analysis. Isokinetic sampling parameters are important for reproducibility of the results however this is less concerning in stove combustion because the majority of PM is sub-micron and the sampling probes are located in positions where steady state flow is established. Alternative methods such as light scattering and differential mobility spectrometry offer greater sensitivity for smaller particle sizes and online measurements. However, the use of gravimetric analysis means that samples can be chemically tested for EC/OC, and also used in inorganic digestions and scanning electron microscopy (SEM).

Impactors were used for the majority of PM emission measurements which conforms to BS EN ISO 23210:2009. This method is used for low concentration measurements of PM10-2.5 from stationary source emissions. Dekati 3-stage impactors were used which samples from the dilution tunnel, see Fig. 3.20 or 3.21, at a rate of 10 L min^{-1} ($\pm$10%). The sample is drawn through a nozzle and using momentum inertia separates particles into 4 size bandwidths: >10μm, 10-2.5μm, 2.5-1.0μm and <1.0μm. The separation mechanism is shown in Fig. 3.24. Using the dilution factor described in section 3.5.5.1 an emission factor can be calculated.

The other method used was to sample directly from the flue stack using an Oliver and Richards exhaust smoke metre. The smoke metre is more flexible in

operation because filter papers can be changed rapidly so it is not overloaded. This means emission factors for specific periods of combustion can be determined (e.g. flaming and smouldering). The filter papers and foils can be changed in the impactors but this requires a greater workload and is more time consuming.

Samples were drawn through a 4mm nozzle from the centre of the flue stack. The gas was transferred along a Teflon coated heated line (120°C) into the smoke metre unit. Using glass fibre or micro-quartz filters in duplicate (two filters back-to-back) the flue gas flows through the paper and particles are filtered out. The filter is housed in a heated block at 70°C throughout the duration of sampling, this prevents low volatile tar and hydrocarbons from condensing. The volume of flue gas that flows through the filter papers is measured with a separate gas meter.
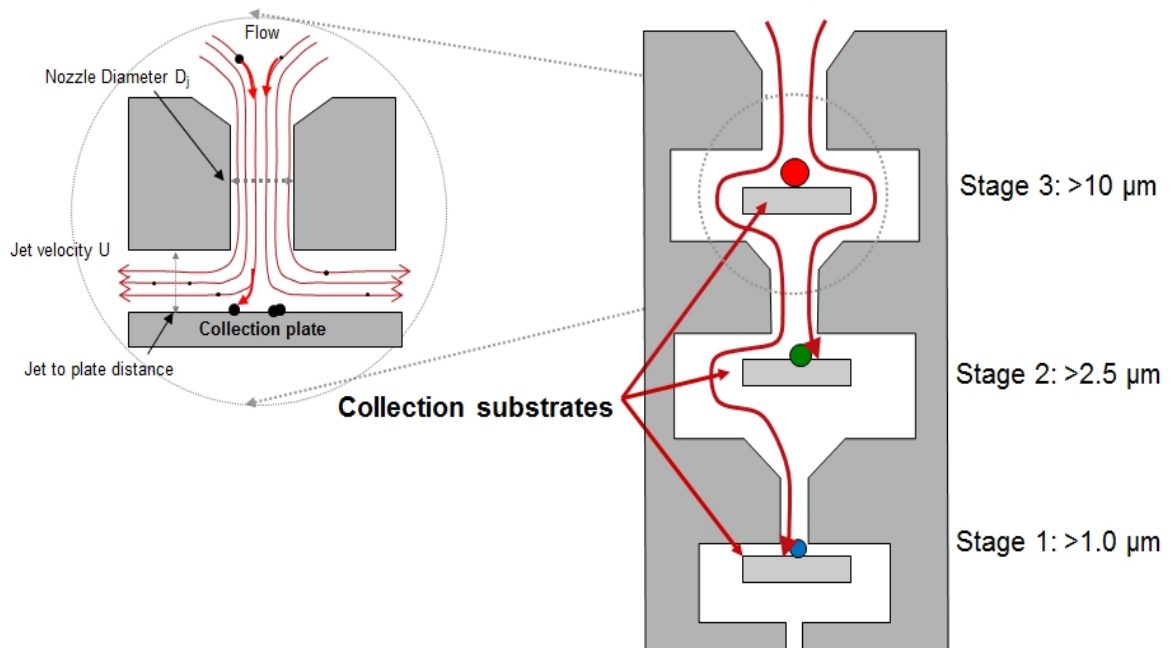
Figure 3.24: Separation mechanism of the Dekati 3-stgae impactors [Dekati, 2017]

3.5.5.3 Emission Concentrations

The units for the measurements are usually shown in ppm or Vol%. International standards require that the emission concentration is shown on a dry basis, at 13% O_2 concentration and at normal room temperature and pressure as shown by Eq. 3.11.

$$C_i \text{ (ppm or Vol\%)} = C_i \times \frac{273 + T_f}{273 + T_P} \times \frac{P}{1013} \times \frac{21 - O_{2,S}}{21 - O_{2,i}} \times \frac{100}{100 - M_c} \quad (3.11)$$

Where C_i is the concentration of species i, T_f is the temperature of the flue gas, T_P is the standard temperature of air (0°C), P is the absolute flue gas pressure, $O_{2,S}$ is the industry standard oxygen concentration (13%), $O_{2,i}$ is the measured oxygen concentration and M_c is the moisture content. This concentration is then converted to mg of emission per m³ of flue gas using Eq. 3.12.

$$C_i \text{ (mg m}^{-3}) = C_i \text{ (ppm)} \times \frac{M_{mol}}{V_{m,S}} \quad (3.12)$$

Where M_{mol} is the molecular mass of the species (i.e. for CO_2 it is 44.01 g mol⁻¹) and $V_{m,S}$ is the molar volume at standard/normal room temperature and pressure (22.4 l).

3.5.5.4 Emission Factors

Calculation of emissions factors (g kg⁻¹ or g GJ⁻¹) is a complex subject and is the main reason for large variations in reported data from literature. EFs on a mass-basis are per kg of dry fuel and on an energy-basis is per GJ of fuel based on the HHV. Within this work two methods of calculation were used:

1. The Specific Dry Flue Gas Volume (SDFGV) method- this method was developed by the AEA for conversion of industrial biomass boiler emission concentrations [AEA, 2012]. This method was used to calculate the emission factors for the gaseous products. Eq. 3.13.

$$EF_i = \frac{C_i \times SDFGV}{1000} \quad (3.13)$$

The SDFGV must be defined at standard temperature and pressure, and corrected for the oxygen concentration.

2. The Total Flow method- this is a scientific method developed to consider the physical combustion properties. This method was used to calculate the emission factors for the particulates. Eq. 3.14.

$$EF_i = \int_{t_0}^{t} \frac{C_i \times Q}{\dot{m}} \, dt \quad (3.14)$$

Where Q is the volumetric flue gas flow rate and $\dot{m}$ is the mass of fuel burnt between t and t_0.

The SDFGV method uses the proximate and ultimate analysis of the fuel to determine the stoichiometry of combustion, volume of flue gas produced from a kilogram or gigajoule of fuel. Whereas the total flow method is an integration of the conversion of fuel to flue gas.

The main advantage of the SDFGV method is that it is relatively simple and effective when comparing between different fuel types. Throughout this work the focus was on the impacts of chemical composition on the emissions produced and to reduce influence of physical properties, therefore the SDFGV method was very useful in analysis. However, the SDFGV is limited by the lack of consideration to the actual combustion process, this is particularly evident when analysing PM emissions. For this reason, the total flow method is used in the analysis of PM.

3.5.5.5 Balance (Burning Rate)

The stove is positioned on a KERN DE 300K5DL balance in the centre of the trihedron. The mass of the stove is recorded online at 1-minute intervals and the change in mass over time is the burning rate.

3.5.5.6 Temperature

Temperature measurements were made using K-type thermocouples positioned at multiple points around the stove. The measurements were made every second by an automated system using a PicoLog bank and software. Positioning of the thermocouples around the stove are shown in Fig. 3.25.
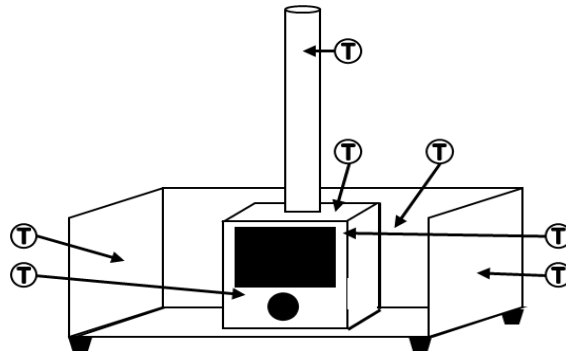
Figure 3.25: Positioning of the thermocouples around the stove test facility

3.5.5.7 Flow Measurements

The dynamic pressure in the flue stack was measured using a S-type Wöhler DC 100 Pressure computer. Initially these measurements were taken every minute manually (Chapters 4 and 5) however in the latter work this was automated (Chapters 6 and 7). The dynamic pressure is then converted to a velocity by Eq. 3.15 at the position of the pitot tube in the flue stack.

$$v = 23.96 \times \sqrt{\frac{\Delta P}{1.4} \times \frac{T}{P_{abs}} \times \frac{1}{\rho_{wet\ flue\ gas}}} \quad (3.15)$$

Where ΔP is the dynamic pressure, P_{abs} is the absolute pressure, T is the flue gas temperature and $\rho_{wet\ flue\ gas}$ is the density of the wet flue gas (assumed to be 1).

3.5.5.8 Assessment of Stove Performance

In order to assess how complete combustion is termed the Modified Combustion Efficiency (MCE) and how much fuel is burnt, the extent of combustion, Eqs. 3.16 and 3.17 are used.

$$Modified\ Combustion\ Efficiency = \frac{Emissions\ of\ CO_2}{Emissions\ of\ CO_2 + Emissions\ of\ CO} \quad (3.16)$$

$$Extent\ of\ Combustion = \frac{Mass\ of\ Fuel\ Input_{daf} - Mass\ of\ Fuel\ at\ the\ End_{daf}}{Mass\ of\ Fuel\ Input_{daf}} \quad (3.17)$$

3.6 Experimental Methods for Pre-treatment

3.6.1 Torrefaction

All torrefaction work was undertaken to produce a torrefied solid sample; no analysis of the gaseous or tar products was undertaken. Torrefaction was performed in a bench top EliteTMH12/75/750 tube furnace. The tube furnace is divided into 3 zones controlled by 3 Eurotherm controllers. A thermocouple monitors the temperature in each zone. A borosilicate glass tube filled with 200g (±30g) of biomass was loaded into the electric furnace per experiment. The sample is positioned in the centre of the tube between two plugs of glass fibre wool, Fig. 3.26. Nitrogen flows at 1.2 L min^{-1}

through the tube throughout the torrefaction process, the flow is controlled by a static flow meter, this is to ensure an inert environment in the tube. The biomass was heated to 150°C at a ramp of 10°C min^{-1} and held for 60 minutes, this was to remove moisture. The temperature was then raised to 270°C at the same heating rate and held for 30 minutes. The sample was removed from the furnace immediately at the end of the process and remained in a nitrogen atmosphere, this was important to prevent any further reactions. The cooling process still takes a significant amount of time to reach a temperature where reactions stop, this is approximately 15 minutes but is dependent on the biomass type. Additionally, the temperatures recorded by the thermocouples shows that the centre of the furnace is up to 20°C hotter than the programme temperature, this is due to exothermic reactions and thermal insulation in the furnace.
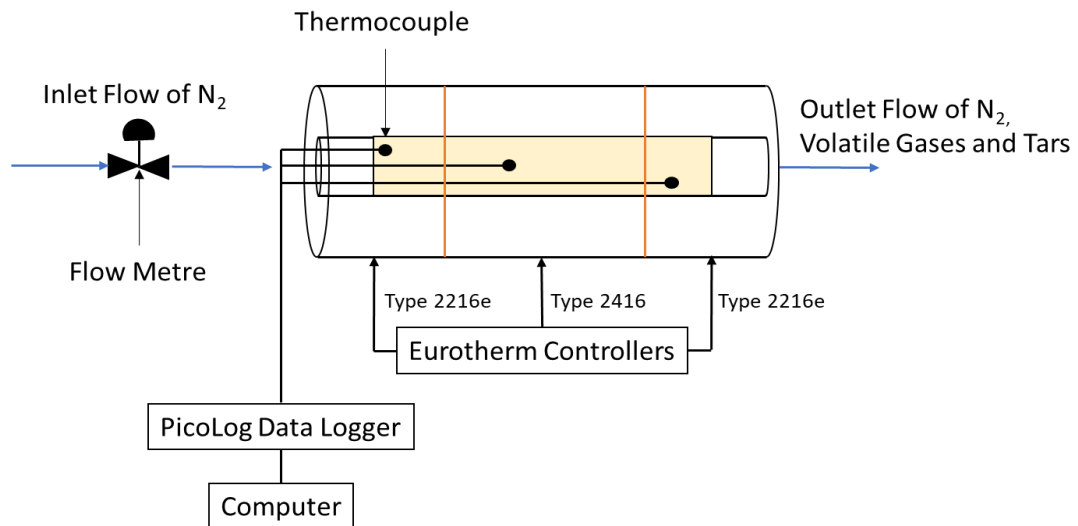
Figure 3.26: Schematic of torrefaction furnace

The conversion of biomass in torrefaction is described predominately by two terms, the mass yield and the energy yield, these are described by Eq. 3.18 and 3.19.

$$Mass\ Yield, \eta_m = \left(\frac{m_{char}}{m_{feed}}\right)_{daf} \times 100 \quad (3.18)$$

$$Energy\ Yield, \eta_E = \left(\frac{HHV_{char}}{HHV_{feed}}\right)_{daf} \times \eta_m \quad (3.19)$$

Where m_{char} is the mass of torrefied product out, m_{feed} is the mass of material input, HHV_{char} is the energy content of torrefied product and HHV_{feed} is the energy content of the material input.

3.6.2 Washing

Washing pre-treatment was based on previous work by Gudka et al. [2016]. Washing methods are designed to remove fine material and leach inorganic elements using distilled water. A rotating drum mechanism was used in a Xtreme Tumblers Rebel 17 Rock tumbler, Fig. 3.27, this instrument is typically used in the polishing of gems and stones for jewellery. The drum is made from powder coated steel with a rubber lining. It is suspended on a pair of parallel rollers held in place by two rubber coated hardened PVC stops. The drum has a rotation speed of 40 RPM.

Figure 3.27: Rebel 17 Rock tumbler

Biomass was loaded into the rock tumbler drum at a ratio of 1:2 to distilled water by volume (approximately 400g (±15g) willow chip to 800g (±10g) of water) and rotated for 20 minutes. After being rotated the biomass and leachate mixture was separated while wet using a series of clarification stages as shown in Fig. 3.28. This separated the washed biomass, fine sediment material and the aqueous phase. This washing procedure was repeated eight times, and all the bulk and fines fractions were

combined. The three products were analysed using a series of methods, Table 3.4, to determine the composition.

>25mm

25mm>x>4mm

>200μm

Leachate
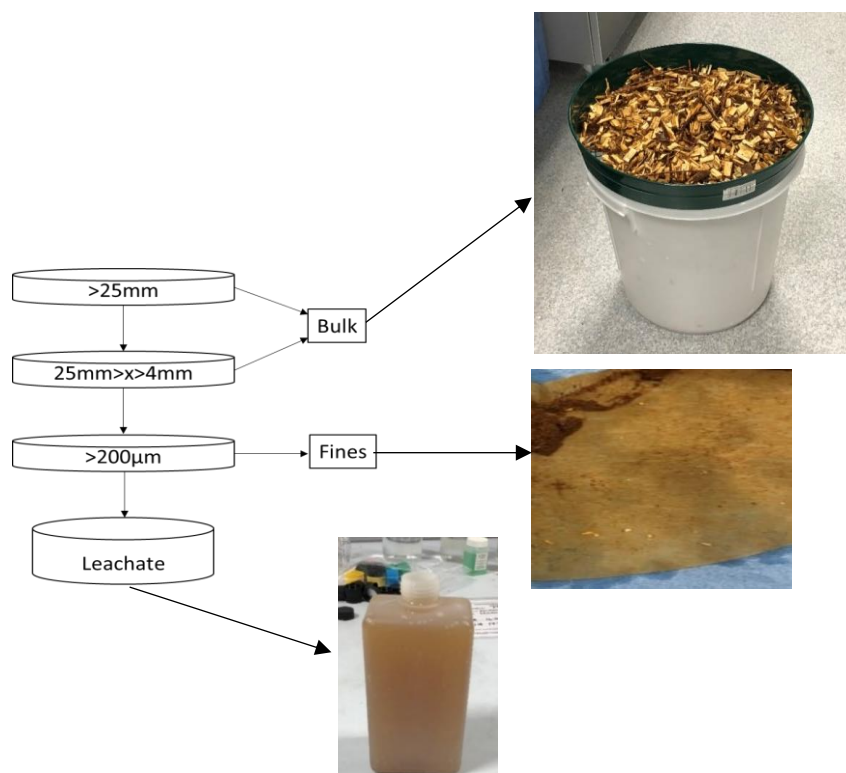
Bulk

Fines

Figure 3.28: Clarification process to distinguish three products from washing

Table 3.4: Analytical methods for each product

Bulk	Fines	Leachate
Proximate	Proximate	IC
Ultimate	Ultimate	ICP-MS
Metals-SOCOTEC	Metals- University of Leeds	TOC
		pH

After washing the bulk and fines, samples were left to dry in a fume cupboard at room temperature for 24 hours, this brought the moisture content down to less than 20 wt.%. The material was then placed in the drying ovens as specified in section 3.3.1. The leachate was immediately bottled and stored in the fridge until analysis, the pH of the leachate was recorded every 24 hours to monitor the condition of the sample. Analysis was within 72 hours of generating the sample.

3.6.2.1 Bulk Biomass Sample

As mentioned in Table 3.6, the collated bulk sample was analysed at the University of Leeds for proximate and ultimate composition as specified in sections

3.4.1 and 3.4.2 respectively. The metals analysis was conducted at SOCOTEC labs as specified in sections 3.3.4.2 and 3.4.5.

3.6.2.2 Fines Sample

Proximate and ultimate analyses were conducted as specified in sections 3.4.1 and 3.4.2. The metals were analysed at the University of Leeds using the acid digestion method as specified in section 3.3.4.1 and then using ICP-MS for its increased sensitivity as specified in section 3.4.5.

3.6.2.3 Leachate Sample

The leachate was kept separate from each run. This was so the reproducibility of the washing processes could be assessed. For leachate samples, Ion Chromatography (IC), see section 3.4.3 for IC make and model, was used for identification of some metals and inorganics. IC works by separating (Cat- or An-) ions using a resin (stationary phase) and an eluent (mobile phase), see Table 3.5 for details. The resin contains the opposite charge to the ions being measured, an ion exchange reaction takes place between ions in the sample and ions on the resin. Next the eluent is passed through the column and releases the sample ions which are bonded to the resin. Depending on the time it takes for the ions to pass through the column to the conductivity detector, the species can be determined and the quantity using standards. Important factors which limit the validity of the results include the pH of the solution, the selection of the eluent and the purity of the solution (fine material can block the column). IC has a detection limit in the ppb range; however, solutions usually have to be diluted to protect the column. Whenever the sample is diluted a repeat at a different dilution concentration should be used to ensure samples are within the detection limit and provide enough sensitivity for more precise analysis. Overall IC has a distinct advantage over ICP methods because it is highly selective, has a high separation efficiency and can tolerate different sample matrices.

Table 3.5: Details of IC instrument

	Anions	Cations
Column	Ion Pac AS14A (4 x 250mm)	Dionex IonPac CS12A (250 x 4mm) column
Eluent	$Na_2CO_3/NaHCO_3$ (8mMol/1mMol)	methyl sulphonic acid solution (1.0nN)

The samples run through both instruments were diluted by 1-part sample to 20 parts deionised water. This was because of the high potassium, calcium, acetate,

phosphate and nitrate concentrations. The IC columns have an optimal range which varies based on the instrument and the sample. If the separation column becomes saturated, then the sample is not sufficiently separated and the results will skew.

For the TOC measurements, samples were diluted 1-part sample to 4 parts deionised water. This was for the same reasons as with the IC, discussed in the previous paragraph. Samples are loaded into an automated sampler, which injects a small amount of sample into a flame. The combustion characteristics and volume of sample injected gives the measurements for the organic and total carbon with the remainder being inorganic carbon (e.g. carbonates). The TOC model is a Hach Lange IL550 TOC/TIC.

For ICP-MS, see section 3.4.5 for details on the analytical method, the samples were loaded into the instrument as collected, no dilution so that elements present in low concentrations could be determined. ICP-MS ionises the sample and then feeds this into the mass spectrometer. This is a fast and accurate technique that can measure multiple metals and non-metals with a small sample and low concentrations. The issue with ICP-MS is small changes in some factors can cause large inaccuracies in the results, these include air contaminating the carrier gas, carbon loading onto the ICP and argon used in the ionisation process inflicting background interference on the detectors. However, for the analysis of leachate it is very robust and accurate.

The analysis for pH was necessary to determine the factors which could be influencing leaching. It is well documented in literature that acidity aids the leaching of elements such as Zn, Na, Ca and K [Deng, Zhang and Che, 2013] [Carillo, Staggenborg and Pineda, 2014] [Yu et al., 2014]. The Apera pH meter is often used in river water sampling. It uses three standard solutions to first calibrate before taking a measurement. The instrument is specially designed to cope with the influence of solid material and lack of water clarity. Colorimetry techniques are typically used in British standards for water pH measurements however these techniques are not applicable in these experiments because of leachate colour as shown in Fig. 3.26.

3.7 Conclusions

In order to summarise, Table 3.6 shows the fuels that have been analysed and the analytical methods that have been used. All of the methods have been discussed in more detail throughout this chapter.

Table 3.6: Matrix of experiments

Chapter 4							
Experiment		**Spruce**	**Torrefied Spruce**	**Willow**	**Torrefied Willow**	**Olive**	**Torrefied Olive**
Fuel Supplied as	Logs	✓		✓			
	Briquettes		✓		✓	✓	✓
	Loose						
	Chipped						
Size Reduction	Cutting Mill (<4mm)	✓	✓	✓	✓	✓	✓
	Cryomill (<100μm)	✓	✓	✓	✓	✓	✓
Proximate	British Standard	✓	✓	✓	✓	✓	✓
	TGA						
Ultimate		✓	✓	✓	✓	✓	✓
Chlorine	IC						
	External Analysis (SOCOTEC)	✓	✓	✓	✓	✓	✓
Minor Metals	ICP-MS						
	External Analysis (SOCOTEC)	✓	✓	✓	✓	✓	✓
Trace Metals	ICP-MS						
	External Analysis (SOCOTEC)						
Stove Combustion	FTIR Gas Analysis	✓	✓	✓	✓	✓	✓
	Particulates (Smoke Metre)	✓	✓	✓	✓	✓	✓
	Particulates (Impactors)						
	Bottom Ash Metals Analysis						
Py-GC-MS		✓	✓	✓	✓	✓	✓

	Chapter 5				
Experiment		**Coffee Logs**	**Mexican Robusta Beans**	**Brewed Mexican Robusta Beans**	**Willow Wood Logs**
Fuel Supplied as	Logs				✓
	Briquettes	✓			
	Loose	✓	✓	✓	
	Chipped				
Size Reduction	Cutting Mill (<4mm)	✓	✓	✓	✓
	Cryomill (<100mm)	✓	✓	✓	✓
Proximate	British Standard	✓	✓	✓	✓
	TGA				
Ultimate		✓	✓	✓	✓
Chlorine	IC	✓	✓	✓	✓
	External Analysis (SOCOTEC)				
Minor Metals	ICP-MS	✓	✓	✓	✓
	External Analysis (SOCOTEC)				
Trace Metals	ICP-MS				
	External Analysis (SOCOTEC)				
Stove Combustion	FTIR Gas Analysis	✓	✓	✓	✓
	Particulates (Smoke Metre)				
	Particulates (Impactors)	✓	✓	✓	✓
	Bottom Ash Metals Analysis				

	Experiment		Bracken	Brackettes	Wheat Straw	Barley Straw	Miscanthus	Wood Briquettes	SRC Willow
				Chapter 6					Chapter 7
Fuel Supplied as		Logs							
		Briquettes		✓	✓	✓	✓	✓	
		Loose	✓						
		Chipped			✓	✓	✓		✓
Size Reduction		Cutting Mill (<4mm)	✓	✓	✓	✓	✓	✓	✓
		Cryomill (<100mm)	✓	✓	✓	✓	✓	✓	✓
Proximate		British Standard	✓	✓	✓	✓	✓	✓	✓
		TGA							✓
	Ultimate		✓	✓	✓	✓	✓	✓	✓
Chlorine		IC			✓				
		External Analysis (SOCOTEC)	✓	✓					✓
Minor Metals		ICP-MS			✓	✓	✓	✓	✓
		External Analysis (SOCOTEC)	✓	✓					✓
Trace Metals		ICP-MS			✓	✓	✓	✓	✓
		External Analysis (SOCOTEC)	✓	✓					✓
Stove Combustion		FTIR Gas Analysis	✓	✓	✓	✓	✓	✓	✓
		Particulates (Smoke Metre)							
		Particulates (Impactors)	✓	✓	✓	✓	✓	✓	✓
		Bottom Ash Metals Analysis							✓
TGA		Combustion	✓						
		Pyrolysis	✓						
	Single Particle Combustion		✓						
Pre-Treatment		Washing							✓
		Torrefaction							✓

114

Chapter 4. Comparison of the Combustion Emissions and Performance from Various Biomass and their Torrefied Counterparts in a Domestic Stove

4.1 Introduction

Replacement of coal combustion has been an objective since the 1980's because of acid rain and smog related issues. In 2019 global coal energy generation fell by 3%, the highest on record [Myllyvirta, Jones and Buckley, 2019]. This was because of large decreases in coal usage in Europe and the US whilst big coal users China and India kept usage stable and even a small reduction in the latter [Myllyvirta, Jones and Buckley, 2019].

The replacement of coal by biomass continues to be an area of high research activity. Within this research torrefaction is an area of priority. The objective of torrefaction is to homogenise the fuel composition, reduce the moisture, increase the energy density and produce a fuel with physical properties similar to coal so existing technology can be used. This is particularly important for grinding and milling where the more elastic properties of biomass require significantly more energy for size reduction.

Replacement of large-scale coal power generation has been largely by gas, solar and wind, this is mainly because of the high costs associated with abatement technology, maintenance and fuel preparation for solid fuel combustion [Thomas, Hook and Tighe, 2019] [Breeze, 2014]. However, domestic usage of solid fuels is increasing. In the UK, domestic stove appliances have been on the rise since 2005 because of their appealing aesthetic appearance and direct heating incentives [DEFRA, 2018].

Domestic stove combustion has since been found to be a major contributor to increased particulate matter (PM) concentrations. A report by Font and Fuller [2017] for DEFRA found that wood burning on open fires and stoves was responsible for 31% of $PM_{2.5}$ in urban areas of London and 38% of PM emissions across the UK. Health conditions related to increased PM concentrations in immediate and local air quality studies has shown concerning correlations with increased risks of cancer, irreversible

lung conditions and neurological damage [Valvanidis, Fiotakis and Vlachogianni, 2008] [Bølling et al., 2009] [Orasche et al., 2013] [Mukhopadhyay et al., 2012].

Past research has shown that torrefaction can reduce PM emissions by removing soot forming components [Mitchell et al., 2016] [Trubetskaya et al., 2019]. Formation of soot particles is a complex process and many routes exist based on various combustion parameters and fuel chemical composition [Torvela et al., 2014] [Lamberg et al., 2013]. Different organic products from biomass pyrolysis have different influences on certain soot formation routes [Atiku et al., 2016]. Using the fingerprint method, comparisons between raw and torrefied fuels has shown that torrefaction can completely remove or substantially reduce the concentrations of some of the known soot forming compounds [Atiku et al., 2017] [Akinrinola, 2014] [Ramos-Carmonal et al., 2017].

The aim of this chapter is to demonstrate the direct improvements from torrefaction by combusting a biomass fuel and its torrefied counterpart on a domestic stove. Within literature many comparisons have been made. However, this work furthers that by comparing resultant emission profiles between the original and torrefied forms. Some fingerprint characterisation analysis (Py-GC-MS) was also used to help understand and interpret the measured emissions.

4.2 Materials and Experimental Methods

4.2.1 Sample Preparation

The sample fuels studied were detailed in Chapter 3, section 3.2.1. All fuels were supplied from external sources and were in briquetted and log form when received. For proximate analysis, ultimate analysis and Py-GC-MS, samples were milled according to methods described in 3.3.2. Because of the form in which the fuels were supplied, a small amount of each sample had to be milled in the Jaw Crusher (briquetted fuels) or sawn (logs) before being milled. For Ultimate analysis and Py-GC-MS, the sample had to be cryomilled as well before analysis. For stove combustion tests the samples were tested as supplied as would be the case in a real domestic situation.

4.2.2 Experimental Methods

Proximate analysis, ultimate analysis and Py-GC-MS were conducted as stated in sections 3.4.1, 3.4.2 and 3.5.3 respectively. Stove combustion studies were conducted in accordance with 3.5.5 with a few specific details:

- Each batch consisted of 0.7-0.9 kg of fuel. This was subject to higher levels of variation with the log fuels compared to the briquetted fuels because of the limits on their size and shape.

- Each combustion run was ignited using 50g of Zip High Performance kerosene-soaked firelighters with a single batch of fuel from room temperature.

- The data from the ignition batch was excluded because of the influence of the firelighters.

- Gaseous emissions were analysed from measurements by the FTIR with the exception of NOx which was by the Testo because of the interference around the NOx detection signal in the FTIR.

- Gas emissions data was analysed using the SDFGV method because this considers compositional properties of the fuel over operation parameters.

- PM emission factor analysis was solely by the use of the smoke metre and direct sampling from the flue using Munkter 50mm micro-quartz filters. Particle size analysis was by the Dekati Impactors sampling 4500mm from the top of the stove in the dilution tunnel- Fig. 3.18.

- Only when the batch mass was below 30% of the original mass was a new batch loaded.

4.3 Results and Discussion

4.3.1 Proximate and Ultimate Analysis

Results for the proximate and ultimate analysis as well as some inorganic analysis (Cl, K and Ca) and the higher heating values (HHV) are shown in Table 4.1. The effects of torrefaction are evident, Table 4.1, on the composition when comparing the torrefied fuel and the untreated fuel. Past research has shown that torrefaction decreases the moisture and volatile matter but concentrates the ash and fixed carbon [Akinrinola, 2014]. Moisture is removed during two phases of torrefaction, the

majority is removed during drying at around 100°C, the rest is removed as the material dehydrates and volatiles are emitted from the particle. The resulting amount of moisture is not dependent on the peak torrefaction temperature because moisture is reabsorbed once the samples are removed from the heat in equilibrium with localised vapour pressure [Bridgeman et al., 2010]. Torrefied fuels are hydrophobic because of the decomposition of OH functional groups which can bond with water hence they have much lower moisture contents than the untreated fuels.

The trend for the volatile concentration is W+O>S>T.W>T.S>T.O this is the exact inverse of the fixed carbon trend where T.O>T.S>T.W>S>W+O. The degree of torrefaction (extent of) can be defined using the work of Li et al. [2013] by the % loss in volatile matter from the parent wood. In this work the degree of torrefaction is highest for the torrefied olive (20.7%), followed by the torrefied willow (11.0%), and the lowest is the torrefied spruce (7.8%). This trend was anticipated because the torrefaction conditions were most severe for the torrefied olive with the hottest peak temperature and longest residence time (280°C, 100 minutes)- see Table 3.1.

Table 4.1: Proximate and ultimate analysis of the fuels studied

Sample	Spruce (S)	Torrefied Spruce (T.S)	Willow (W)	Torrefied Willow (T.W)	Olive (O)	Torrefied Olive (T.O)
Moisture (wt.%)^{ar}	18	4.6	10	7.6	14.8	6.4
Volatiles (wt.%)^{db}	77	71	82	73	82	65
Ash (wt.%)^{db}	0.4	1.0	1.0	2.8	1.2	4.9
Fixed Carbon^{a} (wt.%)^{db}	22.6	28	17	24	17	30
C (wt.%)^{daf}	51	58	49	56	56	70
H (wt.%)^{daf}	6.1	6.1	6.3	5.2	5.2	3.7
N (wt.%)^{daf}	0.27	0.49	0.56	0.64	0.50	0.56
S (wt.%)^{daf}	0.04	0.04	0.04	0.06	0.13	0.16
O^{a} (wt.%)^{daf}	42	35	44	38	38	27
Cl^{b} (wt.%)^{db}	0.04	0.01	0.06	<0.01	0.17	0.04
K^{b} (ppm)^{db}	840	1280	3295	3650	1600	1900
Ca^{b} (ppm)^{db}	980	8770	3050	6020	1000	4800
HHV^{c} (MJ kg^{-1})^{db}	19.70	23.03	18.98	21.25	21.51	25.34

$^{ar-}$ as received basis, $^{db-}$ dry basis, $^{daf-}$ dry ash free basis $^{a-}$ calculated by difference, $^{b-}$ measurement was by an external accredited laboratory, $^{c-}$ calculated using equation in section 3.4.4 from [Friedl et al, 2005]

Because of the nature of the fuels and the method of sampling the degree of variability and error is higher than those specified in the standard analytical method (±0.2%). This is especially significant for the volatile matter and carbon measurements of the torrefied olive fuel because it is blended with the non-torrefied form and speculate that the degree of torrefaction was non-uniform. The measured errors (±1 standard deviation) are shown in Table 4.2.

Table 4.2: Error measurements calculated by ±1 standard deviation

Sample	Spruce	Torrefied Spruce	Willow	Torrefied Willow	Olive	Torrefied Olive
Moisture (wt.%)^{ar}	±0.8	±0.5	±0.7	±0.2	±0.4	±0.7
Volatiles (wt.%)^{db}	±8	±5	±7	±3	±14	±22
Ash (wt.%)^{db}	±0.2	±0.4	±0.5	±0.7	±1.2	±0.4
C (wt.%)^{daf}	±3	±2	±1	±1	±3	±8
H (wt.%)^{daf}	±0.1	±0.2	±0.5	±0.6	±1.2	±0.1
N (wt.%)^{daf}	±0.10	±0.12	±0.21	±0.14	±0.24	±0.4
S (wt.%)^{daf}	±0.03	±0.03	±0.03	n/a	±0.10	±0.11

Comparing the volatile matter, fixed carbon and elemental carbon contents for the fuels in this work with data from the Phyllis2 database and previous work, the numbers are similar, Fig. 4.1. For the spruce fuel used in this study the volatile matter in both the raw and the torrefied was lower than the average from the Phyllis2 database; torrefaction conditions were the same, however the difference between the raw and torrefied is comparable (volatile matter ~7 wt.% daf, fixed carbon ~7 wt.% daf and carbon ~6 wt.% daf). The average for the willow from this work and the Phyllis2 database is within 1 wt.% daf. For the torrefied willow the torrefaction temperature was higher in the Phyllis2 database (300-308°C) compared to the fuel used in this work (250-260°C); the increased degree of torrefaction, explains the difference seen in Fig. 4.1 when comparing the two fuels.

For the olive stone, the volatile matter content and fixed carbon is between the value from Sánchez and Miguel [2016] and Volpe et al. [2016], but is closer in value to the latter. The latter is not just olive stone but a blend of olive stone, branches and leaves which are the common solid residue products in the farming of olives. For the torrefied olive, the comparative analysis between this work, Sánchez and Miguel

[2016] and Volpe et al. [2016] is more significant, since the untreated fuel was used to produce the torrefied products at the same peak torrefaction temperature. The degree of torrefaction is greatest in Sánchez and Miguel [2016] (31.4%), torrefaction at 300°C for 15 minutes, then this work (20.7%) and the lowest is from Volpe et al. [2016] (16.6%), torrefaction at 300°C for 30 minutes. However, the torrefied olive stone analysed in this work was a blend with the raw material meaning a pure torrefied product would have a higher degree of torrefaction. Additionally, the residence time and mixing can have an influence on the final product [Akinrinola, 2014].

Elemental chemical composition changes due to torrefaction are shown in the Van Krevelen diagrams in Figs. 4.2 and 4.3. The trend is that as the process severity is increased the points shift towards the bottom left-hand corner; this process is termed coalification. In Fig 4.2, data from Bridgeman et al. [2008] and Jones et al. [2012] for willow, and Sánchez and Miguel [2016] for olive, are shown for varying torrefaction conditions. The data points from this work for the spruce, torrefied spruce, willow and torrefied willow show strong similarities with those from the other work. The olive and torrefied olive show a similar trend in the direction the points move across the graph however, they are at much lower ratios; they are more enriched in carbon.

Fig. 4.3 from Granados et al. [2017] analyses the composition of a 2-staged torrefaction at various temperatures for poplar wood. The olive and torrefied olive, when plotted on Fig. 4.3, are more analogous with the trend from Granados et al. [2017]. Fig. 4.3 still suggests that the raw olive material has been subjected to some thermal pre-treatment which has resulted in the carbon being concentrated. On Fig. 4.3 biochar produced in Jones et al. [2012] at 1000°C in a helium environment is plotted along with charcoal studied in Mitchell et al. [2019]. Based on these additional points it is evident that the torrefied olive has started to form char and is on a trajectory to form either biochar or charcoal.
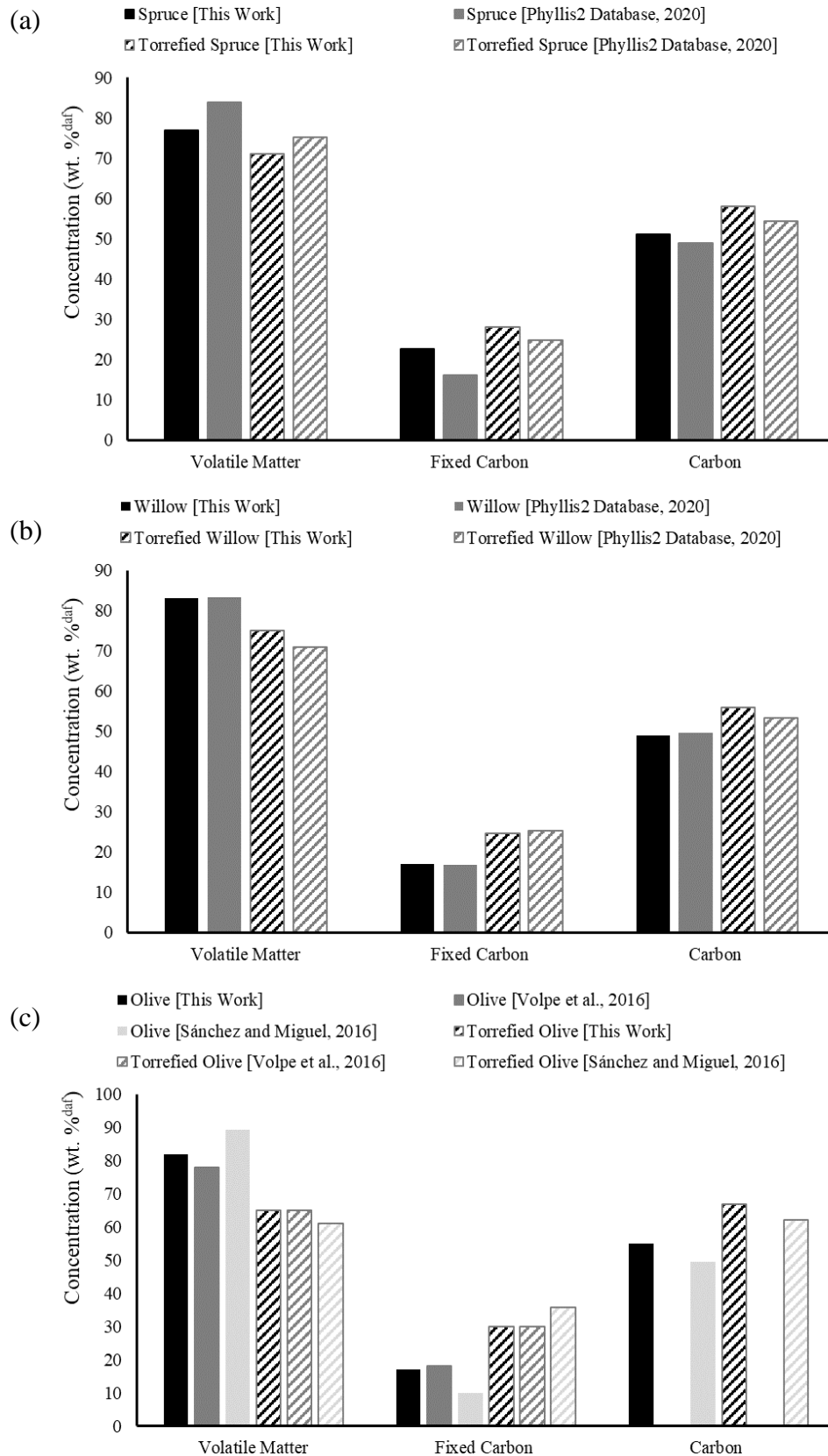
Figure 4.1: (a) Volatile matter, (b) fixed carbon and (c) carbon concentrations on a daf basis for the fuels studied compared to other measured values. Values for the Phyllis2 database are averages.
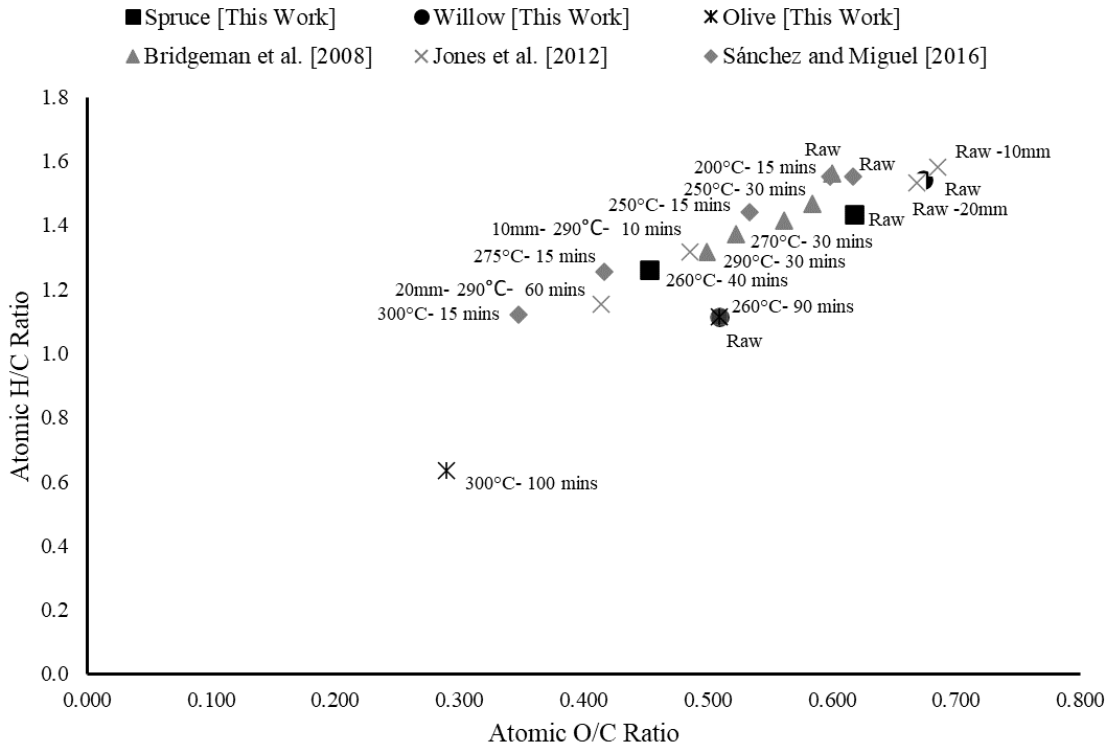
Figure 4.2: Van Krevelen of fuels studied in this work compared to willow in Bridgeman et al. [2008], willow in Jones et al. [2012] and olive stone in Sánchez and Miguel [2016]
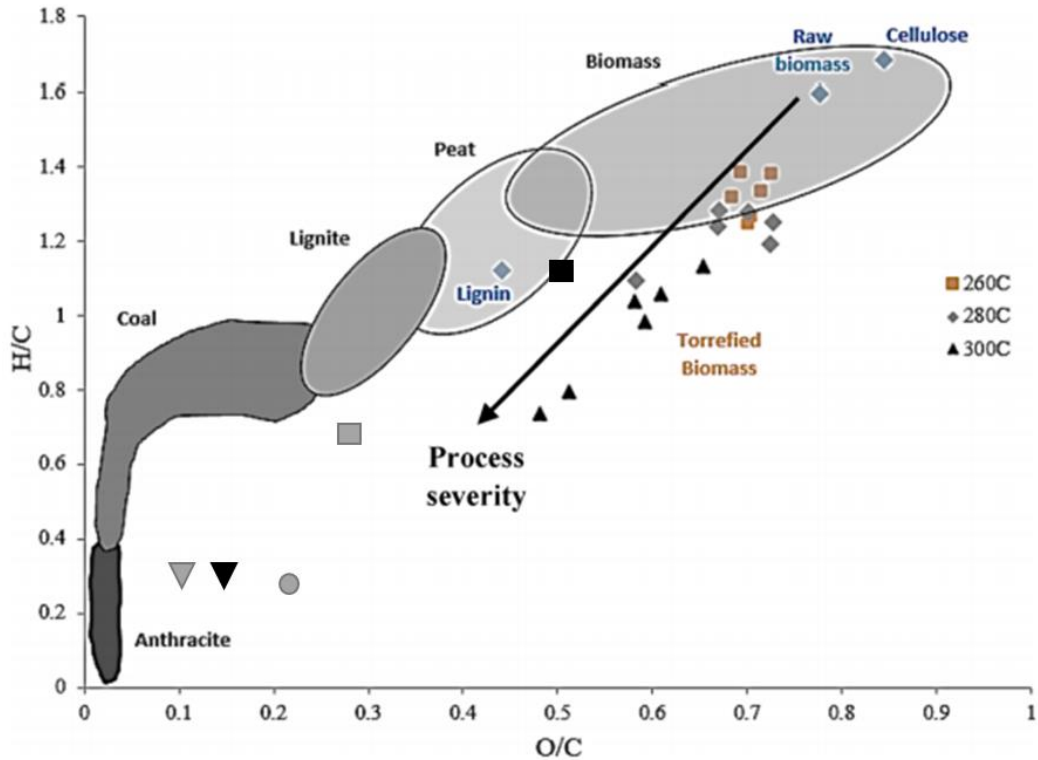
Figure 4.3: Van Krevelen from Granados et al. [2017] ■ Olive [This Work] ■ Torrefied Olive [This Work] ▼ Willow Char 10mm particle size [Jones et al., 2012] ▼ Willow Char 20mm particle size [Jones et al., 2012] ● Charcoal [Mitchell et al., 2019]

Comparing the torrefied forms to the raw fuels, the nitrogen content is higher in all of the thermally treated fuels, Table 4.3. This is the same conclusion as Akinrinola [2014] for torrefaction of different native Nigerian biomass torrefied at temperatures between 260-300°C for 15-60 minutes. When analysing the N to C ratio there is no discernible trend besides in the work of Bridgeman et al. [2008]. The final column of Table 4.3 shows the N content on an energy basis. Based on the fuels in this work and the results from Bridgeman et al. [2008] once the torrefaction temperature exceeds 250°C the increase in energy content is greater than the nitrogen content. This means on an energy basis the nitrogen content of the torrefied olive is lower than in the raw olive material.

Table 4.3: Comparison of nitrogen content between untreated and torrefied fuels from this work, Bridgeman et al. [2008] and Sánchez and Miguel [2016]

			N (Wt. %)[daf]	Atomic N/C	HHV (MJ kg^{-1})[db]	N (kg GJ[-1])[db]
This Work	**Spruce**		0.27	0.0053	19.70	0.14
	Torrefied Spruce		0.49	0.0072	23.03	0.21
	Willow		0.56	0.0098	18.98	0.30
	Torrefied Willow		0.64	0.0098	21.25	0.30
	Olive		0.5	0.0077	21.51	0.23
	Torrefied Olive		0.56	0.0069	25.34	0.22
Bridgeman et al. [2008]	**Willow**	**Raw**	0.2	0.0034	20.00	0.10
		230°C	0.2	0.0034	20.20	0.10
		250°C	0.2	0.0033	20.60	0.10
		270°C	0.2	0.0032	21.40	0.09
		290°C	0.1	0.0016	21.90	0.05
Sánchez and Miguel [2016]	**Olive Stone**	**Raw**	0.4	0.0069	21.05	0.19
		200°C	0.3	0.0051	20.99	0.14
		250°C	0.2	0.0032	21.99	0.09
		275°C	0.4	0.0059	24.64	0.16
		300°C	0.3	0.0041	25.79	0.12

Compositional changes in the C, H and N concentration will impact on the HHV calculated using Eq. 3.7 from Friedl et al. [2005], Table 4.1. The HHV rank in the order of T.O>T.S>O>T.W>S>W (25.34, 23.03, 21.51, 21.25, 19.70, 18.98 MJ kg^{-1} db respectively).The difference between the untreated and torrefied forms are 3.33, 2.27 and 3.83 MJ kg^{-1} db for the spruce, willow and olive respectively. The difference in the C contents between the raw and torrefied forms suggests that the difference in the HHV of the olive fuels should be much larger than the spruce or willow (difference

in C content of 14 wt.% daf compared 7 wt.% daf). This is explained by the loss of H which is significantly lower in the torrefied olive. Past work [Bridgeman et al. 2008] [Sánchez and Miguel, 2016] [Jones et al., 2012] [Akinrinola, 2014] has not seen such significant compositional differences upon torrefaction. This is analogous with the conclusions from the Van Krevelen diagrams, Figs. 4.2-3, that suggest the torrefied olive has started to form char.

4.3.2 Stove Combustion

The results for the stove combustion experiments are discussed in this section. The results are split into sections based upon their objective measurement parameters.

4.3.2.1 Burning Rate and Temperature

Combustion of solid fuels is split into three key phases: ignition, flaming and smouldering. As previously mentioned, this work is not concerned with ignition because of the influence of firelighters on starting the combustion runs. Defining when these phases occur is complex and previous work by Faschinger et al. [2017] has shown that multiple phases can exist and there is a significant amount of overlap between phases. These phases are also subjective to operator influence. Therefore, in order to minimise these factors and keep an ordered comparison between the fuels, flaming combustion is defined as when the burning rate is ≥ 0.85 kg h^{-1}, smouldering is a burning rate of < 0.85 kg h^{-1} but ≥ 0.3 kg h^{-1}, and combustion has ended when a mass of 200g of fuel remains (of the order of 25% of the initial dry mass of each batch).

Figs. 4.4a-c show the burning rate profiles for the spruce, willow and olive pairings respectively. Even though in Figs. 4.4a-c it appears that more fuel has been burnt in some experiments, all experiments burnt 4 batches of fuel (1 ignition and 3 reloads). Not all the batches are shown in Figs. 4.4a-c however a similar amount of fuel (within $\pm 10\%$) has been burnt for all the experiments. With the exception of the willow comparison, the torrefied form has a longer burning time per batch than the untreated form. The willow comparison differs because the torrefied willow are small briquettes and they disintegrate rapidly when exposed to the flame (larger surface area and greater porosity). The average batch burning time is ranked in the order of T.S (~55 mins) >S+T.O (~38 mins) >O+W (~32 mins) >T.W (~18 mins).
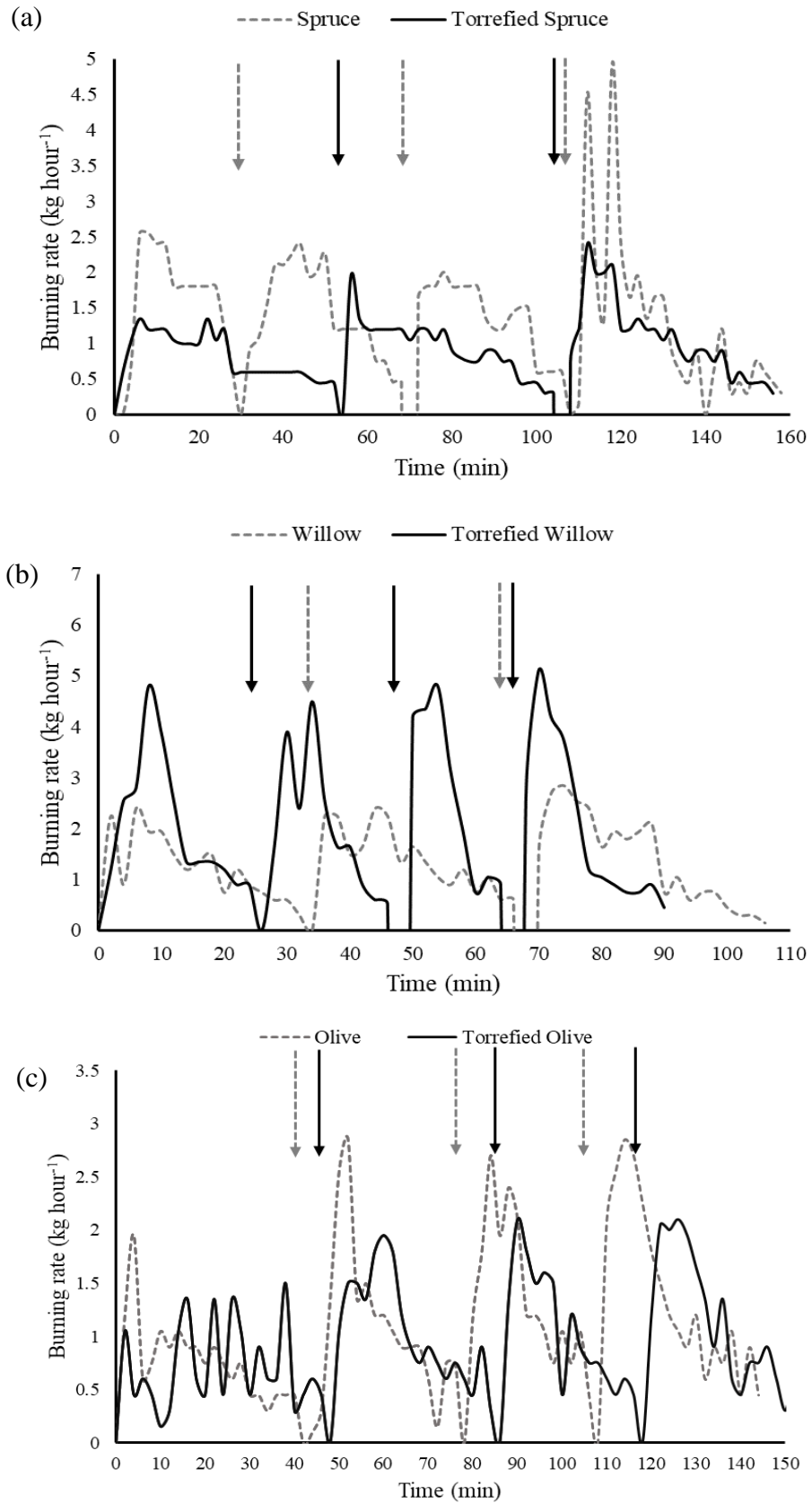
Figure 4.4: Variation of burning rate with time (a) spruce and torrefied spruce (b) willow and torrefied willow (c) olive and torrefied olive. Arrows indicate reloading points- this is consistent throughout this thesis. Not all fuel batches are shown for all the fuels.

For the spruce and olive comparisons, the raw profiles show a sharp peak which has a greater magnitude than the torrefied fuel after the reload. The torrefied fuel peaks are not as high in magnitude and are much broader. This is particularly noticeable for the olive (average peak height 2.75 kg h^{-1} and peak width 8 ± 3 mins) compared to the torrefied olive (average peak height 2.08 kg h^{-1} and peak width 17 ± 4 mins). For the willow the trend is reversed for the peak height, T.W (~4.2 kg h^{-1}) > W (~2.1 kg h^{-1}), however for the peak width the two fuels are very similar (~13 mins), this result is unexpected because the volatile matter content is over 10 wt.% db lower for the torrefied fuel. This result occurs because of the overlap in combustion phases in the torrefied willow described by Faschinger et al. [2017].

The broader and lower peak burning rates just after the fuel is loaded for the torrefied fuels is particularly noticeable in Fig. 4.4c for the torrefied olive. This could be from two factors: The first could be the rate of devolatilisation is lower in the torrefied fuels, this is because the fuel has already been partially devolatilised in the torrefaction process [Saddawi et al., 2011], or it could be because of the nature of the volatiles released, this is explored more in section 4.3.3 on Py-GC-MS.

It should be noted that binders and briquette density (or porosity) can have a large impact on the burning rate and in some cases can outweigh the fuel effects. No binders were used in preparation of the fuels in this study however the density did vary. Although this is discussed in more detail, related to emissions in section 4.3.2.2, it is evident from Figs. 4.4a-c and Table 3.1 that the more dense and harder briquettes have longer burning times and lower burning rates.

Table 4.4: Average burning rates for each fuel, average temperature in each combustion phase and the % of the initial batch mass when the combustion phase changes

Average burning rate, kg h^{-1}, flue gas temperature in parenthesis					
	Flaming		Smouldering		Average per load
Fuel	Average	% of initial mass	Average	% of initial mass	
Spruce	1.55 (225°C)	38 (±5)	0.67 (175°C)	15 (±3)	1.27
T. Spruce	1.19 (240°C)	35 (±3)	0.65 (180°C)	12 (±2)	0.94
Willow	1.86 (320°C)	27 (±3)	0.72 (255°C)	14 (±2)	1.41
T. Willow	2.85 (395°C)	21 (±3)	0.73 (325°C)	12 (±2)	2.30
Olive	1.41 (370°C)	40 (±6)	0.51 (300°C)	16 (±2)	1.24
T Olive	1.21(380°C)	43 (±2)	0.62 (300°C)	20 (±4)	1.02

Table 4.4 shows the average flaming and smouldering burning rate and the average flue gas temperature (measured 1.43m above the combustion zone) for each fuel (excluding ignition). Past work [Faschinger et al., 2017] [Mitchell et al., 2016] has shown that the volatile matter content is directly proportional to the burning rate during flaming combustion, this is because of homogeneous reactions in the gaseous phase above the fuel surface from devolatilisation. This trend is not clearly seen in this work as shown in Fig. 4.5. Comparing the torrefied spruce and torrefied willow, these are both briquetted wood fuels with low moisture contents (minimal influence) [Price-Allison et al., 2019] (4.6 and 7.6 respectively) and similar volatile contents (71 and 73 wt.% db respectively), however their average flaming burning rates are 1.66 kg h^{-1} different. This difference is from the physical structure of the fuels (Table 3.1) mainly the durability and the ease of disintegration as the fuel is heated and converted. The torrefied spruce held its structure throughout the entire batch until fresh fuel was loaded on top of it when it would break under the new fuel's weight. Whilst the briquette held its shape this reduced the surface area for combustion and lowered the surface area to volume ratio. This is the opposite to the torrefied willow mentioned previously which disintegrated on heating, increasing the surface area. It also explains why the torrefied willow has the hottest flaming combustion flue gas temperature (395°C).
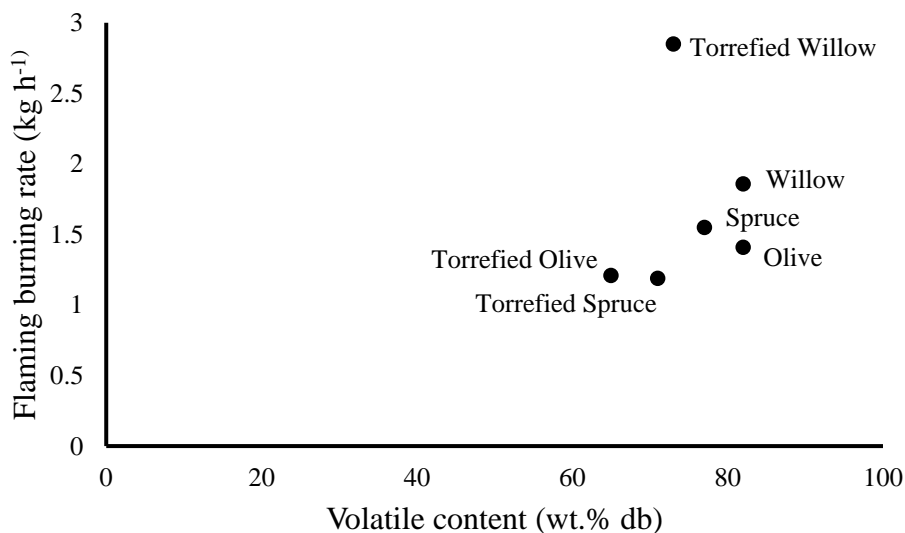
Figure 4.5: Plot of fuel volatile content and average flaming burning rate

Increases in fixed carbon can result in an increase in the smouldering combustion burning rate [Mitchell et al., 2016] which is observed in this work for the

willow, torrefied willow, olive and torrefied olive pairings, Fig. 4.6. For the spruce and torrefied spruce, the smouldering rates are similar, this can be attributed again to the physical structure of the torrefied spruce described earlier. The untreated willow and olive fuels have the same fixed carbon contents (17 wt.% db) but have a large difference in the smouldering combustion rate (0.72 and 0.51 kg h^{-1} respectively). Reasons for this are not clear especially considering the olive disintegrated faster and smouldered at a hotter temperature than the willow, but are most likely due to overlapping of combustion phases, reaction surface inhibitors/catalysts (ash) and inefficient air mixing in the combustion zone [Ozgen et al., 2014]. It should also be added that as discussed in section 3.5.5 there is a 10% margin of error, when applied to Fig. 4.6 (error bars) the changes seen are within the experimental error.
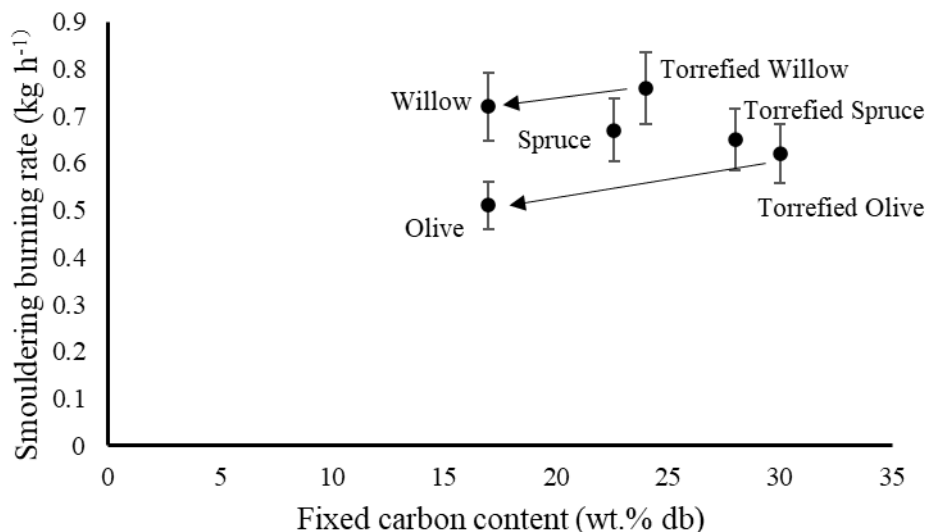
Figure 4.6: Plot of fuel fixed carbon content and average smouldering burning rate. Error bars are for a 10% experimental error.

4.3.2.2 Carbon Emissions

The majority of carbon-based emissions are as carbon dioxide (CO_2), carbon monoxide (CO) and methane (CH_4). Figs. 4.7a-f show the emission profiles for CO_2 and CO on a dry basis at 13% oxygen concentration (industry standard) and normal room temperature (20°C) and pressure. In all of the profiles t=0 is when the fire lighters were started and the stove door was closed, this first ignition batch differs because of the influence of kerosene combustion in the firelighters. The ignition batch is used to heat up the stove and create a hot fuel bed to reload new batches of fuel onto. Reload batches are indicated by arrows on the profiles.
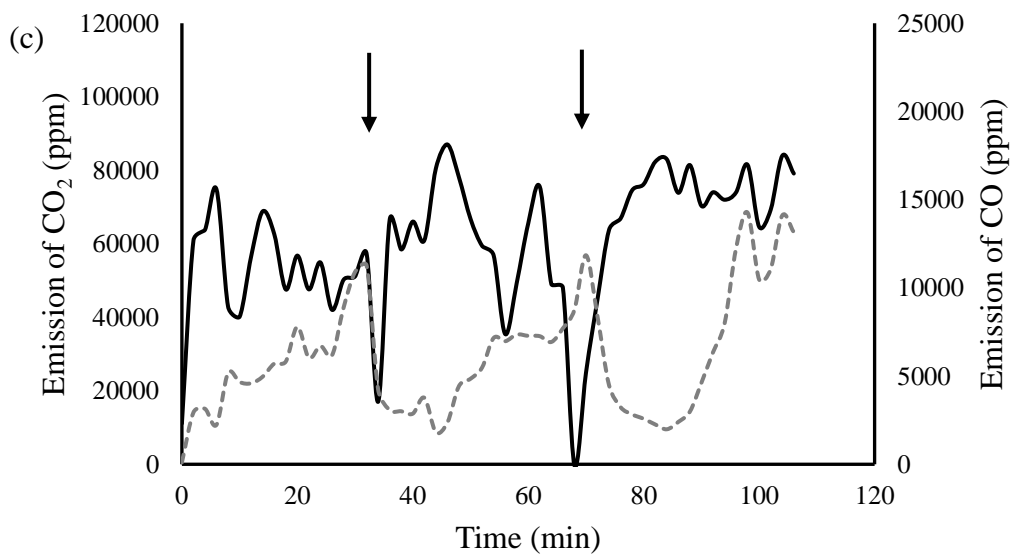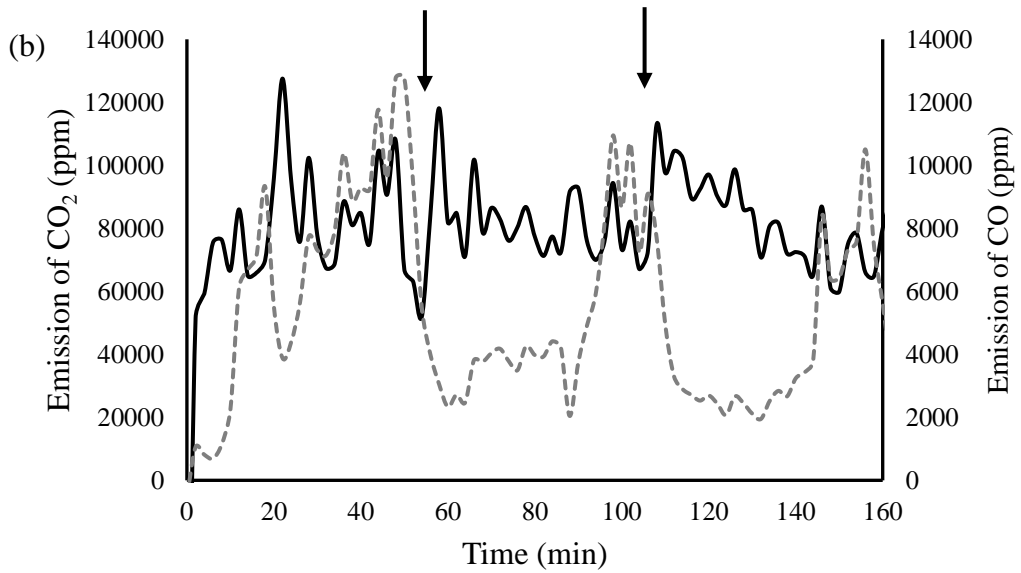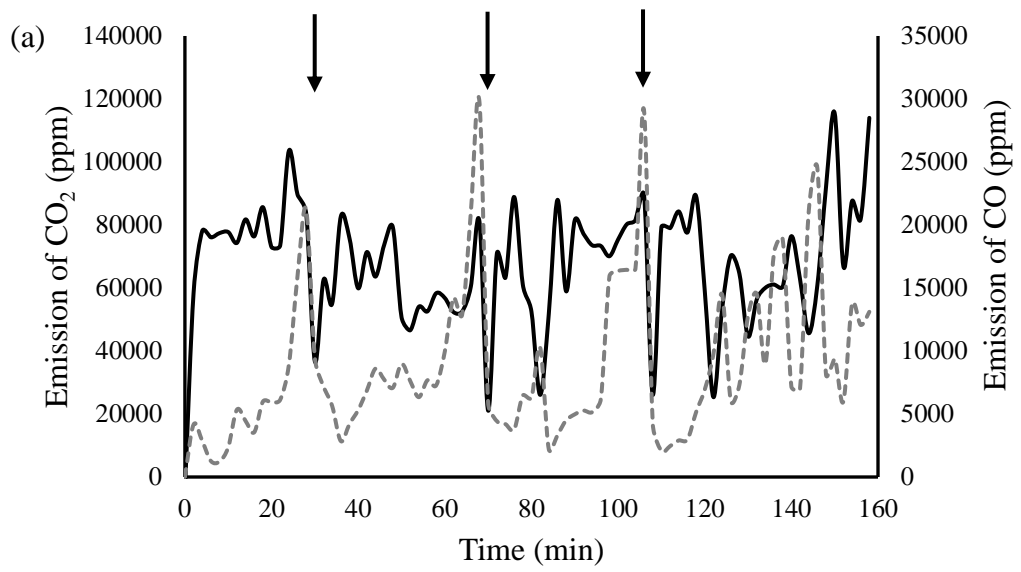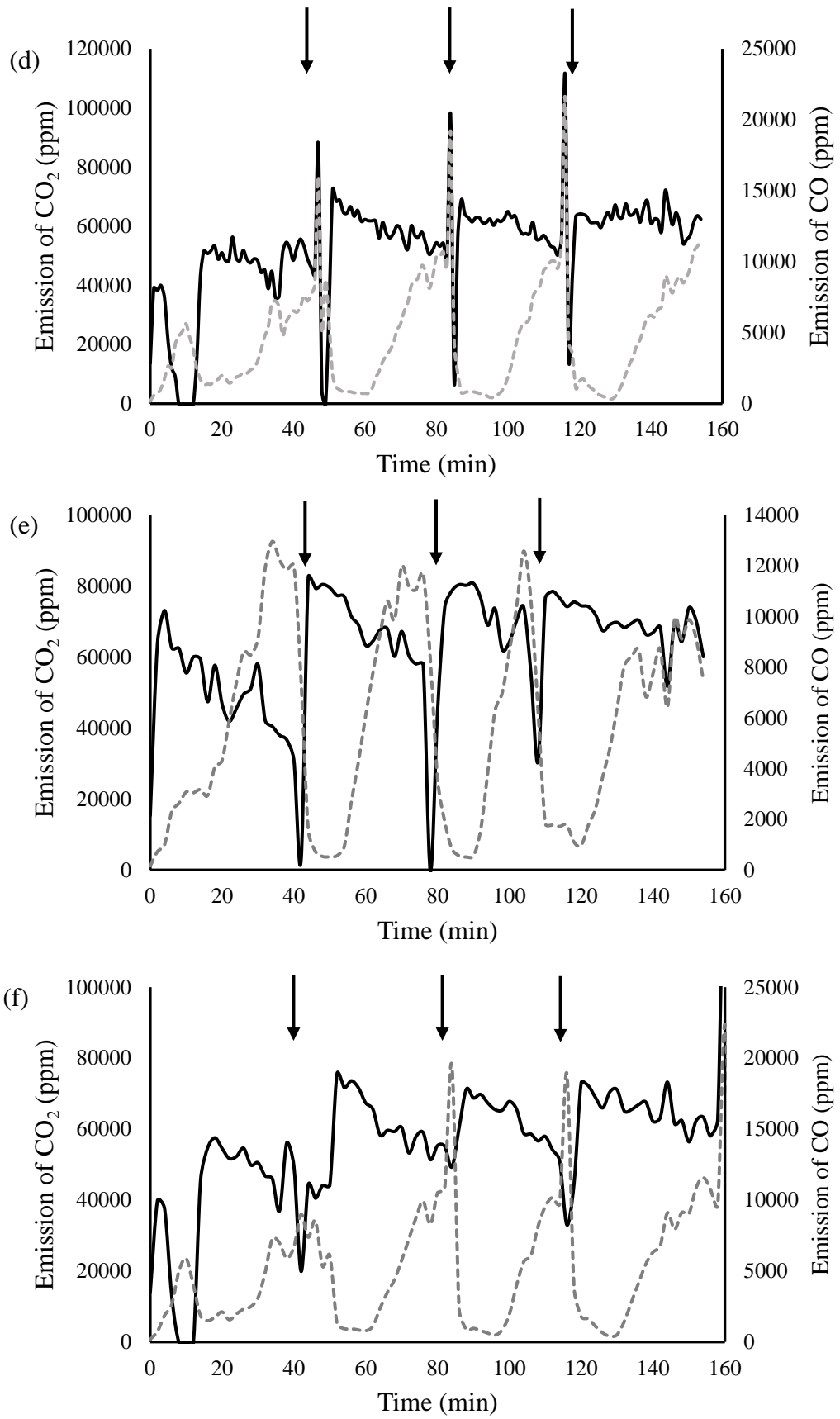
Figure 4.7: Evolution of CO₂ (solid black line) and CO (dashed grey line) over combustion cycles, arrows indicate batch reloads, (a) Spruce (b) T. Spruce (c) Willow (d) T. Willow (e) Olive (f) T. Olive

130

When the fuel is reloaded, the stove door is opened in order to manually place the fresh batch of fuel into the stove, during this process a sudden large influx of air causes the CO emissions to spike. This peak is from the rapid oxidation of volatiles emitted from devolatilisation of the fuel, however slow mixing and lack of energy from heat or radiation sources prevents conversion to CO_2.

The reaction from CO to CO_2 is a much slower process than the initial oxidation step, and is the rate determining step in the reaction mechanism to CO_2 formation. Once the bed is flaming the CO concentration rapidly declines and the CO_2 concentration increases, the stove conditions are now more favourable for complete combustion (hotter temperatures). The CO gradually increases as the flaming phase progresses and more char combustion occurs (smouldering phase). The CO concentration peaks again during smouldering combustion because of the heterogeneous reaction of oxygen with the char surface, at this point the stove temperature has dropped (Table 4.4). The trend of higher CO_2 emissions during flaming combustion and then decreasing during smouldering combustion and the associated increase of CO emissions is also seen in profiles of work by Bertrand et al. [2017], Win and Persson [2014], Mitchell et al. [2016] and Ali Mami et al. [2020].

Table 4.5: Average emission factors over the whole combustion cycle for the fuels studied, margin of error is shown in the parenthesis for a 95% confidence interval

	kg GJ^{-1}			g m^{-3} at 13% O_2		
Fuel	CO_2	CO	CH_4	CO_2	CO	CH_4
Spruce	65 ($\pm$20)	5.8 ($\pm$0.44)	0.37	115 ($\pm$32)	9.1 ($\pm$1.2)	0.56
T. Spruce	90 ($\pm$5.2)	3.2 ($\pm$0.1)	0.18	145 ($\pm$10)	6.0 ($\pm$0.32)	0.47
Willow	67 ($\pm$16)	4.2 ($\pm$0.24)	0.18	110 ($\pm$33)	7.0 ($\pm$0.69)	0.34
T. Willow	78 ($\pm$16)	4.2 ($\pm$0.53)	0.04	120 ($\pm$32)	6.9 ($\pm$1.4)	0.10
Olive	73 ($\pm$10)	4.0 ($\pm$0.25)	0.05	110 ($\pm$28)	6.6 ($\pm$0.71)	0.18
T. Olive	74 ($\pm$5)	4.2 ($\pm$0.44)	0.05	98 ($\pm$17)	6.0 ($\pm$1.2)	0.13

Table 4.5 shows the average emission factors over a whole combustion cycle for the reload batches of each fuel. The most notable observation is that the emission factors for CO_2 from the torrefied fuels are higher than the untreated fuels, this is because of the higher fixed carbon/carbon contents in the torrefied fuels. The CO emissions are similar for all the fuels with the exception of the untreated spruce fuel, which is 1.6 kg GJ^{-1} higher than the torrefied spruce, this is because of the higher

moisture content of the spruce (18 wt.% ar.) which cools down the fuel bed and combustion zone temperature because of the energy consumed drying the fuel and removing the excess moisture.

Methane (CH_4) emissions for the spruce, willow and olive pairings are shown in Figs. 4.8a-c respectively. The emissions from the wood logs (spruce and willow) and the torrefied spruce are significantly higher than the smaller briquetted fuels (torrefied willow, olive and torrefied olive). This suggests that there is some influence of the physical properties on these emissions, fuels that don't disintegrate readily result in higher CH_4 emissions, however this result could also be from the fuel composition discussed later. Emissions of CH_4 are typically from fuel rich combustion, more common with dense briquettes, without the ability to react further to CO or CO_2 [Ndiema, Mpendazoe and Williams, 1997]. The profiles in Figs. 4.8a-c are analogous with this conclusion: the CH_4 emissions either peak towards the end of the combustion cycle when there is still unreacted fuel because the fuel hadn't disintegrated and the temperatures were too low to support further reaction mechanisms (temperature profiles in Appendix A, Fig. A.1-3), or the peak occurs just after reloading when the burning rate spikes, the fuel is rapidly devolatilising but the temperature is still too low, the residence time is too short or the air-to-fuel ratio isn't favourable for further reaction.

Methane is produced from the decomposition and gasification of volatile species as shown in the reaction mechanisms in Eq. 4.1-4.3 [Ndiema, Mpendazoe and Williams, 1997]. There is a partial equilibrium between the emissions of CO and CH_4. The ratio of atomic C/H largely dictates these reactions and using Fig. 4.9 there is a moderate power order trend ($x^{-2.43}$) between the C/H ratio and the CH_4 emission factors. In the spruce and willow pairings, torrefaction improves the C/H ratio and there is a substantial effect on the CH_4 emission factors (Fig. 4.9). In the case of the olive and torrefied olive there is a large increase in the atomic C/H ratio however there is minimal change in the emissions of CH_4. It should be noted that all the fuels in Fig. 4.9 have a similar moisture content, as this would also greatly influence the result [Price-Allison et al. [2019].
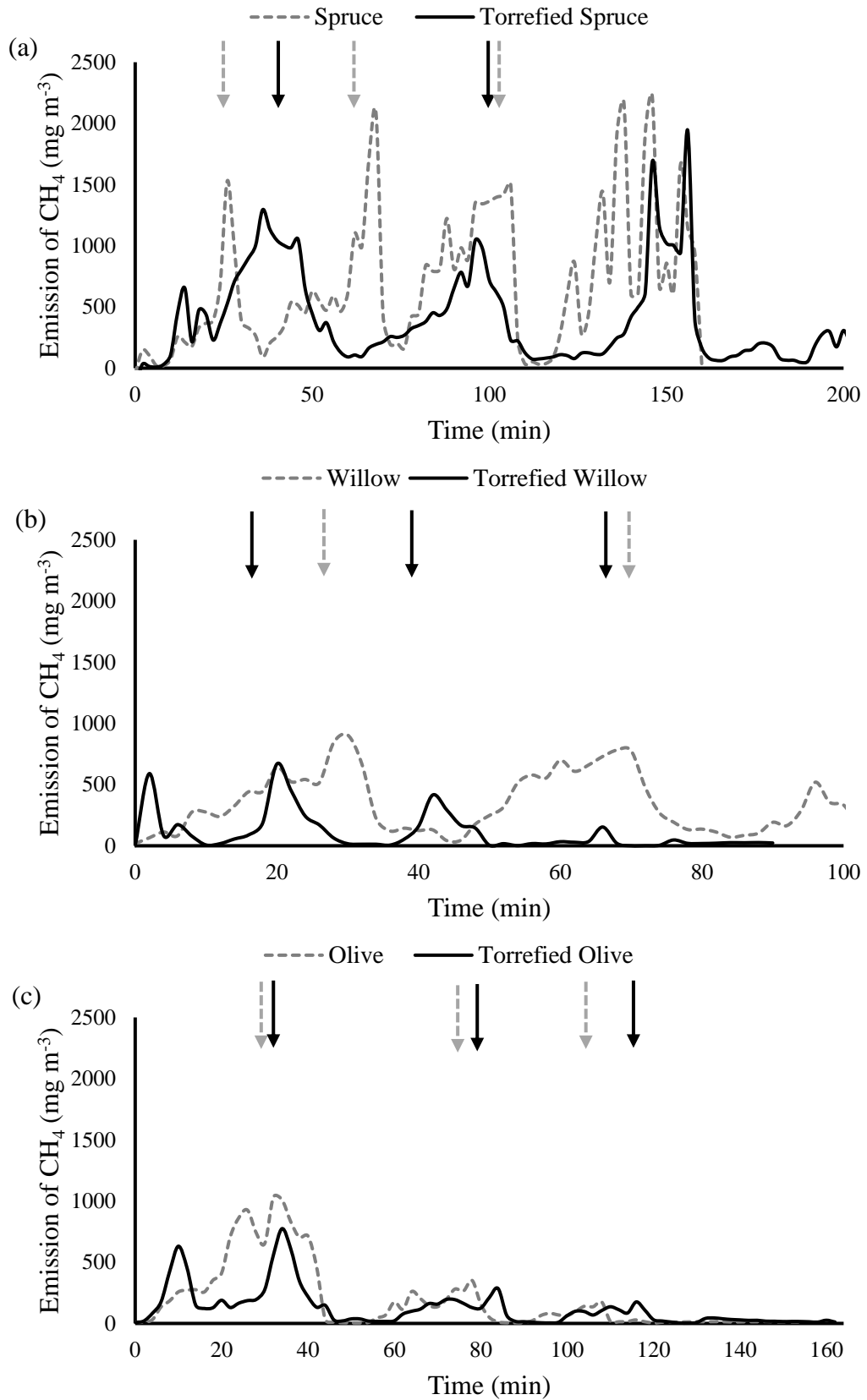
Figure 4.8: Methane emissions over combustion cycles (a) Spruce and T. Spruce (b) Willow and T. Willow (c) Olive and T. Olive

$$Biomass + O_2 \rightarrow CO + C/H/O \; Species \quad (4.1)$$

$$CO + H_2O = CO_2 + H_2 \quad (4.2)$$

$$CO + 2H_2 = CH_4 + 0.5O_2 \quad (4.3)$$
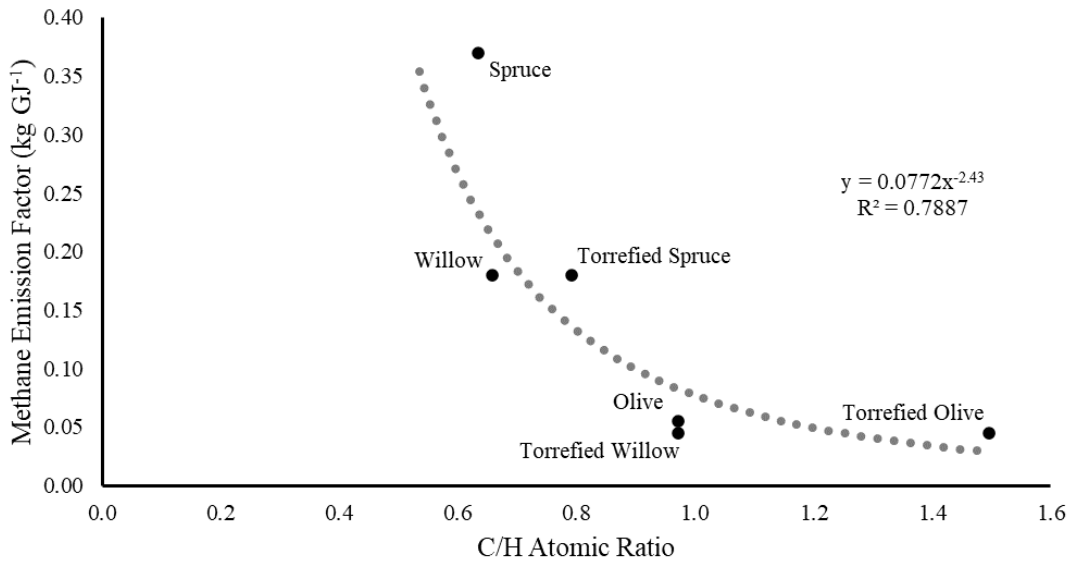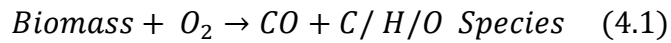
Figure 4.9: Methane emission factors plotted against the C/H ratio from the fuel analysis.

4.3.2.3 Nitrogen Emissions (NOx)

NOx emissions in stove combustion systems are primarily from fuel-N sources, this is because the temperature at which thermal NOx forms (1500°C) is much higher than the average temperature in the stove, this is also a conclusion seen in past research [Mitchell et al., 2016] [Atiku et al., 2017]. Even in research of much larger fixed bed systems temperature profiles show that the fuel bed temperature rarely exceeds 1000°C [Rokni et al., 2017] [Ali Mami et al., 2020].

NOx profiles over the combustion cycle are shown in Figs. 4.10a-c for the spruce, willow and olive pairings respectively. In all of the untreated fuel cases the magnitude of the NOx peak is greater than the torrefied fuel, there is also more of a delay between the batch reload point and the peak occurrence for the untreated fuel. This suggests that the nitrogen release in the untreated biomass occurs very rapidly, the rate of devolatilisation is higher, which is analogous with earlier discussions relating to the burning rate. The larger time lag between reload and peak emissions is because of the higher moisture content in the untreated fuel, this was also observed by

Rokni et al. [2017] for a comparison of untreated and torrefied corn straw. The NOx peaks in the torrefied fuel cases are much broader, which when comparing to Figs. 4.4a-c shows that nitrogen release persists into char combustion (smouldering phase). This was a conclusion also seen in Mitchell et al. [2016] where NOx emissions continued into the smouldering phase and stabilised to a consistent emission rate.
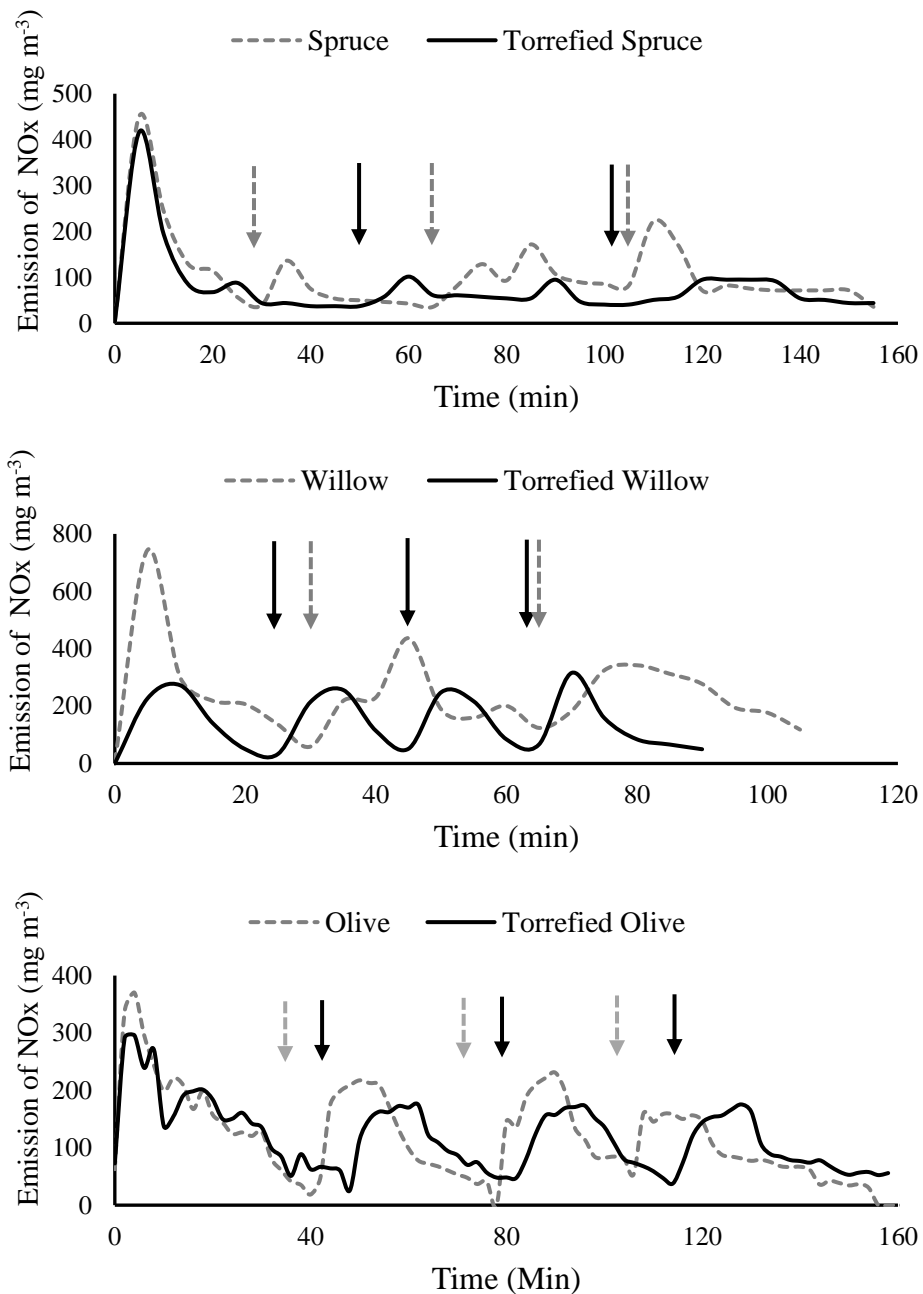
Figure 4.10: NOx emissions profiles (a) Spruce and Torrefied Spruce (b) Willow and Torrefied Willow (c) Olive and Torrefied Olive

Table 4.6 shows the emissions factors for NOx on both a g kg^{-1} and a g GJ^{-1} basis as well as the fuel-N content. On a mass basis (g kg^{-1}) the results show that emissions of NOx are highly variable and there is no definitive correlation between the fuel nitrogen content and the emission factor. Converting this to an energy basis, Fig. 4.11, an improvement in emissions is achieved through torrefaction. Fig. 4.11 includes data from other work [Mitchell et al., 2016] and the values from the untreated fuels (spruce, willow and olive stone) all fit this previous data trend. Arrows indicate the reduction of the NOx emissions by the torrefied fuels. A part of this reduction is from the increase in energy, compensating for the increase in the fuel-N concentration. However, past work [Trubetskaya et al., 2019] has shown in the case of torrefied olive, the torrefied fuel contains char-like particles in which the fuel-N is more tightly bonded in the char matrix. Combustion of char particles encourages a reducing environment and therefore more fuel-N will be released as N_2 instead of NO [Williams et al., 2012]. Analysis of the bottom ash/char mix, Table 4.6, (material remaining after 80% mass burnout) shows that similar amounts of nitrogen remain, this supports the speculation that more nitrogen in torrefied fuels is being evolved as N_2 which is the same conclusion shared by Trubetskaya et al. [2019].

Table 4.6: Average NOx emissions over the whole combustion cycle to 80% burnout, margin of error at a 95% confidence interval are shown in the parenthesis, fuel nitrogen and standard deviation from Tables 4.1 and 4.2 are included

Fuel	NOx Emission Factors		Fuel-N content	Residual Char-N
	g kg^{-1}	g GJ^{-1}	wt.% daf	%
Spruce	1.07	65 (±12)	0.27±0.10	18
T. Spruce	1.04	45 (±5.1)	0.49±0.12	17
Willow	2.56	135 (±8.5)	0.56±0.21	7
T. Willow	1.91	90 (±20)	0.64±0.14	8
Olive	1.61	75(±24)	0.50±0.26	10
T. Olive	1.52	60 (±17)	0.56±0.04	10
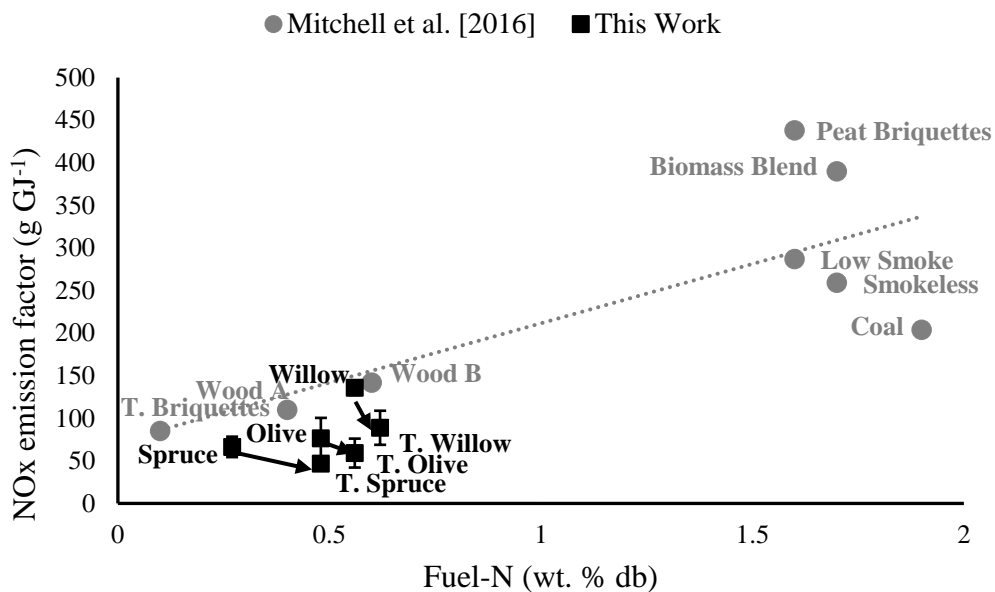
Figure 4.11: NOx emission factors on an energy basis plotted against the fuel-N content, includes data from Mitchell et al. [2016]. It should be noted that changes are within the experimental error (10%).

To explore this further, chars were prepared from each fuel using TGA (nitrogen environment at a heating rate of 20°C min^{-1} to 850°C and held for 60 minutes) and these chars were used to calculate the nitrogen partitioning by elemental analysis and mass balance, Table 4.7. In all of the cases, over 70% of the nitrogen is released in the volatile phase. There is a significant increase in the retention of fuel-N in the char matrix for the torrefied fuels. Previous work has shown that shorter residence times and lower torrefaction temperatures create more nitrogen enriched chars whereas hotter temperatures result in nitrogen being released faster than the volatiles are released [Glarborg, Jensen and Johnsson, 2003] [Werther et al., 2000]. The torrefied spruce had the mildest torrefaction conditions and also has the greatest retention of nitrogen in the char (26%). The olive stone had the most severe torrefaction conditions and retained 21% of the nitrogen in the char, this suggests the trend in this work is analogous with Glarborg, Jensen and Johnsson [2003] and Werther et al. [2000]. However, the willow only retained 14% which breaks the trend. Riaza et al. [2019] reported increased retention of nitrogen in char for olive waste material compared to wood which is consistent with the results seen in this work. Using the results from Tables 4.6 and 4.7, it can be concluded that torrefied fuels will

retain more nitrogen in the char matrix and have lower NOx emissions and, and so nitrogen emissions from biomass must occur more as N_2.

Table 4.7: Nitrogen partitioning in fuels studied

Fuel	Fuel-N Content (wt.% daf)	Char-N Content (wt.% daf)	Char Yield (%)	Fuel-N in Volatiles (%)	Fuel-N in Char (%)
Spruce	0.27 (±0.10)	0.31 (±0.11)	17.5	80	20
Torrefied Spruce	0.49 (±0.12)	0.37 (±0.06)	31.9	74	26
Willow	0.56 (±0.21)	0.27 (±0.08)	13.2	94	6
Torrefied Willow	0.64 (±0.14)	0.32 (±0.04)	28.4	86	14
Olive	0.50 (±0.26)	0.29 (±0.07)	15.2	91	9
Torrefied Olive	0.56 (±0.04)	0.33 (±0.11)	36.2	79	21

4.3.2.4 SO₂ Emissions

Emissions of SO_2 are complex because they are not only dependent on the amount of S in the fuel but also the form in which the S is present and also the nature of minerals/salts. SO_2 emissions for the torrefied fuels are significantly lower than the emissions from the untreated fuels, Table 4.8. Calcium (Ca) in fuels has been thoroughly researched and shown to greatly reduce the emissions of SO_2. Niu, Han and Lu [2010] showed that using a Ca/S atomic ratio of between 1 and 2 can have significant benefits at temperatures of 1000-1200K in fixed bed fluidised combustion of coal. This temperature region is higher than observed in domestic stoves and is most likely encouraging the release of inorganic sulphur from char destruction and decomposition of stable calcium salts (CaS, $CaSO_4$) [Williams et al., 2012] [Yan et al., 2015]. However, Zhang et al. [2020] has shown that in the Ca/S mass ratio range of 1-3 in the temperature region of 200-400°C the percentage of S released is significantly reduced for combustion of high-sulphur containing oil sludge. For the data in this work, the Ca/S mass ratio range is much greater, with the torrefied spruce having the highest mass ratio (~22) and the untreated olive having the lowest (~0.8). All of the torrefied forms have improved Ca/S mass ratios and the emission factors are lower, Fig. 4.12. The relationship between Ca/S and SO_2 emission factors gives a power trend ($x^{-0.297}$). The trend shows that over a Ca/S range of 0.5-2.5 the improvement in emissions is substantial and more significant than improvement made above this ratio. This result was also observed by Zhang et al. [2020]. However, the more interesting result is the comparison between the Ca/S ratio and the % of S emitted as SO_2, Fig. 4.13.

Table 4.8: Emission factors of SO$_2$ for the fuels study

Fuel	S (wt.% daf)	Ca (ppm db)	SO$_2$ Emission (g kg^{-1})
Spruce (S)	0.04	980	0.36
Torrefied Spruce (T.S)	0.04	8770	0.32
Willow (W)	0.04	3050	0.39
Torrefied Willow (T.W)	0.06	6020	0.36
Olive (O)	0.13	1000	0.95
Torrefied Olive (T.O)	0.16	4800	0.58

Fig 4.13 shows that the spruce and willow fuels emit a much larger proportion of their S contents (45 and 48% respectively) compared to the olive fuel (36.5%) even though the S contents of the olive is 4 times greater. This could be to do with the nature of the fuels, high amounts of sulphur in the bark of woods are burnt in early combustion stages as they are exposed [Phillips et al., 2016]. Alternatively, it could be that the S within the woods is present more as organic S which decomposes at lower temperatures [Knudsen et al., 2004]. The % S emitted from the spruce is much lower than reported in previous work by Van Lith et al. [2008] at a similar temperature range, this is most likely due to the nature of combustion in the stove and the fuel being as a log instead of a powder.
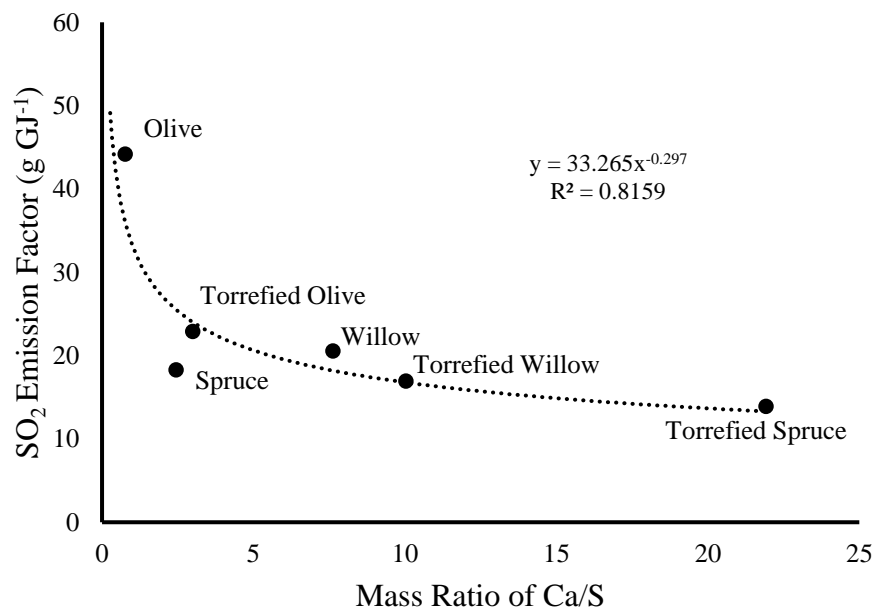
Figure 4.12: SO$_2$ emission factors as a function of Ca/S ratio
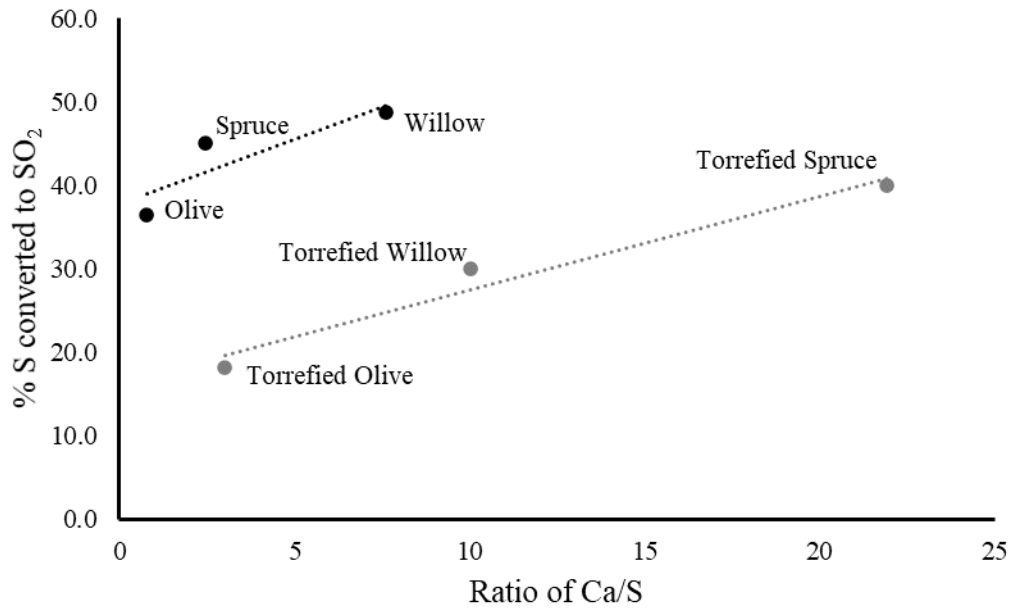
Figure 4.13: Percentage of sulphur emitted from the fuel as SO$_2$ as a function of Ca/S ratio

4.3.2.5 Particulate Matter (PM) Emissions

PM emissions pose many threats to both the environment and human health. Mechanisms for particulate (soot) formation are complex and have been extensively researched to be a function of many variables- see section 2.3.2.6. Table 4.9 shows the emission factors for the fuels studied; the submicron percentage of sampled PM is also shown.

Sampling and determination of PM emission factors is a difficult process and is made more complex by the nature of stove combustion. The majority of PM emissions are during flaming combustion [Mitchell et al., 2016] [Atiku et al., 2016], however as discussed earlier in section 4.3.2.1, definition of the different combustion phases is not simple and analysing the start and end points has some subjectivity. Additional differences between smouldering and flaming combustion, mainly combustion temperature and radiative energy, also makes sampling PM difficult, and in the case of this work the change in the way fuels burn once they are torrefied means that there is no one model fits all approach. The final consideration is the stove operator impacts which can in most cases be the most influential factor [Pettersson et al., 2011], placing the fuel in too late can cause a pre-flaming smoulder which can be described as the release of volatiles into a cold combustion zone, this can cause large

140

amounts of PM to form and this continues until the gaseous mixture reaches a point where it can self-combust. Measurement reliability has been tactically reduced by using the same operator and sticking to key procedure points, such as reloading the fuel when 25% of the initial batch mass remains. Using Table 4.9, comparing the results from the smoke metre and the Dekati impactors (sampling from the dilution tunnel), the numbers are within 15% of each other for each fuel and the trend is consistent: torrefied fuels produce less PM than untreated fuels. The estimated experimental error within this data set is ±20% to account for small perturbations between experimental runs, which cannot be prevented, such as fuel movement within the stove.

Table 4.9: PM emission factors, C/H ratio and Percentage of emission as sub-micron particles

Fuel	VM (wt.% db)	Atomic C/H	EF, PM_t (g kg^{-1})		PM_1 (%)
			Smoke Metre	Impactors	
Spruce	77	0.70	4.2	3.9	97.6
T. Spruce	71	0.79	2.2	1.9	98.6
Willow	82	0.65	6.4	6.1	96.5
T. Willow	73	0.90	4.9	4.4	96.6
Olive	82	0.90	6.7	5.8	99.0
T. Olive	65	1.58	4.6	4.2	98.3

The results show that torrefaction reduces PM_t (total particulate matter) emissions from combustion in a domestic stove. This is because of the reduced VM content of the torrefied fuels. Mitchell et al. [2016] shows that there is a trend between the reduction in volatile matter and the PM_t emission factor which was also seen for the data in this work, Fig. 4.15. This is closely linked to the aforementioned increases in aromaticity and removal of low CV volatile compounds. Additionally, from Fig. 4.14 the values for the torrefied spruce and the torrefied briquettes (which are spruce) are very similar to each other.

Some research has also shown that PM emissions are increased by torrefaction [Khalil et al., 2013] [Shao et al., 2013]. This is mainly because of the concentration of K and S in the torrefied form, resulting in K_2SO_4 being released into the gas phase. There are key reasons this is not observed during combustion of torrefied fuels in a domestic stove: (1) reduced Cl content from torrefaction results in reduced formation of KCl; (2) increased S is accompanied by a large increase in Ca, which as discussed in section 4.3.2.4, reacts with S and prevents emission to the gaseous phase; (3) the stove combustion temperature is too low for significant evaporation or sublimation of K and the majority is retained in the char [Li et al., 2019] [Johansen et al., 2011].
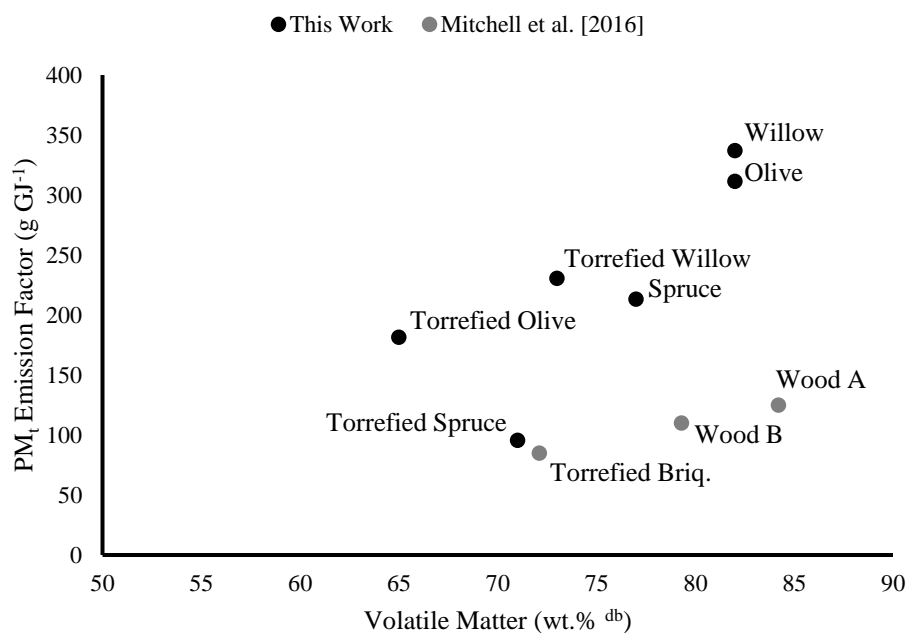
Figure 4.14: Correlation between PM_t and volatile matter, data from Mitchell et al. [2016] included

4.3.3 Pyrolysis-Gas Chromatography-Mass Spectrometry (Py-GC-MS)

Py-GC-MS was used to investigate and compare the organic species released during volatile release. Figs. 4.15-4.17 show the chromatograms for the fuel pairings; spruce, willow and olive respectively. Using the NIST database and previous work [Simoneit, 2002] [Nowakowski and Jones, 2008] [Fahmi et al., 2007] peaks were identified that were common in both the untreated and torrefied forms. Initial observation of the chromatograms, in the spruce and olive cases, shows there is a visible reduction in the magnitude of the main peaks; upon torrefaction this is not observed in the case of the willow. In the case of the untreated olive, late eluding fatty acids create multiple peaks in the latter time period. These peaks are unresolved and not included. It should also be noted that because of the very high heating rate and the inert nature of the carrier gas secondary reactions do not occur.

The selected GC column and operating conditions are optimal for detection of compounds from lignin sources. Based on the area of the identified peak components, lignin products make up 50-60% of the peak area. Volatile components have been well-researched and shown to be closely linked to soot formation routes [Atiku et al., 2017]. The two most notable are the HACA (hydrogen abstraction, carbon addition) method and the CPD (cyclopentadiene), these are both described in more detail in Chapter 2. Table 4.10 describes identified components and defines these into categories based on their source, carbohydrates, lignin or fatty acids.

Figs. 4.18-4.20 compare the percentage of identified components from carbohydrate, lignin and propylphenol sources. Looking at Fig. 4.18, volatilisation of carbohydrate sources increases in the torrefied woods compared to the untreated. This is an unexpected result since during torrefaction almost all of the hemicellulose is degraded and up to 75% of the cellulose (dependent on severity of torrefaction), these are both the main carbohydrate sources [Li et al., 2015] [Saddawi et al., 2012] [Ndiema, Mpendazoe and Williams, 2012]. Further analysis of the individual carbohydrate components from Table 4.10 show that the key component responsible for the increase is levoglucosan (supplementary data Fig. B.4). Levoglucosan is a key tracer compound used in detection of biomass burning in atmospheric chemistry and is the subject of much research. It is formed from the pyrolysis of starch and cellulose and is often difficult to detect in gases directly from a stove because of the hotter

temperatures. No levoglucosan is detected in either of the untreated wood samples however up to 11% peak area is detected in the torrefied samples. Previous work [Hosoya, Kawamoto and Saka, 2009] [Meng et al., 2012] [Boateng and Mullen, 2012] have shown that thermally treated biomass can result in the increased production of anhydrous sugars. This is because of the increase of cellulose-lignin interaction as opposed to hemicellulose-cellulose interactions. In the case of the olive there is a substantial decrease in the products from carbohydrate sources, this result is from the reduction of detected levoglucosan. This is in contrary to the previous work mentioned above however is most likely because of the extreme severity of the torrefaction conditions for this fuel which has been extensively described throughout this chapter.

Torrefaction increases the proportion of lignin that makes up a biomass [Horvat et al., 2016]. This combined with the reduced moisture inherently encourages a small increase in production of tar as shown in Fig. 4.19. Looking at individual species this increase is mainly from increases in phenols especially methoxy-phenol, methyl-phenol and cresol (Fig. A.4), the latter more than doubles in all three cases. Propylphenols (eugenol, methoxyeugenol and homovanillyl alcohol, Fig. A.4) are of the most interest as these compounds have an increased ability to form soot since they can be used in both the HACA and CPD mechanisms. Looking at Fig. 4.20 the reduction in the eluting of these compounds is significant, in the case of the torrefied olive they are almost completely eliminated. The propylphenols make up approximately a quarter of the lignin volatile products in the untreated fuels (~22, 27 and 25% for spruce, willow and olive respectively) which is a substantial difference to the torrefied forms which make up ~9, 13 and 2% (T.S, T.W and T.O respectively). Combining this information with the reduction in cellulose-derived volatile components [Berrueco et al., 2014] goes someway to explaining the reduction in PM_t discussed in the previous section (4.3.2.5).
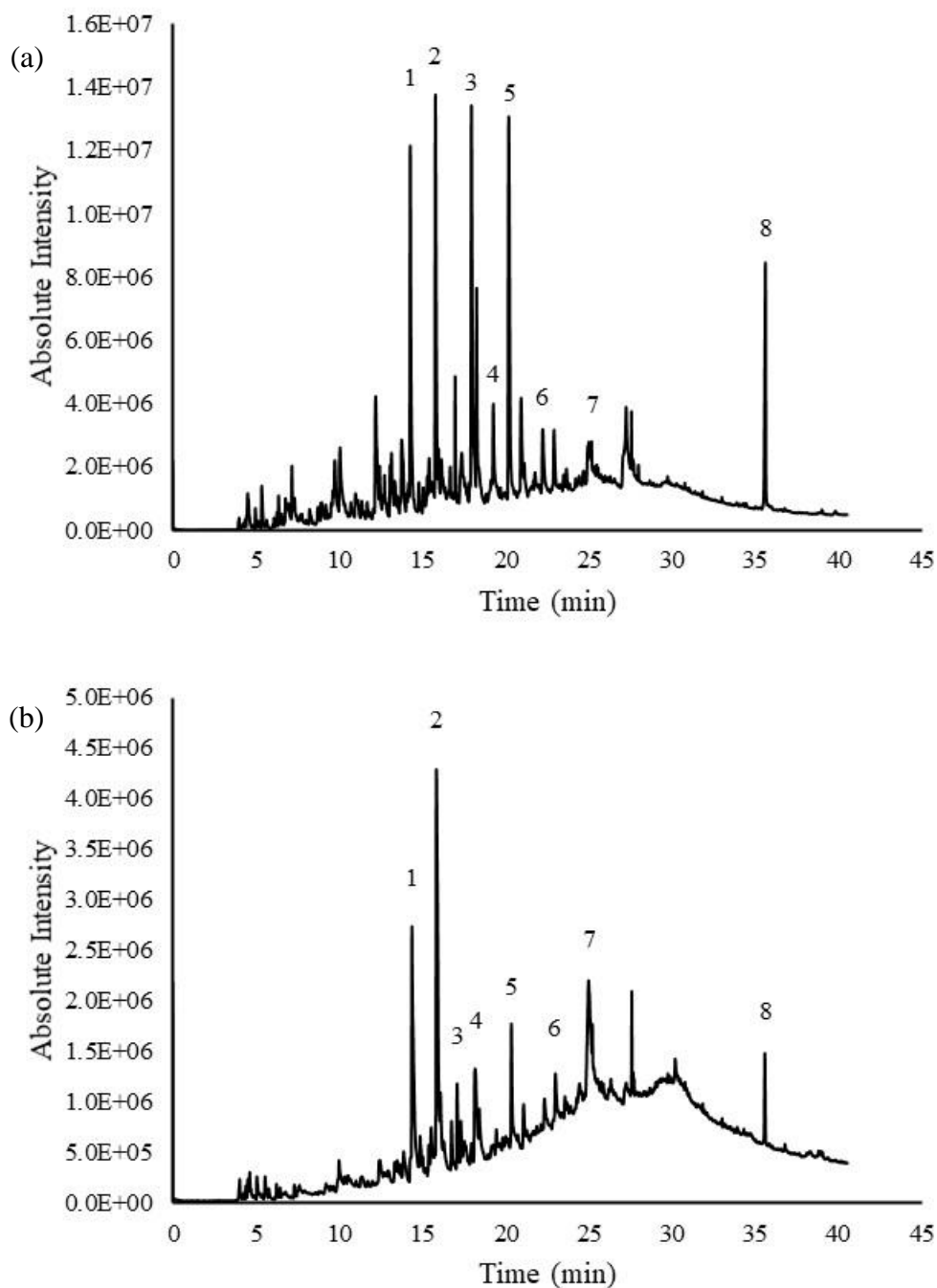
Figure 4.15: Py-GC-MS Chromatograms of (a) Spruce (b) Torrefied Spruce. Peak identification (most likely): 1. Guaiacol 2. Cresol 3. Methoxyacetophenones 4. Methoxypropenyl phenols 5. Eugenol 6. Acetovanillone 7. Homovanillic acid or Levoglucosan 8. Squalene. Peaks up to peak no.1 (not including) are from cellulose sources, from peak no.1 up to no.8 are from Lignin, the remaining are from extractives.
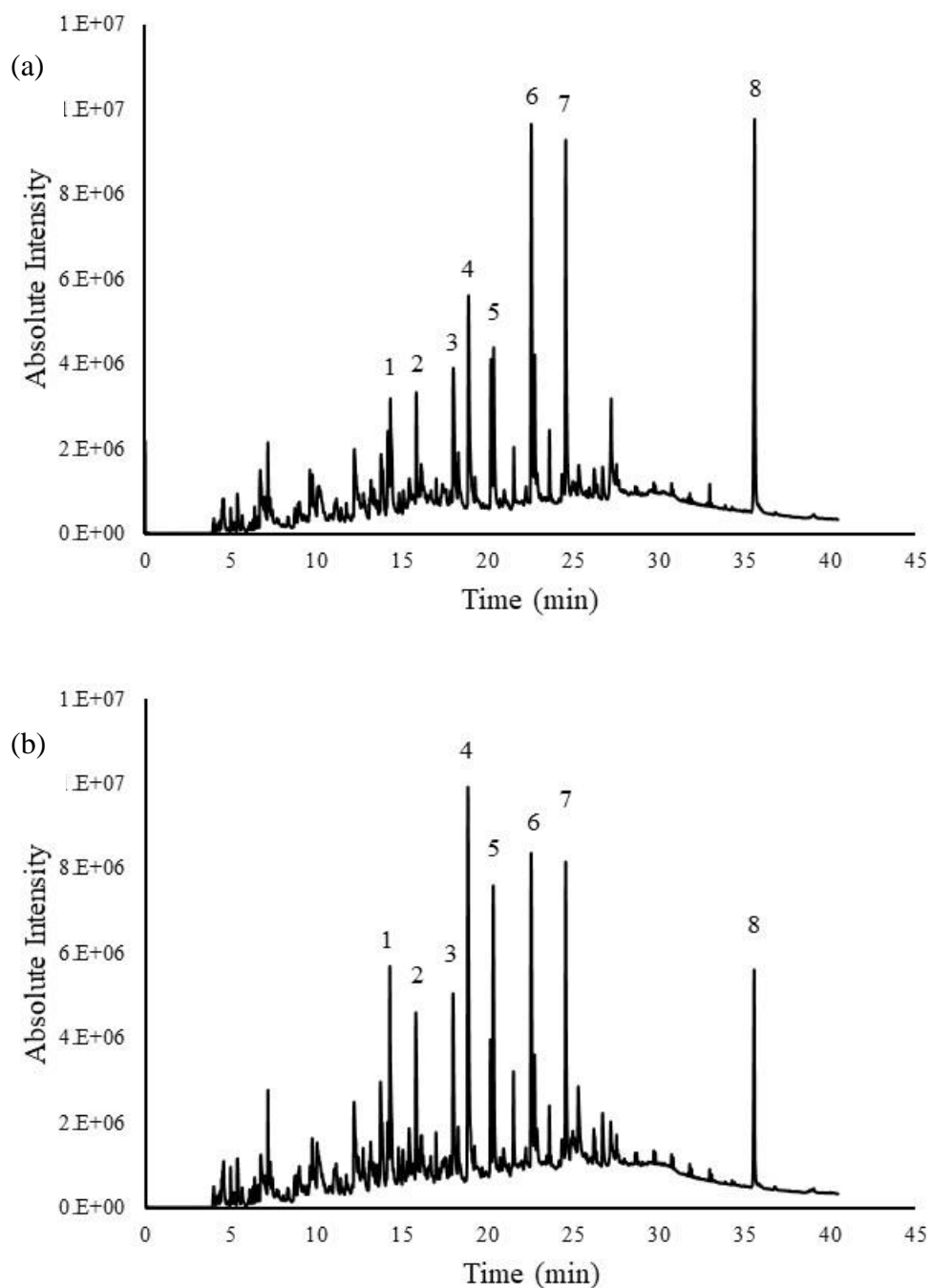
Figure 4.16: Py-GC-MS Chromatograms of (a) Willow (b) Torrefied Willow. Peak identification (most likely): 1. Guaiacol 2. Cresol 3. Methoxyacetophenones 4. Dimethoxyphenols 5. Eugenol 6. Dimethoxyacetophenones 7. Propenyldimethoxyphenols 8. Squalene. Peaks up to peak no.1 (not including) are from cellulose sources, from peak no.1 up to no.8 are from Lignin, the remaining are from extractives.
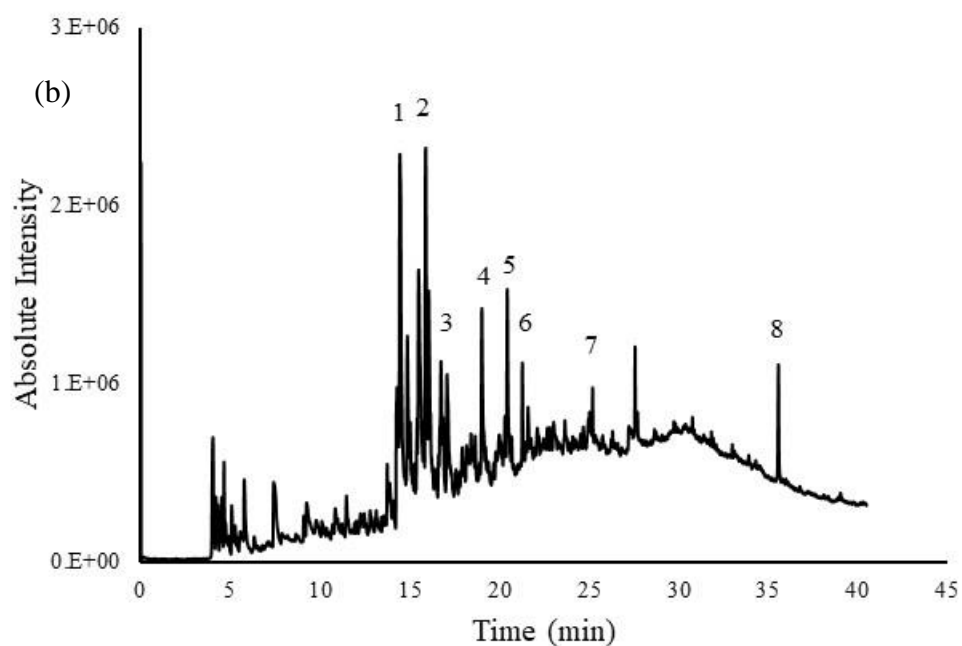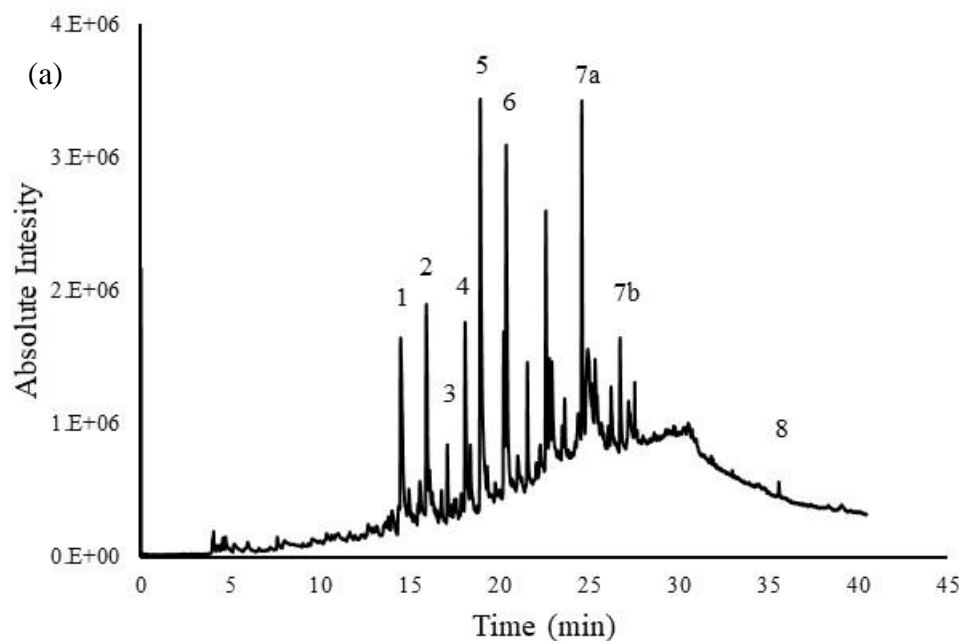
Figure 4.17: Py-GC-MS Chromatograms of (a) Olive (b) Torrefied Olive. Peak identification (most likely): 1. Guaiacol 2. Cresol 3. Methoxyacetophenones 4. Dimethoxyphenols/Syringol 5. Eugenol 6. Dimethoxyacetophenones 7a. Propenyldimethoxyphenols (7) 7b. Levoglucosan 8. Squalene. Peaks up to peak no.1 (not including) are from cellulose sources, from peak no.1 up to no.8 are from Lignin, the remaining are from extractives.

Table 4.10: Classification of identifiable components into carbohydrate sources, lignin source and extractives

Source	Type	Evolved compound	Boiling Point
Carbohydrates	Acids Ketones Sugars	2-Propenoic acid	110-390°C
		Acetic acid	
		Cyclohexanone	
		2-hydroxy-3-methyl-2-cyclopenten-1-one	
		3-ethyl-2-hydroxy-2-cyclopenten-1-one	
		2,5-dimethylfuran	
		2(5H)-furanone	
		Levoglucosan	
Lignin	Toluene Phenols Methoxybenzenes	Toluene	110-260°C
		Phenol	
		2-methoxyphenol	
		2-methylphenol	
		2-methoxy-4-methylphenol (Creosol)	
		2,6-dimethylphenol	
		4-hydroxy-3-methylacetophenone	
		2,6 dimethoxyphenol (Syringol)	
		Eugenol	
		1,2,4-trimethoxybenzene	160-320°C
		Vanillin	
		1,2,3-trimethoxy-5-methylbenzene	
		Acetoguaiacon	
		3,5-dimethoxyacetophenone	
		Homovanillylalcohol	
		2,6-dimethoxy-4(2-propenyl)-phenol	
		4-hydroxy-3,5-dimethoxybenzaldehyde	
Oils	Fatty Acids Fats	Hexadecanoic acid methyl ester	270-420°C
		n-hexadecanoic acid	
		Squalene	
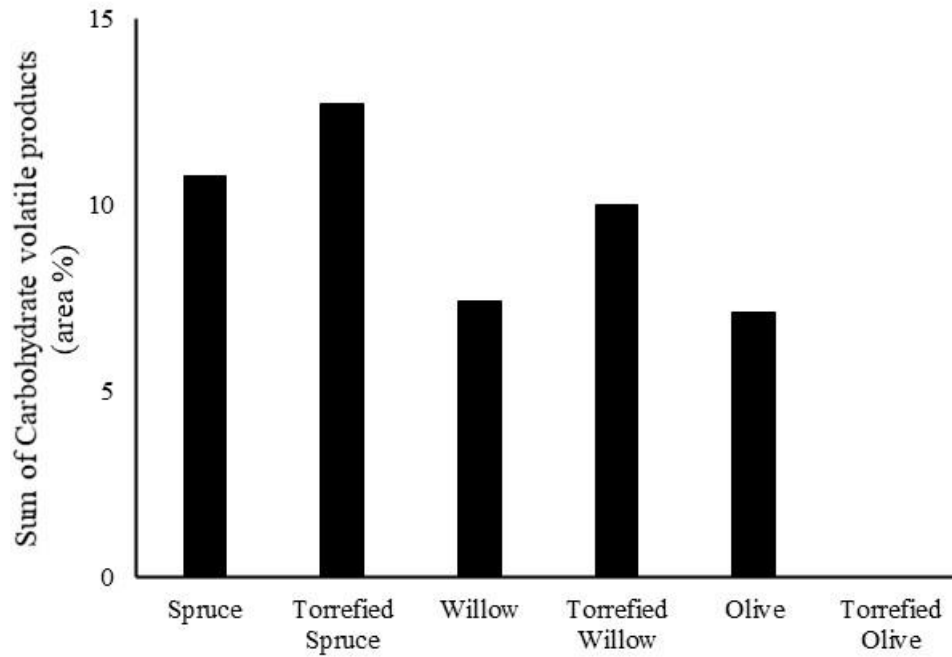
Figure 4.18: Comparison of decomposition products from carbohydrate sources for biomass studied
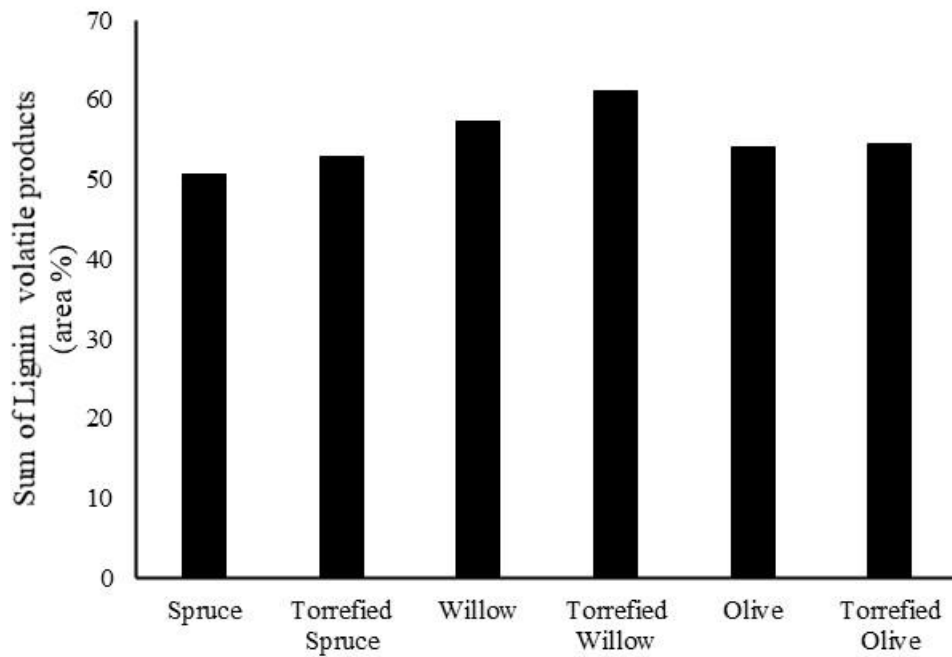
Figure 4.19: Comparison of decomposition products from lignin sources for biomass studied
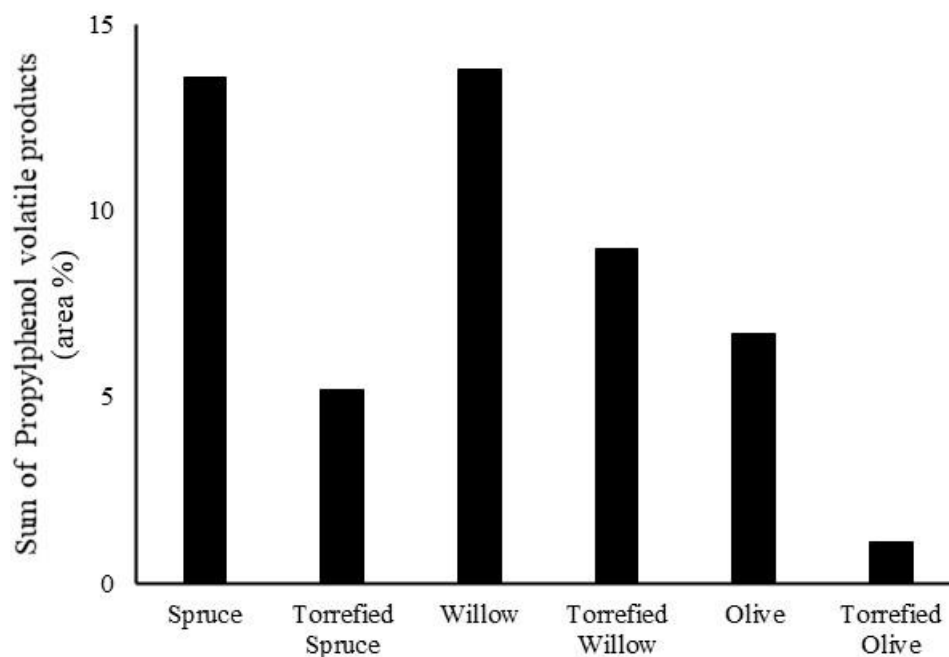
Figure 4.20: Comparison of propylphenol decomposition products for fuels studied

4.4 Conclusions

In this work, two wood fuels (spruce and willow) and a food-processing waste (olive stone) were compared to their torrefied counterparts. In the case of the woods, the untreated and torrefied form came from a different source, however for the waste the torrefied form was from the same source and a blend of 1:1 untreated and torrefied.

Initial composition analysis showed that the torrefied fuels were higher in fixed carbon, carbon, nitrogen, ash, potassium and calcium, but lower in moisture, volatiles, oxygen and chlorine. These trends are common and have been seen in a lot of previous research including that of Mitchell et al. [2016] and Trubetskaya et al. [2019]. The torrefied olive fuel had the highest carbon content (70 wt.% daf.) and lowest concentration of volatiles (65 wt.% db.), when comparing these to the other fuels and fuels from other work it is evident that the torrefied olive has been 'over torrefied' and resembles more of a biochar then a torrefied fuel. This also resulted in large amounts of variation in the analysis (carbon ±8%, volatiles ±22%).

Combustion of the fuels on a domestic stove was used to compare combustion performance (burning rate and flue gas temperature) and emissions. The torrefied fuels burnt slower than the untreated fuels, this is because of the lower volatile content. In the case of the torrefied spruce the burning rate was considerably lower (0.94 kg h^{-1})

150

and this was a result of the dense briquetting which prevented effective break down of the fuel, reduced air flow and heat transfer through the fuel bed. The torrefied willow on the other hand exhibited the opposite results, the burning rate was the highest (2.30 kg h^{-1}) and this also resulted in the hottest average flue gas temperatures (flaming 395°C and smouldering 325°C). The torrefied willow briquettes were very loosely bound and disintegrated rapidly.

For all of the torrefied fuels the emission of CO_2 was larger than in the untreated fuel. The hotter combustion temperatures measured in the torrefied fuels increases the rate of oxidation of CO to form CO_2. The CO emission factors are similar for the untreated and torrefied fuels except in the case of the spruce (untreated 5.8 kg GJ^{-1} torrefied 3.2 kg GJ^{-1}). The emission factor for the spruce is the highest and can be attributed to the higher moisture content, 18 wt. %, the highest of all the fuels used. Methane emissions result from the thermal decomposition and gasification of volatiles and tars released during devolatilisation (pyrolysis) of the fuel. Emission factors of CH_4 have a power law trend ($x^{-3.863}$) with the C/H ratio of the fuel. In the spruce and willow cases the increase in C/H ratio reduces the CH_4 emission factor, however because of the reduced sensitivity when the C/H ratio exceeds 10 the trend is less visible for the olive comparison.

Emissions of NOx continues to be of increasing importance because of the health and environmental impacts from these compounds. The majority of NOx emissions is in the form of NO, this is common to domestic stoves because of the reduced combustion temperatures and residence times. This also means the NOx can be assumed to be only from fuel-N sources and the trend from Fig. 4.11 is linear between the two parameters. Even though the nitrogen content increases when a fuel is torrefied, this is offset by the energy increase. Additionally, torrefaction results in more strongly bonded fuel-N within the fuel matrix. This nitrogen enrichment into the char is increased by milder torrefaction conditions but is also dependent on the fuel type. During combustion of the char, there is more of a reducing environment which converts the fuel-N into N_2 instead of HCN/NO.

Understanding emissions of sulphur are difficult since they are not only dependent on the amount of S in the fuel but also the nature of the sulphur. The mass ratio of Ca/S compared with the emission factors of SO_2 has a power relation ($x^{-0.297}$).

151

The mass ratio is highest in the torrefied spruce (22) and lowest in the olive (0.8), these are also the lowest (0.32 g kg^{-1}) and highest (0.95 g kg^{-1}) emission factors of SO_2.

Particulate matter emissions are lower for the torrefied fuels. There are a few reasons for this. Initial observation shows that the reduced volatile content of the torrefied fuels reduces the emission factors, previous work has shown that moisture is also responsible for this reduction however this was to a lesser extent in this work. During torrefaction almost complete decomposition of hemicellulose and the majority of cellulose limits soot formation by either the HACA or CPD routes. Torrefied fuels also have reduced propylphenol emissions (measured in the Py-GC-MS analysis), amd these volatile components contribute to soot formation by both the HACA and CPD routes. A combination of these factors can be attributed to the reduction seen by the torrefied fuels.

Based on the data in this work, the overall performance of torrefied fuels is superior to that of the untreated counterparts. Emissions from torrefied fuels are higher in CO_2 but lower in CH_4, NOx, SO_2 and PM_t. Because of the higher price at which domestic fuels are purchased at; the effort should be being made to pretreat these fuels by torrefaction. Future work should explore the effects of torrefaction on HCl emissions in stoves and also the optimisation of torrefaction to produce the best performing fuel.

Chapter 5. Combustion of Waste Coffee Grounds in a Domestic Stove

5.1 Introduction

Combustion of waste including energy from waste (EfW), is a growing field of interest both from a research and industry point of view. Drivers for the increased use of waste for power and heat generation include efficient resource use, zero waste to landfill and net carbon zero emissions. Looking at Fig. 5.1 from a report for the UK government [Tolvik Consulting, 2019], the number of EfW facilities continues to grow and this is increasing the throughput of waste. In 2018 this was up by 5.6% to 11.5 Mt of waste processed [Tolvik Consulting, 2019]. The biggest challenges for using waste in combustion facilities is the lack of homogeneity. Even compared to biomass, which has a greater variability than coal, waste can often be very low in calorific value because of non-combustible components being fired into the combustion vessel. Removal of some waste constituents, such as metals, ceramics and composites are difficult because they are often blended or pose separation problems.
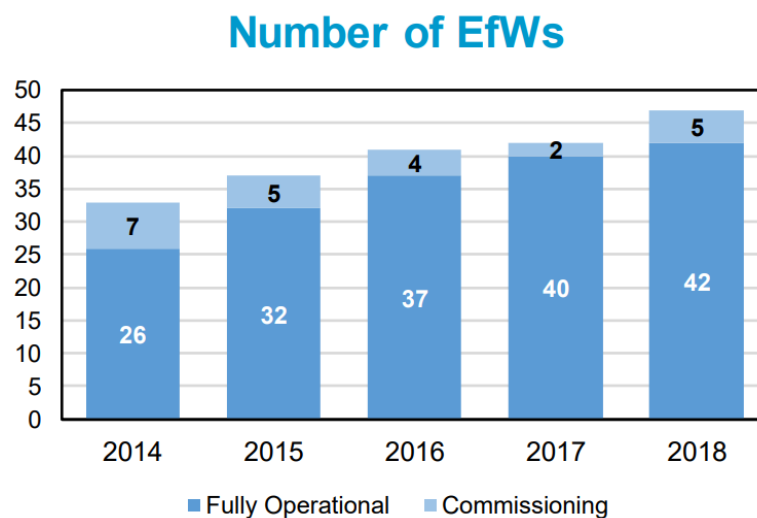
Figure 5.1: Number of EfW facilities in the UK [Tolvik Consulting, 2019].

Waste coffee grounds can be considered a unique type of fuel. This is because they are both a waste and a pretreated biomass (torrefied). Estimation from a UK company suggests that around half a million tonnes of coffee waste is produced annually in the UK [The British Coffee Association, 2019]. A report from the

International Coffee Organization (ICO) predicts that coffee markets in Europe and North America will increase by 1 and 2.5% respectively [2018]. Use of coffee grounds as a food product and then the waste as an energy source provides a solution to the fuel vs food debate, improves the prospects of a bio-economy and increases revenue in poorer countries.

The potential to use waste coffee grounds is an ongoing subject of research. Because the supply is too inconsistent, use in large scale power generation is a less favourable option unless in energy from waste plants. Biodiesel production from waste coffee grounds is an area of increasing interest however low free fatty acid content means that the yield of biodiesel is relatively low (~10.8% on a g of biodiesel/ g of waste coffee grounds) this process also requires the use of a high purity NaOH catalyst reducing the financial feasibility of the process [Kim and Yeom, 2020].

Production of bio-oil through pyrolysis is also an area of interest. In the work of Ktori, Kamaterou and Zabaniotou [2018] pyrolysis at 540°C manufactured a yield of 36 wt.% of bio-oil, 9 wt.% gaseous products (wet gas) and 29 wt.% biochar, these were seen to be the optimal conditions for bio-oil yield. Other processes such as fermentation for bioethanol production and extractive processes for bio-oil are also ongoing subjects of research interest. However direct combustion is still of interest because of the more favourable energy yields to alternative processes.

In this study commercial coffee briquettes have been studied for their composition and combustion properties in a domestic stove. Analysis of the combustion performance (burning rate and temperature) and the emissions have been compared to standard kiln dried willow logs. Some additional analysis has been used to further understand the combustion and emission properties.

5.2 Materials and Experimental Methods

5.2.1 Sample Preparation

Samples were prepared according to the methods described in Chapter 3. The commercial coffee briquettes were supplied in their briquetted form along with a small amount of non-briquetted loose ground spent coffee. Willow logs were supplied with bark in ½ split logs. The willow logs had to be cut and milled for elemental analysis.

The Mexican Robusta Beans (MRB) were ground using a conventional coffee grinder and the samples were then milled appropriately for analysis. For the Brewed Mexican Robusta Beans (BMRB) the ground coffee was used to make solely double shot espressos and the waste grounds were collected dried and then milled accordingly.

5.2.2 Experimental Methods

Elemental analysis was carried out as described in Chapter 3- proximate and ultimate analysis. Metals analysis was conducted by SOCOTEC using the method described in section *3.3.4.2*. For the ground coffee material, a particle size distribution analysis was performed by manually sieving the material through a series of discrete sized sieves (>1mm, 750-1000μm, 500-750μm, 250-500μm and <250μm). Using the mass collected the percentage particle size was calculated.

Combustion analysis was conducted on the domestic stove using the method specified in section 3.5.5. Some alterations to the method were made and these were:

- Three batches of fuel were combusted, one ignition batch and two reload batches. The ignition batch data is displayed but was not used in the calculation of emission factors.

- Each batch of fuel was approximately 1.5kg in mass (±100g). This was more repeatable with the briquettes compared to the logs since they are a regular size and shape.

- The ignition batch was started using 110g of firelighters (±5g). The effect of these on the bottom ash analysis was assumed negligible since it contributed less than 1% to the overall mass of ash after the complete experiment.

- Each run was continued until 0.3kg of batch mass remaining. At this point all the flames had been extinguished, the fuel was no longer glowing and the burning rate was consistently zero.

- The ash was collected and sent to SOCOTEC for composition analysis.

- Particulate measurements were conducted using only the Dekati Impactors, emission factors were calculated using this data and the filter papers were sent to Sunset Labs for EC/OC analysis.

5.3 Results and Discussion

5.3.1 Proximate and Ultimate Analysis

The proximate analysis (moisture, volatile matter, ash and fixed carbon) for the coffee grounds, willow logs, MRB and BMRB are shown in Table 5.1. Additional data from Kang et al. [2017] and Soysa et al. [2015] are also shown in Table 5.1 for comparison.

Table 5.1: Proximate analysis of fuels studied and fuels from Kang et al. [2017] and Soyosa et al. [2015]

	Fuel	Moisture (wt.%)[ar]	Volatiles (wt.%)[db]	Fixed Carbon[a] (wt.%)[db]	Ash (wt.%)[db]
This Work	Commercial Coffee Logs	7.5	79	17.9	3.01
	Willow Wood Logs	5.0	82	16.3	1.68
	Mexican Robusta Beans (MRB)	2.3	78	16.7	5.32
	Brewed Mexican Robusta Beans (BMRB)	9.7	78	17.6	3.99
Kang et al. [2017]	Wood Pellet	7.4	81	18.6	0.59
	Coffee Bean (before brewing)	2.1	78	17.6	3.96
	Dried Spent Coffee Ground	11.7	79	18.4	2.33
Soysa et al. [2015]	Douglas Fir	3.7	81	17.2	2.08
	Spent Coffee Ground (two staged drying)	0.9	79	16.2	4.84

[a]*Calculated by difference*

The results from this work show good consistency with the results from Kang et al. [2017] and Soysa et al. [2015]. The main difference is between the moisture content. The main reason for this is the various methods used for drying; in this work the fuels were dried in an oven at 40°C, in Kang et al. [2017] the fuels were dried in direct sunlight and air, and in Soysa et al. [2015] a two-staged drying process was used at 105°C and then 80°C. Additionally when the coffee is ground, the particle size is much smaller than the size generated in the cutting mill, discussed in more detail in section 5.3.3. The ground coffee is a coarse powder, this means it has a relatively high specific surface area and has a fairly porous structure which can absorb and retain more moisture.

The ash content shows a significant degree of variability between the fuels. Coffee beans are formed from a mild torrefaction process of coffee cherries, their identity is therefore complex as they are neither an herbaceous or fruit biomass, but a

mixture of both. Vassilev et al. [2010] showed that herbaceous biomass can have a mean ash content of between 4.8-8.6 wt.% db compared to 3.5 wt.% db for common woods. This explains the observed lower ash content for the Douglas fir, willow and wood pellets. The highest ash content was measured in the MRB, 5.32 wt.% db, most likely because during torrefaction the ash material is concentrated. The ash content is then reduced when the coffee is brewed as seen for the BMRB, 3.99 wt.% db. This is a decrease of 1.32 wt.%, a slightly smaller decrease than seen in Kang et al. [2017] of 1.63 wt.% between the original and brewed ground coffee. Brewing washes the ground coffee which leaches inorganic elements [Wang et al., 2016].

There is a small difference in the volatile matter between the fuels. Typically, the volatile matter is much lower for torrefied fuels, however the torrefaction process for producing coffee is often at much lower temperatures (between 200-250°C) than used in conventional biomass torrefaction for energy purposes. The volatile matter is highest in the wood logs, although there is only 1 wt.% db between the wood fuels. Based on the results collectively from Table 5.1 the spent coffee and the raw coffee have nearly identical VM and FC contents.

The ultimate and chlorine analysis is shown in Table 5.2. From Table 5.2 it is clear that the coffee prior to brewing, MRB, has the highest HHV (22.29 MJ kg^{-1}) and this is because of the high concentrations of carbon and hydrogen (57.0 wt.% daf and 7.4 wt.% daf respectively). There is a result of torrefaction [Akinrinola, 2014] [Trubetskaya et al., 2019]. The coffee bean fuel from Kang et al. [2017] has the second highest carbon content (55.0 wt.% daf) however the HHV is equal to the spent coffee bean fuel from the same reference (21.97 MJ kg^{-1}). During the brewing process carbon is extracted in the form of light oils. This result was observed for the MRB and the BMRB and for the spent and unused coffee in Kang et al. [2017]. The carbon content for the spent coffee from this work, Kang et al. [2017] and Soysa et al. [2015] are within 1 wt.% daf, showing a significant level of consistency and homogeneity between spent coffee collected from different sources. All of the coffee-based fuels have a significantly higher HHV. Between the lowest HHV for a coffee-based fuel, spent coffee grounds from Soysa et al. [2015], and the highest HHV for a wood-based fuel, wood pellets from Kang et al. [2017], this is a difference of 1.57 MJ kg^{-1} (20.92 and 19.35 MJ kg^{-1} respectively). The carbon and hydrogen content of the wood-based fuels are substantially lower than the coffee fuels which explains the lower HHV.

The nitrogen content of the coffee-based fuels (1.48-2.40 wt.% daf) is considerably higher than the wood fuels. The N content of wood is typically low including when using barked wood, average of 0.4 wt.% daf [Vassilev et al., 2010]. This is significantly lower than in herbaceous biomass, 1.2 wt.% daf [Vassilev et al., 2010]. The N content reduces by approximately 0.2 wt.% daf when brewed in both this work (MRB and BMRB) and the work of Kang et al. [2017]. In the work of Abelha et al. [2019] and Carillo, Staggenborg and Pineda [2014] there are some fuels (miscanthus, road side grass and sorghum) which decrease slightly in N content when torrefied and washed. This reduction must be from the leaching of soluble N compounds such as ammonium salts and amines [Quilin, Lujia and Guangqun, 2017] [Yu et al., 2014].

The sulphur content for all the fuels is below 0.06 wt.% daf except for the MRB which is significantly higher at 0.22 wt.% daf. Vassilev et al. [2010] reported that coffee husks (a shell that coats the bean) to have a sulphur content of 0.35 wt.% daf, which suggests coffee plants are naturally high in S. However, the BMRB has a substantially lower S content (0.06 wt.% daf) meaning that the brewing process can remove up to 70% of the S content. A similar result was observed in Yu et al. [2014] for Jose wheat grass, which went from 0.23 wt.% db to 0.06 wt.% db using deionised water at room temperature with agitation. A similar process by Deng et al. [2013] of using deionised water at room temperature but using a water bath to agitate the leaching process resulted in similar S reductions for wheat straw, rice straw, corn stalk, cotton stalk and rice hulls. A study by Sun, Salisbury and Tomkinson [2003] explains that S will leach into a solution as both inorganic anions or organic compounds depending on its natural presence within a biomass. However, limits on S removal can be dependent on competition with other organic compounds usually because of temperature influences [Sun, Salisbury and Tomkinson, 2003].

Leaching of chlorine has been extensively researched by various washing techniques [Knudsen, Jensen and Dam-Johansen, 2004] [Jenkins, Bakker and Wei, 2003] [Björkman and Strömberg, 1997]. Water washing is highly effective at removing chlorine from biomass because it is usually present as a free anion or loosely bonded at ion exchange sites [Marschner, 2012] [Knudsen, Jensen and Dam-Johansen, 2004]. Similar to S the Cl content for the MRB, 0.21 wt.% db, is reduced after brewing, BMRB, 0.03 wt.% db, by 85%. It is expected that there would be competition between

the sulphur anion, SO_4^{2-}, and the monovalent chloride ion, Cl^-. Usually. this competition is generated by ion saturation of water bodies [Jenkins et al., 1996] however because the brewing process in commercial coffee machines simulates a continuous flow process more than a batch process this would prevent saturation and thus aid removal of both ions.

Table 5.2: Ultimate and chlorine analysis of fuels studied

	Fuel	Carbon (wt.%)[daf]	Hydrogen (wt.%)[daf]	Nitrogen (wt.%)[daf]	Sulphur (wt.%)[daf]	Oxygen[a] (wt.%)[daf]	Chlorine[b] (wt.%)[daf]	HHV[c] (MJ kg^{-1})[db]
This Work	**Commercial Coffee Logs**	53.0	7.1	1.89	0.03	37.9	0.04	21.1
	Willow Wood Logs	49.0	6.8	0.54	0.00	43.8	n/d	19.28
	Mexican Robusta Bean (MRB)	57.0	7.4	1.86	0.22	33.7	0.21	22.29
	Brewed Mexican Robusta Bean (BMRB)	54.0	7.4	1.66	0.06	36.5	0.03	21.51
Kang et al. [2017]	**Wood Pellet**	49.0	6.4	0.42	0.01	44.5	n/a	19.35
	Coffee Bean (before brewing)	55.0	7.2	1.69	0.06	35.6	n/a	21.97
	Dried Spent Coffee Ground	54.0	7.4	1.48	0.05	36.8	n/a	21.97
Soysa et al. [2015]	**Douglas Fir**	49.0	6.1	0.00	0.00	44.8	n/a	19.04
	Spent Coffee Ground (two staged drying)	54.0	7.1	2.40	0.00	36.8	n/a	20.92

[a]Calculated by difference, [b]determined by SOCOTEC external analysis, [c]calculated using Eq.3.7 by Friedl et al. [2005]

5.3.2 Metals Analysis

Analysis of the metals in the ash are shown in Table. 5.3 for the fuels studied and some other domestic stove fuels.

As mentioned in the previous section understanding the nature of coffee as a fuel is difficult. Using Table 5.3, the SiO_2 concentration is ranked in the order miscanthus> coal> mixed waste paper> sawdust> BMRB> commercial coffee logs> MRB> willow wood logs> salix. Straws and coal are often high in SiO_2 this comes from natural processes during growth or formation. The mixed waste paper and sawdust are high in SiO_2 from anthropogenic sources during manufacturing. The

BMRB and commercial coffee logs are higher in SiO_2 then the MRB, this is because Si is in more stable structures that do not leach in water. Wood is notoriously low in SiO_2, the difference between the salix and the willow logs is most likely the amount of bark as bark is often lower in SiO_2 compared to the actual wood [Vassilev et al., 2010].

Table 5.3: Metals in ash analysis of the fuels in this work and comparison with other fuels for domestic stoves, all values are in wt.%

Reference	Fuel	SiO_2	Fe_2O_3	CaO	MgO	Na_2O	K_2O
This Work	**Commercial Coffee Logs**	20.12	6.11	30.31	1.62	0.22	23.26
	Willow Wood Logs	9.25	1.25	39.65	5.06	1.35	22.11
	Mexican Robusta Bean (MRB)	16.51	4.51	26.76	1.54	0.97	32.21
	Brewed Mexican Robusta Bean (BMRB)	22.31	6.56	32.51	1.46	0.19	20.81
[Zevenhoven-Onderwater et al., 2000]	**Salix**	6.1	0.74	46.09	4.03	1.61	23.4
[Wigley et al., 2007]	**Miscanthus**	56.42	0.94	10.77	3.01	0.47	19.75
	Sawdust	26.17	1.82	44.11	5.34	2.48	10.83
[Vassilev and Vassileva, 2007]	**Coal**	54.06	6.58	6.57	1.83	0.82	1.6
[Miles et al., 1995]	**Mixed Waste Paper**	28.62	0.82	7.63	2.4	0.54	0.16

The concentrations of Fe_2O_3 are in the decreasing order of coal> BMRB> commercial coffee logs> MRB> sawdust> willow wood logs> miscanthus> mixed waste paper> salix. The Fe_2O_3 measured in ash has low mobility and is usually found in high concentrations in contaminated biomass and agricultural residues [Vassilev et al., 2010]. Based on Table 5.3 the highest containing Fe_2O_3 biomass have been torrefied. Torrefaction causes ash to become concentrated [Akinrinola, 2014]. The brewing process also concentrates the Fe_2O_3 based on the results from Table 5.3, between the MRB and the BMRB the Fe_2O_3 concentration increases by 2.05 wt.%, this is 45% increase after brewing.

The MgO concentration is ranked in the order sawdust> willow wood logs> salix> miscanthus> mixed waste paper> coal> commercial coffee logs> MRB> BMRB. According to Vassilev et al. [2010] there is a moderately strong positive correlation between the MgO concentration and the CaO concentration. The CaO

concentration ranks in the order salix> sawdust> willow wood logs> BMRB> commercial coffee logs> MRB> miscanthus> mixed waste paper> coal. The two trends are similar with the exception of the coffee derived fuels. In both Abelha et al. [2019] and Yu et al. [2014] during torrefaction and washing the concentration of CaO increases. In the latter leaching alone increases the concentration on average by 19% for a mixture of straws and woods. In this work the increase on brewing is 21%. Therefore, the exception in the correlation between MgO and CaO could be from pre-treatment.

The Na_2O concentrations are in decreasing order of sawdust> salix> willow wood logs> MRB> coal> mixed waste paper> miscanthus> commercial coffee logs> BMRB. The solubility of Na ions in water is very high and therefore it is anticipated any mobile Na will be readily removed during the brewing process. Yu et al. [2014] noted that the concentration of Na_2O is reduced for most of the fuels studied (grasses and woods). There is one exception to this in Yu et al. [2014] which is switchgrass where the Na_2O increases after the washing process. This is most likely due to the presence of Na in insoluble structures for example within silica. However, for the MRB and BMRB in Table 5.3 it can be assumed that the Na is present as soluble Na, since the concentration decreases by 0.78 wt.% after brewing.

The K_2O ranks in the order of MRB> salix> commercial coffee logs> willow wood logs> BMRB> miscanthus> sawdust> coal> mixed waste paper. Based on the data in Table 5.3, 40% of the K_2O is removed between the MRB and the BMRB. Yu et al. [2014] observed that 75% of the K_2O is removed when wheat and rice straw is washed, this was lower than seen in the work of Deng, Zhang and Che [2013] for the same fuels (78% and 84% respectively). However, both are substantially higher than measured for the brewing process in this work. Before brewing the K_2O content is high and is comparable to herbaceous and agricultural residues such as hazelnut shells (30.40 wt.%) and walnut shells (33.03 wt.%). After the coffee has been brewed the reduction is substantial, and the fuel is now comparable to the wood fuels (in terms of K_2O content in the ash).

5.3.3 Particle Size Distribution

Particle size distribution has been shown to have significant impacts on the combustion performance in various boilers and stoves [Russo et al., 2014] [Caposciutti

et al., 2020] [Kang et al., 2017]. Fig. 5.2 shows the particle size distribution for the commercial coffee logs and BMRB from this work and compared to the results of Kang et al. [2017] for the spent coffee grounds.
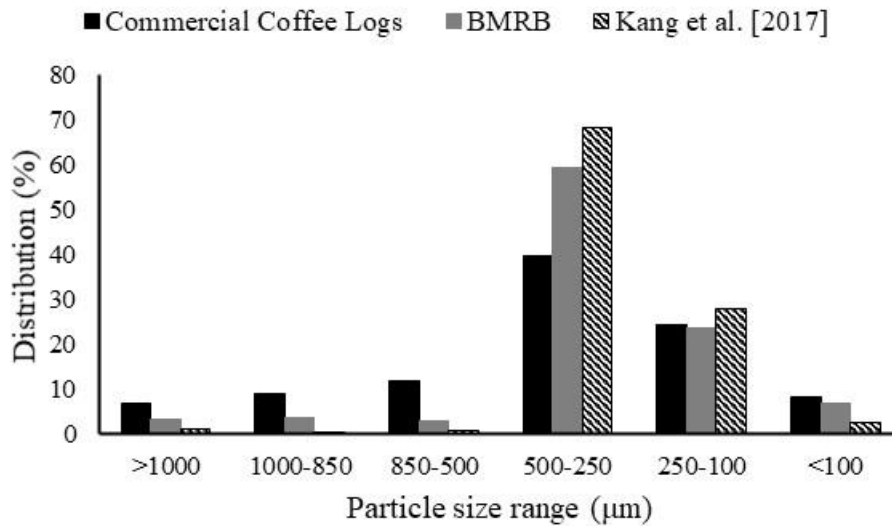
Figure 5.2: Particle size distribution of used ground coffee from commercial coffee logs, BMRB and Kang et al. [2017]. A standard error of 5% applies to the measurements in this work to account for lost mass.

From Fig 5.2 it is clear that the majority of spent coffee grounds have a particle size in the region of 500-250μm. Additionally, over 90% of particles in the BMRB and in the work of Kang et al. [2017] are below 500μm, for the commercial coffee logs this percentage is smaller (72.4%) but still represents the majority of particles in the briquettes. For the commercial coffee logs the distribution is much more evenly spread creating a much smaller skew towards the smaller particles. Reasons for this are not definitive however are most likely the result of collecting from multiple sources, each coffee machine user can decide how coarse they want the coffee ground. Other reasons could include differences in beans and agglomeration from moisture, temperature and pressure.

5.3.4 Stove Combustion

5.3.4.1 Stove Performance

Stove performance focuses on three key measurements: burning rate, conversion efficiency and temperature. Fig. 5.3 shows the burning rate over the whole combustion period, arrows indicate when new batches of fuel (~1.5kg) were placed in

the stove. From Fig 5.3a for the coffee logs, the plot shows an initial peak (in the black box) after reload followed by the main broader peak which continues to the end of combustion. The initial peak is caused by the rapid combustion of the thin carbon rich wax coating which encases each briquette. Once this coating is combusted the briquette loses all its integral shape causing it to form a bed of soft powdered fuel. This bed then begins flaming very rapidly hence the burning profile restores its shape very quickly.
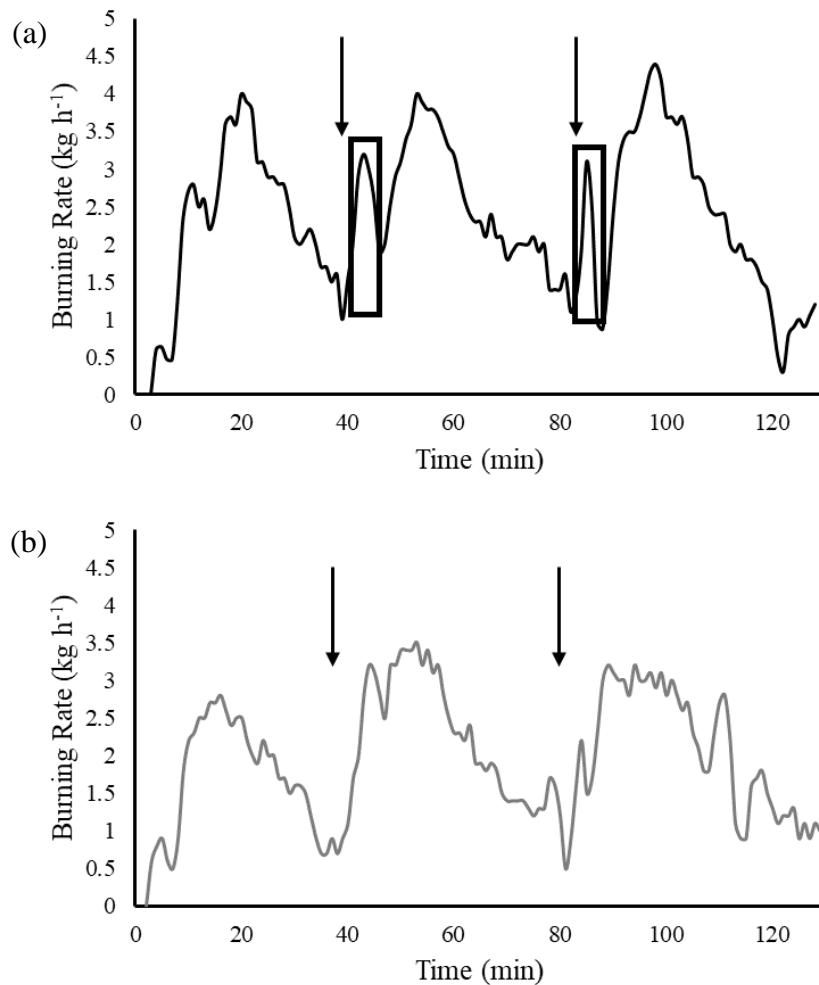
Figure 5.3: Burning rate profiles for (a) Commercial coffee logs (b) Willow wood logs. Arrows indicate fuel reloading points.

Profiles for both commercial coffee logs and the willow wood logs have a regular shape. This means that the fuel is loaded, it begins to flame, flaming progresses to a peak burning rate and maintains for a period, after which the burning rate steadily declines as the fuel progresses through char combustion and until combustion ends. The main differences (besides the aforementioned initial peak from the coating) are in

163

the magnitude and width of the peaks. For the coffee logs the peak is sharper and narrower for the flaming period, and then during the smouldering phase the profile is more gradual in its decline. This is especially important since the characteristic time for each batch of fuel is nearly identical.

Table 5.4 shows the average burning rates for flaming and smouldering combustion, the peak and average temperatures during each phase and the percentage conversion of each batch of fuel. The average burning rate for the coffee logs in both flaming and smouldering combustion is higher than the willow wood logs which results in an overall greater conversion of the fuel. The average and peak temperatures for the both combustion phases are higher for the coffee logs which is expected since the calorific value is greater (21.1 and 19.8 MJ kg^{-1}).

Past work has shown that the flaming burning rate is related to the volatile matter content [Faschinger et al., 2017] [Mitchell et al., 2016]. However, when referring back to Table 5.1 the volatile matter for the willow wood logs (81 wt.% daf) is higher than the commercial coffee logs (76 wt.% daf). Caposciutti et al. [2020] demonstrated that smaller particles during combustion can ignite much faster due to a high surface area to volume ratio. This is relevant to the fuels studied in this work, the coffee logs are made from 72.4% sub-500μm particles. The willow wood logs combust as a complete unit with a much lower surface area to volume ratio. Therefore, the particle size is the main influencing factor increasing the burning rate and the extent of combustion, Eq. 3.17.

Table 5.4: Average burning rates, average temperatures and peak temperatures for each batch and combustion phase, and the overall percentage batch conversion efficiency

Fuel		Commercial Coffee Logs		Willow Wood Logs	
	Batch	1	2	1	2
Flaming Combustion	**Burning rate (kg h^{-1})**	3.15	3.26	3.05	2.91
	Average Temperature (ºC)	510	530	435	410
	Peak Temperature (ºC)	590	600	470	480
Smouldering Combustion	**Burning rate (kg h^{-1})**	2.58	2.33	1.75	1.68
	Average Temperature (ºC)	410	390	310	300
	Peak Temperature (ºC)	435	420	375	355
(%) Extent of Combustion		86	89	84	82

5.3.4.2 Carbon Emissions

Carbon emissions specifically refers to CO_2, CO and CH_4 emissions in this section. Fig. 5.4 shows the CO_2 and CO emission profiles for the coffee logs and willow logs. Comparing the two profiles, the willow wood follows a profile typical of wood stove combustion where by the CO_2 emissions increase after the new batch of fuel has been loaded, this increases to a peak and a plateau which declines as the fuel bed transfers from flaming to smouldering combustion. As the phase transition occurs the CO emissions increase to a peak and then decrease indicating combustion is ending. This transition is common in domestic stoves because it reflects the changing stoichiometry (lower mixing), temperature (decreasing) and reaction phase (homogeneous gas phase reactions to heterogeneous char combustion).

Compared to the burning rate profiles in Fig. 5.3, the concentration profiles in Fig. 5.4 are not as consistent. When fresh fuel is loaded into the stove the heat within the stove initiates decomposition of the fuel, the high amount of carbon from the new batch of fuel accelerates the burning rate. The relationship between the burning rate and emissions is not consistent. During the combustion of the coffee logs and the wood logs even though the burning rate profiles are uniform the CO_2/CO profiles suggest that oxidation reactions were being restricted, this could be from multiple factors such as air flow, turbulence, stoichiometry or residence time. This explains the disparity between the two parameters.

Comparatively the coffee logs show a different scenario. The emissions of CO_2 and CO directly correlate to the burning rate in Fig. 5.3 for the willow, however there is no correlation for the coffee logs. Instead in the coffee log profiles there are random sharp spikes. This is more noticeable in the first reload batch compared to the second. The profile for the coffee logs is more characteristic of a pellet boiler as seen in Sippula et al. [2017]. The particle size is believed to be the main parameter influencing this result. Once the coffee log disintegrates into a powder the transfer of heat and mass is more consistent across the fuel bed because of the high surface area to volume ratio. The spikes seen on the CO_2 profiles are being driven by localised rapid volatile release at specific moments.
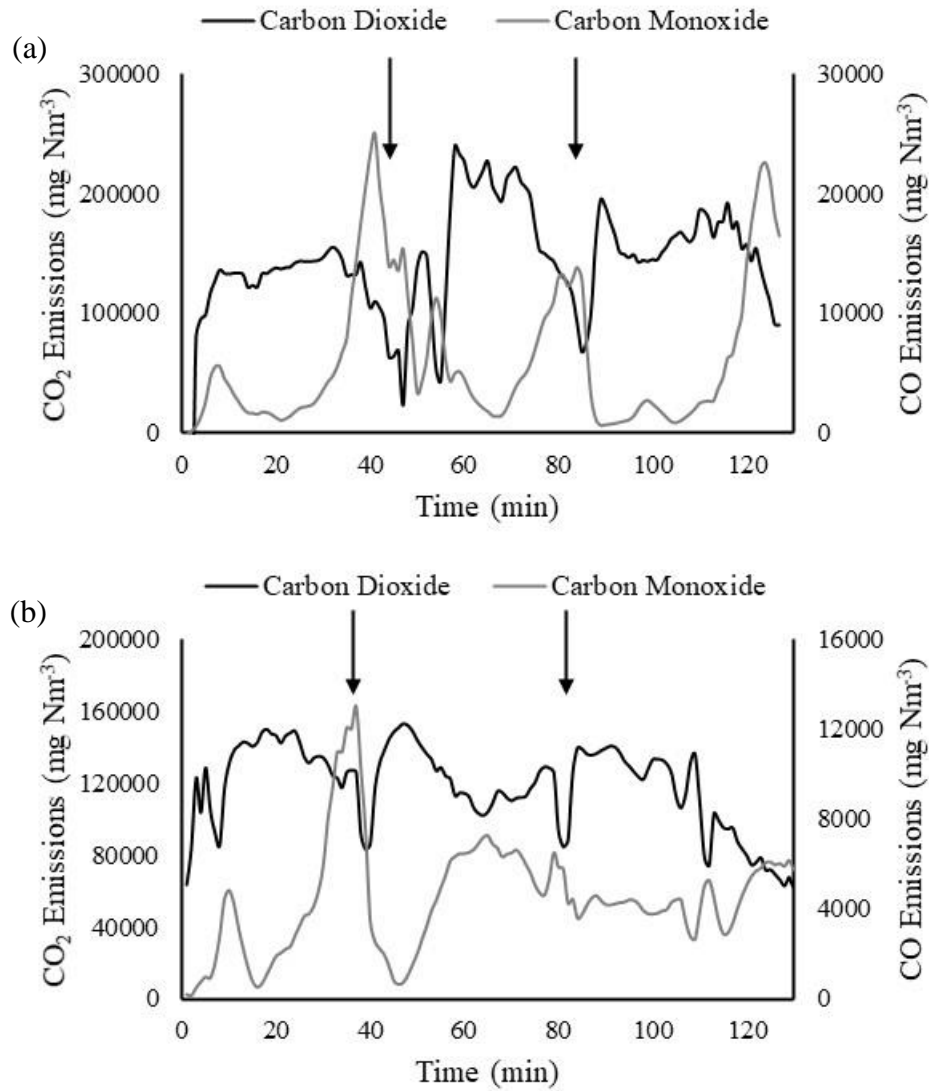
Figure 5.4: Emission profiles for CO_2 and CO for (a) Commercial coffee logs (b) Willow wood logs. Arrows indicate fuel reloading points.

The results also show that the small particle size of the coffee logs maintains a longer time period of flaming combustion and the change from flaming to smouldering is more rapid. This is the opposite to the willow logs where the logs retain their shape throughout combustion until fragmentation in the very latter stages of char combustion causing the fuel to disintegrate. Hence char combustion for the outer layers of the log is progressing whilst devolatilisation of inner areas of the log have just started, heat and mass transfer are determining the rate of combustion.

Table 5.5: Average emission factors for a batch of fuel (~1.5 kg) for CO_2, CO and CH_4 on a mg Nm^{-3} and kg GJ^{-1} basis

Fuel	Average Emission Factors (13% O_2, STP)						MCE	Residual Carbon in the Bottom Ash (%)
	mg Nm^{-3}			kg GJ dry fuel^{-1}				
	CO_2	CO	CH_4	CO_2	CO	CH_4		
Commercial Coffee Logs	160000	7300	400	100	5	0.26	95.6	7.5
Willow Wood Logs	115000	4600	300	75	3	0.16	96.2	18.8

Table 5.5 shows the average emissions of CO_2, CO and CH_4 for a batch (~1.5 kg) of fuel. The emissions for the coffee logs are substantially higher than the willow wood logs on both a mass and energy basis. However, when analysing the emissions using the modified combustion efficiency (MCE) equation, Eq. 5.1, the ratio of complete to incomplete combustion, the two fuels are very similar, both have high efficiency. Additionally, as seen in Table 5.4 because the willow wood logs burn in a sequential method from the outside to the inside, this reduced the percentage of the batch mass that was reacted, between 2-7% less than the coffee logs. In Table 5.5 the residual reactive carbon in the bottom ash of the wood logs is higher, this means that the extent of reaction (conversion efficiency) is significantly higher for the coffee logs (>10%).
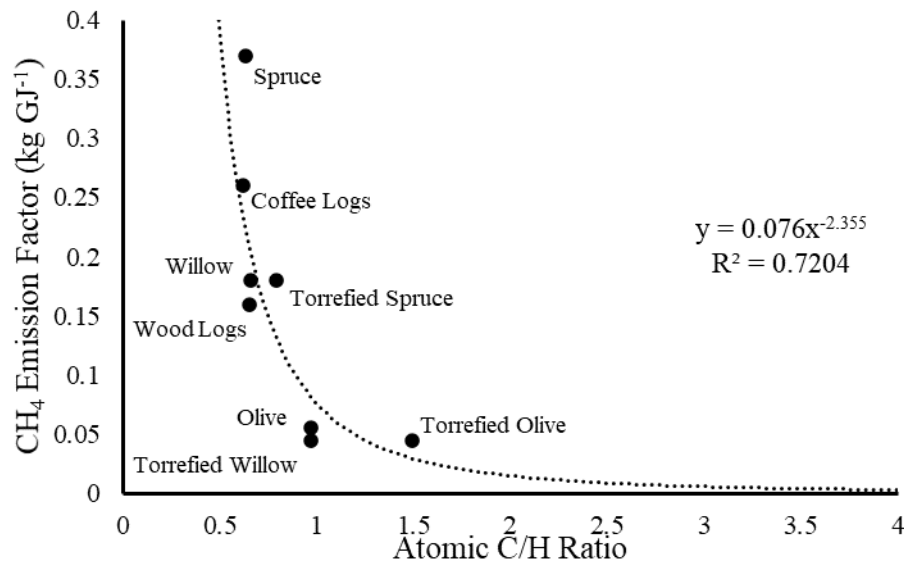
Figure 5.5: Methane, CH₄, emission factors plotted against the C/H ratio from the fuel analysis. Points from Chapter 4 are included.

As mentioned in Chapter 4 using Eq. 4.1-4.3, the CH_4 emissions are from the decomposition and gasification of volatiles. A correlation between the C/H ratio and the CH_4 emissions was evident from Fig 4.9. Fig. 5.5 shows the same data from Chapter 4 as well as the two fuels from this work. As can be seen in Fig. 5.5 a similar trend line ($x^{-2.355}$) with a good R^2 value (0.7204) is plotted; the value is still substantially short of being a definitive correlation. However, this does still present a reasonable argument for the correlation between the CH_4 emissions and the C/H ratio for fuels with a similar moisture content (<15 wt.%).

5.3.4.3 Nitrogen Emissions

Table 5.6 shows the average NOx emissions, NOx emission factor and the residual N measured in the bottom ash, as well as a comparison to data collected by Nosek et al. [2020] and Limousy et al. [2013]. As can be seen from Table 5.6 the coffee logs emit much higher concentrations of NOx compared to the willow wood logs combusted on the same system. This result was expected since the N content was higher in the coffee logs. As can be seen in Table 5.6, the N partition for the wood logs is more in the ash compared to the coffee logs.

Table 5.6: NOx emissions, emission factor, and residual N in the bottom ash. Additional data from Nosek et al. [2020] and Limousy et al. [2013] are shown.

Ref.	Fuel	Fuel-N (wt. % db)	NOx Emissions		Residual N in bottom ash (%)
			mg m^{-3}	g GJ^{-1}	
This Work	Commercial Coffee Logs	1.84	300	190	6
	Willow Wood Logs	0.53	140	80	14
Nosek et al. [2020]	Spent Coffee Grounds (SCG)	2.03	120	n/a	n/a
	SCG/Sawdust-50/50 blend	8.6	190		
Limousy et al. [2013]	Spent Coffee Grounds (SCG)	2.91	206		
	Pine	<0.1	45		
	50/50 blend-Pine/SCG	n/a	201		

Compared to Nosek et al. [2020] and Limousy et al. [2013] the emissions for the spent coffee in this work are much higher when the fuel-N content is much lower. In both Nosek et al. [2020] and Limousy et al. [2013] the fuels were combusted in pellet boilers where emissions are measured during a steady-state combustion process (fresh fuel is continuously loaded). Additionally, air staging is common in such combustion systems which is used as a NOx reduction technique and has been shown to reduce NOx emissions by up to 50% [Li et al., 2017] [Wang et al., 2018] [Wang et al., 2020]. However, there is a big difference in the results from the two references, Nosek et al. [2020] explains that the spent coffee grounds result is low because of incomplete combustion, fuel rich combustion conditions.
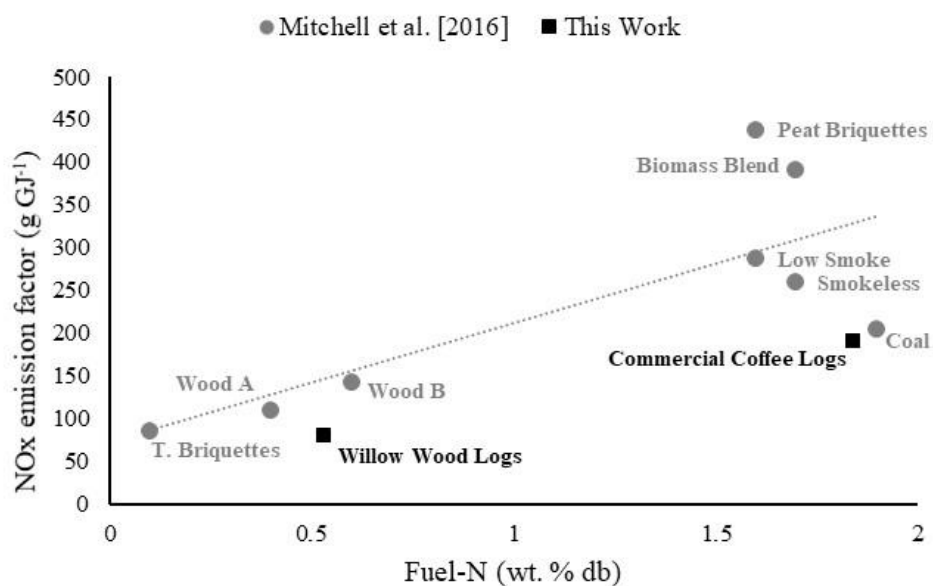
Figure 5.6: Emissions of NOx on an energy basis compared to the fuel-N content

As seen in Fig. 4.11, there is a linear correlation between the fuel-N content and the NOx emissions on an energy basis. Using the original points from Mitchell et al. [2016], Fig. 5.6 shows the data for the coffee logs and the willow wood logs on this trend. The two fuels are consistent with the fuels studied by Mitchell et al. [2016] however the magnitude is lower than expected based on the trendline. For the willow wood logs this most likely reduced combustion efficiency (i.e some fuel-N is retained in the ash). For the coffee logs, Fig. 5.6 suggests that torrefaction of the fuel causes the NOx emissions to be lower than predicted. The same result as seen in Chapter 4 and by Trubetskaya et al. [2019] for torrefied olive residue, where torrefaction binds

N tighter to C in the fuel matrix which delays its release during char combustion and promotes the NO reduction reaction with C to N_2.

5.3.4.4 Particulate Emissions and EC/OC Analysis

The PM_t emission factor is shown in Table 5.7 as well as results from the EC/OC analysis- EC is the same as black carbon (BC). The coffee logs PM_t emission factor is substantially higher than for the wood logs. Based on the work of Roy and Corscadden [2012] it could be said that this is because of the higher C/O ratio of the coffee logs however more data would be need to make establish this trend as it is not analogous with the data trend by Roy and Corscadden [2012], Fig. B.2.

Table 5.7: Total PM (PM_t) emission factors and EC/OC/ash emissions. Values are an average of two filters.

Fuel	PM_t Emission Factor (mg MJ^{-1})	Average Composition (wt. %)			% K released[a]
		EC	OC	Ash	
Coffee Logs	338	34.9	32.8	32.3	27.15
Willow Wood Logs	204	24.2	36.6	39.2	32.19

[a]*Calculated from ash analysis of the bottom ash*

Looking at Fig. 5.7 which are photos taken of the filter papers/foils from the impactors immediately after combustion, there is an apparent difference in the collected samples. The PM collected for the coffee logs has a more powder-like appearance and hence has scattered irregularly across the collection surfaces. For the wood logs there are much clearer scatter patterns and the PM looks to have partially coalesced so is less powder-like. Similar observations were observed in Wiinikka and Gerbart [2004] and suggest that the main constituent in the collected samples for the coffee logs is soot (EC). This is confirmed by the analysis of the filter papers (collecting sub-micron PM), which show a greater proportion of EC compared to the wood smoke which has a greater proportion of OC (organic carbon and tars). Additionally, assuming that any material collect that is not carbonaceous is ash material, as defined by Sippula et al. [2009] and Schmidl et al. [2011], the proportion of fly ash in the PM is significantly higher for the wood logs.

The PM constituent make-up (EC, OC and Ash) for the willow wood logs in this work is comparable to the results of Atiku et al. [2016] (EC ~30-50%, OC ~20-

40% and ash ~40%) for softwood fuels. The only difference is in the EC value for willow which could be from better stoichiometry during combustion or the reduced conversion efficiency. When comparing the coffee logs and the wood logs the ratio of OC/EC (0.93 and 1.51 respectively) shows that the PM from coffee logs is more similar to that from coal than biomass, although the nature of the OC will differ. The NOx emissions from coffee logs were also similar to levels seen in coal combustion.

Figure 5.7: Impactor foils and filters for a) commercial coffee logs b) willow wood logs

The most intriguing observation is the lower PM ash content for the coffee logs compared to the wood logs when the initial fuel analysis shows that the ash and K content is greater. A similar result was observed for rice straw pre-treatment (torrefaction followed by washing) and combustion by Wang et al. [2020]. Chemical analysis of the PM_1 for the pre-treated rice straw was lower in K even though the fuel content was higher [Wang et al., 2020]. During combustion at temperatures between 600-1000°C K salts form as chlorides and sulphates; however, Si and Ca can prevent the formation of these salts by retaining K or S in the char or ash matrix. Both Si and Ca are not readily leached from biomass because of their structural stability and often require acids or harsher chemicals to remove them. As can be seen in Table. 5.3, the SiO_2 content of the coffee logs is significantly higher than the wood logs and from Table 5.7, by analysing the chemical composition of the bottom ash, 5% more K was released from combustion of the wood logs than the coffee logs. This could explain the increased ash content of the PM from the wood logs.

5.4 Conclusions

In this work, analysis of the suitability of waste coffee grounds for domestic combustion applications was assessed in comparison to other more conventional fuels. Proximate, ultimate and metals analysis was used to compare the composition of the spent coffee grounds to willow wood logs. Additionally, analysis of the coffee grounds before and after brewing were analysed to assess the impacts of the brewing process and to establish the variability of spent coffee grounds. Combustion of the commercial coffee logs was investigated on a domestic stove and compared to the willow wood logs. Comparison was based on combustion performance (burning rate and temperature) and emissions (CO_2, CO, CH_4, NOx and PM).

Volatile content in the spent coffee grounds (78-79 wt.% db) was lower than the conventional wood fuels (>80 wt.% db) this is common with thermally treated fuels, as was the higher ash content which had a large degree of variability (3.01-5.32 wt.% db) and was substantially higher than the wood logs analysed in this work (1.68 wt.% db). After the coffee had been brewed the ash content was significantly reduced, 1.33 wt.%.

The carbon content in the ultimate analysis was approximately 5 wt.% (db) higher in the spent coffee ground. The coffee grounds were very high in nitrogen, values were greater than 1.66 wt.% (db) and were more comparable to coal than biomass. The overall differences in the composition from proximate and ultimate analysis resulted in the calculated HHV of the coffee being approximately 2 MJ kg^{-1} (db) higher than the wood-based fuels.

Metals analysis was focused on major inorganic species. The SiO_2 content of the coffee increased after being brewed (20.12-22.31 wt.% compared to 16.51 wt.%) and was analogous with other industrial residues such sawdust (26.17 wt.%) [Wigley et al., 1995] and mixed waste paper (28.62 wt.%) [Miles et al., 1995]. The CaO content was substantially lower in the spent coffee (30.31-32.51 wt.%) compared to the wood fuels, wood logs (39.65 wt.%) and salix (46.09 wt.%) [Zevenhoven-Onderwater et al., 2000]. The most significant change after the coffee had been brewed was in the Na_2O and K_2O content, 0.78 wt.% and 11.6 wt.% was removed respectively.

The overall conversion during combustion of spent coffee grounds in the form of commercial coffee logs was much greater than the wood logs. This was mainly

attributed to the smaller particle size and the ease and speed at which the coffee logs disintegrated when in the stove. After the coffee logs had disintegrated the surface area to volume ratio was substantially higher. This also resulted in much sharper peaks on the burning rate profile (Fig. 5.3) which were greater in magnitude than the wood logs ($\sim$4 kg h^{-1} compared to 3.5 kg h^{-1})

The carbon-based emission factors (CO_2, CO, and CH_4) were greater for the coffee logs than those measured for the wood logs. Interestingly the MCE for the two fuels were almost identical (95.6 to 96.2%). There was more C in ash for the wood logs, which corresponds to the aforementioned lower conversion of the wood logs compared to the coffee logs. The C/H ratio correlation to the CH_4 emission factor in this chapter was in agreement with the data from Chapter 4 and Mitchel et al. [2016].

The NOx emissions from the coffee logs were more comparable to coal [Mitchell et al., 2016] than conventional biomass. This was anticipated since the fuel-N content was also similar to coal. There was a greater amount of residual N in the ash from the wood logs.

Analysis of the PM_1 collected indicated that the PM from the coffee logs was greater in EC and lower in OC and ash (assumed based on residual mass) compared to the PM_1 from the willow logs. This was intriguing since the coffee was higher in ash species. Based on the work of Wang et al. [2020] the higher Si content of the coffee logs reduced the release of K by retaining it in the bottom ash, this was confirmed by analysing the K in the bottom ash.

Chapter 6. Characterisation of Bracken for Combustion Applications

6.1 Introduction

In the UK current electricity generation is rapidly moving from the use of coal to alternative fuels. Although part of this is being replaced by oil and natural gas; wind, solar, nuclear, biomass and wastes are also being used. Biomass is particularly advantageous as it can easily be retrofitted to existing coal fired power stations and localised heat and energy systems without large capital investment or new plant commission.

In the first quarter of 2019, bioenergy and waste accounted for 11% of the UK's total energy production [BEIS National Statistics, 2019]. This will continue to grow as the UK moves towards no waste to landfill and stricter limitations on the uses of fossil derived fuels. Within the biomass sector natural agricultural wastes are a growing area for research and investment. A survey in 2003 by the Chartered Institution for Waste Management (CIWM) [2003] showed that 90% of agricultural holdings burned agricultural waste, with 83% admitting to burning on open fires. This presents many opportunities for the management of waste to be utilised as fuels for power generation or in space heating systems.

Bracken *(Pteridium aquilinum)* is considered an agricultural waste which is commonly burned in open fires. It is found annually on farmland, lowland heath, moorland, grassland, woodland, coastal areas, in towns and cities. It is the UK's most common fern and is described as opportunistic, pernicious and invasive [EUR (1985) 10013 EN, final]. Globally bracken grows in every continent except Antarctica. Across Northern Europe, North America and New Zealand problems persist with the growth of bracken and its damage to the ecosystem [Callaghan, Scott and Whittaker, 1981]. There is more detail on the growth, structure and problems with bracken in section 3.2.3.

Current management options are limited because of the ban on the herbicide asulox by the European Union in 2012 and the price of straw being cheaper; meaning the market for animal bedding is no longer profitable [Lyme Disease Action, 2011]. It

is clear that should an alternative use for bracken be available it would prevent land management agencies from open burning [Donnelly, Robertson and Robinson, 2002]. There is roughly ¼ of a million hectares of open land harvestable bracken available in the UK. There is little recent literature on the considerations of bracken as an energy crop, therefore it is important to analyse its potential use as a fuel from both an energy and environmental point of view in order to modernise current practices. This chapter aims to characterise the properties of bracken and compare them with currently used energy crops and biomass described in section 3.2.3.

6.2 Materials and Experimental Methods

6.2.1 Sample Harvesting

Samples were obtained from Budby Moor in Sherwood Forest, Nottinghamshire at four different time points between July- October 2018, Table 6.1. Five sampling sites were chosen based on their similarity in growing conditions- sunlight exposure, proximity to woodland area and potential for water logging. The site locations along with the GPS codes are shown in Fig. 6.1. Only the fronds were sampled, this was decided as it represented a realistic management technique for future harvesting.

6.2.2 Sample Preparation

The samples studied and details of machinery used in sample preparation are detailed in Chapter 3. All the samples were dried in air for 96 hours at 40°C before being milled to a size of less than 4mm. A small amount of sample was cryomilled to a size range of 10-100µm for use in ultimate analysis, metals analysis, and TGA. For ash fusion tests and metal analysis some sample was ashed before being milled, the ashing procedure used was the same as used in the British Standard Test for the determination of ash in solid biofuels; BS EN ISO 21404:2020, this method is outlined in section 3.4.6.

6.2.3 Experimental Methods

The details of all the experiments conducted in this chapter can be found in Chapter 3.

Table 6.1: Sampling times and weather conditions

Sampling period	Temp. High (°C)	Temp. Low (°C)	Historical Temp. High (°C)	Historical Temp. Low (°C)	20-day prior total rainfall (mm)
1- 5th July	29	12	19	12	2
2- 30th July	26	14	20	13	19
3- 26th September	23	11	16	9	52
4- 24th October	15	10	12	6	32

Figure 6.1: Sample sites in Budby Moor, Sherwood Forest and GPS co-ordinates, Map from RSPB (2018)

6.3 Results and Discussion

6.3.1 Proximate and Ultimate Analysis

Results from the proximate analysis are shown in Table 6.2, this includes miscanthus, two straws, willow logs and torrefied willow (willow and torrefied willow data is extracted from Chapter 4). When the bracken is harvested, its moisture content is very high (ar), >50 wt.%, therefore it was dried as detailed in section 6.2.2 and this reduced the moisture to less than 10 wt.% ad. The main reason for drying the bracken was to prevent the biological degradation of the samples. The moisture is always

higher in the first harvest than the final harvest, this is because of senescence in the latter part of the growth cycle.

The volatile content is higher during the earlier harvests. However, the overall change over the sampling time period was very small; at every site this change was less than 2 wt.% db. The volatile content of the bracken is lower than that of other frequently used UK energy plant species. Pakeman, Marrs and Jacob [1994] identify that bracken has a C_4 photosynthetic pathway and a perennial growth cycle. This is the same as miscanthus; however, there is a significant difference in the volatile matter content, ~15 wt.% db.

Table 6.2: Proximate analysis of fuels studied

Sample	Site	Sample Period	Moisture (wt.%)^{ar}	Moisture (wt.%)^{od}	Volatiles (wt.%)^{db}	Fixed Carbon ^{a} (wt.%)^{db}	Ash (wt.%)^{db}
Bracken	**1**	**1**	69.7	8.1	72.0	19.9	8.1
		2	71.1	7.3	71.8	20.9	7.3
		3	62.5	6.8	71.0	22.2	6.8
		4	50.1	5.7	72.0	22.4	5.6
	2	**1**	68.4	6.4	69.7	23.9	6.4
		2	73.5	6.0	70.4	23.6	6.0
		3	63.5	5.9	70.1	24.1	5.8
		4	51.1	5.1	68.1	26.8	5.1
	3	**1**	71.2	8.7	67.3	24.0	8.7
		2	72.3	8.5	68.6	22.9	8.5
		3	64.2	8.4	67.8	23.8	8.4
		4	53.1	7.3	67.5	25.3	7.2
	4	**1**	67.8	8.7	67.3	24.0	8.7
		2	68.9	8.5	67.9	23.6	8.5
		3	61.2	8.3	67.7	24.0	8.3
		4	52.1	7.9	66.4	25.7	7.9
	5	**1**	72.1	8.7	70.1	21.4	8.5
		2	69.8	8.3	70.7	21.1	8.2
		3	63.4	7.8	70.8	21.4	7.8
		4	51.7	5.9	68.9	25.2	5.9
'Brackettes'			5.1	n/a	68.7	26.7	4.9
Miscanthus			9.1	n/a	87.0	8.4	4.6
Barley Straw (423)			7.4	n/a	75.1	19.0	5.9
Wheat Straw (093)			5.8	n/a	79.6	16.2	4.2
Willow			10	n/a	82.0	17.0	1.0
Torrefied Willow			7.6	n/a	73.0	24.2	2.8

^{ar} as received, ^{od} oven dried, ^{db} dry basis, ^{a} calculated by difference. Sample period is the time of year at which the sample was harvested.

The fixed carbon content for the bracken is significantly higher at the last harvest than during any other time period; Site 5 showed an increase of 3.8 wt.% db

between harvests 3 and 4. The FC is also considerably higher in the bracken in comparison to the other energy crops with the exception of the torrefied willow briquettes. The torrefied willow briquettes have a FC content of 24.2 wt.% db compared to 22.4, 26.8, 25.3, 25.7 and 25.2 wt.% db for the final harvest at sites 1-5 respectively. The miscanthus, 8.4 wt.% db, and bracken site 2 harvest 4, 26.8 wt.% db, have the lowest and highest FC contents respectively.

The ash content shows a significant degree of variability over the bracken sites and harvesting. The highest and lowest contents being 8.7 wt.% db and 5.1 wt.% db, sites 3 and 2 respectively. The change in ash content over the sampling time period is also variable between sites. Sites 1 and 5 experience a large change of ≥2.5 wt.% db, this represents a change of over 30% in the ash content at both sites. Whilst, the smallest change is at site 4, 0.8 wt.% db, which is a change of ~9% in the ash content. The ash content in the bracken is typically higher than the other energy plants. Of the other fuels the willow has the lowest ash content, 1.0 wt.% db, and the barley straw has the highest, 5.9 wt.%. The final harvests of sites 1, 2 and 5, have an ash content which is comparable to the barley straw, 5.6, 5.1 and 5.9 wt. % db respectively.

Results from the CHNS analysis are shown in Table 6.3. The carbon content of the bracken increases as time progresses by about 2 wt.% db. Compared to the other energy species the bracken has a similar carbon content with the exception of the torrefied willow; this is expected since torrefaction is used to energy densify a fuel. Using Eq. 3.7 by Friedl et al. [2005] in section 3.4.4, the HHV can be calculated based on the elemental composition. In most of the bracken samples the increases in carbon content result in an increase in the HHV. There are a few exceptions to this, for example bracken sites 2 and 3 sample period 3 where the decreases in hydrogen content compensate for the increase in carbon content resulting in the HHV being lower than expected. The HHV of the bracken is greatest after the fourth harvest for all the sites, this is also when the largest increase in carbon content occurs. The average HHV over the growth cycle of the bracken is lower than most of the alternative energy species with the exception of the willow, 18.98 MJ kg^{-1} db. The fourth harvest HHV for the bracken sites 1-5, 19.03, 19.40, 19.79,19.69 and 19.55 MJ kg^{-1} db respectively, are comparable to the barley and wheat straws, 19.75 and 19.71 MJ kg^{-1} db respectively.

The hydrogen content of the bracken peaks at the third sampling period, this then drops by approximately 1 wt.% db. All the sites have a significant change in hydrogen between sampling periods 3 and 4, >12% of the relative total. The highest bracken hydrogen content is site 2 harvest 3, 6.0 wt.% db, which is similar to the willow, 6.2 wt.% db. The average hydrogen content over the growth cycle is between 4.6-4.7 wt.% db which is lower than the other energy pants.

Table 6.3: Ultimate analysis, CHNSO, of fuels studied

Sample	Site	Sample Period	C (wt.%)^{db}	O^a (wt.%)^{db}	H (wt.%)^{db}	N (wt.%)^{db}	S (wt.%)^{db}	Cl (wt.%)^{db}	HHV^b (MJ kg^{-1})^{db}
Bracken	1	1	45.7	39.8	4.3	1.86	0.26	0.28	18.42
		2	47.1	39.1	4.5	1.56	0.29	0.26	18.77
		3	46.5	38.9	5.6	1.92	0.25	0.29	18.52
		4	48.2	39.8	4.8	1.38	0.20	0.18	19.03
	2	1	47.8	38.8	4.7	1.97	0.29	0.22	18.88
		2	47.6	39.3	5.0	1.87	0.27	0.26	18.62
		3	48.1	38.1	6.0	1.75	0.15	0.25	18.79
		4	49.6	39.6	4.6	1.09	0.15	0.17	19.40
	3	1	46.6	38.1	4.7	1.99	0.05	0.33	19.27
		2	47.0	38.2	4.3	1.80	0.14	0.34	19.28
		3	46.9	38.3	5.3	1.03	0.03	0.43	19.16
		4	48.9	38.2	4.7	0.92	0.12	0.10	19.79
	4	1	46.5	38.0	4.7	1.99	0.15	0.36	19.27
		2	47.1	37.6	4.7	2.01	0.16	0.42	19.33
		3	46.8	37.9	5.4	1.60	0.10	0.44	19.28
		4	48.2	38.3	4.6	1.02	0.09	0.32	19.69
	5	1	46.7	37.9	4.8	1.85	0.19	0.21	19.17
		2	46.4	38.2	5.2	1.73	0.28	0.19	19.00
		3	47.7	37.3	5.4	1.69	0.18	0.18	19.35
		4	49.4	39.0	4.7	0.98	0.16	0.10	19.55
'Brackettes'			49.5	39.7	4.4	1.11	0.20	0.14	19.41
Miscanthus			47.3	41.5	5.7	0.80	0.10	0.25	20.02
Barley Straw (423)			48.7	39.3	5.1	0.90	0.10	0.11	19.75
Wheat Straw (093)			50.3	39.4	5.5	0.50	0.06	0.03	19.71
Willow			48.5	43.6	6.2	0.55	0.04	n/d	18.98
Torrefied Willow			54.4	36.9	5.1	0.62	0.06	n/d	21.25

^{db}- dry basis, ^{a}- calculated by difference, ^{b}-calculated using Eq. 3.7 from (friedl et al, 2005), n/d- outside the detection limits of the instrument. Sample period is the time of year at which the sample was harvested.

Fuel nitrogen content is a significant parameter when considering a fuel for combustion, especially in domestic applications; previous research has shown direct correlations between fuel N and NOx emissions [Mitchell et al., 2016]. The bracken N content is highly variable; the highest and lowest values being 2.01 and 0.92 wt.% db. In the case of site 3 the N content is half of the initial content by the fourth harvest,

1.99 to 0.92 wt.% db. At every site the nitrogen content is substantially lower at the fourth sampling period compared to the other sampling periods. The N content of the alternative energy species, are lower than the bracken however the barley straw and miscanthus are not too dissimilar, 0.9 and 0.8 wt.% db respectively.

The sulphur content is also highly variable. The S content peaks during the early sampling periods and is at its lowest by the fourth harvest, in some cases this is outside the detection limit of the elemental analyser. With the exception of site 1, the S content by the fourth harvest is comparable to the alternative energy species and is lower than the miscanthus and barley straw, both 0.1 wt.% db.

Chlorine content reduces in the bracken between the third and fourth sampling period for every site and ranges from 0.10 to 0.44 wt.% db over the growth cycle. No Cl was detected in the willow and torrefied willow samples, past research has shown that this is common in willow [Vassilev et al., 2017]. The bracken on the fourth harvest at sites 3 and 5 was 0.1 wt.% db, and they have a Cl content that is similar to the barley straw, 0.11 wt.% db. It is also significantly lower than the miscanthus, 0.25 wt.% db. Site 4 has the highest chlorine content at the fourth sampling period, 0.32 wt.% db; this site produced bracken which was higher in Cl at all the sampling periods.

6.3.2 Metals Analysis

Results for the trace metals from ICP-MS of the bracken are shown in Table 6.4 as well as the typical contents for miscanthus, barley straw and reed canary grass from the British ISO standard 17225-1:2014 (E) [2014]. The British standard does include typical variations for each of the fuels aforementioned; however, for the purposes of comparison in this work only those variations that are significant have been mentioned in the text.

Looking at the results for the barium concentration, the data is very scattered. The general trend across all the sites is that the barium concentration increases with time. The lowest concentration is site 3 sample period 1, 14.7 mg kg^{-1} db, and the highest is site 4 sampling period 4, 45.5 mg kg^{-1} db. The original source of this barium is unknown, past work concludes it is a result of soil particles in the fuel [Vassilev et al., 2017].

The contents of both chromium (Cr) and lead (Pb) species in the bracken change insignificantly and there are no observable trends over the sampling periods.

Cr contents varies between 0.8 to 1.4 mg kg^{-1} db and the Pb concentration between 0.7 and 1.9 mg kg^{-1} db; the Pb concentration is usually higher at the fourth harvest. Comparing to the typical values for miscanthus and barley straw, the Cr content is comparable to the miscanthus, 1 mg kg^{-1} db, but considerably lower than the barley straw, 10 mg kg^{-1} db. British ISO standard 17225-7:2014 (E) [2014] specifies the concentration of Cr and Pb must not exceed 50 and 10 mg kg^{-1} db respectively for herbaceous, fruit bearing, aquatic or blended biomass without additives. The highest concentrations of Cr, 1.4 mg kg^{-1} db, and Pb, 1.9 mg kg^{-1} db, for the bracken do not exceed these limits.

Table 6.4: Trace metal analysis results for the fuels studied

Sample	Site	Sample Period	Ba	Cr	Cu	Pb	Sr	Mn	Ni	Zn
			mg kg^{-1} db							
Bracken	1	1	14.8	0.9	7.8	0.8	5.1	311.7	2.5	30.8
		2	15.1	1.2	6.5	1.0	6.7	389.5	1.9	32.5
		3	16.2	1.0	5.3	0.9	8.9	568.9	1.5	36.4
		4	17.5	1.0	4.0	1.1	8.8	601.2	1.3	36.9
	2	1	15.3	1.0	8.9	1.0	4.7	281.9	2.4	29.5
		2	20.2	1.4	6.2	1.3	6.9	321.6	2.1	34.6
		3	22.5	0.9	5.1	1.2	10.1	480.9	1.8	38.5
		4	26.9	0.9	3.7	1.0	10.4	545.8	1.4	39.1
	3	1	14.7	0.9	6.1	1.4	4.1	286.6	2.5	29.4
		2	17.6	2.0	5.1	0.6	6.2	485.9	2.2	36.4
		3	26.9	1.2	3.9	1.8	9.4	606.2	2.0	43.1
		4	23.9	1.0	2.8	1.9	8.4	530.7	1.5	32.9
	4	1	18.6	0.8	9.0	0.8	4.2	265.5	2.4	31.3
		2	27.8	1.0	8.3	0.5	5.8	363.9	1.6	28.2
		3	39.1	1.3	4.6	1.1	9.4	647.3	1.4	39.7
		4	45.5	1.3	3.4	1.1	10.6	697.2	1.2	39.4
	5	1	19.5	0.9	8.8	0.7	4.5	276.8	2.6	30.6
		2	18.6	1.1	7.1	1.2	7.8	342.9	2.3	32.1
		3	22.1	1.2	5.6	0.8	8.2	589.4	1.8	34.5
		4	24.7	1.0	3.4	1.1	7.9	566.2	1.5	38.7
'Brackettes'			26.3	0.9	4.1	1.1	10.2	510.3	1.4	38.6
ISO Standard 17225-1:2014(E)	Miscanthus		n/a	1.0	2.0	2.0	n/a	20	2.0	10
	Barley Straw		n/a	10	2.0	0.5	n/a	40	1.0	10
	Reed Canary Grass		n/a	n/a	n/a	1	n/a	160	n/a	n/a

Relative error for the bracken values is ±7%, calculated from standard deviation of measured values.

Sample period is the time of year at which the sample was harvested.

Past research shows that uptake of copper (Cu) by plant species is highly dependent on the plant species, the presence of inorganics in soil and the moisture of the soil [Chigbo, Batty and Bartlett, 2012]. The Cu content of the bracken decreases as the annual cycle progresses. The highest concentration is measured at site 4 sampling period 1, 9.0 mg kg^{-1} db. The limit specified in ISO 17225-7:2014 (E) [2014] is 20 mg kg^{-1} db. Compared to the miscanthus and barley straw, both 2.0 mg kg^{-1} db, the average concentration for the bracken in the fourth sampling period is 50% higher, 3.5 mg kg^{-1} db. The concentration range for barley straw, from ISO 17225-1:2014 (E) [2014], is between 1 to 10 mg kg^{-1} db which is much broader than for the bracken over the growth cycle, 3.4-9.0 mg kg^{-1} db.

The strontium (Sr) in the bracken increases as time progresses; the highest measured concentration is 10.6 mg kg^{-1} db at site 4 sampling period 4. Sr is not typically considered very important in fuel analysis because of its low concentration in most biomass. Although there is very little research on the impacts of Sr in fuels during combustion, it is reported that strontium has similar chemical properties to calcium, both are alkaline metals. According to Sullivan and Glassman [1971] during combustion strontium and calcium in the vapour phase have very similar homogeneous characteristics. Therefore, if there were significant quantities detected further discussion of Sr would be appropriate in relation to slagging and fouling characteristics. This is not the case for the bracken sampled in this work.

Manganese (Mn) is an area of interest for bracken because the measured concentration is greater than typically found in most biomass. As the bracken cycle progresses the Mn concentration increases, this is from 280 mg kg^{-1} db to 580 mg kg^{-1} db. Comparing this to the other fuels in Table 6.4 the Mn concentration is substantially higher in bracken, reed canary grass being the next highest at 160 mg kg^{-1} db with a reported variation of up to 200 mg kg^{-1} db. In ISO 17225-1:2014 (E) [2014] the only other comparable biomass is grass hay which has a typical concentration of 1000 mg kg^{-1} db but can have a concentration of between 200 to 2600 mg kg^{-1} db. Mn can be considered a heavy metal specie in geochemical research [Kuramshina et al., 2014] and an important ash forming element, it is moderately mobile and has a strong and important association with Ca and Mg [Vassilev et al., 2017].

Both nickel (Ni) and zinc (Zn) have concentration limits, these are 10 and 100 mg kg^{-1} db respectively [ISO 17225-7-2014 (E), 2014]. As can be seen in Table 6.4, the highest concentrations are 2.6 (Ni) and 43.1 (Zn) mg kg^{-1} db, both are substantially below the limit. The general trend for Ni is that its concentration deceases by about 1.0 mg kg^{-1} db as the cycle progresses. For the Zn it generally increases however it is highly variable depending on the site. The Ni concentration of the bracken is comparable to both the miscanthus and barley whereas the Zn concentration is higher. The variation reported in ISO 17225-1:2014 (E) [2014] for Zn in miscanthus ranges from 3 to 30 mg kg^{-1} db and the barley straw from 3 to 60 mg kg^{-1} db. The variation on the bracken is much narrower, 13.6 wt.% db, than the other two alternative fuels.

6.3.3 Ash Composition, Slagging and Fouling Indices

One of the main concerns with solid fuel combustion is ash slagging and fouling. It is important when considering novel fuels in combustion systems that the risks of slagging and fouling are understood to prevent operational and technical problems. The fuel ash composition is shown in Table 6.5. The ash composition of each fuel in Table 6.5 does not add up to 100%, this is because it is an estimate of the ash composition where all the species are assumed to be oxides, these make up the majority of the ash. Carbonates, hydrogen carbonates and sulphates will also be part of the composition.

Typically, biomass has higher concentrations of certain ash species as they are crucial nutrients and have specific critical biological functions in the plant. Some of these elements are vaporised and then condensed in low temperature areas in boilers and combustion systems. The ternary diagram in Fig. 6.2 from Boström et al. [2012] shows the interaction of $K_2O(+Na_2O)$-$CaO(+MgO)$-SiO_2; adding the fuels from this work to the diagram, the bracken at the fourth harvest is predicted to have the highest slag formation temperature- above the 1200°C isotherm line from Morey et al. [1930]. The order of slagging temperature based on Fig. 6.2 goes bracken harvest 4 >bracken harvest 3 >bracken harvest 2 >miscanthus >wheat straw >bracken harvest 1 >barley straw. Over the annual cycle, the slagging temperature increases from about 1000°C to above 1200°C. Comparing to the fuels used by Boström et al. [2012] the bracken performs similar to conifer stumps which are considered to be a woody biomass, the bracken has a significantly higher slagging propensity than the stem and bulk woods.

Table 6.5: Ash Composition of Fuels Studied (wt. %)

Sample	Site	Sample Period	SiO$_2$	Al$_2$O$_3$	Fe$_2$O$_3$	TiO$_2$	CaO	MgO	Na$_2$O	K$_2$O	Mn$_3$O$_4$	P$_2$O$_5$	SO$_3$
Bracken	1	1	17.9	0.1	0.1	<0.1	5.1	0.7	0.7	37.5	0.7	6.8	5.7
		2	22.7	0.2	0.2	<0.1	7.1	0.9	1.5	31.1	1.1	5.7	5.8
		3	27.1	0.2	0.3	<0.1	9.3	1.1	2.4	24.0	1.4	3.1	5.9
		4	40.1	0.3	0.3	<0.1	13.9	0.7	2.8	15.3	2.3	2.4	5.7
	2	1	17.8	0.1	0.1	<0.1	5.0	0.9	0.6	37.8	0.7	7.4	6.1
		2	23.1	0.2	0.2	<0.1	7.8	1.1	1.9	30.9	1.1	5.9	6.0
		3	26.5	0.2	0.3	<0.1	8.9	0.8	2.7	24.1	1.6	3.4	5.9
		4	42.4	0.3	0.3	<0.1	14.2	0.8	2.7	14.8	2.3	2.5	6.0
	3	1	18.0	0.1	0.2	<0.1	4.9	0.4	0.1	38.9	0.7	6.6	5.8
		2	23.5	0.2	0.2	<0.1	6.7	0.4	0.5	29.9	1.1	5.4	6.1
		3	25.5	0.2	0.2	<0.1	6.9	0.4	0.6	24.3	1.3	2.8	6.3
		4	47.1	0.3	0.3	<0.1	12.6	0.7	0.8	14.1	2.3	2.6	6.2
	4	1	17.7	0.1	0.1	<0.1	5.4	1.2	0.8	38.8	0.7	7.8	5.8
		2	20.8	0.2	0.2	<0.1	9.3	1.7	1.7	32.4	1.2	6.2	5.5
		3	27.2	0.3	0.3	<0.1	12.4	0.8	3.1	23.3	1.7	4.1	5.7
		4	38.0	0.3	0.2	<0.1	16.6	1.4	3.3	15.9	2.3	2.0	4.7
	5	1	17.9	0.1	0.1	<0.1	5.3	0.8	0.7	38.4	0.7	7.7	5.5
		2	21.9	0.2	0.1	<0.1	8.2	1.4	1.5	31.5	1.2	6.1	5.6
		3	26.9	0.3	0.2	<0.1	10.8	1.1	2.9	23.8	1.7	3.8	5.8
		4	44.5	0.3	0.2	<0.1	15.0	1.3	3.0	14.3	2.3	2.2	5.5
'Brackettes'			40.8	0.2	0.3	<0.1	13.8	0.9	3.0	15.2	2.0	2.5	6.0
Miscanthus			33.2	0.3	0.3	0.1	13.4	2.0	0.5	29.1	0.1	3.0	3.8
Barley Straw (423)			62.8	0.2	0.3	0.1	9.6	1.7	0.6	11.1	0.1	1.5	2.1
Wheat Straw (093)			55.8	0.3	0.2	0.1	11.5	1.5	0.2	13.9	0.1	2.1	1.3

Relative error for bracken measurements is ±10%. Sample period is the time of year at which the sample was harvested. Sample period is the time of year at which the sample was harvested.
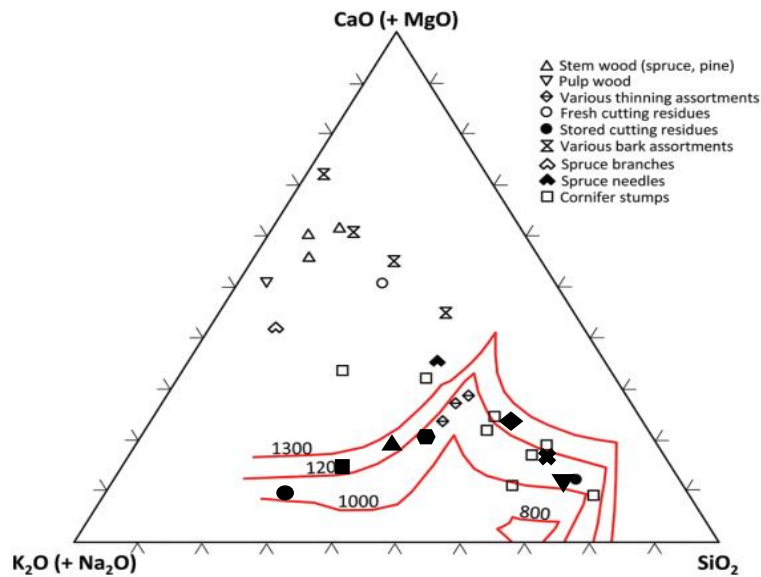
Figure 6.2: The K₂O(+Na₂O)-CaO(+MgO)-SiO2 system; • Bracken Harvest 1* ■ Bracken Harvest 2* ▲Bracken Harvest 3* ◆Bracken Harvest 4* ⬟Miscanthus ▼Barley straw ✖Wheat Straw. *values are averages over all sites.* Figure taken from [Boström et al., 2012]

Fig. 6.3 is from Wang et al. [2017] and shows a different interaction series which considers the mobility of inorganics in the structures of biomass; these can be categorised into 3 groups:

- Highly mobility- K_2O, P_2O_5, SO_3, and Cl_2O
- Moderately mobility- CaO, and MgO
- Low mobility- SiO_2, Al_2O_3, Fe_2O_3, Na_2O, and TiO_2

Vassilev et al. [2017] discusses the problems with classification of Na in this system. Traditionally Na was classified as a low mobility element because it typically forms silicates however in some biomass species which are more salt tolerating Na is present more as chlorides and sulphates- highly mobile species. Bracken does not typically grow well in coastal and wet areas and therefore it is reasonable to assume that Na will exist more as silicates and use of the traditional interactions is appropriate. Additionally, Mn_3O_4 has limited interactions with other ash elements so can be excluded for the interactions above [Boström et al., 2012].

Fig. 6.3 shows that all the bracken samples are in the high deposition risk areas, S and K types. As the bracken goes through the annual cycle it moves from a K type to an S type, this is an increase in the acidity of the biomass meaning there will be

more issues of corrosion. This trend moves towards the straw results from Wang et al. [2017]. The barley and wheat straws from this study are in the same region as the results from Wang et al. [2017] meaning the results from this work show reliable consistency.
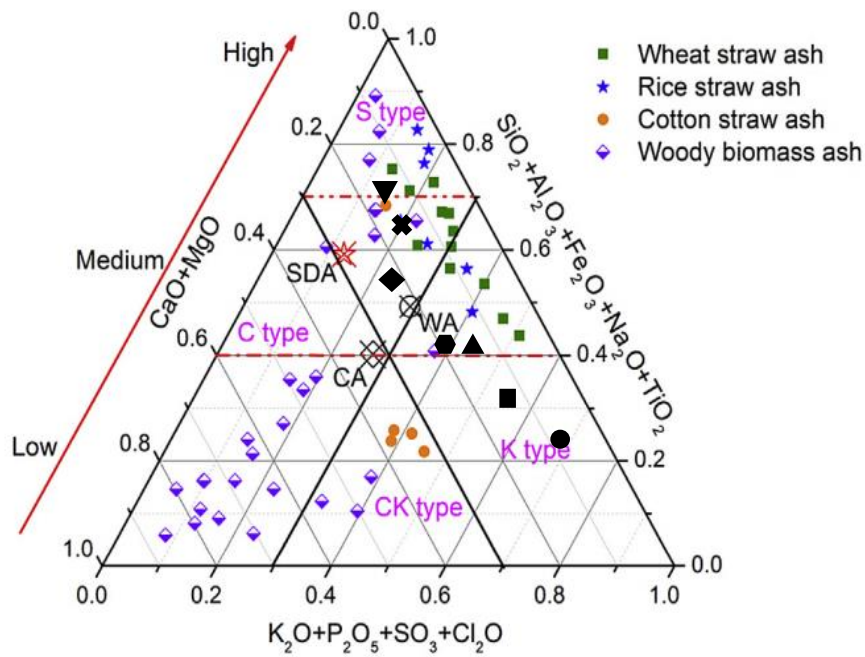
Figure 6.3: The K2O(+Na2O)-CaO(+MgO)-SiO2 system; • Bracken Harvest 1* ■ Bracken Harvest 2* ▲Bracken Harvest 3* ◆Bracken Harvest 4* ⬟Miscanthus ▼Barley straw ✖Wheat Straw. *values are averages over all sites.* Figure taken from [Wang et al., 2017]

Table 6.6 is a series of slagging and fouling parameters used by academics and industry to estimate the slagging propensity of a fuel. These indices are described in section 2.3.3.1. The base to acid ratio ($R_{b/a}$), alkali index (AI) and slagging viscosity index are calculated by Eqs. 2.10-2.12 respectively. For the $R_{b/a}$, as the bracken goes through the annual cycle the probability of slagging goes from high to moderate. The fourth sampling period for the bracken has an $R_{b/a}$ of between 0.70 and 0.89 which is approximately double the number for the straw fuels but is considerably lower than the miscanthus fuels.

All of the fuels in this study except for the wheat straw have a high probability of slagging based on the AI. The final sampling of the bracken is between 0.41 and 0.69 which is approximately a reduction of 1 kg alkali GJ^{-1} from the first sampling period to the last.

Table 6.6: Calculated slagging and fouling indices

Sample	Site	Sample Period	Base to Acid Ratio (Inc. P_2O_5)[a]	Base Percentage (%)	Alkali Index (kg alkali GJ^{-1})[b]	Slagging Viscosity Index[c]
Bracken	1	1	1.75	43.4	1.51	75.2
		2	1.40	39.9	1.14	73.5
		3	1.18	36.0	0.87	71.7
		4	0.75	32.3	0.48	72.9
	2	1	1.72	43.5	1.17	74.8
		2	1.40	40.8	0.95	71.7
		3	1.20	36.0	0.75	72.6
		4	0.71	32.0	0.41	73.5
	3	1	1.79	44.1	1.58	76.6
		2	1.28	37.3	1.21	76.3
		3	1.12	32.0	0.98	77.3
		4	0.56	27.8	0.49	77.6
	4	1	1.76	45.1	1.61	72.5
		2	1.60	43.6	1.35	66.0
		3	1.24	39.1	1.02	66.8
		4	0.89	36.0	0.69	69.6
	5	1	1.73	44.5	1.56	74.3
		2	1.46	41.3	1.28	69.3
		3	1.22	37.7	0.97	69.0
		4	0.70	32.9	0.47	72.5
Miscanthus			1.19	43.3	0.68	67.9
Barley Straw			0.33	21.6	0.35	84.4
Wheat Straw			0.44	25.8	0.30	80.9

a- calculated by equation 2.10, b- calculated by equation 2.11, c - calculated by equation 2.12. Sample period is the time of year at which the sample was harvested. Sample period is the time of year at which the sample was harvested.

For the slagging viscosity index, the bracken results show a more complex trend compared to the other indices but generally the bracken from harvests one and four are above 72 so have a low slagging propensity whilst harvests two and three show moderate slagging tendencies. None of the fuels studied show a high slagging propensity. The straws show superior slagging properties which is in agreement with the other calculated indices.

6.3.4 Ash Fusion Tests

Ash fusion tests (AFT) were carried out under oxidising conditions as described in Chapter 3.4.6. The results for the bracken from sites 3 and 4 only are shown in Table 6.7; these results are averages from the two test pieces. Selection of sites 3 and 4 was based on the previous results from section 6.4; site 3 showed the best anti-slagging properties whilst site 4 showed some of the worst anti-slagging properties.

Table 6.7: Ash fusion test characteristic temperatures

Sample	Site	Sample Period	ST (°C)	IDT (°C)	HT (°C)	FT (°C)
Bracken	3	1	960	1000	1010	1030
		2	910	930	980	1020
		3	930	950	1000	1010
		4	1000	1030	1160	1180
	4	1	960	980	1020	1030
		2	910	920	980	1020
		3	920	950	1010	1030
		4	1010	1040	1160	1180
Miscanthus[a]			800	900	1010	1100
Barley Straw[b] (423)			970	1010	1200	1250
Wheat Straw[c] (093)			950	980	1095	1140

*a- values from Pang et al. [2013], b- values from Wang et al. [2012], c- values from Akinrinola [2014]. Sample period is the time of year at which the sample was harvested. Sample period is the time of year at which the sample was harvested.

Results of AFT are subjective to the analyst looking at the images, meaning there is an inherent error in the reading of the temperature at which the characteristic change occurs. The errors for the ST, IDT, HT and FT, are between 0-15°C, 0-13°C, 0-10°C and 0-10°C respectively. The contrast of the images makes it difficult to identify the first stage of ash melting, hence the largest error is for this measurement. Compared to the results from Akinrinola [2014] these errors are much smaller; this could be due to a number of reasons but it is most likely from differences in the method of analysis and confidence interval.

Looking at Table 6.7 the characteristic temperatures are highest for the fourth bracken harvest. Softening and initial deformation happen at above 910°C for the bracken meaning the ash is very stable up to this temperature. The four characteristic temperatures occur over a relatively small temperature range, approximately 180°C. As the harvest time period progresses the stability of the test piece between the initial deformation and hemisphere increases. The test piece retains its stability to the hemisphere temperature and about 20°C later collapses; although this is not a sudden collapse as described by Gudka [2012] it is also not as gradual as described by Baxter et al. [2012].

Past work has shown that the process of ash melting can be variable, some biomass types experience shrinkage and swelling at different temperatures [Roberts et al., 2019]. This can have significant impacts on the results and is inherent to different fuel properties. Fig. 6.4 shows the test pieces at the characteristic ash melting

temperatures for the bracken samples. The bracken does not experience any swelling and follows a uniform process of ash fusion until it reaches its flow temperature.
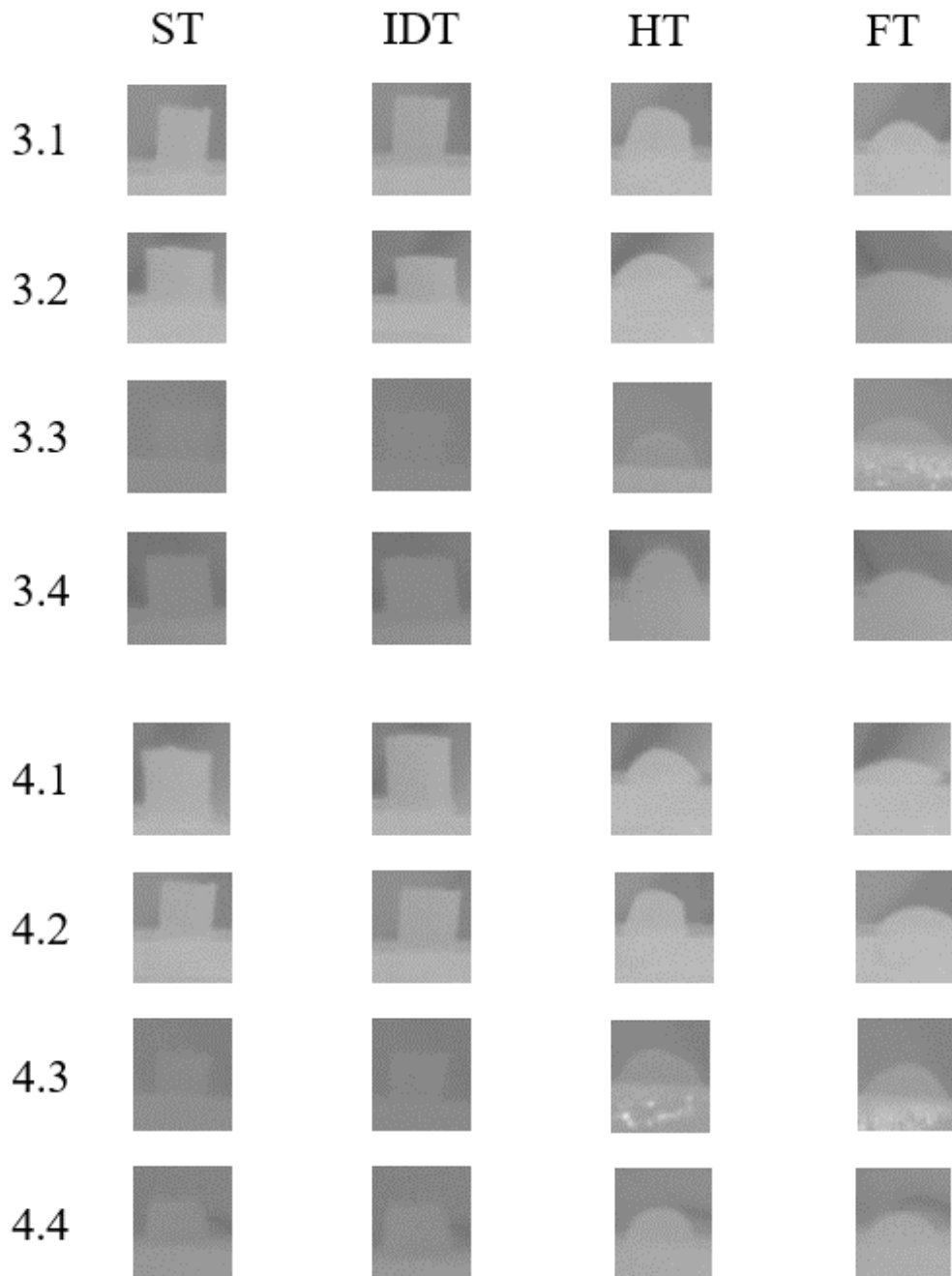
Figure 6.4: Ash melting characteristic temperatures. *The first number is the sampling site and the second number is the sample period.*

Bryers [1996] plotted the hemisphere temperature against the base percentage for a number of lignites and biomass. The plot produces a parabolic curve with a minimum between 35 and 55 wt.% basic oxides. Using the base percentage from Table 6.6 and the hemisphere temperatures from Table 6.7 the bracken fuels are plotted onto the figure from Bryers [1996] in Fig. 6.5. Relative to the fuels studied by Bryers [1996] the bracken has a similar correlation, however the results from Bryers [1996] were from AFT conducted in reducing environments, this typically means that the temperatures are lower (about 100°C) than in an oxidising environment. Therefore, as with any fuel used, careful monitoring and considerations as to technology applications would be required to prevent slagging and fouling.
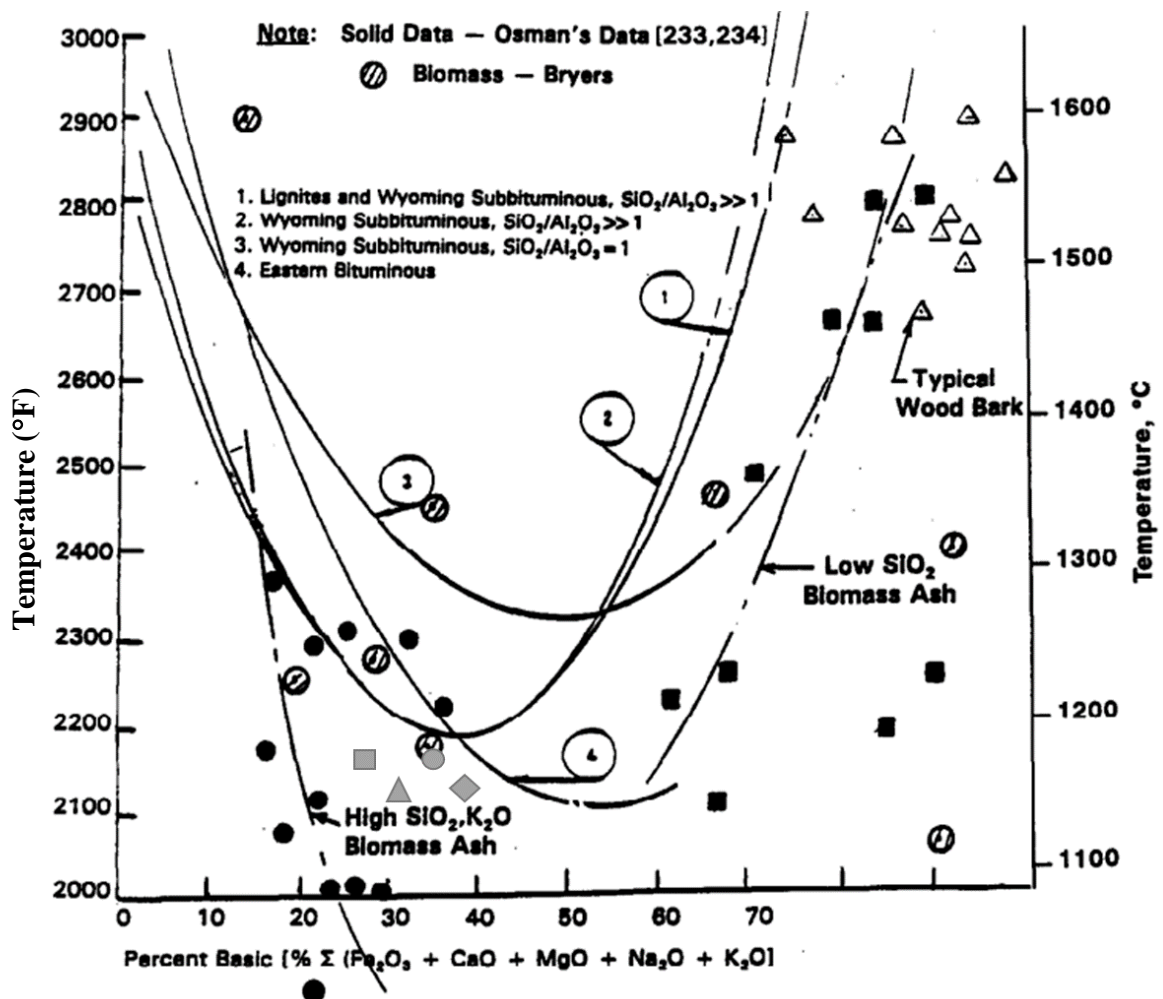
Figure 6.5: Hemisphere temperatures and base percentage values for bracken at different sampling periods, figure from Bryers [1996]. ▲ **bracken site 3 harvest 3,** ■ **bracken site 3 harvest 4,** ◆ **bracken site 4 harvest 3,** ● **bracken site 4 harvest 4.**

6.3.5 Pyrolysis and Combustion Studies

6.3.5.1 Thermogravimetric Analysis (TGA) and Differential Gravimetric Analysis (DTG)

TGA and DTG analysis was carried out according to the method in section 3.5.1 in order to analyse the combustion and pyrolysis kinetics. All the raw samples (cryomilled) were heated to 900°C at 10°C min^{-1} in air and nitrogen for combustion and pyrolysis respectively. Samples from different harvest time periods were compared, all the samples studied came from site 4. It should be noted that the error in TGA analysis is within 2% as determined by Phillips [2018].

Analysis involved identification of the peak temperatures and mass loss rates from the mass loss profiles in Figs. 6.6-6.10. For combustion of biomass fuels, it is evident from past research that two peaks form for the two key stages, devolatilisation and char combustion [Jones et al, 2015]. This is different to coal combustion, which only has a single overlapping peak, because of the higher VM content and reactivity of biomass. The initial mass loss temperature (T_{IM}), the temperature at which maximum mass loss occurs during devolatilisation (T_v), the rate of mass loss at this temperature (dm/dt_v), the temperature at which maximum mass loss occurs during char combustion (T_c), the mass loss rate at this temperature (dm/dt_c) and the burnout temperature (T_B) are listed in Table 6.8. The T_{IM} and T_B are measured when the mass loss equals 0.016 wt.% s^{-1} at the start and end of the combustion runs, this is excluding any drying periods. For pyrolysis (Figs. 6.9 and 6.10) there is a single peak which is for devolatilisation; therefore, the temperature and mass loss parameters above still apply except for the absence of T_c, dm/dt_c and T_B.

The initial mass loss on the TGA curves is due to moisture, Figs. 6.6 and 6.7. This occurs at the same temperature for all the fuels. All the moisture is removed before the sample reaches 120°C.

For the combustion profiles there are two main peaks, the first represents devolatilisation and the second is for char combustion. Looking at the combustion profiles from Table 6.8 and Figs. 6.6, 6.7 and 6.8; the devolatilisation peak, T_v, increases as the bracken is harvested later (occurs at ~20°C hotter for the fourth harvest compared to the other harvests). Additionally, from Fig. 6.7 harvests 1 and 2 have a flat pre-tail before the main peak. This was also evident in the pyrolysis analyses. This

phase was also seen in Miranda et al. [2008] for olive pits, pulp and residue cake and is concluded to be from the evolution of light volatiles such as oils and resins.

The T_{IM} also increases as the bracken is harvested later meaning the reactivity is decreasing. There is an increase of 50°C between the first harvesting period to the last. Dooley [2017] says volatile content is the main factor affecting the reactivity of the fuel, however as discussed in section 6.3.1 and Table 6.2 the change in volatile content is within 2 wt.% db. Decreases in K content can also reduce the reactivity of a fuel since it slows the catalysed rate of thermal decomposition of lignocellulose. From Table 6.5 it is clear that the K content decreases as the bracken growth cycle progresses. Therefore, this is most likely causing the decreases in reactivity. This change in K content is also relevant to differences in the pyrolysis analyses discussed later in this section.

For the char combustion phase, the second peak, both T_c and dm/dt_c increase as the bracken is harvested later. Comparing to the pyrolysis analyses the fourth bracken harvest has the lowest rate of mass loss during devolatilisation but the highest mass loss rate during char combustion. This is because more char is produced for the fourth harvest based on the fixed carbon content, Table 6.2. This is also coherent with the ultimate analysis of C, Table 6.3. The C changes are small; however past research has shown that in TGA applications char yield is strongly influenced by the pseudo-components of biomass (cellulose, hemicellulose and lignin) as well as the K concentration. Small changes in the carbon content can actually be the result of large changes at a cell level and yield significantly different amounts of char [Skreiberg et al., 2011].

The burnout temperature, T_B, is more interesting as there is no discernible trend. The third harvest of bracken has the lowest burnout temperature (464°C) followed by harvest 2 (482 °C), harvest 1 (500 °C) and harvest 4 (508 °C). This is linked to the differences in the shapes of the char combustion mass loss profiles. From Fig. 6.7 harvest periods 1 and 2 have two peaks. One peak occurs between 350-440°C and the other between 450-510°C. This same result was seen by Darvell et al. [2010] for shea and olive residue and Akinrinola [2014] for wheat straw (which as seen in earlier sections shows similar properties to bracken) and is caused by the combustion of two different char matrices. In the case of the early bracken harvests this is most

likely from the differences in the stipe (soft fleshy material) and the pinna/leaflet (thin brittle material), both of which make up roughly 50% by volume of the harvested material. Additionally, from Fig. 6.8 bracken from harvest 4 has a shoulder on the main char combustion peak at approximately 480-490°C; a small peak also occurs at a similar temperature in the pyrolysis profile in Fig. 6.10; these two peaks are expected to be from the decomposition of $CaCO_3$ [Skreiberg et al. 2011]. As seen in Table 6.5 the Ca in the fuel increases the later the bracken is harvested.

The rate of peak volatile release, dm/dt_v, is lowest for the fourth harvest in combustion and pyrolysis. This is most likely due to changes in the mineral concentrations, especially K. High Cl, and low Si and Al facilitates release of KCl and KOH to the vapour phase in devolatilisation [Clery et al., 2018]. As the bracken cycle progresses the K and Cl decreases and the Si increases so the volatile release rate slows and more K is retained in the ash. This K is also known to promote more char formation reactions [Nowakowski and Jones, 2008]. PM emissions are also dependent on KCl and KOH and this is discussed later in Section 6.3.5.5.

Table 6.8: Characteristic temperatures (°C) and mass loss rates (wt.% s^{-1}) measured in TGA combustion and pyrolysis of bracken at different sampling time periods from site 4

Method	Parameter	Harvest Time Period			
		1	2	3	4
Combustion	T_{IM}	207	207	242	257
	T_v	308	310	313	332
	dm/dt_v	0.117	0.128	0.134	0.106
	T_c	408	411	413	432
	dm/dt_c	0.049	0.051	0.064	0.069
	T_B	500	482	464	508
Pyrolysis	T_{IM}	237	222	255	263
	T_v	335	337	343	338
	dm/dt_v	0.0967	0.0929	0.0861	0.0738
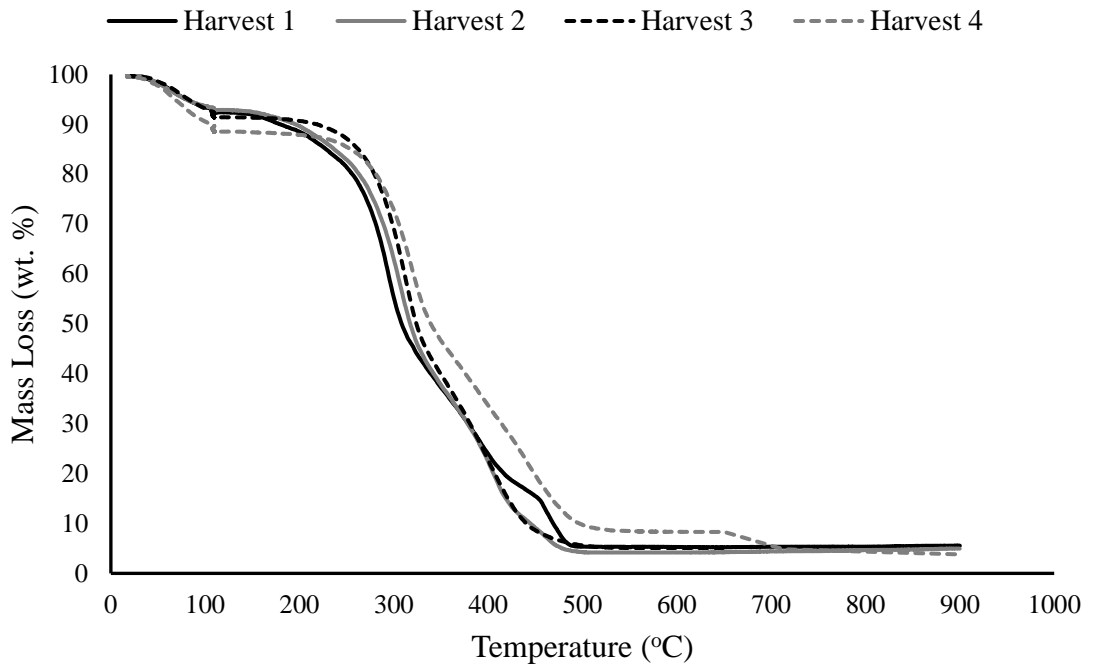
Figure 6.6: Plot of mass loss with temperature from combustion-TGA analyses of bracken from harvests 1-4
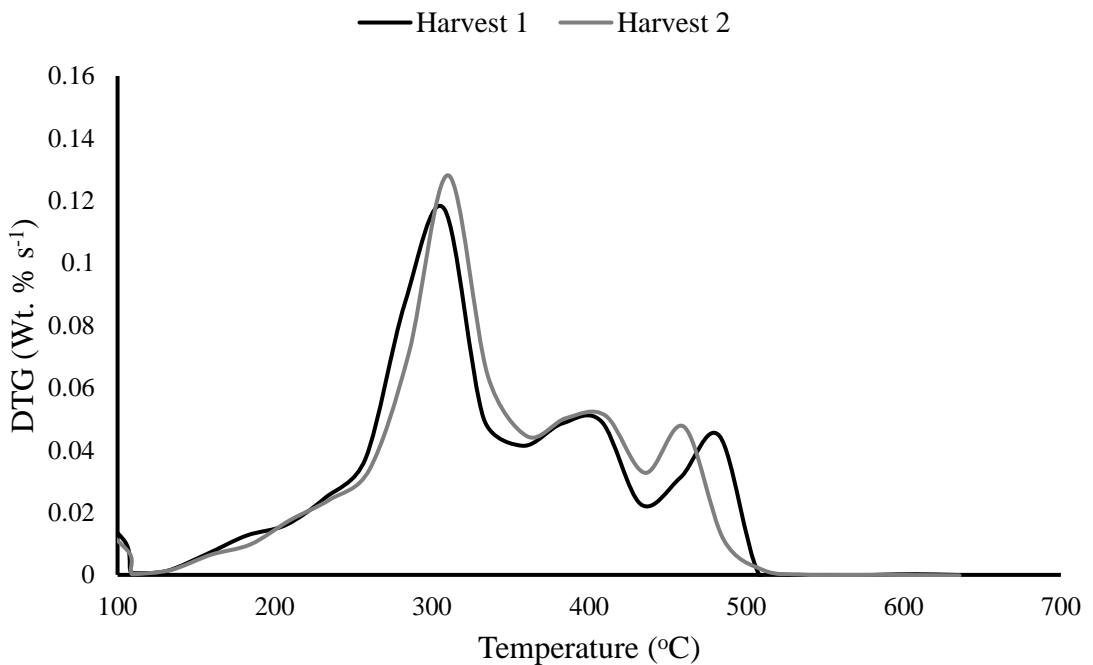
Figure 6.7: Plot of the time derivative mass loss (DTG) with temperature from combustion-TGA analyses of bracken from harvests 1 and 2
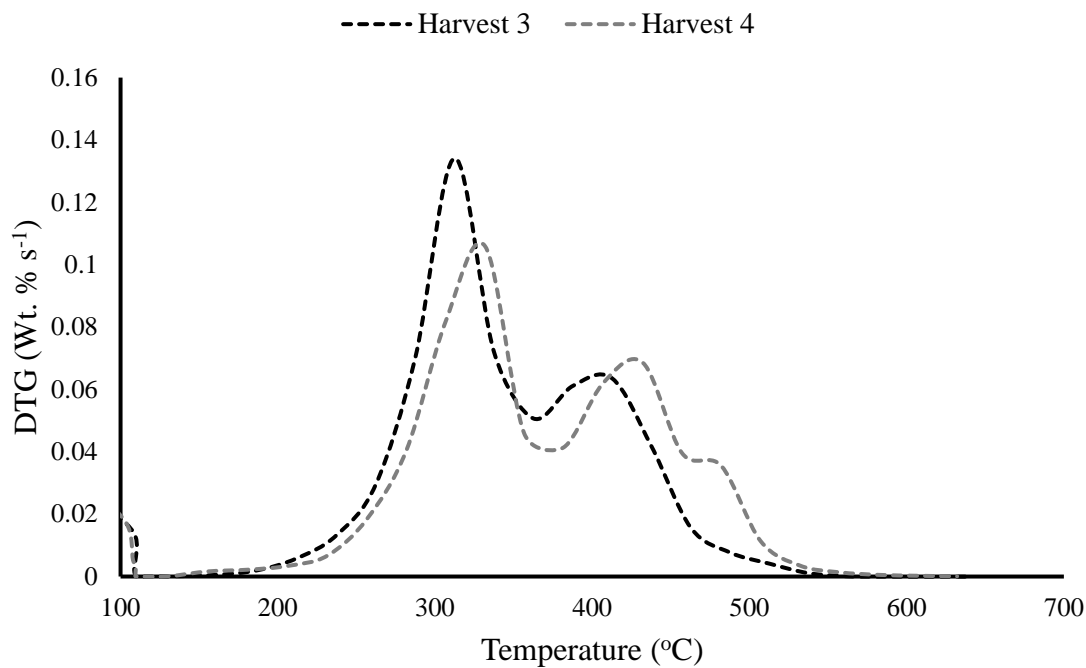
Figure 6.8: Plot of the time derivative mass loss (DTG) with temperature from combustion-TGA analyses of bracken from harvests 3 and 4
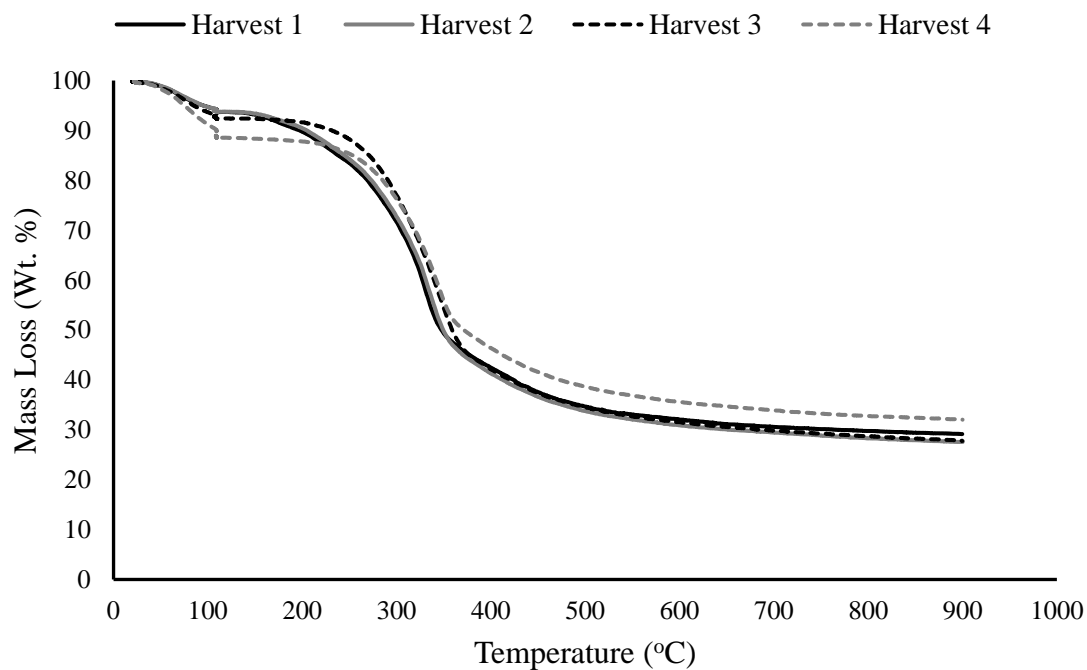
Figure 6.9: Plot of mass loss with temperature from pyrolysis-TGA analyses of bracken from harvests 1-4
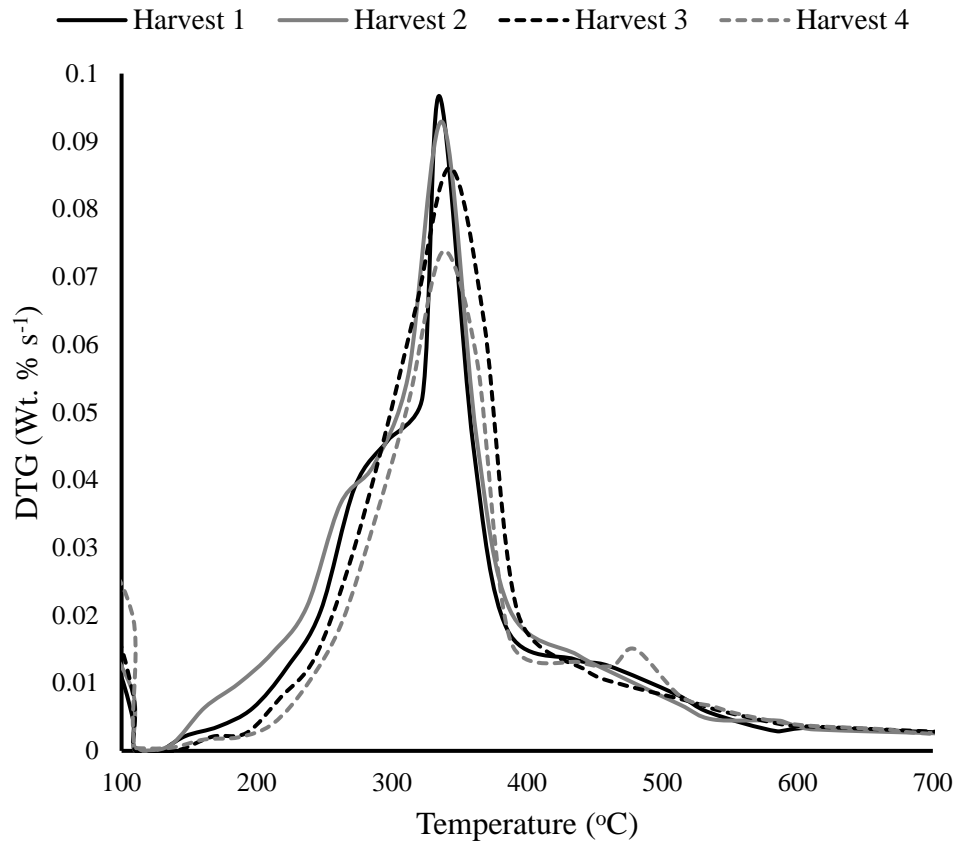
Figure 6.10: Plot of the time derivative mass loss (DTG) with temperature from pyrolysis-TGA analyses of bracken from harvests 1-4

For the pyrolysis analyses, the temperature of peak mass loss, T_v, are within 8°C. This was also seen by Dooley [2017] for different white wood pellets and was most likely from the similarities in fuel-O content which aided surface reactions. The maximum mass loss rate, dm/dt_v, did decrease significantly as the bracken was harvested later mostly likely associated with changes in the mineral content- this was discussed in the preceding paragraph.

Compared to other fuels in work by Dooley [2017] and Akinrinola [2014] as the bracken is harvested later its char combustion rate is closer to that of a torrefied fuel- torrefied spruce in Dooley et al. [2017] dm/dt_c is 0.105 wt.% s^{-1}. Additionally, the temperature range in which peak char combustion occurs is closer to straw for the first three harvests and more like wood for the fourth harvest.

The final point to note from Fig. 6.10 is the profiles for the first and second bracken harvests have a shoulder to the main peak. The shoulder is usually ascribed to

hemicellulose decomposition whilst the main peak is cellulose decomposition [Darvell et al., 2010].

6.3.5.2 Apparent First Order Kinetics

The kinetic parameters were calculated using the data from the mass loss curves for pyrolysis. This is only an estimate and requires two key assumptions:

1. Any combustion and decomposition are assumed to take place in a single step, this is considered to be a first order Arrhenius reaction described by Eq. 6.1. [Kastanaki and Vamvuka, 2006]
2. Reactivity is a function of conversion; conversion is measured by mass loss so any mass loss is considered to be conversion.

$$k = Ae^{\frac{-E_a}{RT}} \quad (6.1)$$

In order for kinetic evaluation to be valid, a temperature boundary must be used; this is because in non-isothermal analysis decomposition of different pseudo-components happen at variable rates. Therefore, a boundary is used to obtain kinetic parameters which reflect analogous conversion mechanisms [Fisher et al., 2002] [Saddawi, Jones and Williams, 2010] [Gudka et al., 2010]. Assessment of the compatibility of these conversion methods is done by R^2 statistical analysis, Table 6.9, of linear plots shown in Figs. 6.11 and 6.12.

Table 6.9: Key kinetic parameters for devolatilisation/ pyrolysis of bracken from TGA analysis using the first order constant reaction rate method

Pyrolysis Kinetic Analysis				
Harvest	1	2	3	4
Temperature Range (^{o}C)	145-170	200-225	205-270	200-275
Ln A	3.13	3.57	5.57	8.31
Ea (kJ mol^{-1})	44.99	47.34	58.41	71.93
R^2	0.93	0.938	0.994	0.996

The pre-exponential factors (A) and the activation energy (E_a) are shown in Table 6.9- these are only applicable to the temperature range stated. The E_a is highest for the fourth harvest (71.93 kJ mol^{-1}) followed by harvest three (58.41 kJ mol^{-1}), two (47.34 kJ mol^{-1}) and one (44.99 kJ mol^{-1}). This ranking is analogous with the

observations from the DTG combustion profiles, Figs. 6.7 and 6.8, in that the reactivity decreases as the bracken is harvested latter. However, this is not analogous with the T_v for pyrolysis, Fig. 6.10. This is most likely because the T_v for all the harvests are within 2.5%, which is just outside the 2% margin of error determined by Phillips [2018] for repeat TGA analyses on the same fuel.

As discussed in Section 6.3.5.1, the bracken harvested earlier contained low CV oils and resins which were evaporated at low temperatures. Therefore, it is more challenging to determine the temperature range at which only hemicellulose decomposition is assumed to be occurring because these phases overlap. This means that only a small temperature range is used for the determination of the pyrolysis kinetics for harvests one and two.

Fig. 6.13 shows the pyrolysis reaction rate at 300°C plotted against the K content; which produces a strong positive linear correlation (R^2=0.934). Compared to Saddawi, Jones and Williams [2010] for pyrolysis of raw willow chip, demineralised willow chip and K-impregnated willow chip, the reaction rate is slower. From the trendline in this work, when the K content is 0 the reaction rate at 300°C would be 0.0006s^{-1}. This is similar to the measured value for willow, 0.00043 s^{-1}, by Saddawi, Jones and Williams [2010].

Based on the trend in Fig. 6.13, the reactivity of the bracken is directly dependent on the time of harvest (K content). Saddawi, Jones and Williams [2010] also observed this relationship at low K concentrations however it deviated from linearity as the K content increased. During the linear phase the K is both catalysing the degradation as well as being evolved from the fuel. When the trend deviates the fuel is saturated and some of the K is no longer being released from the fuel during devolatilisation. This also means the efficacy of this K as a catalyst is lower. Although more data would be required to confirm this, the data from this work does suggest that the bracken deviates from linearity when the K content exceeds 2.2 wt.% (harvests one and two). This is a similar observation to the composition and slagging and fouling analyses in that the differences between harvests one and two are minimal.

If bracken was used in combustion systems typically fired with woody biomass, the TGA data shows the feed in rate would have to be altered because of the differences in reactivity. The lower reactivity of bracken means the volatile gases

would be released from the fuel at a slower rate and thus would need a longer residence time to achieve the same burnout rates. This is an important consideration as it will require additional control measures to ensure the same energy requirements are fulfilled.
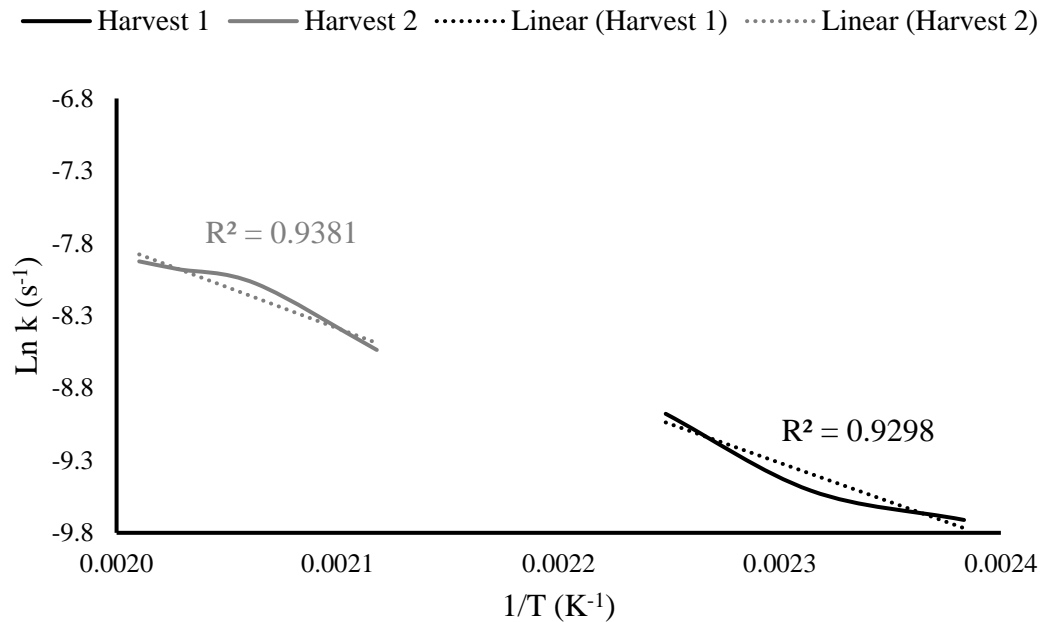
Figure 6.11: Pyrolysis kinetics for harvests 1 and 2. The solid lines are the actual experimental values and the dashed line is the linear best fit.
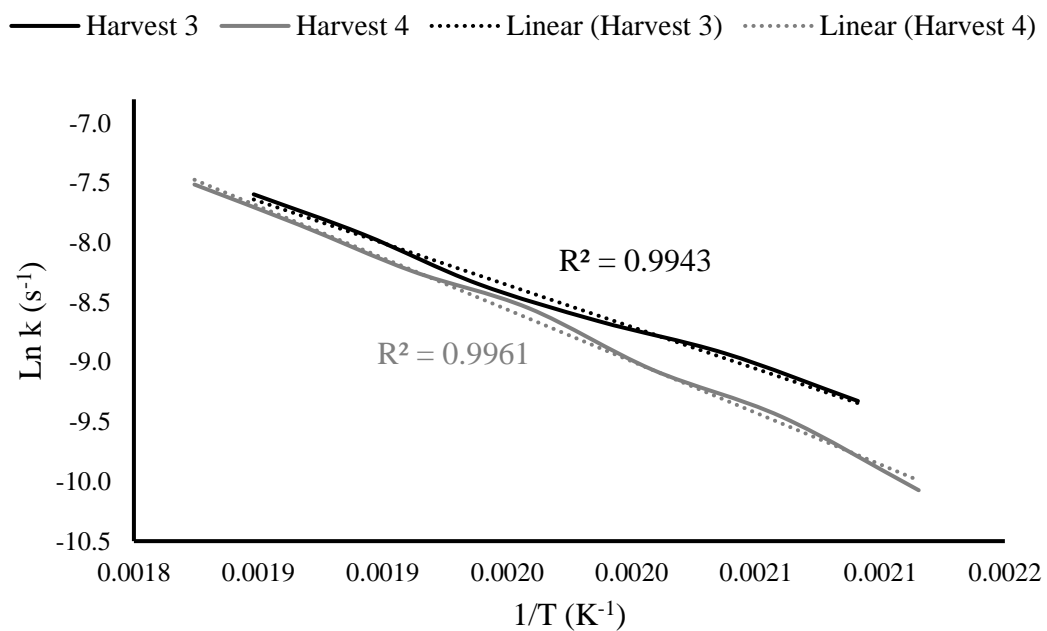
Figure 6.12: Pyrolysis kinetics for harvests 3 and 4. The solid lines are the actual experimental values and the dashed line is the linear best fit.
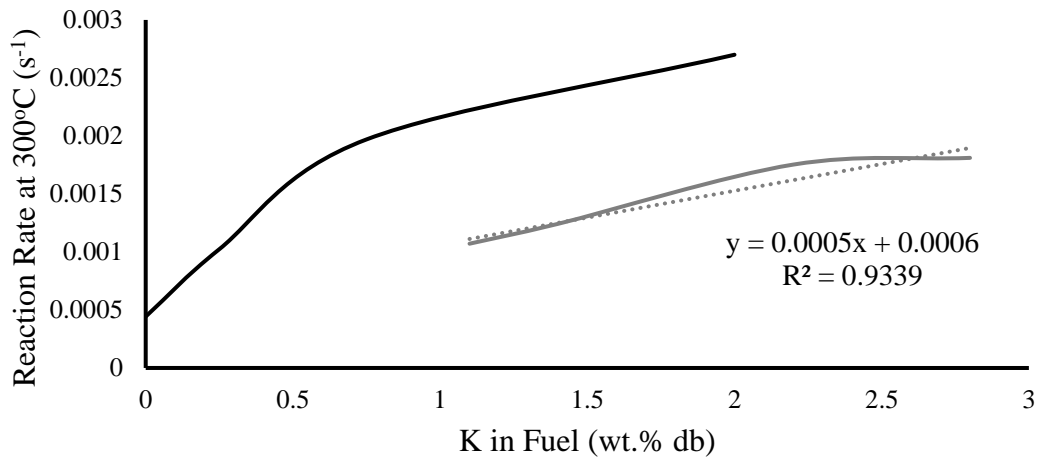
Figure 6.13: Reaction rate constants calculated at 300oC vs K content in the fuel, comparison with the work of Saddawi, Jones and Williams [2010]. The solid grey line is experimental data.

6.3.5.3 Single Particle Combustion- Video data
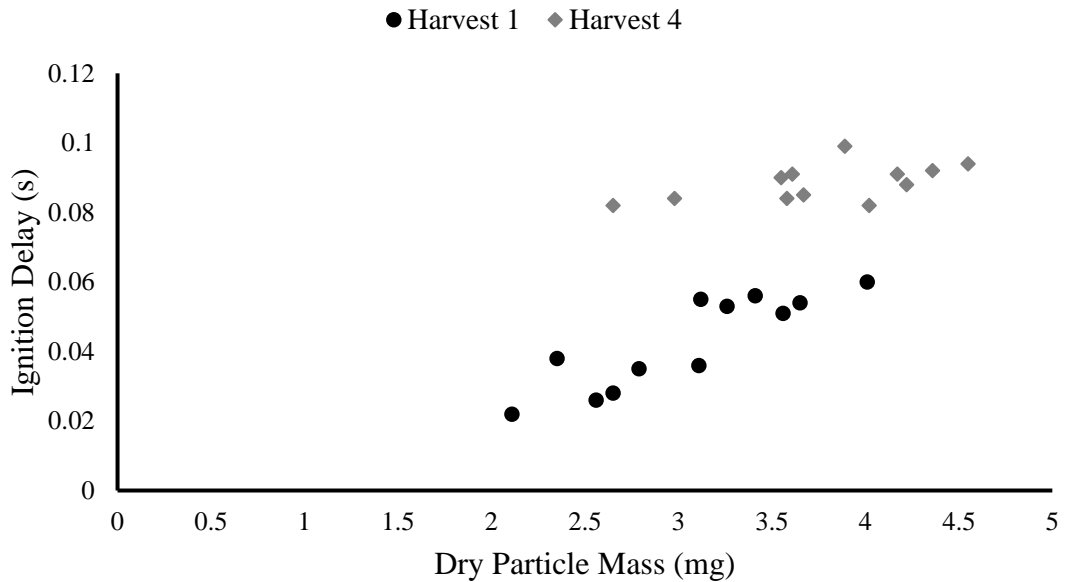
Figure 6.14: Ignition delay versus dry particle mass. *Particles are between 2-4mm in size.*

Single particle combustion experiments were conducted as stated in section 3.5.4. Single particle combustion analyses the stages of combustion at a higher heating rate that is more representative of combustion of pulverised fuels in power stations.

200

Only bracken samples from site 4 at the first and fourth harvests were used as these were considered to have the largest differences in properties. Using a high-speed camera (standard error of ±0.008 due to the frame speed) four key points are identified: ignition, volatile release, char burnout and ash cooking. The times at which these occur is variable depending on the type of fuel, the chemical composition and dimensions of the particle. Moisture can have the most significant impact on the results particularly on the ignition delay because of the drying process slowing the volatile release and creating an unstable flame. For this reason, the fuels were oven dried to less than 10% moisture content.

The first characteristic to identify from the video frames is the ignition delay time, this is characterised by the time lag between the first exposure of the particle to the flame and the development of a luminous flame above the particle surface. When the particle starts flaming this is ignition. The plot of the ignition delay time against the dry particle mass is shown in Fig. 6.14. The spread of the data in Fig. 6.14 is caused by the variation in the particle geometry, density and moisture content. The bracken samples have a unique make-up, common with ferns, in that some particles were more straw like and others more grass like- this made it difficult to establish a common repeatable particle. However, it is clear from Fig. 6.14 that the bracken harvested earlier has a much shorter ignition delay time (between 0.02-0.06s) compared to the fourth harvest (>0.08s). It is clear that the reactivity is decreasing as the bracken is harvested later, this is in agreement with the results from Table 6.8 for combustion. This is most likely to be from oils and resins present in harvest 1 that evolve at lower temperatures and aid ignition. However, other factors such as the biochemical composition and thermal conductivity can also influence the result.

Identification of volatile release and char combustion from the video frames is measured by monitoring the flame above the particle and when the particle starts to glow. During devolatilisation volatile organic compounds are released, these are combusted above the fuel particle in homogeneous gaseous phase reactions which produces a luminous flame. After the release of these gases a change in the pressure gradient allows oxygen to reach the fuel particle surface and diffuse through the char matrix meaning heterogeneous combustion can take place which results in the particle heating up and glowing. It is assumed that when char burnout begins volatile release has stopped- they are absolute individual stages. However, in reality this isn't the case

and there is an overlap. In these experiments, because the Meker burner is below the particle, char combustion will start at the bottom of the particle whilst volatiles are still being release from the top of the particle.
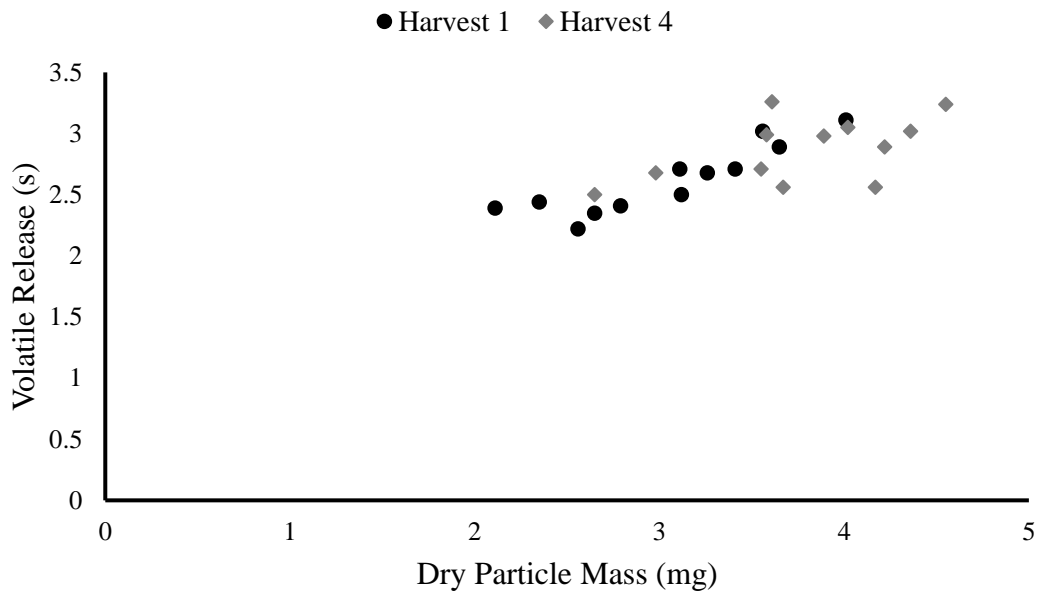
Figure 6.15: Volatile release time versus dry particle mass. *Particles are between 2-4mm in size.*
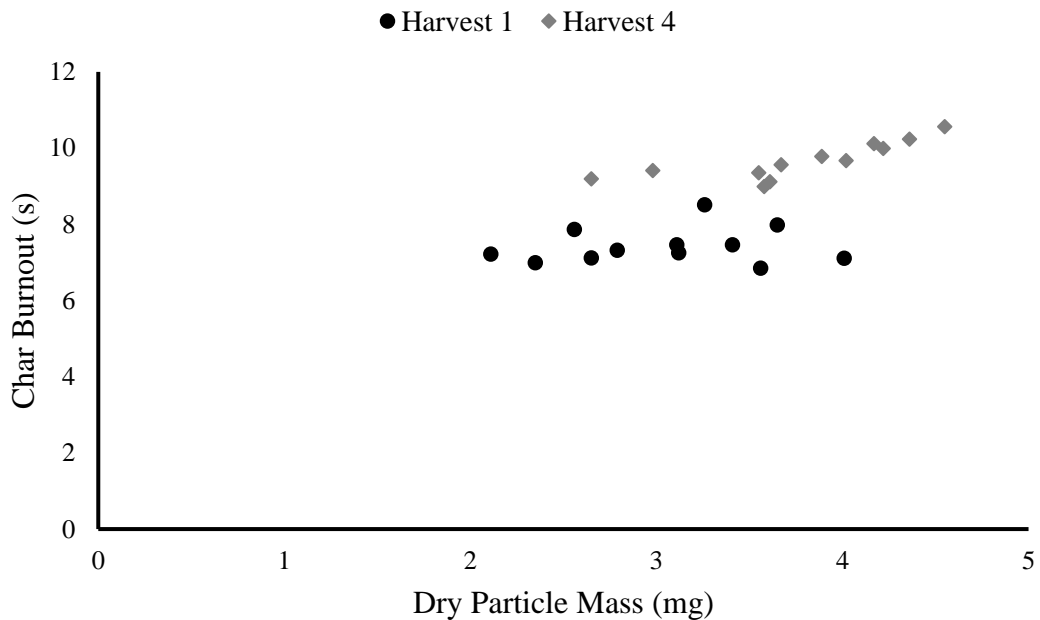
Figure 6.16: Char burnout time versus dry particle mass. *Particles are between 2-4mm in size.*

Figs. 6.15 and 6.16 show the time taken for volatile release and char combustion against the dry particle mass respectively. Surprisingly in Fig. 6.15 the time taken for volatile release is similar between the two bracken harvests. This was unexpected since the K content, discussed more in the next section, and reactivity discussed in the preceding sections (6.3.5.1 and 6.3.5.2) was much higher for the first harvest. The volatile release phase occurs very quickly and it is therefore difficult to judge the point at which the change in combustion phase occurs. A small difference in the value read such as 0.3s can in fact have a 10% deviation in the result for the devolatilisation measurements. This is most likely the reason for not seeing a difference in the time taken for volatile release of the two harvests.

The time taken for char combustion (Fig. 6.16) is longer for the fourth harvest than the first. There are 5 key contributing factors to the char burning rate: (i) the mass of char after devolatilisation (ii) chemical factors which influence the porosity of the resultant char after devolatilisation (iii) the presence of catalytic metals and metals which could form structures to retain elements within the ash (iv) the chemical reaction rate of the char and (v) the diffusion rate through the char matrix. Based on Table 6.2 there is a small increase in the char produced because of the slight increase in FC content (3 wt.%) of the fourth harvest. Additionally, from Table 6.5 the Si content increases by more than 20 wt.% which retains K in the char/ash matrix. A combination of these two factors is causing the increase in char burnout time.

6.3.5.4 Single Particle Combustion- Potassium Release Detection

Photodiodes are used to monitor potassium release (the times measured by the change in spectral intensity) and can be used as a comparison with the times measured from the video frames [Mason, 2016]. Figs. 6.17 and 6.18 show the potassium release profile over the combustion time of the particle for particles from harvest 1 and 4 respectively. Comparing Figs. 6.17 and 6.18, harvest 1 and 4 respectively, it is clear that the ignition delay for the particles from the fourth harvest is much greater, this is because there is a gap between t=0 and the first peak. However, it was not possible from Figs. 6.17 and 6.18 to distinguish between K evolving during volatile release and K evolving during char combustion. Additionally, in Fig. 6.17 the first harvest bracken was so high K the signal became saturated. This is common when analysing fuels high in K [Mason et al., 2016].
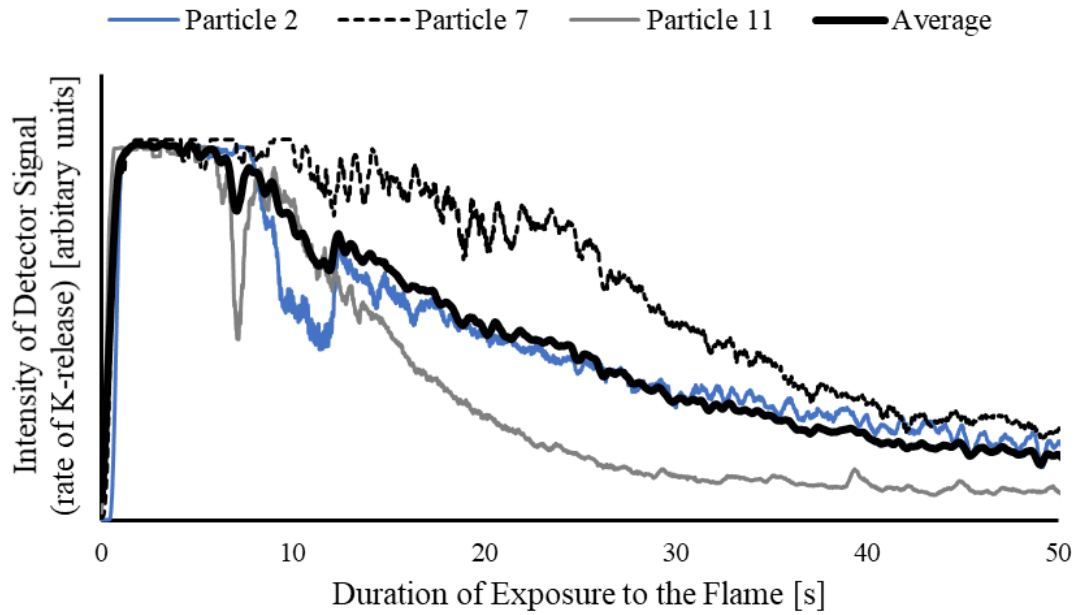
Figure 6.17: Plot of potassium release profiles for bracken from the first harvest
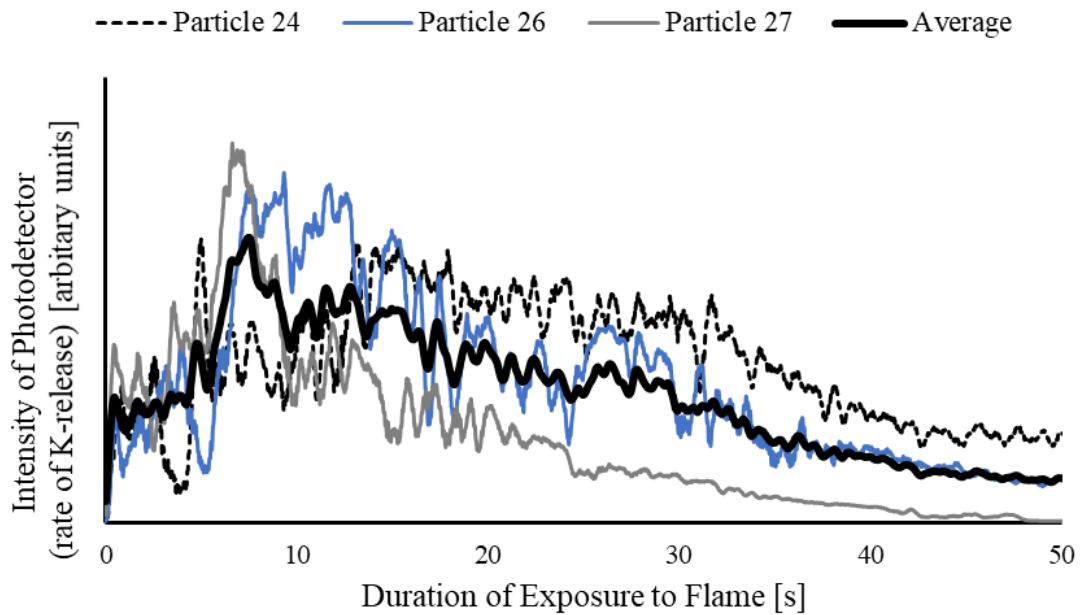
Figure 6.18: Plot of potassium release profiles for bracken from the fourth harvest

Fig. 6.19 compares the average potassium release rates from the first and fourth harvests for particles identical in mass and size. The area under the profile represents the amount of K released which was larger for the first harvest particle, this is coherent with K measurements in Table 6.5. The most interesting comparison is between the shapes of the profiles. For the first harvest particle, the ignition delay time is very short

and is followed by a sharp peak which then regresses parabolically (x^{-2}). Comparatively, the fourth harvest particle peaks and then regresses linearly. This was a result also observed by Mason [2016] and suggests that K is being retained in the char/ash matrix. Based on the metal analysis from Table 6.5, this will be because of the high concentration of Si which prevents K release in the earlier stages of combustion.

Figs. 6.20 and 6.21 show the average K release rate and a single standard deviation from the profiles of 12 particles from the first and fourth harvests respectively. The results from the fourth harvest show a lower degree of variability over the whole particle combustion period. Although this is a very limited analysis, because of the sample number, the standard deviation for the composition analysis (Appendix C) also showed greater variation in bracken from the first harvest. Homogeneity within a fuel is a key property for creating stable flames within power station applications.
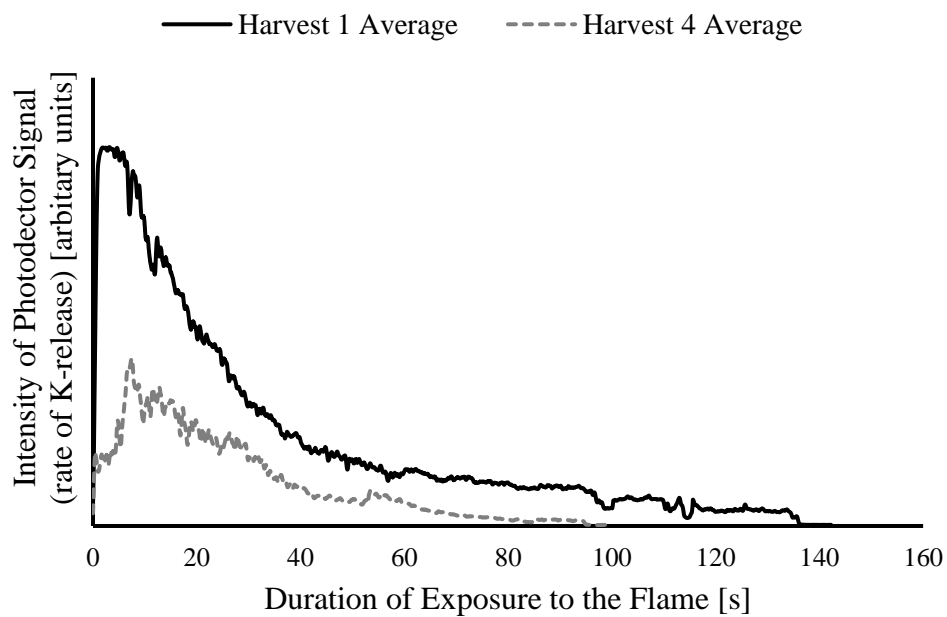
Figure 6.19: Comparison of the average potassium release profiles from the first and fourth harvests
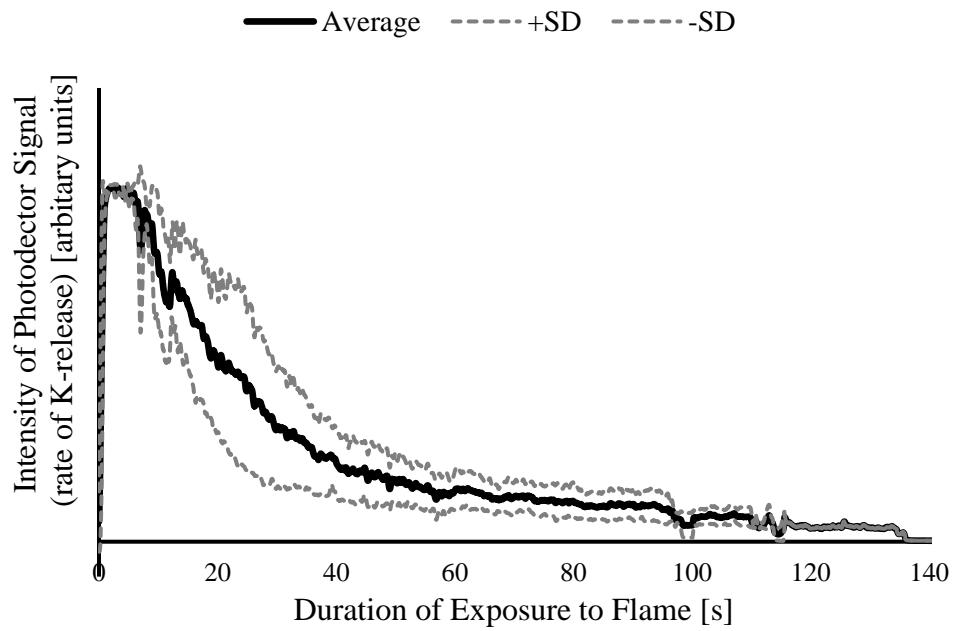
Figure 6.20: Average potassium release profile with standard deviation from twelve harvest 1 particle combustion runs
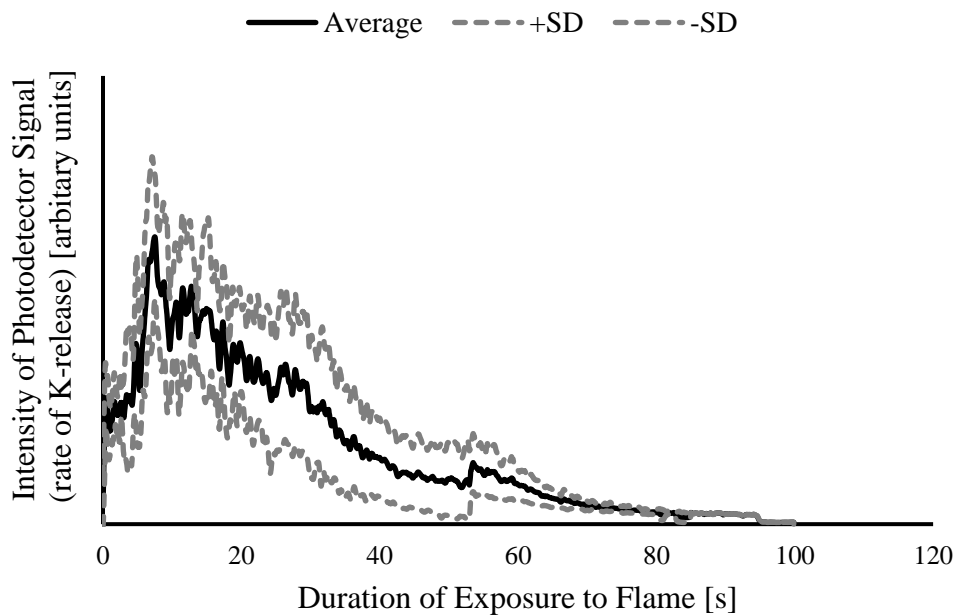
Figure 6.21: Average potassium release profile with standard deviation from twelve harvest 4 particle combustion runs

6.3.5.5 Stove Combustion

Bracken briquettes were combusted in the domestic stove and compared to miscanthus, barley straw, wheat straw and commercially made 'heatlogs[TM]' (wood briquettes). The bracken briquettes composition was within 3% of the bracken from site 2 harvest 4 in Tables 6.2-6.5. Therefore, even though the bracken briquettes are from a different source they are representative of the bracken harvested from Budby Moor. Information on the briquettes and their forming can be found in section 3.2.3. There was no binder used in the production of the brackettes. During the combustion runs it was observed that the bracken briquettes were too dense, preventing efficient combustion of the fuel. Therefore, after the first two batches, smaller briquettes were loaded into the stove made by splitting the larger briquettes into four, the same mass of fuel was loaded in each batch (±5%).
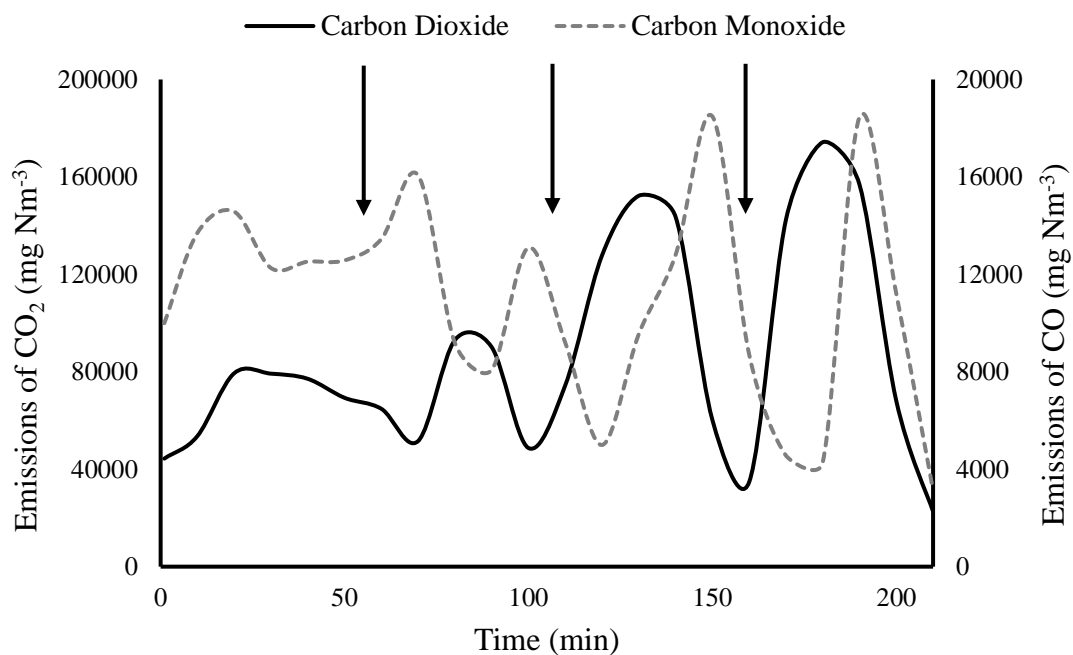
Figure 6.22: Emission profile for whole combustion run for CO₂ and CO. Arrows indicate fuel reloading. The profile up to the second arrow is for whole bracken briquettes and the after is for broken bracken briquettes.

Fig. 6.22 shows the emissions of CO₂ and CO over the whole combustion experiment, black arrows indicate reload points. Typical combustion runs show peaks in emissions of CO_2 during flaming combustion and peaks in CO during smouldering combustion [Mitchell et al., 2016] [Atiku et al., 2016] [Johansson et al., 2004]. For the smaller briquette batches this is evident in Fig. 6.22 however for the larger briquettes

207

the relative emissions of CO are much greater and are sustained for longer time periods. This is because of the aforementioned dense briquetting which reduces the porosity and prevents the fuel from decomposing, thus decreasing the surface area to volume ratio. The ability of air and heat to transfer through the briquettes is much lower in the larger briquettes, this results in a greater proportion of smouldering combustion and a reduction in the efficiency of both the modified combustion efficiency (MCE) expressed by Eq. 3.16 and the extent of combustion, Eq. 3.17, in Table 6.10. Additionally, lower temperatures, shorter gaseous residence times and fuel rich combustion also contribute to higher emissions of CO [Tissari et al., 2009] [Gonzalez et al, 2004] [Kristensen and Kristensen, 2004], these are discussed more later in this section.

The average emissions (g Nm^{-3}) and the average emission factor on an energy basis (kg GJ^{-1}) are shown in Table 6.10. The reduction in CO emissions is 26.4% from splitting the briquettes and this increases the fuel consumption by over 20%. The average emission factors for CH_4 are also shown in Table 6.10. Emissions of CH_4 are the result of pyrolysis during fuel-rich stoichiometry and they are dependent on many factors including stove design, air-to-fuel ratio and temperature. The emissions of CH_4 are 18.7% higher for the smaller briquettes, this is because there is an increase in the devolatilisation rate, based on the higher average burning rate. This produces a more fuel-rich gas and so CH_4 is able to exit the combustion zone without being reacted [Ndiema, Mpendazoe and Williams, 1997].

Table 6.10: Organic emission factors and combustion efficiency measurements

Batch	g Nm^{-3}			kg GJ^{-1}			MCE	Extent of Combustion (%)	Average Burning Rate (kg h^{-1})
	CO_2	CO	CH_4	CO_2	CO	CH_4			
1	70	13	0.51	40	7	0.32	0.86	60	0.74
2	70	15	0.53	40	9	0.34	0.85	65	0.76
3	110	10	0.63	70	5	0.40	0.91	81	1.21
4	120	11	0.60	70	6	0.38	0.89	87	1.34

Other key emissions from combustion systems include total organic carbon (TOC), NOx, SO_2 and HCl as shown in Table 6.11. TOC includes organic species such as formaldehyde, furan, propane, hexane, acetylene, ethane, ethylene, ethanol and benzene. All of these compounds are volatile and condensable and they contribute to

the formation of soot. Concentrations of TOC are greater from domestic stoves because they operate at temperatures below 700°C. As mentioned previously the larger bracken briquettes had lower average combustion temperatures and reduced turbulence which prevented the efficient conversion of TOC [Williams et al., 2012] [Fitzpatrick et al., 2008]. By breaking down the larger briquettes this increases the proportion of flaming combustion and increases the average temperature and turbulence resulting in a 25% reduction of TOC emissions.

Comparing the emissions of the bracken briquettes to the alternative fuels there are some similarities in results. The CO emissions for the wood briquettes are the lowest and over 10% lower than the other fuels. These briquettes were very high in volatiles (90.1 wt.% db) with a moderate burning rate (1.6 kg h^{-1}). Therefore, the release of volatiles persisted for a greater proportion of the batch burning time and hence flaming combustion dominated reducing the amount of smouldering combustion. The emissions of CO and TOC for the barley straw, like the large bracken briquettes, are high. These fuels are characteristically the opposite of the wood briquettes with lower VM contents, 68.1 (bracken) and 75.1 (BS 423) wt.% db, and slower burning rates, 0.74 (bracken) and 1.4 (BS 423) kg h^{-1}. Therefore, a stable flaming phase was only achieved for a short time period, which was inconsistent between fuel batches.

Table 6.11 Emissions factors for fuels studied on the domestic stove

	g kg^{-1}				
Fuel	CO	TOC	NOx	SO$_2$	HCl
Bracken Large Briquettes	180	1.3	2.5	1.6	0.50
Bracken Small Briquettes	140	0.8	4.0	1.7	0.60
Miscanthus	160	0.6	1.8	0.8	0.30
Barley Straw (423)	180	1.3	3.6	0.8	0.30
Wheat Straw (093)	140	1.1	2.0	0.5	0.20
Wood Briquettes	120	0.7	1.4	0.3	0.06
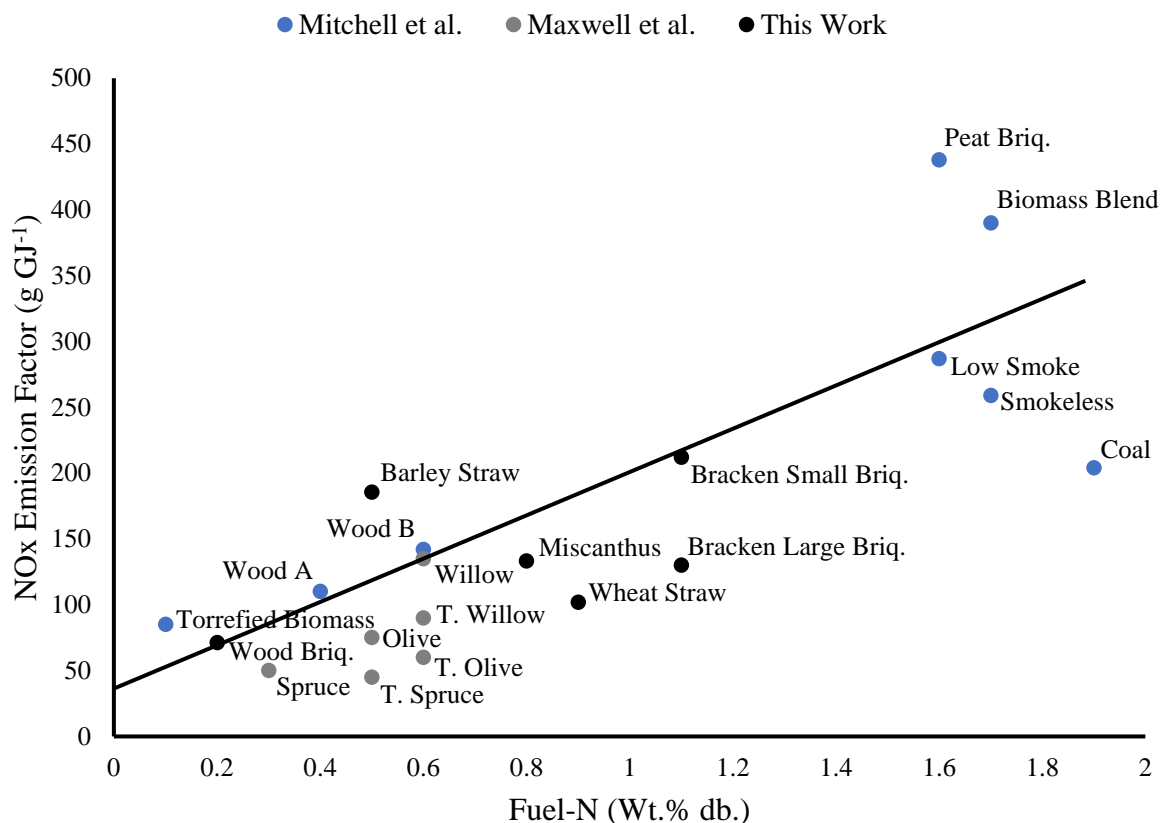
Figure 6.23: Emissions of NOx against fuel nitrogen content, data from chapter 4 and Mitchell et al. [2016] included

It is well established in past research that NOx emissions in domestic stoves from solid fuels are dependent on the fuel nitrogen content. Fig. 6.23 shows the emission factors for the fuels in this study as well as the fuels from Chapter 4 and the fuels from Mitchell et al. [2016]. It is visible that there is a correlation between the emissions of NOx and the fuel nitrogen content. All these studies were conducted on the same stove which mitigates any differences in operation or physical combustion conditions. The emission factor for the small briquettes is greater than the large briquettes. There was a lower burnout for whole briquettes, thus more N was retained in the char, this nitrogen was released from the increased burnout of the broken briquettes. This is an inherent flaw of using the specific dry flue gas volume (SDFGV) method where by characteristics of the combustion are assumed consistent and only fuel composition varies.

Sulphur dioxide, SO_2, emissions can also be dependent on the quantity of sulphur in the fuel. However, in biomass the relationship is more complex because of the nature in which the sulphur is bound within the fuel. Stove combustion of biomass results in higher emissions of SO_2 during devolatilisation. This is from the thermal decomposition of organically bound sulphur in amino acids and other compounds for protein synthesis [Han et al., 2019]. Past work by Johansen et al. [2011] shows that thermal decomposition of organically bound sulphur can happen at temperatures as low as $200^{\circ}C$ (based on decomposition experiments of cysteine). Figs. 6.24a-f show the emission and temperature measurements over a single batch of fuel. Using Figs. 6.24a-f the results from this work show that the emissions of SO_2 peak when the temperature in the stove peaks (temperature reading is the temperature of the flue gas) for all the fuels. The temperature peak is from flaming combustion and therefore all SO_2 emissions during that peak are the result of decomposition of organically bound sulphur.

Inorganically bound sulphur such as in K_2SO_4 found in xylem and phloem of biomass can also be released in biomass combustion but usually these salts are decomposed in char burnout stages at high temperatures (>900°C). Presence of high amounts of silicates and chlorine can reduce the temperature at which potassium-sulphur salts decompose because of the high affinity of K to Si and Cl. Some of this SO_2 (g) can be retained in the ash matrix by calcium interactions [van Lith et al., 2009] [Johansen et al., 2011]. Looking at Fig. 6.24f for the wood briquettes a second peak occurs when the temperature is decreasing, this peak is during char burnout which suggests there is release of either SO_2 from the ash matrix or from the destruction of K_2SO_4 [Knudsen et al., 2004]. A second peak is also visible on Fig. 6.24a for the large bracken briquettes, this is another peak during flaming combustion as the breakup of the fuel is more random compared to the other fuels, this is another characteristic of the dense briquettes.
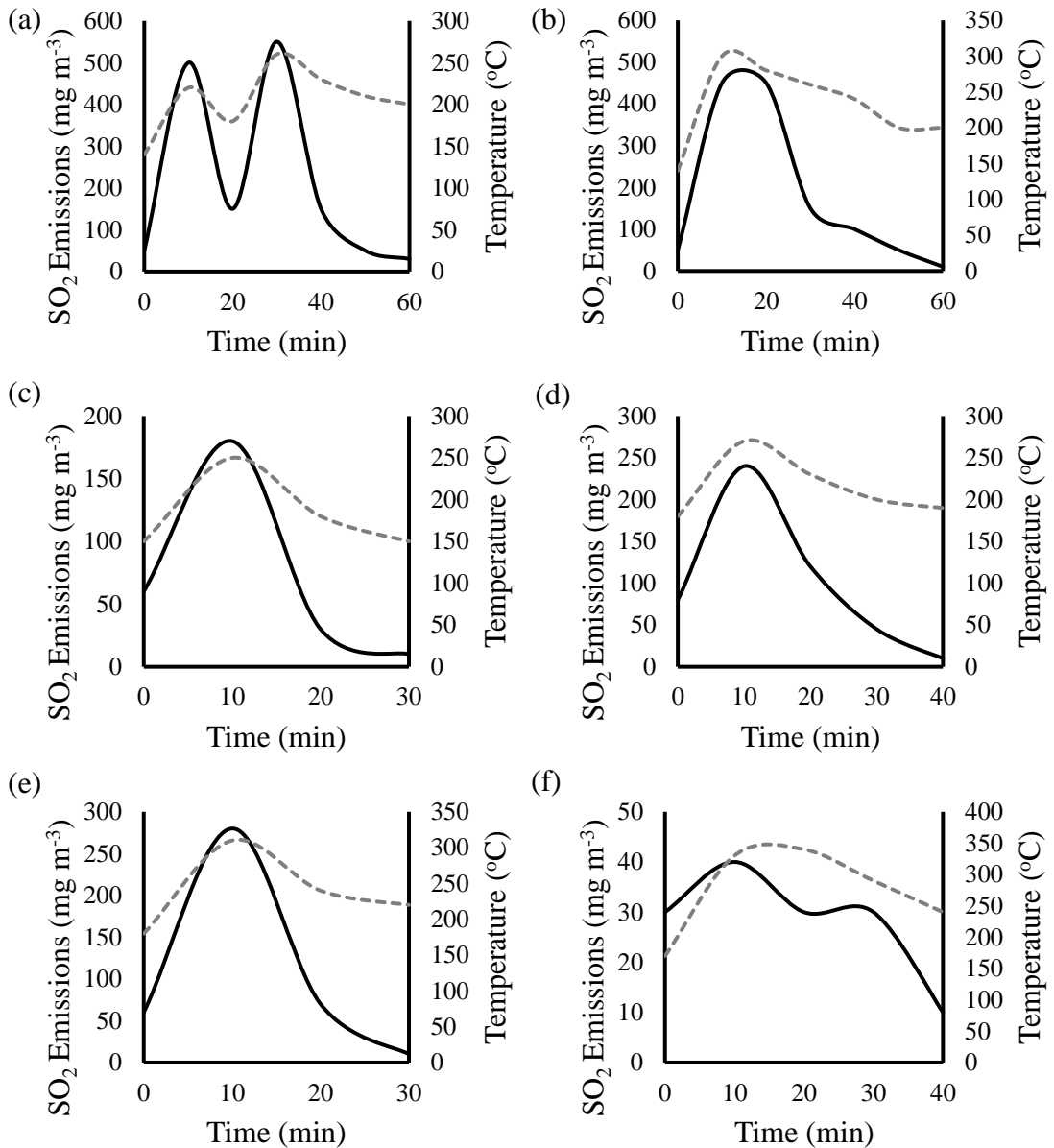
Figure 6.24a-f: Emissions of SO₂ and flue gas temperature for a single batch of fuel combustion (a) bracken large briquettes (b) bracken small briquettes (c) miscanthus (d) barley straw (e) wheat straw (f) wood briquettes

To assess further the relative partitioning of sulphur release, Table 6.12 uses a mass balance of the emissions and CHNS analysis of the bottom ash from the stove to establish what percentage of the sulphur in the fuel is released. The results show that the emission factors for the bracken briquettes is significantly higher, because of the higher fuel sulphur content, however the emissions are only 40% of the sulphur in the fuel. This is also the case for the miscanthus, barley straw and wheat straw where by only approximately 40% of the sulphur in the fuel is emitted. The wood briquettes release 75.1% of the fuel sulphur content and this will be because of the hotter

combustion temperatures, greater relative time in flaming combustion and the release of sulphur during char combustion (not seen in the other fuels). Using the work of Johansen et al. [2011] it can be assumed that there is a greater proportion of organically bound sulphur in the wood briquettes compared to the other fuels.

Table 6.12: Sulphur partitioning in combustion of fuels.

	SO_2 EF (g kg^{-1})	S in Fuel (kg/ kg of fuel)	%S emitted	%S in Ash (Calculation)	%S in Ash (CHNS)	%Difference
Bracken Large Briquettes	1.6	0.002	40.0	60.0	63.5	5.9
Bracken Small Briquettes	1.7	0.002	42.5	57.5	61.2	6.1
Miscanthus	0.8	0.001	40.0	60.0	66.5	9.8
Barley Straw	0.8	0.001	40.0	60.0	64.1	6.5
Wheat Straw	0.5	0.0006	41.7	58.3	55.1	5.5
Wood Briquettes	0.3	0.0002	75.1	24.9	28.6	12.8

The calculated S content in the bottom ash from a mass balance of the combustion process is within 10% of the measured reading from the CHNS, with the exception of the wood briquettes, which suggests good reliability in the emissions data. The results from the CHNS are expected to show a degree of difference to the calculated values since the calculated value is based on an average emission factor. Because the fuel was lighted using fire lighters, and in the cases of the straws a small starting batch of coal was used, the measurement from the CHNS could introduce errors. However, it is reasonable to assume the results are representative in all cases since the majority of the ash is from the fuels being investigated because by mass the fuel contributes over 85% of the ash to the stove.

PM emissions can be dependent on many variables and defining the origin of soot particles is difficult. More detail on the factors affecting the formation and composition of PM, are discussed in section 2.3. In Table 6.13 the total PM (PM_t) emission factor is compared for the fuels studied. It must be noted that the bracken measurements were made using the Dekati impactors in the dilution tunnel whilst the other fuels were measured by the smoke metre from the flue stack. Typically, hotter combustion temperatures result in more complete combustion and reduced PM emissions. However, comparing the two types of bracken briquettes the PM_t emission factor for the large briquettes (lower combustion temperature) is lower than the smaller

briquettes. This is because of the greater proportion of smouldering by the large briquettes compared to the smaller briquettes, the majority of PM_t is released during flaming combustion [Price-Allison et al., 2019]. PM_t emission factors in Table 6.13 are calculated using the total flow method which accounts for the fuel burnt and the time for combustion which annuls the problems discussed earlier with the SDFGV method for the reduced amount of fuel burnt per batch by the large briquettes.

Table 6.13: PM_t for all the fuels studied

	PM_t EF (g/kg)	Volatile Content (wt.% db)	C/O	K content (wt.% db)
Bracken Large Briquettes	3.5	68.1	1.25	0.8
Bracken Small Briquettes	3.9	68.1	1.25	0.8
Miscanthus	2.7	87	1.14	2.0
Barley Straw	5.0	75.1	1.24	1.7
Wheat Straw	6.4	79.6	1.28	1.5
Wood Briquettes	3.0	90.1	1.16	0.2

Work by Mitchell et al. [2016] and Roy and Corscadden [2012] show relationships between PM_t and volatile matter, C/O fuel mass ratio and K fuel content, Figs. 6.25-27 show these relationships respectively. Using Fig. 6.25 the relationship between volatile matter content and PM_t relates to the proportion of flaming combustion which has already been discussed as having a significant impact on the results. Mitchell et al. [2016] established some discrete categories of biomass represented by three trendlines on Fig. 6.25. These categories discretise coals, agricultural residues/decomposing organic matter and biomass fuels. In the case of the bracken the results sit between the agricultural residue and biomass trends.

The bracken briquettes correlate to the C/O mass ratio trend better as seen in Fig. 6.26. Intriguingly the two trends from this work and the work of Roy and Corscadden [2012] individually show strong correlations (defined from the R^2 values of the trendlines) but more so they both intercept the x-axis at the same point. From these trends it can be concluded, assuming there is no deviation from linearity, that fuels with a C/O mass ratio of less than 1 would result in zero PM_t emissions (i.e highly oxygenated fuels). The difference in the gradients of the trendlines will be due to the differences in the stoves, method of particulate collection or experimental method differences.

Fig. 6.27 shows the impact of fuel potassium content on the PM_t emissions. Higher concentrations of fuel potassium will result in faster pyrolysis and increase the formation of fly ash, discussed earlier in sections 6.3.5.2-6.3.5.4. Only fuels from this work are plotted and the miscanthus was excluded because the correlation was much stronger after excluding that single point. The trend is the higher potassium content in agricultural residues the higher the PM_t emission factor. It cannot be determined if this comes from increased soot or fly ash formation.
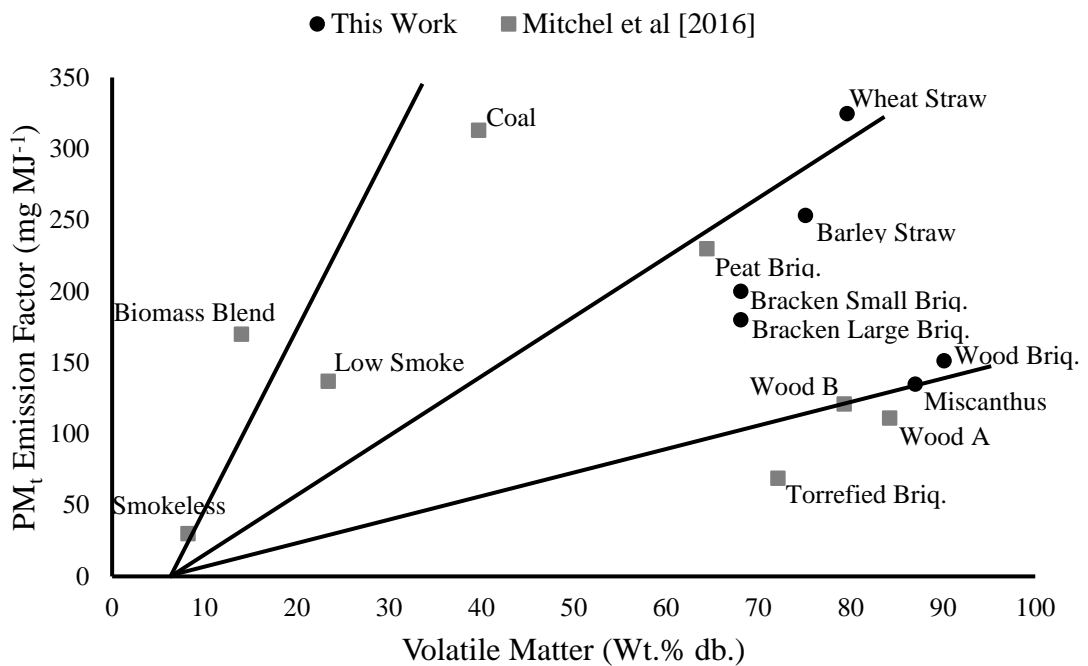
Figure 6.25: PM_t emission factor versus volatile matter, including data from Mitchell et al. [2016]
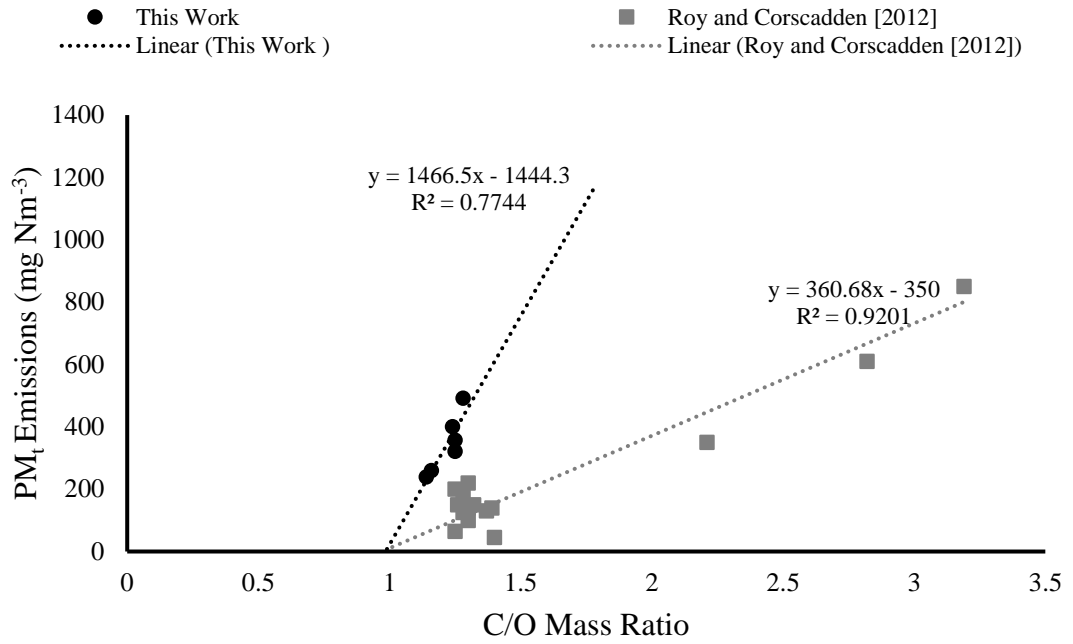
Figure 6.26: PM$_t$ emissions as a function of C/O ratio in the fuel, including data from Roy and Corscadden [2012]
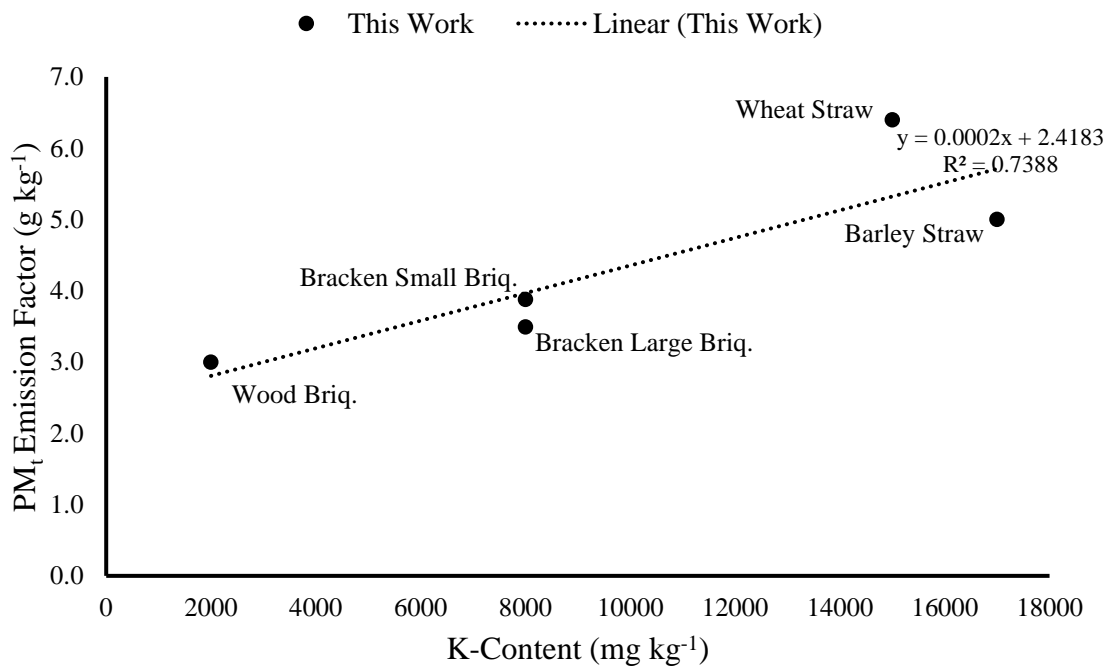
Figure 6.27: PM$_t$ emissions with fuel potassium content

216

6.4 Conclusions

In this work bracken harvested at different time periods was compared to other agricultural residues and currently-used combustion fuels. Proximate analysis of the bracken showed that as the annual cycle progressed the fixed carbon content increased significantly, more than 4% increase. This also resulted in the bracken fuel having a fixed carbon content which was much greater than the other traditional fuels. The variability between the sampling time periods (harvests) showed that the increase in fixed carbon was compensated for by decreases in the volatile content and the ash content. The ash content of the bracken was greater than compared to traditional woody fuels.

Ultimate analysis showed agreement with the proximate results since the C content of the fuel was also significantly higher at the latest harvest. Both the S and Cl decreased slightly but were still relatively high in concentration compared to the woods, residues, straws and grasses. The only major observation for the trace metals analysis was the drastic increase in the Mn content of the bracken as the annual cycle progressed. None of the other trace metals showed any discernible results. The minor metals analysed from the ash created an interesting trend, the K_2O concentration in the ash decreased particularly between the last two harvest whilst the SiO_2 and CaO both increased. These changes resulted in both the calculated and measured slagging and fouling propensities being lowest in the final harvest. The softening and initial deformation occurred above 900°C but all the key stages of ash fusion occurred within 180°C for all the harvests.

Combustion studies used the devolatilisation and char combustion profiles from the bracken samples to compare the reactivities. The bracken harvested earliest was the most reactive. Using the video footage from the single particle combustion the decreased reactivity of the final harvest bracken was evident by the increase in the ignition delay time which doubled in most cases from particles of the same mass. This was thought to be from the presence of oils and resins which evolve at low temperatures and aid ignition in the early harvests. Comparing results from the potassium release detection and the video footage it was not possible to identify the stages of volatile release and char burnout in the potassium release profiles. This was because the potassium release rate was too high to identify between the two stages.

217

However, it was possible to conclude from the video footage by crudely assuming there was a single point when combustion switches from volatile to char combustion. The results from the high heating rate experiments and the low heating rate experiments drew the same conclusions.

Stove combustion studies showed that there is a significant impact of the fuel physical properties on the emissions. Large bracken briquettes burned poorly and emitted higher amounts of CO and TOC because of reduced temperatures and gaseous mixing. NOx emissions fitted the trend with fuel nitrogen content previously explored earlier in this work and by Mitchell et al. [2016]. However, flaws in the SDFGV method results in the NOx data being slightly skewed by not accounting for the mass of fuel combusted. SO_2 emissions in the cases of the bracken, miscanthus, wheat straw and barley straw only represented 40% of the S within the fuel. Increased SO_2 emissions were the result of increased fuel-S content and all SO_2 emissions were from the thermal decomposition of organically bound S during devolatilisation. Previous work has examined many correlations between different fuel properties and the emissions of total PM (PM_t). The results from the bracken were inconclusive when correlated against the volatile matter content suggesting that the bracken could be classified neither as a woody biomass or an agricultural residue. A better correlation was found with the fuel C/O content ratio. This produced a linear relationship whereby above a C/O ratio of 1 soot formation will occur. Finally, the relationship between the soot formation and potassium content, based on the bracken, barley straw, wheat straw and wood briquettes, was linear with an R^2 of 0.7388. Thereby suggesting increased fuel-K content will result in higher PM_t emissions, however it is not possible to determine if this impact increases the formation of soot or fly ash.

Chapter 7. Washing and Torrefaction of SRC Willow grown on Contaminated Land for Combustion Applications

7.1 Introduction

As fossil fuel resources reduce, and renewables increase, energy security becomes more of a concern. Global efforts to ensure society's needs requires use of alternative fuels. Biomass is one of the key alternative fuels available. Solid biomass has the advantage of being easily implemented into the existing technology currently used for coal. Power stations can now co-fire coal with biomass or with higher capital investment and time convert to sole biomass usage.

Ash related problems are ubiquitous to solid fuels. Slagging and fouling historically have been the largest contributors to power station shutdown [Skrifvars et al., 1999]. In addition, ash causes particulate emissions which are of current concern because of the damage they cause to human health [Dilger et al., 2016].

In nature, biomass type and composition vary considerably since biomass properties are subject to its surrounding environment. Energy crop growth is forming a larger part of national economies, however more recent projects have focused on the importance of preserving agricultural land for food production [Harvey and Pilgrim, 2011]. This has created a conundrum within society of land for food or energy.

A solution to this problem is to grow energy crops on contaminated land unsuitable for food production. Under BS EN ISO 17225-4:2020 crops grown in contaminated conditions [British Standards, 2020] must undergo further testing to analyse whether they are acceptable for use as solid fuels. If they fall outside the limits expressed in the British standards shown in Table 7.1, then they cannot be used in conventional systems and are deemed as waste.

Phytoremediation is a key part of the strategy to reduce metal pollution. Metals and metalloids quickly bioaccumulate in soils and water body's which cannot be effectively removed using anthropogenic techniques. Vamerali, Bandiera and Mosca [2010] collated data which showed that certain plant species, which can be defined as hyperaccumulators (i.e *Brassica juncea L.*, *and Helianthus annus L.*), can remove over 1000 mg of Zn and Pb, over 500 mg of Cu and 200 mg As per kg^{-1} of harvested crop.

219

Experiments involving fast growing crops such as miscanthus and *salix* (willow) have also shown promising phytoextraction properties [Barbosa et al., 2015] [Korzeniowska and Stanislawska-Glubiak, 2019]. Utilisation of these crops would enhance both the reconditioning of the soil and the economic feasibility of the process.

The impacts of washing and torrefaction to upgrade biomass grown in contaminated conditions is less extensively studied. Using these pre-treatment methods this Chapter analyses the impacts they have on biomass focusing on the removal of metals and other inorganics. This concludes by using mass balances to demonstrate how ash elements are removed through pre-treatment and also their fate during combustion.

Table 7.1: Limits for SRC willow that is suspected to be grown on contaminated land, also applicable to any contaminated chipped fuel [British Standards. 2020].

Property	Limit	Units
Nitrogen, N (ISO 16948)	N1.0 ≤ 1,0	w-% dry
Sulphur, S (ISO 16994)	S0.1 ≤ 0,1	w-% dry
Chlorine, Cl (ISO 16994)	Cl0.05 ≤ 0,05	w-% dry
Arsenic, As (ISO 16968)	≤ 1	mg/kg dry
Cadmium, Cd (ISO 16968)	≤ 2,0	mg/kg dry
Chromium, Cr (ISO 16968)	≤ 10	mg/kg dry
Copper, Cu (ISO 16968)	≤ 10	mg/kg dry
Lead, Pb (ISO 16968)	≤ 10	mg/kg dry
Mercury, Hg (ISO 16968)	≤ 0,1	mg/kg dry
Nickel, Ni (ISO 16968)	≤ 10	mg/kg dry
Zinc, Zn (ISO 16968)	≤ 100	mg/kg dry
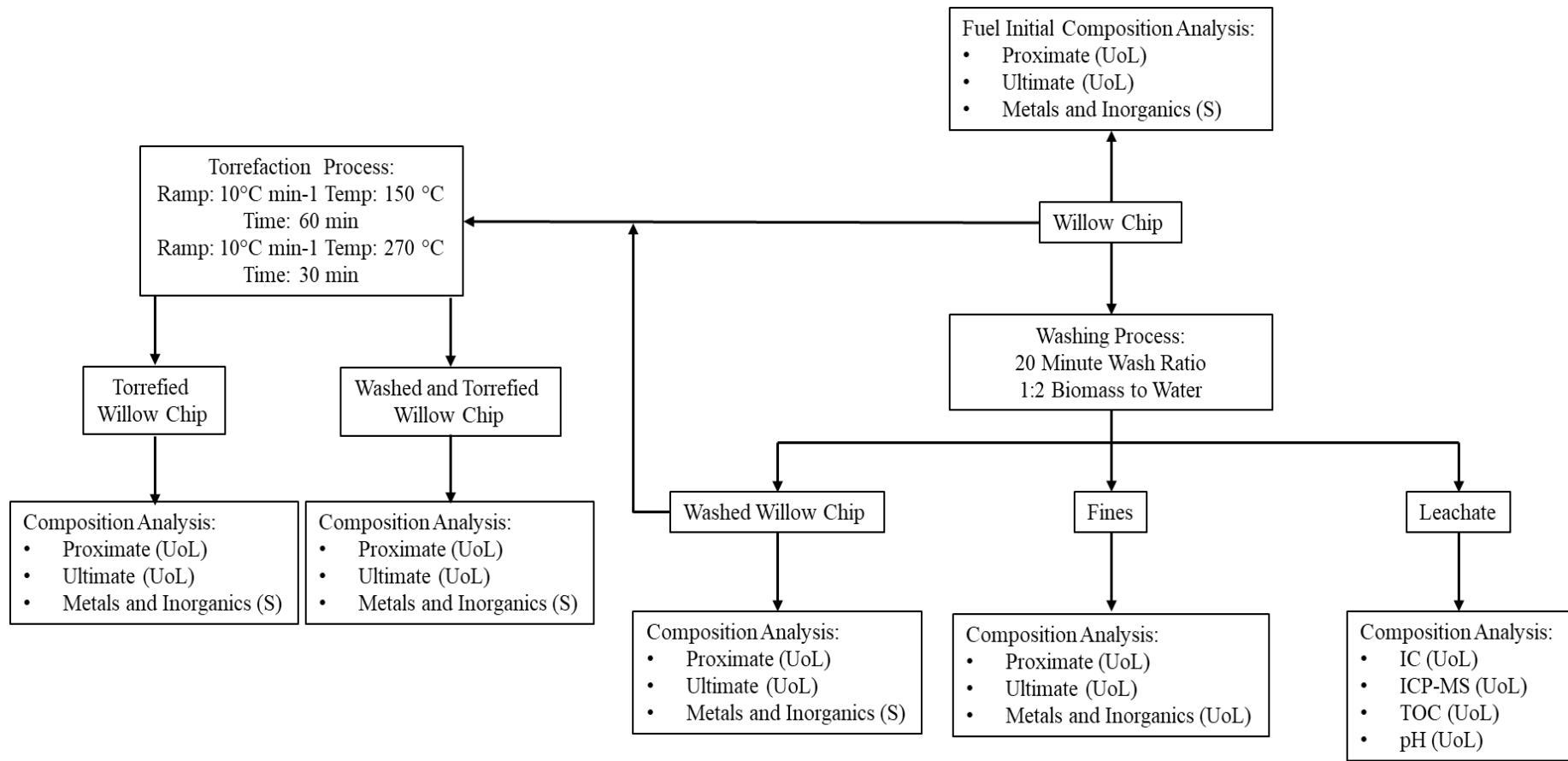
Figure 7.1: Work flow diagram

7.2 Materials and Experimental Methods

7.2.1 Sample Preparation

Samples were prepared according to methods specified in Chapter 3.

7.2.2 Experimental Methods

The overall experiment design is shown in Fig. 7.1. Initially the willow chip supplied from Rothamsted was dried in a drying oven as specified in section 3.3.1. A kilogram of sample was sent to SOCOTEC (S) for metals and inorganic analysis. Proximate and ultimate analysis was done in accordance with British Standards at the University of Leeds (UoL).

A fraction of the willow chip was washed according to the process in section 3.6.2. Once washed, the product was split into three sections the washed willow chip, the leachate and the fine materials. The washing process was repeated eight times and the washed willow chip and fines from all of the batches was combined. The leachate refers to the liquid phase after separation. The fines are the small solid particles which can be removed through simple filtration. An example of each of these factions can be seen in Fig. 3.26.

Some of the bulk washed willow (~1.2kg) was torrefied under the same conditions as the raw torrefied material, details are in section 3.6.1. This was so that a comparison of the impacts of washing on pyrolysis could be deduced and assess the product quality of washed and torrefied fuel. Composition analysis was investigated as shown in Table 3.6.

Combustion analysis was conducted for briquettes on the domestic stove using the method specified in section 3.5.5. Some alterations to the method were made and these were:

- Three batches of fuel were combusted, one ignition batch and two reload batches. The ignition batch data is displayed but was not used in the calculation of emission factors.
- Each batch of fuel was approximately 0.9kg in mass (±40g). Since only briquettes were used with no binder the reproducibility and reliability of the results improved.

- The ignition batch was started using a butane torch. This prevented minimal contamination of the bottom ash.

- Each run was continued until 0.2kg of batch mass remained. At this point all the flames had been extinguished, the fuel was no longer glowing and the burning rate was consistently zero.

- The ash was collected and sent to SOCOTEC for composition analysis.

- Particulate measurements were conducted using only the Dekati Impactors with glass fibre filter papers. Emission factors were calculated using this data and the filter papers were analysed using SEM-EDX at the University of Leeds.

7.2.3 Experimental Materials

The SRC willow was grown on land at the Renishaw Colliery, near Chesterfield in Derbyshire (Fig. D.1). The mine opened in 1860 and ceased operations in 1989. The crop was grown on the open cast mine site which was heavily contaminated in Zn (137.8 mg kg^{-1}), Pb (100.5 mg kg^{-1}), Cu (39.8 mg kg^{-1}), Ni (31.8 mg kg^{-1}) and Cr (36.5 mg kg^{-1}). This was more than three times the concentration than found in local agricultural soil for all the metals with the exception of Cr which was double the concentration. Concerningly, these concentrations, except for Zn, were similar to those measured in the average urban soil across the UK found in the Environment Agency's UK soil and herbage pollutant survey [2007] (Table D.1). The Zn concentration was 44.9% higher than the average measured in urban soil (95.1 mg kg^{-1}). It is evident that the historical activity of the site means the land is unsuitable for growing food, grazing or development without a large investment to remediate the land. The SRC willow was harvested in 2017 after a three-year growth cycle.

7.3 Results and Discussion

Analysis of the biomass before pre-treatment (raw) and after various treatment methods is shown in the following sections. The initial focus is on composition and the latter sections compare the combustion properties. Stove combustion of the torrefied fuels was not possible because of briquetting difficulties.

7.3.1 Biomass Composition

Table 7.2 shows the elemental analysis of the willow chip before and after pre-treatment.

Table 7.2: Chemical composition of Raw Willow chip (RW), Washed Willow chip (WW), Torrefied Raw Willow chip (TRW) and Torrefied Washed Willow chip (TWW). Error is in parenthesis.

		Raw Willow	Washed Willow	Torrefied Raw Willow	Torrefied Washed Willow
wt%	Moisture (ar)	3.35 (±0.8)	4.86 (±0.9)	1.7 (±0.4)	1.9 (±0.4)
	Volatiles (daf)	85.8 (±2.4)	84.15 (±1.2)	69.23 (±0.9)	71.2 (±0.7)
	Fixed Carbon^a (daf)	14.2	15.9	30.72	28.9
	Carbon	47.6 (±0.25)	49.1 (±0.15)	59.7 (±0.1)	57.0 (±0.1)
	Hydrogen	6.02 (±0.05)	6.14 (±0.03)	5.83 (±0.03)	5.53 (±0.02)
	Nitrogen	0.69 (±0.08)	0.40 (±0.07)	0.53 (±0.04)	0.51 (±0.03)
	Sulphur	0.06	0.00	0.00	0.00
	Oxygen^a	45.7	44.4	33.9	36.9
	Chlorine	n/d	n/d	n/d	n/d
	Ash (db)	1.8 (±0.3)	1.32 (±0.15)	2.39 (±0.4)	1.77 (±0.1)
mg/kg (db)	Antimony	*	1.6 (±0.05)	2.7	1.1
	Arsenic	*	*	0.5	0.4
	Barium	6.9 (±0.2)	6.1 (±0.1)	54.4	24.3
	Beryllium	n/d	n/d	n/d	n/d
	Cadmium	1.3 (±0.05)	1.2 (±0.05)	2.1	1.9
	Chromium	0.8 (±0.1)	0.6 (±0.05)	2.6	0.8
	Cobalt	0.5 (±0.0)	0.1 (±0.0)	1.1	0.6
	Copper	6.1 (±0.25)	4.3 (±0.15)	21.7	11.8
	Lead	3.1 (±0.15)	1.2 (±0.0)	9.9	3.9
	Strontium	8.7 (±0.25)	8.1 (±0.1)	14.2	13.1
	Manganese	22 (±0.6)	18.3 (±0.2)	27.8	23.5
	Mercury	*	*	*	*
	Molybdenum	*	*	0.6	*
	Nickel	1.3 (±0.15)	1.4 (±0.1)	6.5	3
	Tin	*	*	1.1	*
	Vanadium	*	*	3.6	1.3
	Zinc	98.5 (±3.5)	105.8 (±1.5)	207.7	154.4
	Silicon	2300 (±250)	1800 (±100)	3000	2300
	Aluminium	38 (±3.5)	35 (±1.5)	139	84
	Iron	44 (±1.0)	46 (±1.0)	401	124
	Titanium	11 (±0.0)	8 (±0.5)	43	32
	Calcium	4098 (±350)	3137 (±150)	5381	4238
	Magnesium	310 (±4.5)	295 (±2.0)	562	416
	Sodium	40 (±1.5)	35 (±0.5)	248	38
	Potassium	2480 (±300)	1797 (±50)	3036	2351
	Phosphorus	1029 (±100)	801 (±25)	1179	989
	Sulphur	425 (±15)	238 (±15)	526	333
daf	HHV (MJ/kg)	18.9	19.5	24.1	22.7
	Mass Yield, Y_m (%)	n/a	n/a	71.7	80.4
	Energy Yield, Y_e (%)	n/a	n/a	91.4	93.6

n/d- none detected, n/a- not applicable, *- below the instrument detection limit, ^{a}calculated by difference.

Four fuels are listed- raw, washed, torrefied raw and torrefied washed. The values in the parenthesis are error margins based on the standard deviation. Errors for the proximate and ultimate analysis are based on three measurements, the metals analysis for the raw and washed willow are based on two measurements. Only a single measurement was made for the metal's analysis of the torrefied fuels. Looking at the raw willow data, although none of the species exceed the limits specified within Table 7.1, Zn, Cu and Cd are the closest to exceeding their limits. No chlorine was detected in the raw willow chip.

After washing all of the detected metals in the raw fuel reduce in concentration with the exception of Ni and Zn, the latter exceeding the limit (100 mg kg^{-1}) specified in Table 7.1. In the case of antimony (Sb) the concentration is only measurable after washing. Additionally, the variability after pre-treatment for both washing and torrefaction decreases. In the cases Si, Al, Ca, K and P the variability in the raw willow measurements is approximately 10%, whereas after washing this variability reduces in all of the species to ≤5%.

As seen in previous research [Akinrinola, 2014] [Vassilev et al., 2017], torrefaction causes metals to become concentrated in the biomass, and this is seen in Table 7.2. The values for all the metals and inorganics are highest in the torrefied willow chip. In the cases of Cd, Cu, Pb and Zn the concentrations exceed the limits in Table 7.1. However, since the fuel has now been thermally treated British Standard 17225-8:2016 [British Standards, 2016] would now apply. Based on the values in Table 7.3 from British Standard 17225-8:2016 for a TW3H category fuel (thermally treated woody biomass with a net calorific value ≥21.0 MJ kg^{-1} on a dry basis) all of the same elements would exceed the limits making it unsuitable for combustion.

In the washed and torrefied willow chip the concentration of all the metals are lower than in the torrefied willow chip. In the cases of Cd, Cu and Pb the concentration decreases significantly, enough to be below the limits specified Table 7.3 and for Cd and Pb below the limits in Table 7.1. Although there is a 25.7% decrease in the concentration of Zn it is not sufficient to be below the limits specified in Tables 7.1 or 7.3.

225

Table 7.3: Limits for a TW3H fuel that can be briquetted and is thermally treated. Limits can be applied to the torrefied fuels in Table 7.2.

Property	Limit	Units
Chlorine, Cl (ISO 16994)	Cl0.1 ≤ 0,1	w-% dry
Arsenic, As (ISO 16968)	≤ 2	mg/kg dry
Cadmium, Cd (ISO 16968)	≤ 2	mg/kg dry
Chromium, Cr (ISO 16968)	≤ 15	mg/kg dry
Copper, Cu (ISO 16968)	≤ 20	mg/kg dry
Lead, Pb (ISO 16968)	≤ 10	mg/kg dry
Mercury, Hg (ISO 16968)	≤ 0,1	mg/kg dry
Nickel, Ni (ISO 16968)	≤ 10	mg/kg dry
Zinc, Zn (ISO 16968)	≤ 100	mg/kg dry

Table 7.4 summarises the trends in Table 7.2 for specific species. In the case of volatiles although washing can remove some volatiles the majority are removed by torrefaction. However, once the willow chip has been washed, there is a lower extent of devolatilisation in the torrefaction process increasing the mass (Y_m) and energy (Y_e) yields as shown in Table 7.2. Past research [Takeshita and Kenji, 2002] [Trubetskaya et al., 2018] has shown that the concentration of potassium can greatly influence the rate of pyrolysis and thus the extent of torrefaction, however this is discussed in more detail in section 7.3.5.

For C, FC, Ni, Zn and Fe the losses during washing are outweighed by the total mass loss, this results in them being concentrated in the WW. The extent of torrefaction is much higher for the RW than for the WW and thus these species are less concentrated in the TWW than the TRW.

For the ash, K, P and S, washing substantially reduces their concentration and any concentration of these species during torrefaction is offset by the losses made by washing. For Si and Cr, the impact of washing and torrefaction is equal resulting in the TWW having the same composition as the RW. The majority of elements follow the trend of having a loss during washing but then the impact of torrefaction is much greater concentrating them to more than in the raw willow chip. Overall, from the trends in Table 7.4 it is evident that washing before torrefaction mitigates any impact

of ash/inorganic species concentration of the willow chip composition that would otherwise normally occur in torrefaction.

Table 7.4: Ranking of fuels from Table 7.2 for individual elements.

Component (Element)	Ranking
C, FC, Ni, Zn & Fe	TRW>TWW>WW>RW
Cd, Cu, Pb, Al, Ti, Ca, Mg & Na	TRW>TWW>RW>WW
Ash, K, P & S	TRW>RW>TWW>WW
Si & Cr	TRW>RW=TWW>WW
Volatiles	RW>WW>TWW>TRW

Raw Willow chip (RW), Washed Willow chip (WW), Torrefied Raw Willow chip (TRW) and Torrefied Washed Willow chip (TWW).

7.3.2 Fine Material Analysis

In order to perform an acid digestion to analyse the composition of the fine material removed, the fine material collected from all of the eight washing batches had to be combined. This was then ashed and digested at the University of Leeds using the method in section 3.3.4.1. The sample was analysed using ICP-MS (section 3.4.5) and only specific elements were analysed (K, Ca, P, S, Si, Mg, Zn, Na, Fe, Al, Cu and Cd). This was done to try to improve the accuracy of the quantitative result by reducing the potential for interference for analysing multiple elements.

Table 7.5 shows the composition of the fines, all values are on a dry basis. The values for the volatiles and ultimate results are similar to a typical woody biomass [Vassilev et al., 2017] and show a strong resemblance to the values for the raw willow in Table 7.2. The main difference is the value for the ash which is 8.3 times greater than in the raw willow and 3 times greater than in a typical woody biomass [Vassilev et al., 2017].

The composition of the ash is largely made up of Ca. The nature and structure of this Ca was not the focus of this work however based on the work of Zárubová et al. [2015] and Sugier and Sugier [2018] Ca is in higher concentrations in willow bark and soil than typically found in willow stems and branches. Based on this and Fig. 3.26 which shows a photograph of the fines collected from the willow washing in this work, the collected material is a combination of willow bark and soil (entrained from harvesting).

Table 7.5: Composition of collected fine material from washing using ICP-MS.

		Average	Standard Deviation	Error (%)
Wt. % (db)	**Ash**	19.6	0.48	2.4
	Volatiles	60.5	0.99	1.6
	C	47	1.87	4.0
	H	6	0.49	8.2
	N	1.2	0.13	10.8
mg g^{-1} of fine material (db)	**Ca**	212	2.49	2.2
	K	0.3	0.11	38.0
	P	1.1	0.23	21.2
	S	22	6.74	30.7
	Mg	1.22	0.09	7.6
	Si	4.04	0.46	11.3
	Zn	0.07	0.01	4.6
	Fe	1.63	0.08	5.0
	Na	0.05	n/a	n/a
	Al	1.43	0.06	4.2
	Cu	0.83	0.03	3.3
	Pb	0.68	0.01	1.4
	Cd	0.031	0.001	4.7

Comparing the components in Table 7.5 relative to the raw biomass: Mg, Si, Fe, Al, Cu, Pb and Cd are measured in more significant concentrations. These elements are often found in higher concentration in bark and soil comparative to willow stems, similar to Ca [Zárubová et al., 2015] [Sugier and Sugier, 2018]. Analysis of the soil, Table D.1, shows that the soil was heavily contaminated in Zn. Based on this information it could be assumed that the removed Zn in the fines is all from soil residue.

7.3.3 Leachate Analysis

The leachate analysis results have been combined in Table 7.6 as concentration in the leachate. Amounts removed from the fuel are discussed later in section 7.3.4. The value shown is the average of eight separate leachates from eight separate washing experiments. The pH of the distilled water acidifies during washing, Fig. 7.2, as seen in previous research [Deng et al., 2013] [Carillo, Staggenborg and Piñeda, 2014] [Yu et al., 2014] [Liu et al., 2015] [Tonn et al., 2012]. Fluoride, nitrate, sulphate, chloride, calcium, potassium, magnesium, manganese, iron, nickel, copper and lead concentrations all have a standard deviation within 20%. This suggests that the data is reproducible.

It is clear from Fig. 7.2, that the water used as a washing medium became acidic over the washing process. This result was also seen in Liaw and Wu [2013] where further investigation showed that leaching of organic acids such as acetate, oxalate and formate had influenced the leaching of alkaline earth metals that were insoluble in water but soluble in acid. From Table 7.6 acetate accounts for over 10% of the organic carbon leached and over 25% of the K and Ca is leached through washing. This is an analogous observation to Liaw and Wu [2013].

The high amounts of leached K are common in past research [Liaw and Wu, 2013] [Liu et al., 2015] [Runge, Wipperfurth and Zhang, 2013] and it is usually accompanied by high amounts of Na leaching, the common factor being that these are monovalent cations. Divalent ions, alkaline metals, such as Ca and Mg are harder to leach and usually require more acidic solutions to dissolve them [Werkelin et al., 2010]. It is interesting that Ca leaching has been so effective in this work by the use of deionised water. Based on results from Werkelin et al. [2010] for water leaching from a variety of biomass, a ratio of 1:1 for Ca^{2+} to $C_2O_4^{2-}$ (oxalate) is measured implying that calcium oxalate (CaC_2O_4) minerals can be readily dissolved in water. This could explain the result seen in this work but further analysis of the water acids would be required to confirm this.

For the trace metals measured in Table 7.6, Zn leaching is the most effective followed by Cu and Cd. This is the same result as Šyc et al. [2012] and Břendová et al. [2018] in terms of both these three trace metals being leached the most and in that order. The influence of pH, on leaching of these metals as well as Pb, Ni and Al, is disputed amongst current research, as well as the influence of particle size, temperature, mechanical constraints, drying and storage time [Břendová et al., 2018] [Pecorini et al., 2017] [Stals et al., 2010] [Zhao et al., 2017] [Ghosh and Singh, 2005]. Using the data in this work it is evident that with a small, self-induced, change in pH to make a very weak acid solution, at room temperature and with a small mechanical input, leaching of these metals from willow chip (≤30mm) will occur.

Table 7.6: Leachate analysis.

		Average	Standard Deviation	Limits	Reference
pH		5.18	0.05	6.5-8.5	EPA
mg L^{-1}	Fluoride	148	7.04	*4 mg L^{-1}	WHO [2017]
	Acetate	220	59.44	-	
	Nitrate	90	10.18	*10 mg L^{-1}	WHO [2017]
	Phosphate	230	31.02	0.1 mg L^{-1}	Water Research Centre [No Date]
	Sulphate	74	5.30	*250 mg L^{-1}	WHO [2017]
	Chloride	55	3.54	*250 mg L^{-1}	WHO [2017]
	Sodium	10	2.50	*60 mg L^{-1}	EPA [2018]
	Calcium	600	46.02	Soft 0-60 Medium 61-120 Hard 120-179 Very Hard ≥180	DEFRA [2014]
	Ammonium	4.0	0.42	*12 mg L^{-1}	WHO [2017]
	Potassium	700	39.61	411 mg L^{-1}	WHO [2017]
	Magnesium	43	3.08	20-30 mg L^{-1}	DEFRA [2014]
	Total Carbon	1600	268.88	N/A	
	Inorganic Carbon	10	13.56		
	Organic Carbon	1600	266.76		
µg L^{-1}	Aluminium	38	9.35	200	EPA [2018]
	Chromium	1.0	1.14	*50	WHO [2017]
	Manganese	13	2.02	*50	WHO [2017]
	Iron	35	5.95	*300	WHO [2017]
	Nickel	7.0	1.23	100	EPA [2018]
	Copper	490	86.14	*1300	WHO [2017]
	Arsenic	12	5.63	*10	WHO [2017]
	Selenium	26	6.59	*50	WHO [2017]
	Cadmium	110	23.90	*5	WHO [2017]
	Antimony	3.4	0.91	*6	WHO [2017]
	Mercury	0.01	0.023	*2	WHO [2017]
	Lead	18	3.18	*15	WHO [2017]
	Zinc	11 000	6.78	*5000	WHO [2017]

These limits relate to drinking water standards
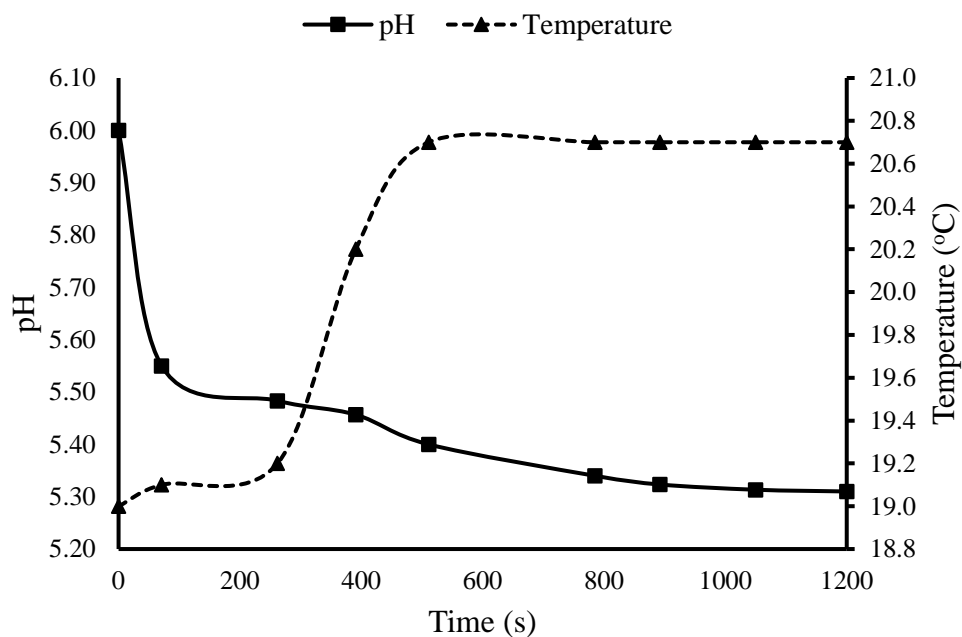
Figure 7.2: pH and temperature over the washing time period.

Although Cl analysis in the fuel was below the detection limit, in the leachate a significant amount of chloride is detected (no chloride was detected in the control water sample). The chlorine in the leachate amounts to 0.04 wt.% in the fuel. Based on previous work, chlorine is readily leached from biomass due to its high solubility [Saddawi et al., 2012]. Therefore, it can be assumed that 100% of the Cl is removed from washing.

Table 7.6 shows limits that have been imposed on water systems by various international and national bodies. In most of these cases, they relate to tap water (drinking water) which has to be treated to prevent infection and disease. It is evident that the water collected after washing (leachate) is not suitable for discharge. In the cases or Ar, Cd, Pb and Zn discharge of these concentrations would cause bioaccumulation in the ecosystem and be toxic without treatment [Khan et al., 2019]. The phosphate concentration is significantly higher than the recommended; this result will cause accelerated eutrophication [Water Research Centre, No Date]. Water treatment would be required before discharging this leachate.

7.3.4 Mass Balances

Evaporated Water, E
Water Evaporated in Drying, $M_E = (M_A + M_B) - (M_Z + M_Y + M_F)$

Willow Chip, A
Willow Chip, A, at 14.8% moisture
Willow, $W_A = A \times 0.852$
Water as moisture, $M_A = A \times 0.148$

Water, B
Water, $M_B = B$

20 Minute Wash
Biomass to Water Ratio
1:2 by Volume
Distilled Water
24 hours drying at Room
Temperature
72 hours drying at 40°C

Willow Fuel, Z
Willow Fuel, Z, at 8% moisture
Willow, $W_Z = W_A \times 0.887$
Water as moisture, $M_Z = W_A \times 0.087$

Leachate, Y
Willow in Leachate (Leached), $W_Y = W_A \times 0.006$
Water in Leachate, $M_Y = (M_A + M_B) \times 0.59$

Losses, L
Material that is unaccounted for.
Willow, $W_L = W_A - (W_Z + W_Y + W_F)$

Fines, F
Fines, F, at 3.5% moisture
Willow, $W_F = W_A \times 0.041$
Water as moisture, $M_F = W_F \times 0.0363$

Figure 7.3: Model for washing experiments conducted in this work

Evaporated Water, E
Water Evaporated in Drying, $M_E = 0.8109$ kg

Willow Chip, A
Willow Chip, A, at 14.8% moisture
Willow, $W_A = 0.852$ kg
Water as moisture, $M_A = 0.148$ kg

Water, B
Water, $M_B = 2.0$ kg

20 Minute Wash
Biomass to Water Ratio
1:2 by Volume
Distilled Water
24 hours drying at Room
Temperature
72 hours drying at 40°C

Willow Fuel, Z
Willow Fuel, Z, at 8% moisture
Willow, $W_Z = 0.756$ kg
Water as moisture, $M_Z = 0.0658$ kg

Leachate, Y
Willow in Leachate (Leached), $W_Y = 0.005$ kg
Water in Leachate, $M_Y = 1.27$ kg (1.27L)

Losses, L
Material that is unaccounted for.
Willow, $W_L = 0.056$ kg

Fines, F
Fines, F, at 3.5% moisture
Willow, $W_F = 0.035$ kg
Water as moisture, $M_F = 0.0013$ kg

Figure 7.4: Washing outputs based on 1kg of willow and 2kg of water input

In order to understand how effective washing is at removing individual species, mass balances were used to analyse how removal occurs. In order to do this an overall mass balance had to be determined first using data in Table D.2. Fig. 7.3 shows the model for the washing process used in the experiments in this chapter; developed from experimental data in Table D.2, any value can be determined as long as the mass of willow input (at 14 wt.% moisture content) and the mass of water is known (kept fixed at a ratio of 1:2 by mass willow chip to water). The model is within 10% of the measured values in Table D.2 with the exception of the fines which is within 30%. This model only applies to the total mass, not the mass of individual species. Fig. 7.4 shows the predicted outputs based on a 1kg input of willow chip and a 2kg input of water. Using these predicted outputs, mass balances for specific elements can be calculated, Fig. 7.5a-l.

Using Fig. 7.5, elements can be split into three categories:

- Removed by leaching: K, P, Zn and Na
- Removed through fine material filtration: Si, Al and Pb
- Removed by both mechanisms: Ca, S, Mg, Cu and Cd

Losses refers to how much material is unaccounted for. How elements are removed is a direct indication of the structures in which they are present in the biomass [Werkelin et al., 2010].

Previous work using chemical fractionation and washing pre-treatments have shown that K, P and Na are easily removed by simple water washing because these are present in water soluble forms [Wang et al., 2020] [Schmidt et al., 2020] [Bandara, Gamage and Gunarathne, 2020] [Wang and Xiong, 2020] [Wigley, Yip and Pang, 2015] [Zhang et al., 2018]. However, looking at Fig. 7.6 the removal efficiency is much lower than shown in previous work. For example, the potassium removal efficiency in this work was 42% compared to Wang and Xiong [2020] which measured an efficiency of 58%, Carillo, Staggenborg and Pineda [2014] measured 62%, Yu et al. [2014] 66% and Abelha et al. [2018] between 50-80%. In all of the aforementioned works the ratio of biomass to water was five times the ratio used in this work, this has a substantial impact on the removal efficiency along with particle size, water temperature and washing time [Bandara, Gamage and Gunarathne, 2020].
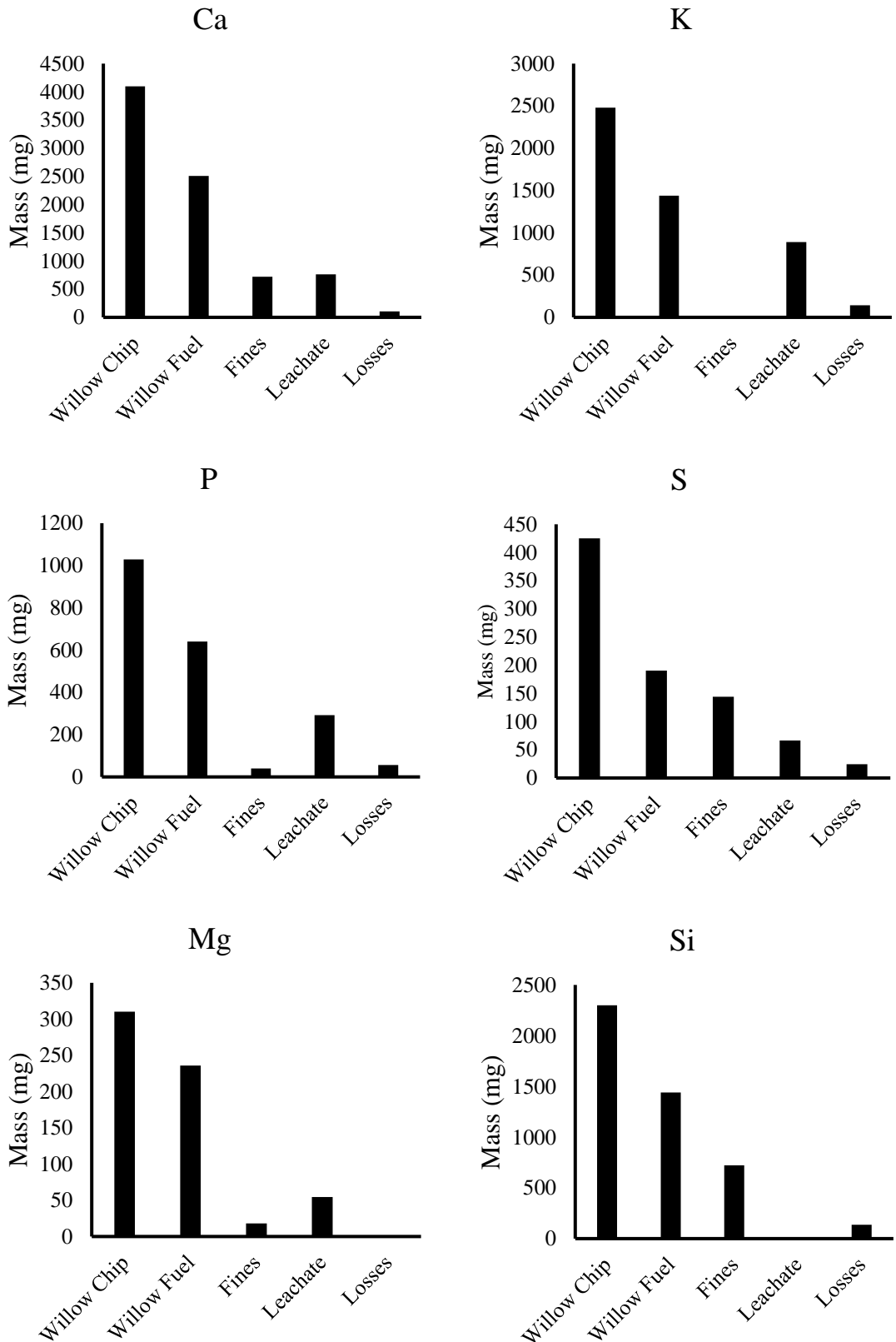
Figure 7.5: Elemental mass balances for washing process based on a 1kg willow input feed (a) calcium (b)potassium (c) phosphorus (d) sulphur (e) magnesium (f) silicon. *Refer to Fig. 7.4 for details.*
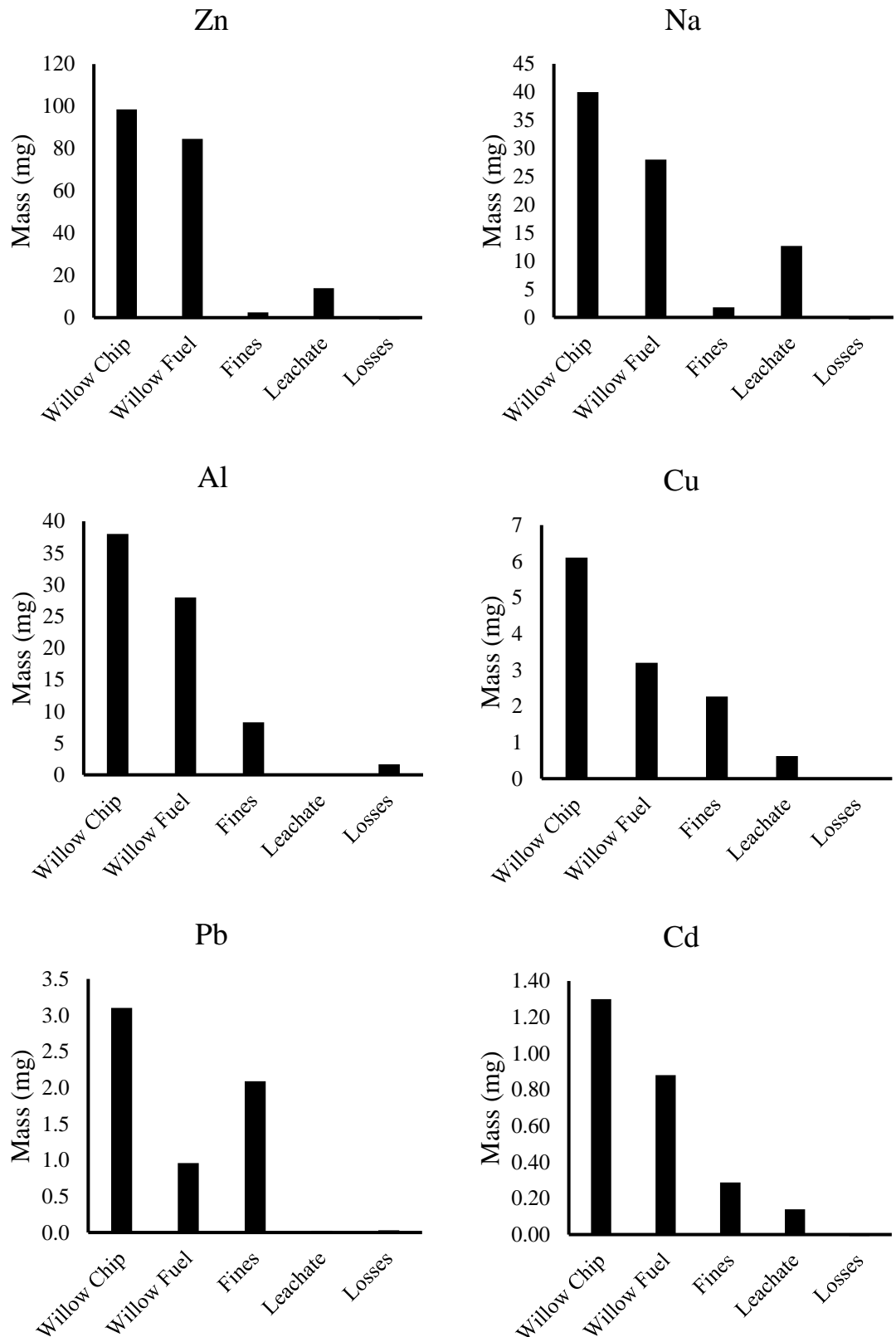
Figure 7.5 *cont.*: Elemental mass balances for washing process based on a 1kg willow input feed (g) zinc (h) sodium (i) aluminium (j) copper (k) lead (l) cadmium. *Refer to Fig. 7.4 for details.*

235

Zn is often measured in past research [Schmidt et al., 2020] [Wigley et al., 2015] however it is usually in much smaller quantities compared to the willow chip used in this work. In Wigley et al. [2015] 11% of the Zn is removed from pine wood chips using deionised water however when washed in 1% HCl the removal efficiency increases to 88%. It is evident that increases in acidity improve Zn leaching and this is also the case in Nazif et al. [2015] and Amrani, Westfall and Peterson [1999] which showed that the solubility of Zn salts such as sulphate, acetate and chloride increase when the pH decreases to 4-5.5. Based on Fig. 7.2, as the washing process progresses the leachate acidifies, from the removal of organic acids, this subsequently results in more Zn salts being dissolved. Based on Fig. 7.5 and 7.6, Zn shows a low removal efficiency, 14%, this is also common with Fe, 16%, and Ni, 14%. However, based on Table 7.2, the concentration of these three elements increases in the washed willow compared to the untreated. This implies that there is a threshold elemental removal efficiency, between 16% (Fe) and 24% (Mg), where below this threshold elements will appear to be concentrated after washing.

Si, Al and Pb were all removed in significant quantities, removal efficiencies of 37%, 26% and 69% respectively, with Pb having the greatest removal efficiency of all the elements analysed. Unlike the previously discussed elements, these elements were measured in the analysis of collected fine material filtered from the leachate. Si removal from washing biomass has been analysed in previous work with the general conclusion that there is no removal of Si compounds from biomass leaching due to its lack of solubility in water [Wang et al., 2020] [Wang and Xiong, 2020] but a small amount can be removed by acid washing [Bandara, Gamage and Gunarathne, 2020] [Saddawi et al., 2012]. Temperature increases have been shown to improve Si removal efficiency [Deng et al., 2013] however the removal mechanism is from leaching of amorphous silica and is dependent on how tightly bonded the silica is to the biomass matrix. The substantial presence of Si in the collected fine material in this work implies that this is the result of the removal of soil and dirt particles from harvesting. This is the same for Al and Pb where no material is detected in the leachate. In Schmidt et al. [2020] analysis of the leachate from beech, oak and fir washing showed the same result where minimal leaching of Al had occurred. However, for willow chips washed in water in Břendová et al. [2018] the Pb concentration in the leachate was significant, 0.63 mg L^{-1}, suggesting that Pb leaching can be the dominant removal mechanism. In

the case of this work, Pb concentration in the original biomass was very low and would have been present as either PbO, $PbCO_3$ or $PbSO_4$ [Cao et al, 2008] [Guo et al., 2019]. Any leached Pb would have readily been reacted with excess P to form pyromorphite [Cao et al., 2002], of which a small amount of P was detected in the fines, and bonded with clay or silt particles [Shen et al., 2017].

Removal of Ca from biomass washing is highly variable. Results from Yu et al. [2014], Deng et al. [2013], Wang et al. [2020] and Bandara et al. [2020] all showed the Ca content increased in the biomass after washing. In contrast, Wang and Xiong [2020] (22%), Wigley et al. [2015] (14.3%) and Zhang et al. [2018] (50%) showed Ca reductions after washing. Saddawi et al. [2012] measured a 3% removal efficiency based on the leachate analysis after filtration for willow washed in deionised water for 20h with agitation. The removal efficiency in this work for Ca was 39%, however this was split between leaching (19.8%) and insoluble fine material (19%). Wang et al. [2020] showed that the insoluble fraction of Ca increased in the fuel when it is washed using chemical fractionation. However, the nature of this insoluble Ca is unknown. It should be noted that wood bark is typically very high in Ca and could be forming part of the fine material. With refined filtration, as in this work, this insoluble Ca could potentially be removed.

S is present in many forms within biomass, this includes organic compounds and inorganic salts [Williams et al., 2012]. Removal of S by leaching has been shown to be highly efficient in water. Deng et al. [2013] showed removal efficiencies of up to 90%, mainly in straws, and a slightly lower result was seen for rice husks in Zhang et al. [2018], ~75%. Both are much more efficient than in this work, 55%. Since S is in many various forms, some of these forms are water soluble whilst others rely on ion exchange reactions to leach from the biomass [Miller and Miller, 2007]. In Deng et al. [2013] when the water temperature increased, the S removal decreased because of increased ion competition in the leachate. An equilibrium between the fuel and leachate forms when the leachate is saturated. This phenomenon is also influenced by reduced ratios of biomass to water. This is most likely the effect being measured in this work and hence the removal efficiency of S (55%) is lower than compared to past work.

Mg removal as with Ca removal is highly variable, Wang et al. [2020] reported removal efficiencies of up to 80% for rice straw whilst Bandara et al. [2020] reported no removal in rice husks. In this work there is a small amount of Mg leaching, which makes up 75% of the removal mechanism, most likely from the acidification of the leachate as is the case with Ca- both elements being divalent ions.

The removal efficiency of copper was the fourth highest of all elements (≈47%), this was removed mainly as fine material and a small amount of leaching. Cu uptake by plants has been studied extensively. Past research has shown that in particular Cu (II) in acidic conditions, pH 5, is adsorbed into the bark of biomass such as radiata pine [Palma, Freer and Baeza, 2003]. Radiata pine is another softwood like willow. Therefore, a reasonable explanation for the removal of Cu is through the removal of bark [Palma, Freer and Baeza, 2003]. Some leaching of Cu does occur but this could be from either the bark or the willow stem (wood) and cannot be determined from the data in this work.

Cd removal from willow leaching has been measured previously by Břendová et al. [2018] with a removal efficiency of up to 39%, based on measurements of the leachate. This is a much larger leaching effect than seen in this work where the majority is removed by fine material. It must be noted that the willow in Břendová et al. [2018] was more contaminated in Cd, twenty times higher, than the willow used in this work. The excess Cd could be present in more water-soluble salts and explain the differences seen in the removal mechanisms.
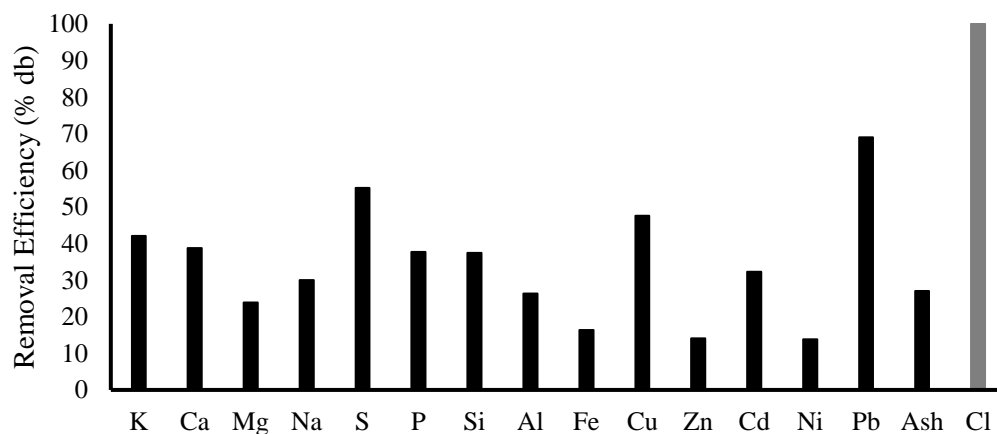
Figure 7.6: Removal efficiency of various elements. *Cl has been assumed to be 100% based on its high solubility and initial concentration in the willow. Below 10% removal efficiency is within the experiment error.*

When comparing results for the removal of ash in this work to other literature, washing is less effective than previously reported as shown in Table 7.7. In Yu et al. [2014] and Chin et al. [2015] between 48 and 85 wt.% of the ash is removed on a dry basis, compared to 28 wt.% in this work. This will be due to differences in the experimental methods and fuel types. Some of these differences are listed in Table 7.7, however other differences include the size of the washing instrument, the particle size and changes in pH.

Table 7.7: Comparison of ash removal efficiencies

	Biomass	Ratio of Washing Medium to Sample	Leaching Temperature	Mechanical Action	Wash Time (min)	Ash Removal (%)
This work	SRC Willow (contaminated)	2		drum rotation	20	27
Yu et al. [2014]	Rice Straw	variable		impeller	6 hours (stirred for 2 minutes every 30 minutes)	85
	Wheat Straw					76
	Corn Stover					47
	Switchgrass					76
	Miscanthus					61
	Douglas Fir					60
Chin et al. [2015]	Acacia	10	room	stirring	30 minutes	50
	Paraserianthes falcataria					62
	Macaranga					48
	empty fruit bunch					80
	olive palm biomass					50
Saddawi et al. [2012]	Willow	60g to 1L			20 hours	6

7.3.5 Stove Combustion

Combustion of willow and washed willow briquettes made at the University of Leeds were combusted on a domestic stove. Batches of the same number of briquettes were uniformly loaded into the stove and the lighted using a butane torch. Emission factors were calculated over the reload batches and ash analysis was used to show the fate of metals during combustion.

Fig. 7.7 shows the burning rate (a) and the temperature (b) profiles over the combustion runs; arrows indicate the reload points. As can be seen in Fig. 7.7 the

peaks formed from combustion of the washed willow are larger in magnitude this is more discernible for the third batch of fuel. The main peak width is slightly wider for the washed fuel however the overall characteristic batch burning time is shorter for the washed fuel, this results in a similar conversion efficiency (based on mass) for the two fuels (willow 79% and washed willow 76%).

On Fig. 7.7b boxes highlight when the temperature plateaus, this is a key property as it represents a phase termed 'pre-flaming smoulder.' During this period after reloading fresh fuel devolatilisation occurs. However, after their release combustion does not occur because the gaseous mixture is not flammable, this is common in the combustion of wet and low calorific fuels, and is characterised by the production of plumes of grey smoke [Chen et al., 2010].
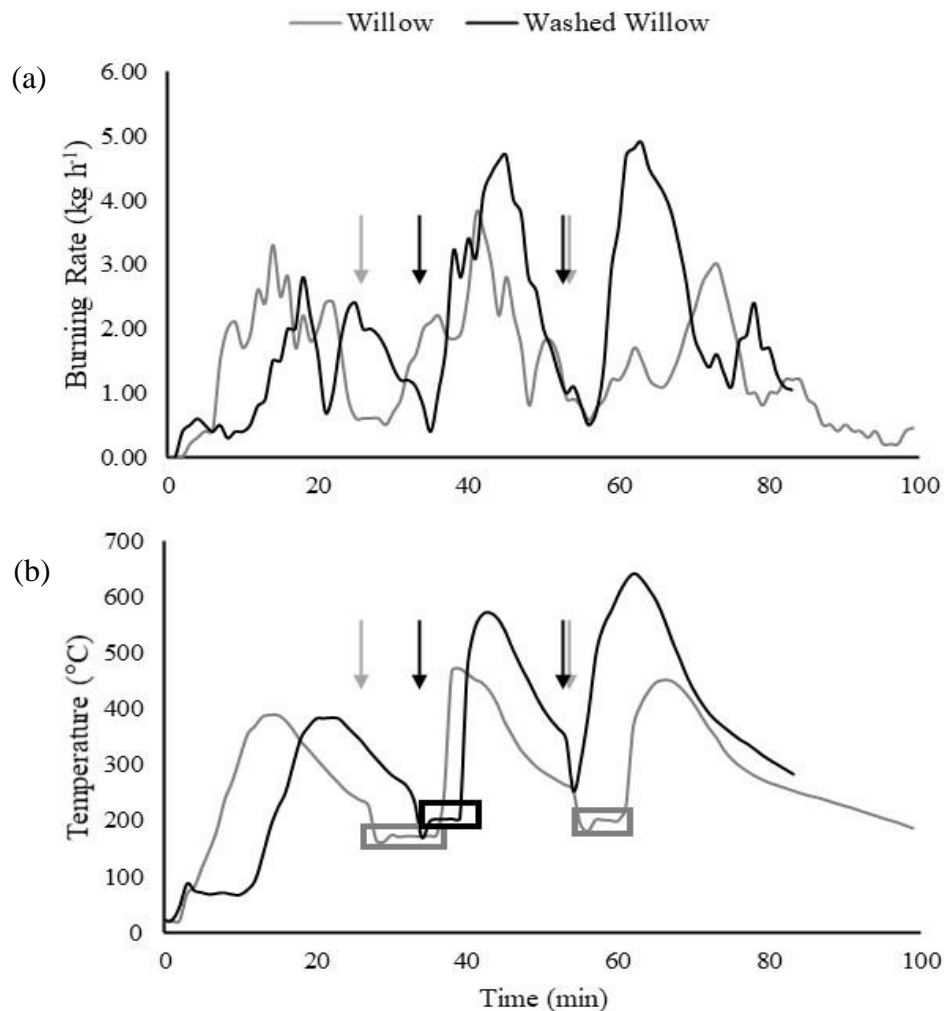
Figure 7.7: Burning rate (a) and temperature (b) profiles for the combustion runs

As time progresses the fuel dries releasing less moisture and volatiles begin to heat up eventually sparking causing ignition and the fuel begins flaming. Fig. 7.8 shows photos of how the combustion process progresses for the washed willow. Comparing this pre-smouldering phase for the willow and washed willow, the time it takes for the system to ignite is faster for the washed willow and also does not occur on the second reload batch. The reduced volatile and K content of the washed willow will increase the activation energy and ignition temperature/delay time (at isothermal heating) [Saddawi et al., 2012] [Chin et al., 2016]. Looking at Fig. 7.7(b) the temperature in the stove for the washed willow remains hotter so when the fuel is reloaded the fuel heats up faster, the reduced fuel ash content and increased HHV aids this. Additionally, from Fig. 7.7(a) the burning rate profile is smoother for the washed willow than the untreated willow, this will be from the increased homogeneity, see Table 7.2. A combination of these factors is most likely improving the flammability and combustion performance.

(a)　　　　　　　　　　(b)　　　　　　　　　　(c)

(d)　　　　　　　　　　(e)
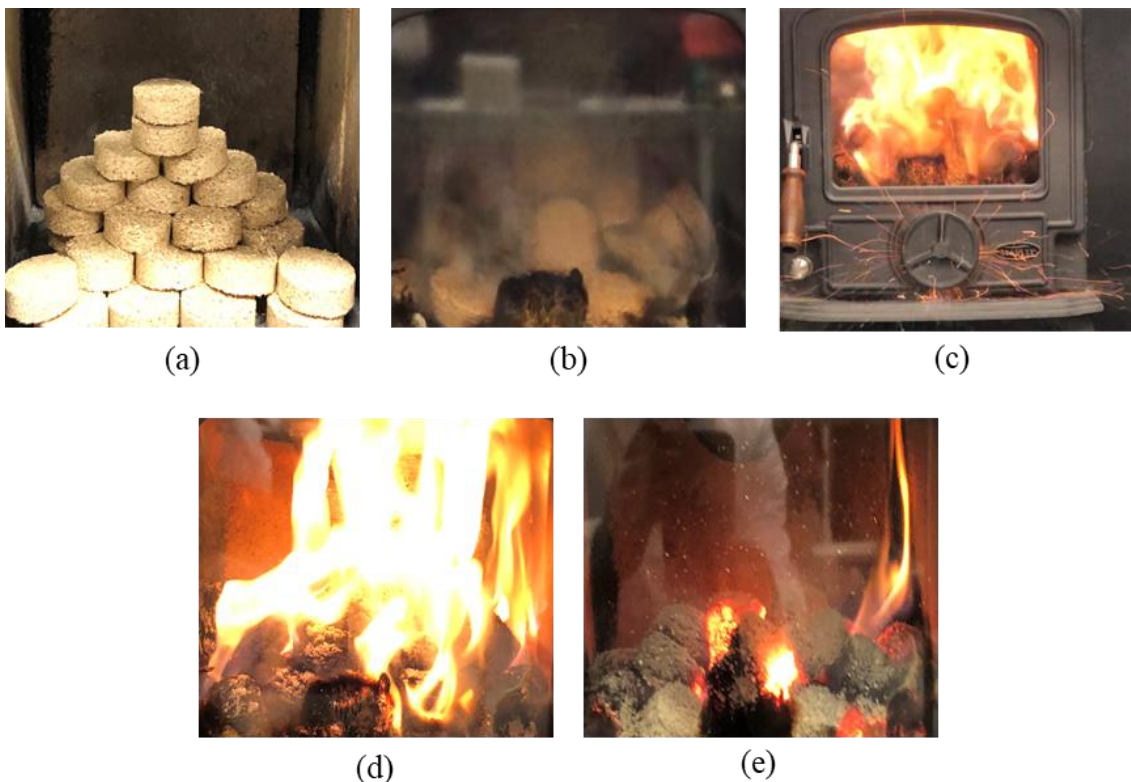
Figure 7.8: Photos during combustion of washed willow showing (a) batch of fuel (b) 'pre-flaming smoulder' (c) spark ignition (d) flaming combustion (e) post-flaming smoulder

During this period of pre-flaming smouldering, the emissions of CO_2 sharply decrease, Fig. D.2, whilst the emissions of CO and THC spike as shown in Figs. D.3 and D.4. The spike in CO emissions indicates that devolatilisation is occurring but conversion to CO_2 is not feasible. There is no impact to NOx and SO_2 emissions, Figs. D.5 and D.6, both peaks coincide with the peak for CO_2 when the fuel starts flaming.

Table 7.8: Emission factors from the combustion of willow and washed willow, factors are for the reload batches.

		Willow			Washed Willow		
		Batch 1	Batch 2	Average	Batch 1	Batch 2	Average
Average Emission Factors (kg GJ^{-1})	CO_2	48	41	45	73	70	72
	CO	5.6	4.7	5.2	2.4	2.5	2.45
	THC	0.24	0.19	0.22	0.12	0.13	0.125
	NOx	0.05	0.053	0.052	0.064	0.065	0.065
	SO_2	0.028	0.026	0.027	0.017	0.018	0.0175
	PM	0.12			0.063		

Table 7.8 shows the emission factors over the reload batches and the average emission factor with the exception of the PM which is a single measurement calculated over a batch of fuel. Current published research on the impact of washing biomass on gaseous emissions is scarce and limited to emissions of CO, NOx and SO_2. Table 7.8 shows that CO_2 emissions increase by 60% for the washed willow. The reasoning for this is most likely because of the increase in flue gas temperature caused by the increased calorific value of the fuel. Since CO is an intermediate in the formation of CO_2 after primary oxidation of volatile species from the fuel particle surface, it is often dependent on the relative emissions of volatile species (THC) and CO_2. Emissions of CO are reduced by 50% for the washed willow compared to the willow, the same result is observed in Ravichandran and Corscadden [2014] for agricultural biomass and a similar reduction range (31-51%) is observed in Schmidt et al. [2018] for washed fir, oak and beech. Nishimura, Iwasaki and Horio [2009] suggest the result is from the reduced potassium and a slower rate of pyrolysis during the early stages of combustion. Leaching of K reduces the rate of gasification of cellulose and pyrolysis of saccharide polymers which reduces the concentration of CO and THC during the heating up and early devolatilisation/pyrolysis phases. Figs. D.3 and D.4 show that the CO and THC spikes are exacerbated during the pre-flaming smoulder period for both the washed and untreated willow, these represent the largest peaks in emissions of

both these species. The reduced period of pre-flaming smoulder for the washed willow fuel has a significant impact on the CO and THC emission factors.

From Table 7.8 the NOx emissions are 25% greater for the washed willow which is surprising since there is a reduction in the nitrogen content when the fuel is washed. In Ravichandran an Corscadden [2014] leaching of reed canary grass caused the fuel-N content to decrease by 33% however the NOx emissions also increased. Within the same work, leaching of barley, switchgrass and wheat all reduce the nitrogen content by up to 50% however the observed impact on the NOx emissions is minimal. Release of fuel-N can be through various mechanisms [Williams et al., 2012] and is dependent on surrounding concentrations of H, C and O, particle size, heating rate and the environment [Ren et al., 2010]. Reducing environments inhibit the formation of NOx from the reaction of NO with the char surface, Eq. 7.1 [Wang et al., 2016]. Na is a catalyst of these reactions and is more effective at lower combustion temperatures (<700°C) [Zhao et al., 2006]. Leaching of Na from washing is highly efficient and in previous work based on coal washing the same result is observed [Liu et al., 2005] [Yang et al., 2007] [Zhao et al., 2006] [Zhao et al., 2003]. This is most likely the reason for the observed increase in NOx emissions.

$$NO + C(char) \rightarrow \frac{1}{2}N_2 + CO \quad (7.1)$$
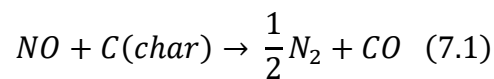
Although the removal efficiency of S is high, ~55%, emissions of SO_2 are still dependent on the form in which the S is present and the Ca content of the fuel. From Table 7.8 the SO_2 emissions decrease by ~40% for the washed willow compared to the willow. S removal occurred from both removal of fine solid particles and through leaching, however the most important factor is the removal of organic S which is more reactive at lower temperatures. The reduction in SO_2 is from the direct reduction in fuel-S content and within the removal a large removal of organic S. Ravichandran and Corscadden [2014] observed a different result when they combusted various washed and untreated agricultural residues, they observed a minimal decrease in the fuel-S content and an increase in the SO_2 emissions, this result was explained to be from averaging spikes in SO_2 during hotter combustion periods when the instrument could detect S. It is well known that S content in agricultural residues such as straws is higher than in woody biomass, and the Ca content, which can prevent SO_2 emissions by reacting to encapsulate S in the char and ash, is lower [Vassilev et al., 2017].

Ravichandran and Corscadden [2014] did not measure the fuel-Ca content and therefore no correlation can be made. However, this is most likely the reason for the difference in observed results.
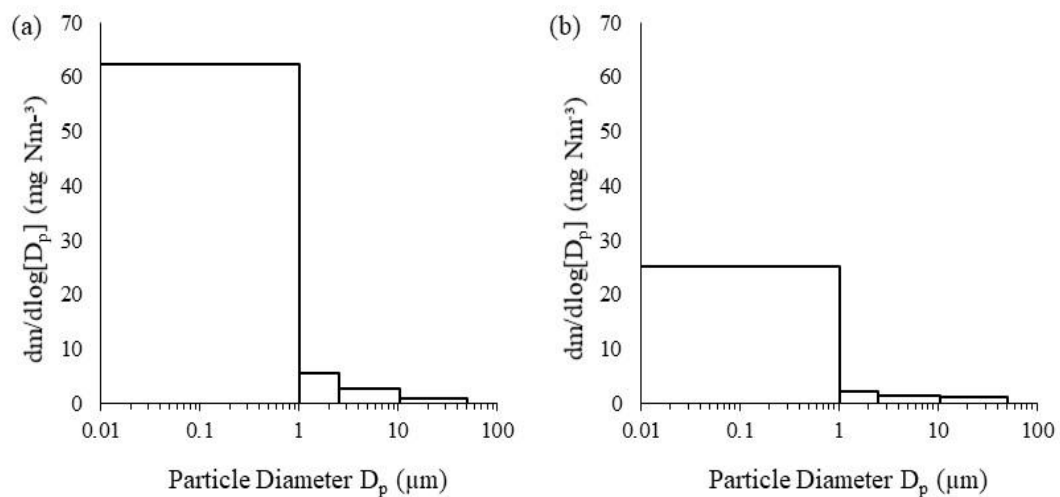
Figure 7.9: Particle size distribution for (a) willow (b) washed willow

The PM emissions were significantly reduced (50%) after washing. Fig. 7.9 shows the particle size distribution for the discrete particle size categories measured by the Dekati impactors. The majority of the reduction is at the sub-1μm level with a small reduction in the 1-5μm range. Since over 95% of PM emissions are from the sub-micron range from domestic stoves it is not surprising that this is where the difference is measured.

Wang et al. [2020] observed the same result for torrefied and washed willow compared to torrefied willow, concluding that the observed difference is from the reduction in K. This is analogous with the results in this work. Nishimura, Iwasaki and Horio [2009] observed the same effect and showed that decreasing K_2CO_3 in a fuel increased the temperature range over which elemental and organic carbon is released and this means that the majority of PAH's are formed at above 600°C. This coincides with work from Ross et al. [2005], Jones et al. [2020] and Atiku et al. [2017] in that slower decomposition of cellulose prevents fuel rich 'pocketing' in the flue gas which can lead to soot formation from the development of PAH's in flaming combustion.

244

However, K can also contribute to PM when it condenses from inorganic vapour, this is discussed more in the following section, 7.3.5.1.

7.3.5.1 Particulate Composition
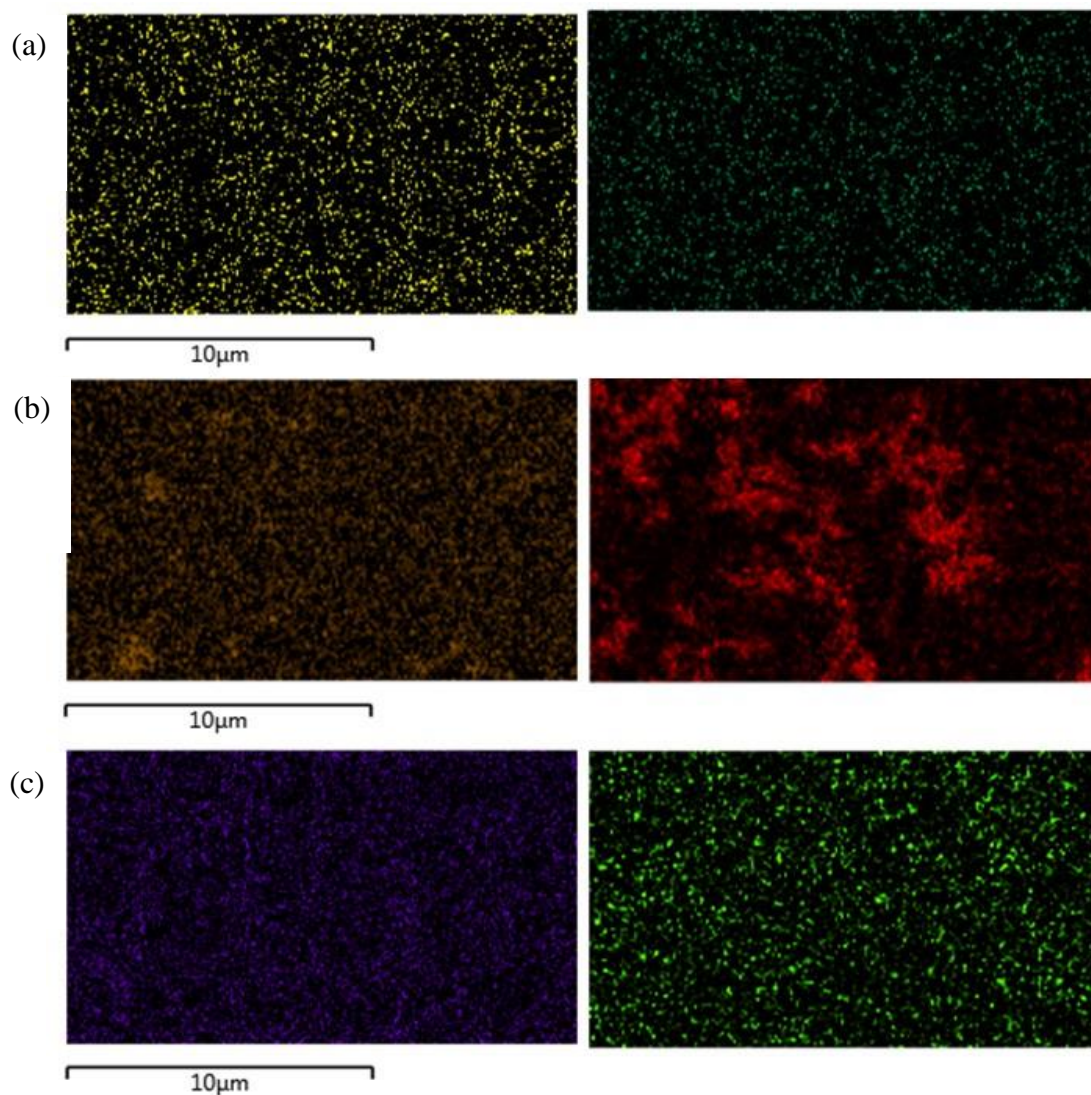
Figure 7.10: Surface analysis using SEM-EDX of collected sub-micron particulates for (a) Ca (b) K and (c) Zn. *Images on the left are from willow particulates and images on the right are from analysis of washed willow particulates.*

SEM-EDX analysis of collected PM was used to compare the composition before and after washing. Figs. 7.10a-c show the surface analysis for Ca, K and Zn for the willow and washed willow sub-micron PM. These elemental analyses are shown since all three elements were detected in the PM_1. The surface analysis shows that in the cases of Ca and Zn, even though the concentration changes, the elements are still

245

evenly distributed across the collected PM surface. A small amount of agglomeration can be seen by brighter spots on Figs. 7.10a and c. In contrast, the K surface analysis, Fig. 7.10b shows a large variation in the particle morphology with increased agglomeration in certain areas for the washed willow.
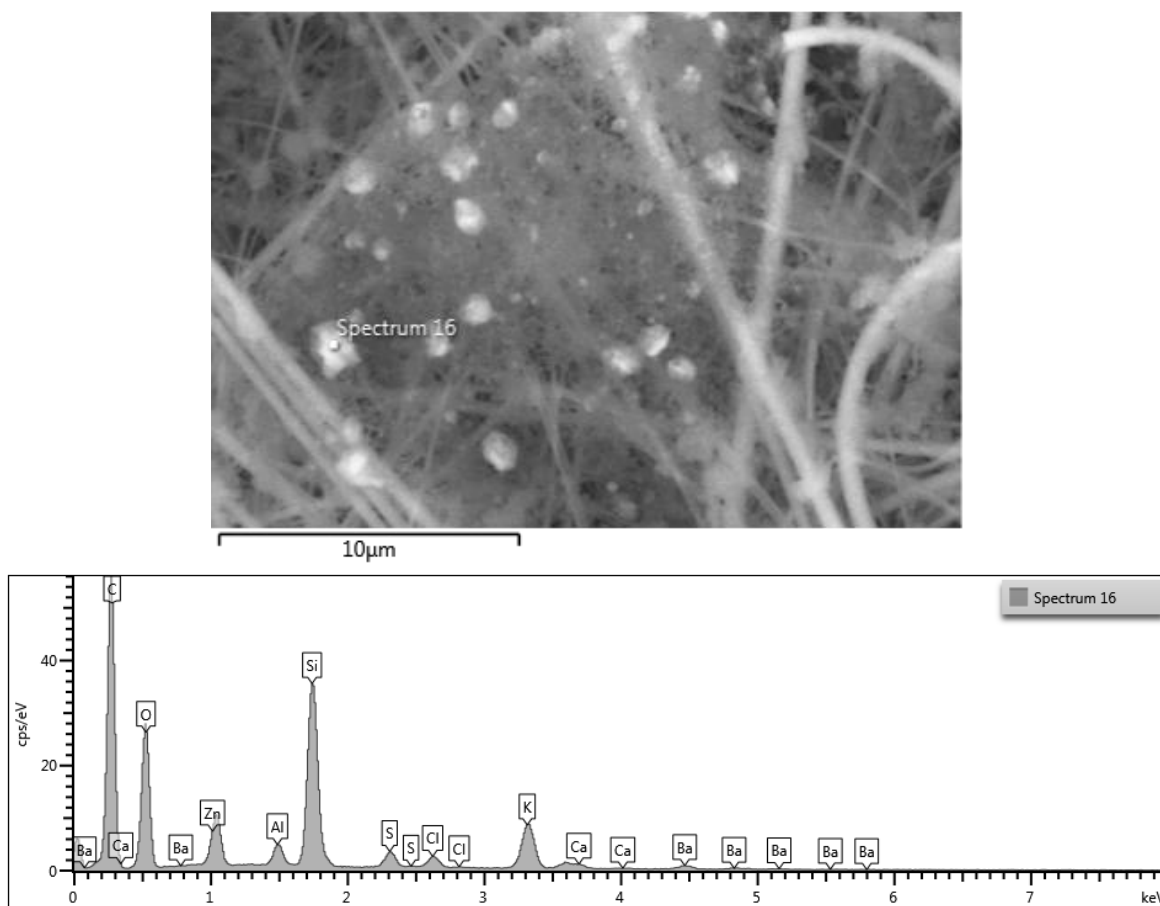
Figure 7.11: Measured composition spectra for PM surface sites from washed willow combustion.

EDX analysis was also used to estimate and compare the inorganic composition of the PM from untreated and washed willow combustion. Fig. 7.11 shows an example of the measured spectra for an area of collected PM. This was performed on multiple sites across the filter surface. The measured spectra were normalised to account for C and O from soot and Si from the glass fibre filters and then averaged for all the measured sites- Table D.3. The estimated average is compared between the untreated and washed willow in Fig. 7.12.
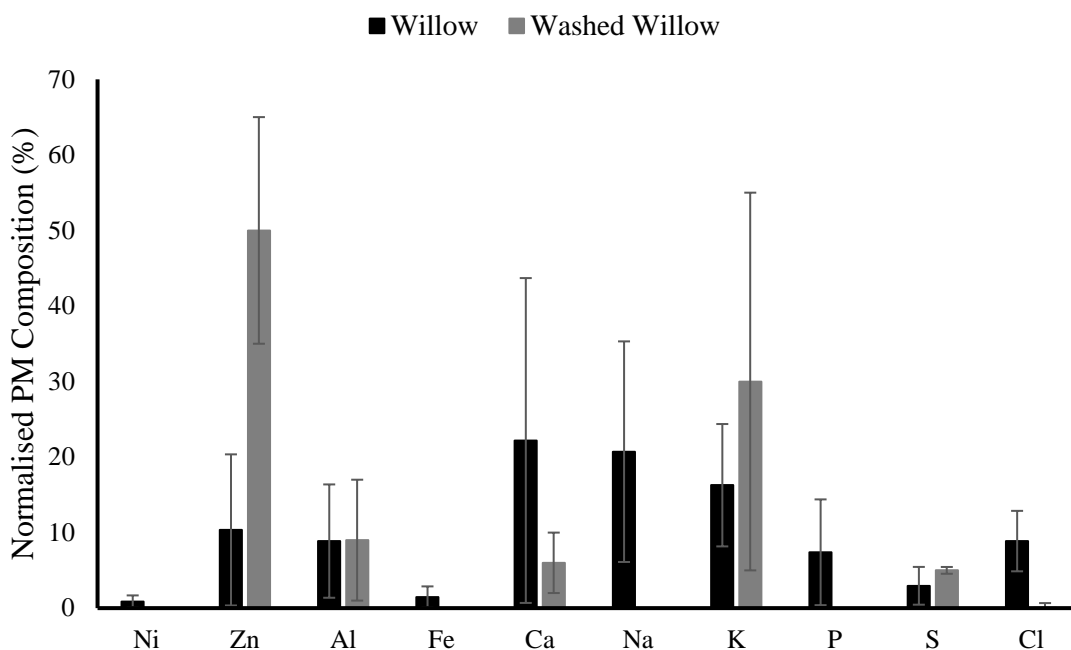
Figure 7.12: Average normalised inorganic PM composition. Estimation based on SEM-EDX analysis.

Based on Fig. 7.12 it is evident that certain ash species are not as prominent in the PM from combustion of the washed willow compared to the untreated willow. Ca is a low volatile metal that is stable in the ash, Fig. 2.7. Therefore, it is surprising that Ca is the most prominent inorganic species in the willow PM. Ca is present in the PM because of fine ash particles that fragment and are entrained into the flue gas coalescing/agglomerating with sticky soot and condensing volatile inorganics and metals. Once the willow is washed, 38.8% of the Ca is removed, Fig. 7.6. Based on the observation from Fig. 7.12, the Ca removed must be more involved in forming fine ash particles. Ca was removed from willow by both leaching and removal of fine material (dirt/bark) in even proportions, Fig. 7.5. Willow bark is typically very high in Ca [Vassilev et al., 2010] and it is therefore possible to speculate that the Ca removed is from bark and links to the formation of fine ash particles increasing the concentration of Ca in PM.

The concentration of Na is also less prominent in the washed willow PM. As a more volatile metal it is interesting that it is not detected in the PM. From Fig. 7.6, 30% of the Na in the fuel is removed which suggests that the remaining Na in the fuel is in complex ash/silica structures and is retained in the ash during combustion, discussed in the following section. A similar conclusion can be deduced for P.

In contrast to the aforementioned species, the concentration of Zn and K in the PM significantly increases for the combusted washed willow compared to the untreated. Zn and K are more volatile species which are expected to form in flyash from both entrained fine ash particles as well as volatile evaporation and condensation/sublimation. As seen in Table 7.2, the Zn concentration increases once the willow was washed (this was despite the detection of Zn in the leachate and fine material discussed in section 7.3.4). This could explain the observed increase in the PM. The K observation is more complex since K can form various volatile salts; KOH, KCl and K_2SO_4. Even though no Cl was detected in the fuel, it was evident from the leachate analysis, Table 7.6, that some was present in the original fuel. This Cl is present in the PM from the untreated willow but is almost completely removed in the washed willow PM. Had the Cl increased a correlation between the K and Cl would have explained the result. The only feasible change in the fuel composition, from Table 7.2, that could have aided the increased formation of K in the PM would be the reduction of Si; reduced formation of K-(Ca)-silicate. However, it is important to remember that the PM emission factor and thus mass of PM collected is significantly lower from washed willow combustion (0.063 kg GJ^{-1}) compared to the untreated (0.12 kg GJ^{-1})- Table 7.8. Therefore, the observed result could simply be the reduced concentration of other metals increases the proportion of K, i.e there was no change in the K volatility.

It should be noted that SEM-EDX is limited in its quantitative capabilities as shown by the error bars on Fig. 7.12. SEM-EDX is a very accurate technique at analysing surface elements however this analysis is for specific sites up to a maximum depth of 2µm. This limits what can be deduced from this data to obvious comparisons. However, combing the observations of the SEM-EDX with combustion data and the bottom ash analysis, in the following section, aids the understanding of the fate of certain species during stove combustion.

7.3.5.2 Bottom Ash Composition

Table 7.9 shows the bottom ash composition. For both the willow and washed willow, the inorganic composition is highest in Ca, followed by K, Si and P. This is the same observation as Schmitt and Kalschmitt [2013]. Based on Fig. 7.13, which is a mass balance on the stove system, any material not measured in the bottom ash can be assumed to be lost. Lost meaning the material has either been entrained in the flue

gas as fine ash particles or released from the fuel as volatile gases. From the composition of the bottom ash in Table 7.9 and the fuel composition in Table 7.2 the partitioning of specific ash species can be determined and thus their retention in the bottom ash, Table 7.10.

Table 7.9: Bottom ash composition

		Willow Bottom Ash	Washed Willow Bottom Ash
Concentration (mg kg^{-1} bottom ash db.)	Arsenic	0.8	0.6
	Cadmium	7.2	5
	Chromium	35.1	14.2
	Cobalt	6.8	5.8
	Copper	203	195
	Lead	7	4
	Nickel	65.6	64.1
	Zinc	3700	3500
	Silicon	57000	58000
	Aluminium	900	660
	Iron	1600	1300
	Calcium	130000	170000
	Magnesium	13000	14000
	Sodium	1700	1100
	Potassium	91000	91000
	Phosphorus	36000	40000
	Sulphur	6300	6200
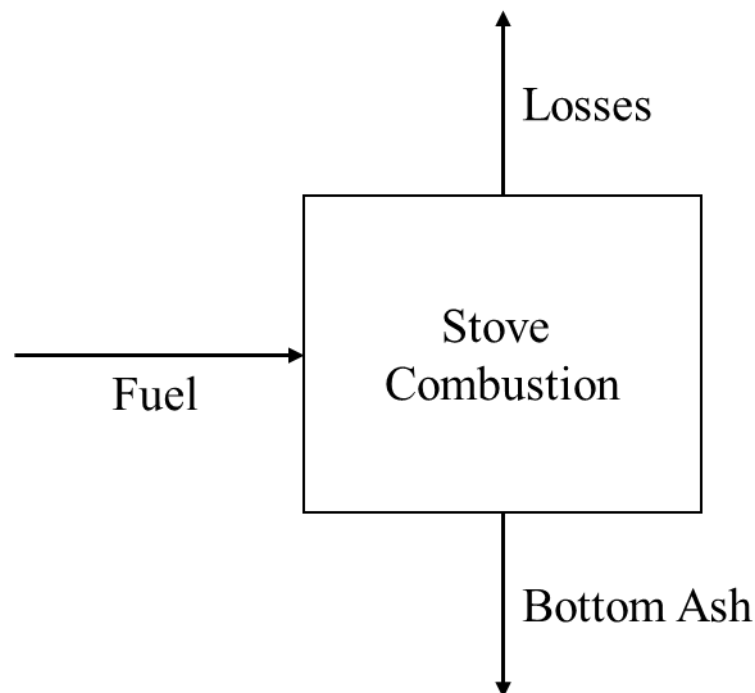
Figure 7.13: Stove Mass Balance

Table 7.10: Mass fractions for the retention of metal and inorganic species in the ash

Element	Willow Bottom Ash	Washed Willow Bottom Ash
Cadmium	0.19	0.08
Chromium	1.00	0.44
Cobalt	0.35	0.54
Copper	0.85	0.85
Lead	0.06	0.06
Zinc	0.95	0.61
Silicon	0.63	0.59
Aluminium	0.60	0.35
Iron	0.92	0.52
Calcium	0.84	0.98
Sodium	0.46	0.87
Potassium	0.84	0.84
Phosphorus	0.89	0.93
Sulphur	0.43	0.47

From Table 7.10, the retention of Pb, K, P, S, Cu, and Si is mostly unaffected by washing the willow; a difference of 0.05 or less. K and Na are considered similar ash forming species, however the retention of Na in the bottom ash of the washed willow is significantly higher (0.41) than in the untreated. This observation is analogous with the results from the SEM-EDX analysis which saw a greater proportion of Na in the willow PM. This suggests that washing removes the more mobile and reactive Na which is then not released into the flue gas.

Zn is also a more mobile ash species however conversely to Na, there is a reduced retention of Zn in the washed willow bottom ash (0.339). This is also in agreement with the SEM-EDX results. Previous work by Zając, Szyszlak-Bargłowicz and Szczepanik [2019] analysed the impact of combustion temperature on the release of Zn from various biomass fuels. In all the fuels, including willow, the amount of Zn retained in the bottom ash was significantly reduced as the temperature increased, especially in the low temperature range (500-600°C) [Zając, Szyszlak-Bargłowicz and Szczepanik, 2019]. From Fig. 7.7 the temperature profiles for the flue gas show that the washed willow releases more heat (peak temperature 640°C) compared to the untreated willow (510°C) and thus the observed result is mostly the effect of

temperature. The same result is seen for Cd, with a smaller magnitude, that is also observed in Zając, Szyszlak-Bargłowicz and Szczepanik [2019].

The Ca retention in the washed willow bottom ash was greater than the untreated willow. This was also analogous with the PM measurements. As discussed in the preceding section because Ca is a stable element its release would be by fragmentation of fine ash particles being entrained into the flue gas. The data from Table 7.10 and Fig. 7.10 suggests that any Ca removed by washing is involved in the formation of fine ash particles.

Conversely, Cr, Al and Fe, that are also stable metals, are retained significantly less in the bottom ash for the washed willow combustion compared to the untreated willow. This observation suggests that the washed willow forms more fine ash particles than the untreated willow and the fragmentation of these particles is increased. This could be linked to the increased combustion temperature inducing bigger temperature/pressure gradients increasing the rate of fragmentation. It could also be a result of changes in the microstructure of the willow chip after it is washed; a more porous structure. In both cases further work is needed to verify if these factors are influencing the retention of these stable metals in the bottom ash.

7.4 Conclusions

Washing willow is a process used to target ash removal, in this work a 28% removal efficiency was achieved. The greatest removal efficiencies of inorganic species were Pb (69%), S (55%), Cu (47.5%), K (42%) and Ca (38.8%). The general trend was that the removal efficiencies measured in this work were lower than those reported previously. This was from differences in the washing process, most notably the washing time, the use of acids and the process temperature. The lowest removal efficiencies were measured for Fe (16.4%), Zn (14.1%) and Ni (13.8%).

Removal from washing can be categorised into three groups: (i) removal by leaching (elements K, P, Zn and Na), (ii) by rinsing off debris (Si, Al and Pb) or (iii) a combination of both mechanisms. During washing the leachate acidifies because of the release of organic acids and the pH changes from 6.0-5.3. This increases the ability of elements such as Ca and Mg to leach; they are more difficult to leach because they are divalent ions. Ca removal by leaching (600 mg L^{-1}) is more effective in this work

compared to previously reported data from Werkelin et al. [2010]. This could be because more Ca in this work is present as CaC_2O_4, calcium oxalate, which is more soluble in water. However, more work would be required to confirm this.

The majority of past research has not considered the impact of removing debris by effective filtration. However, Gudka et al. [2016] showed that removal of debris, such as soil trapped in the biomass from harvesting, can result in large decreases in certain trace metals. Debris was collected from filtration and termed fine material in this work. The fine material was high in Ca (212 mg g^{-1}), S (22 mg g^{-1}) and Si (4.04 mg g^{-1}).

During combustion the washed willow fuel achieved higher peak burning rates (~5 kg h^{-1}), shorter characteristic batch combustion times (~20 mins) and hotter flue gas temperatures (>600°C). When new batches of fuel were reloaded, for both reloads of the willow fuel and for the first reload of the washed willow fuel, a new combustion phase was observed and it was termed 'pre-flaming smouldering.' During this phase, the flue gas temperature plateaued and a dense grey smoke persisted to form until the gaseous mix was flammable and a spark caused ignition. Emissions of CO and THC spiked during this phase whilst emissions of NOx and SO_2 were unaffected. Although the reduced K and volatile content would suggest that the washed willow will take longer to ignite, the increased energy content and homogeneity kept the stove hotter and increased the heating rate of the fuel which reduced the ignition delay time.

CO_2 emissions increased by 60% when the willow was washed. The reason for this is most likely from the increased flue gas temperatures of t he washed fuel which increases the rate of further oxidation of CO to CO_2. Emissions of CO are reduced by 50% for the washed willow and this was the same result reported by Ravichandran and Corscadden [2014] and Schmitt et al. [2018]. This is probably from the leaching of K, in particular in the form K_2CO_3, which slows the rate of gasification and decomposition of cellulose. This results in the reduction of CO emissions during the early stages of combustion.

NOx emissions increased by 25% after washing. Similar findings were observed when washing Chinese coals and were explained by large reductions in Na content. Na can catalyse NOx reduction reactions between NO and char to form N_2. This is most likely the observed result in this work (Na concentration decreased by

12.5% after washing). Emissions of SO_2 are reduced by 40% after washing. This was directly correlated to the reduction in fuel-S content.

PM emissions are reduced by 50% after washing and this was all at the sub-micron level. Reduced K, Cl, S, Si and Ca can all have a large impact on PM formation, the former two having the greatest impact in stove systems. Since the Cl content of the willow was already low and Cl has a high removal efficiency in water, K removal (42%) was considered the main factor in PM reduction. Reduced K can reduce soot formation by slowing the decomposition rate of cellulose and thus reducing the formation of PAHs from fuel rich "pockets" in the flue gas.

The composition of PM, analysed by SEM-EDX, increased in Zn and K, and decreased in Ca, Na and P when the willow was washed. Although the quantification of this analysis was limited by the use of SEM-EDX, it was useful for a comparison between the PM for the two fuels.

Bottom ash analysis was used to determine the fate of metals during combustion. The bottom ash composition was highest in Ca (willow 130 g kg^{-1} db. and washed willow 170 g kg^{-1} db.), K (91 g kg^{-1} db.), Si (57 g kg^{-1} db. and 58 g kg^{-1} db.) and P (36 g kg^{-1} db. And 40 g kg^{-1} db.). The same trend was observed for willow wood ash composition from an ashing oven in Schmitt and Kaltschmitt [2013].

Combining the combustion data, the SEM-EDX data and the bottom ash analysis willow washing has minimal effect on the fate of Pb, K, P, S, Cu, and Si. In the case of Na and Ca their partitioning favoured the bottom ash more after washing. The removal efficiency was relatively (30 and 38% respectively) and so it was concluded that the material removed must have been in structures that were more susceptible to be being vaporised or entrained into the flue gas. The biggest change in partitioning in the bottom ash was for Zn. After washing the partitioning decreased by 0.34 which explained the observed increase in its presence in the PM. Based on previous work this was most likely caused by the increase in the combustion temperature vaporising more Zn to the flue gas [Zając, Szyszlak-Bargłowicz and Szczepanik, 2019].

The desired outcome of this work was to use pre-treatment (washing) to convert an unusable biomass into a fuel that meets British Standards. Unfortunately, this objective was not met in the scope of this work and therefore may not warrant

further research. However, this work has demonstrated some potential in washing to improve the chemical properties of biomass. In order to demonstrate the value of washing pre-treatments more work is required with different types of fuels to see the removal efficiencies of specific elements- this way a more targeted approach can be used. Additionally, concerns over the financial implications of washing need to be addressed. In order to do that effective analysis of the increased product value in the domestic fuels market, considerations of legislation and the operational improvements (mitigation of slagging and fouling) need to be assessed.

Chapter 8. Conclusions and Future Work

8.1 Conclusions to Answer the Thesis Aims

The experiments in this work were focused on analysing the chemical composition and combustion properties of various traditional, novel and pre-treated biomass. These included five woody biomass, five agricultural residues, five torrefied biomass, three biogenic wastes and an energy crop. Combustion experiments were predominantly focused on the use of these fuels in domestic stoves since the emissions from these systems are an area of growing interest and environmental concern.

In order to address the research aims in section 1.5, Table 8.1 compares the emissions of the various fuels in this work compared to the 2022 EU Regulations for eco-stoves [2015]. It should be noted the stove used in the combustion experiments in this work was not an eco-stove. From Table 8.1 none of the fuels meet the CO standard which initially suggests that none of the fuels tested would be suitable for use in such devices. However, this standard is for emissions at the nominal thermal output of the stove used rather than an average across the combustion cycle.

The washed SRC, Chapter 7, was the closest to this standard. This was because the periods of flaming combustion were longer, providing sufficient energy for secondary reactions to convert CO to CO_2. The proportion of flaming combustion to smouldering combustion is the critical factor in the emissions of CO. Throughout this work various properties have influenced this including:

- The physical disintegration of the fuel. Fuels which break apart increase the surface area to volume ratio.
- The concentration of K in the fuel. K increases the rate of thermal decomposition.
- The moisture content of the fuel. Moisture in the flue gas reduces the temperature and flammability.

The first two properties control the rate of devolatilisation. Fuels that devolatilise too quickly, from the fuel physically or biochemically disintegrating too quickly, decrease the air-to-fuel ratio and prevent oxidation of CO. Conversely fuels that disintegrate, and thus devolatilise, too slowly don't sustain flaming combustion because the air-to-fuel ratio is too high.

Table 8.1: Comparison of emissions from the fuels tested in this work compared to the 2022 EU regulatory standard [2015]

Category	Fuel	Chapter	Form	CO (mg m^{-3})	Organic Gaseous C (mgC m^{-3})	NOx (mg m^{-3})	PM (g kg^{-1})	SO$_2$ (g kg^{-1})
				Emissions at 13% Oxygen				
EU regulation 2015/1185 DEFRA Limit	Any fuel except compressed wood	n/a		1500	120	200	2.4	n/a
Woods	Spruce	4	Logs	9100	420	100	3.9	0.36
	Willow (logs)	4		7000	260	180	6.1	0.39
	Wood Logs (Willow)	5		4600	230	140	3.9	n/a
	SRC Willow	7	Briquettes	8600	270	90	2.2	0.51
	Washed SRC Willow	7		3700	140	100	1.2	0.34
Agricultural Residue	Barley Straw (423)	6		8000	200	160	5	0.8
	Wheat Straw (093)	6		7700	110	150	6.4	0.5
	Brackettes	6		10000	420	300	3.9	1.6
Energy Crops	Miscanthus	6		8500	160	260	2.7	0.8
Biogenic Wastes	Olive	4		6600	135	160	5.8	0.95
	Coffee Logs	5		7300	300	300	7.1	n/a
	Wood Briquettes (sawdust)	6		9000	140	150	3	0.3
Thermally pre-treated	Torrefied Spruce	4		6000	350	60	1.9	0.32
	Torrefied Willow	4		6900	80	150	4.4	0.36
	Torrefied Olive	4		6000	100	130	4.2	0.58

Average margin of error based on a 95% confidence level is ±15%

Emissions of organic C are mostly as methane but also include formaldehyde, furan, propane, hexane, acetylene, ethane, ethylene, ethanol and benzene, all of which are measured by the FTIR. These species devolatilise directly from the fuel and develop/exit in fuel rich regions of the flue gas without being combusted. Again, similar to CO, the emissions of these species are depended on the air-to-fuel ratio which is linked to the decomposition rate and the presence of moisture. From Table 8.1, wheat straw, torrefied willow and torrefied olive are all within the limits of eco-stove combustion. This is important since it demonstrates that fuel properties can be tailored to achieve the same performance as eco-stoves with the advantage that they can be implemented without the large investment costs.

The chart shows the relationship between the C/H Atomic Ratio (x-axis, from 0.5 to 1.0) and the CH_4 Emission Factor (kg GJ^{-1}) (y-axis, from 0.00 to 0.35). Data points are labelled: Coffee Logs, Wood Logs, Willow Logs, SRC Willow, Miscanthus, Barley Straw, Washed SRC Willow, Wood Briq., Wheat Straw, Olive, Torrefied Willow. The trendline equation is:

$$y = 4.5769x^2 - 7.4769x + 3.0786$$
$$R^2 = 0.7448$$
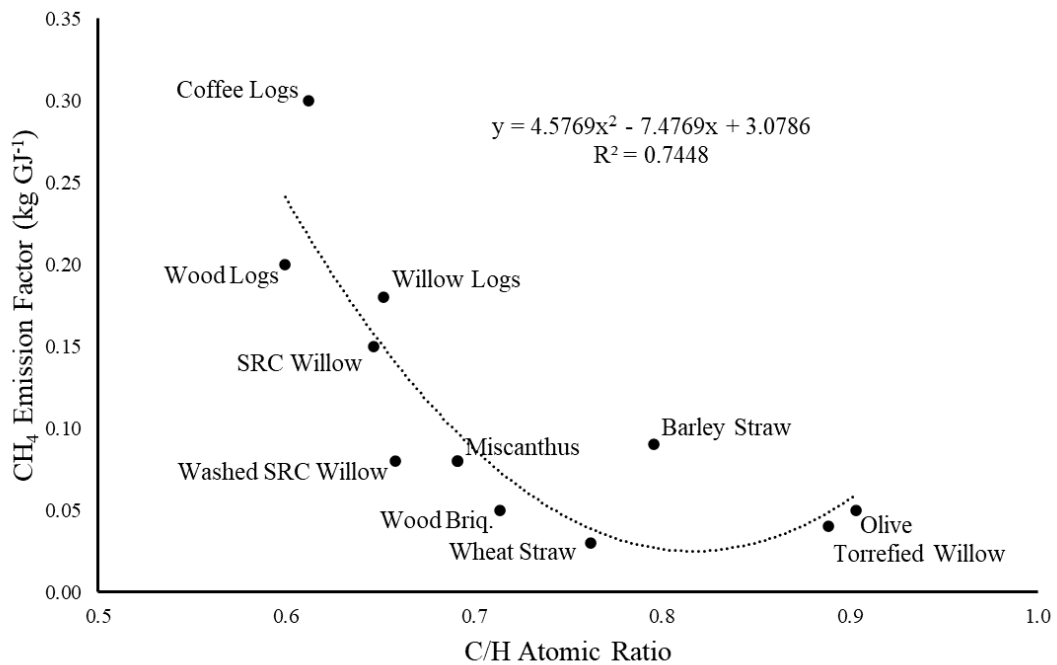
Figure 8.1: Relationship between the C/H ratio and the CH$_4$ emissions

Existing work by Ndiema, Mpendazoe and Williams [2010] demonstrated that fuels with increased aromaticity (C/H atomic ratio) can have lower CH_4 emissions because of a decrease in the thermal decomposition and gasification reactions which dictate the production of CH_4, Eq. 4.1-4.3. This was demonstrated in Figs. 4.9 and 5.5 by comparing the data in those chapters and using a single point from Mitchell et al. [2016]. However, by using only the data within this thesis excluding the fuels where physical disintegration was the determining factor (spruce, torrefied spruce and bracken), Fig. 8.1 shows a reasonable correlation (R^2=0.7448) between the two

parameters. This is not a definitive and there is still a significant influence from other variables, such as the rate of decomposition, however it does suggest that a reasonable prediction of the CH_4 emissions can be obtained from the C/H atomic ratio.

The NOx emissions from all of the fuels except for the brackettes, the coffee logs and the miscanthus were below the limit. Throughout this thesis NOx emissions were correlated to the fuel-N content, Fig. 8.2. It is clear that this trend is well established as is this case in previous work [Mitchell et al. [2016]. However, some new properties were found to have an impact on the NOx emissions particularly for the pre-treated fuels; these included:

- Torrefying biomass increases the char produced during combustion and binds N into the char matrix more tightly, e.g in the form of pyrroles and pyridinic-N rather than amine-type functionalities. N was therefore released during reducing conditions promoting the formation of N_2 instead of NOx.
- Washing biomass can remove Na. Na catalyses the NO+C reduction reactions to form N_2.
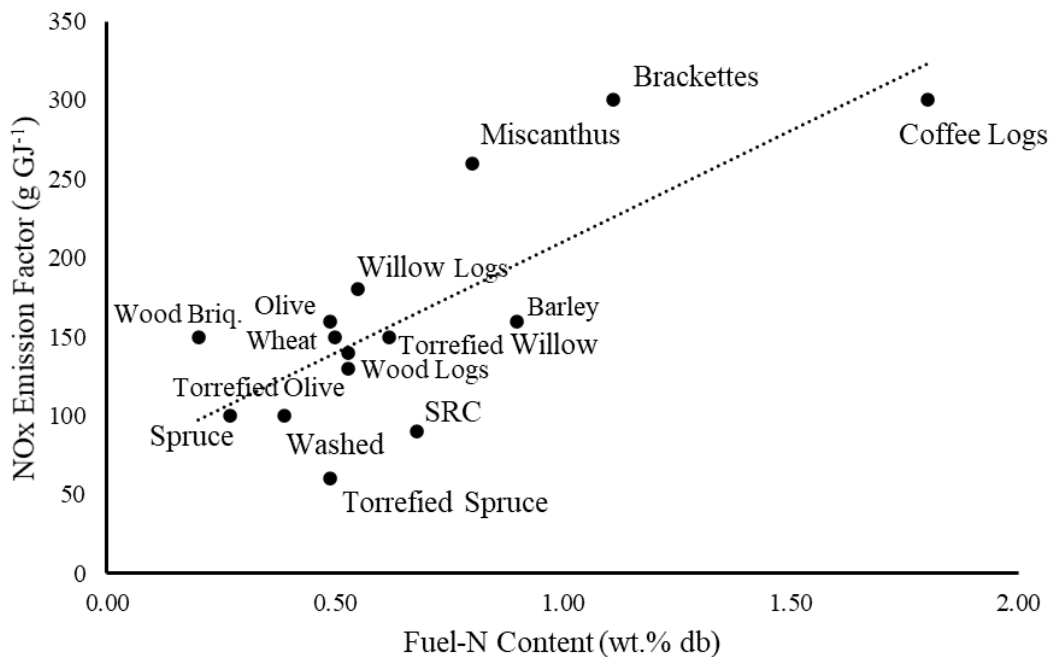
Figure 8.2: NOx emissions versus fuel-N content

Although there is no specified limit on the SO_2 emissions, there was significant analysis on them throughout this thesis. The main observation was the correlation between fuel-S content and the emissions of SO_2, Fig. 8.3. There is a strong

relationship between the two parameters however it is important to recognise that S is present in many various forms. At low temperatures only the organically bound S is released, this can be between 50% to as little as 20% of the fuel-S content as shown in Fig. 4.12. The concentration of minerals such as Ca and K can prevent the release of S during combustion by reacting to form salts that stay in the bottom ash. Fig. 8.4 shows the relationship between the ratio of Ca/S and the emissions of SO_2. It is clear that there is a relationship between these two variables. However more data is required at below a ratio of 3 to establish if this trend is universally applicable.
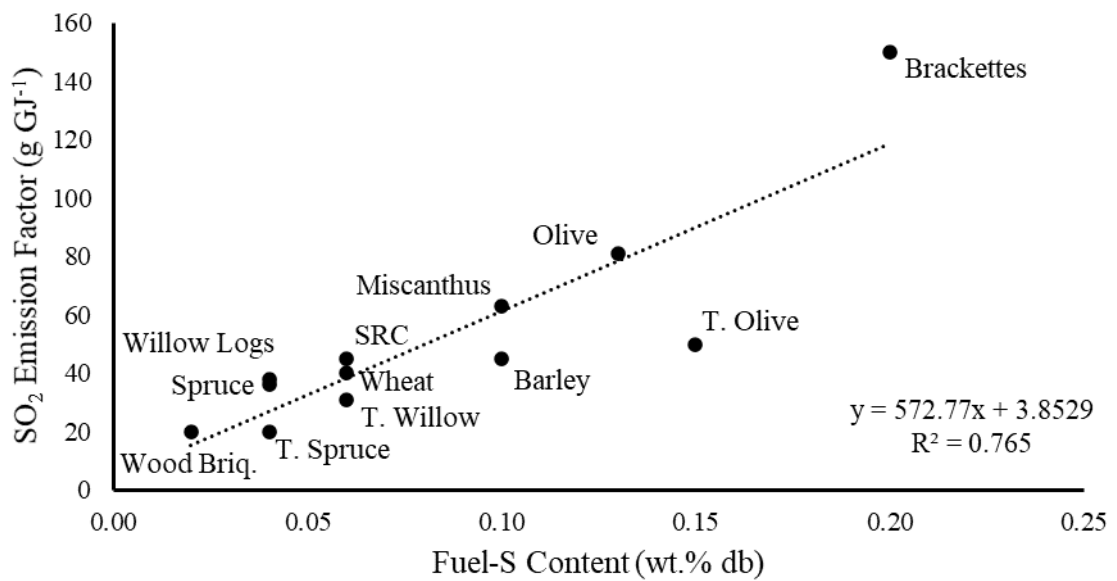
Figure 8.3: Correlation between the fuel-S content and the emissions of SO$_2$
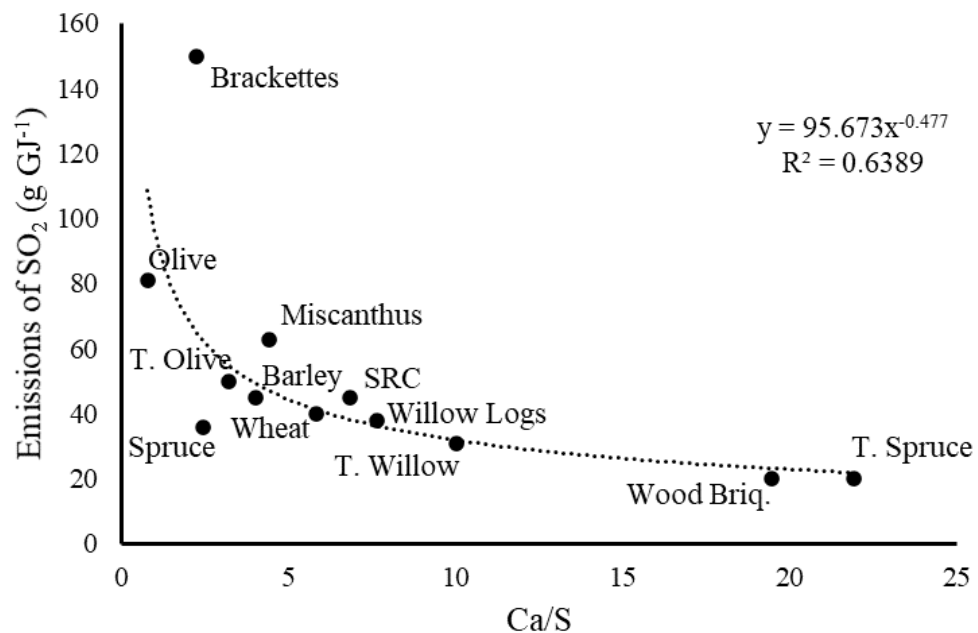
Figure 8.4: Correlation between the mass ratio of Ca/S and the emissions of SO$_2$

The final conclusion from this thesis is the relationship between fuel properties and the PM emissions. It is important to remember that PM is a combination of soot, tar, char fragments and fly ash. Based on these properties, Figs. 8.5 and 8.6 show the correlation between the PM emissions and the C/O ratio and the K content. This is because the C/O ratio is the property associated with the formation of soot and tar whilst K is the most influential mineral in the formation of condensable vaporised salts. There is a trend between the C/O ratio and the PM emissions for all the fuels, with the exception of the torrefied fuels. As described in Chapter 7, section 7.3.5, the mineral content of biomass PM is very varied and no single species dominates over 50% of the composition, Fig. 7.11. Additionally, from Tables 7.9 and 7.10 of the K in the fuel only 16% is released during stove combustion.
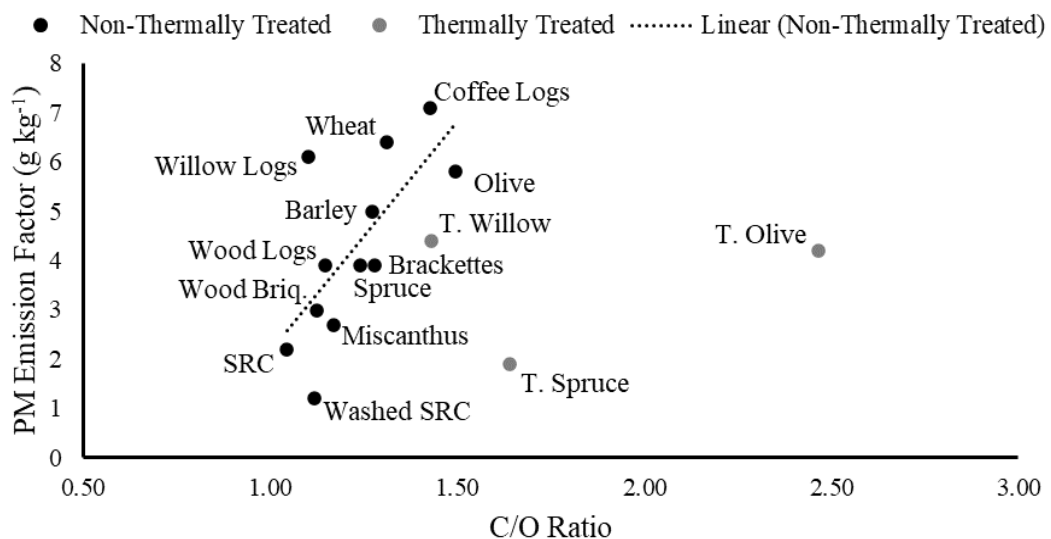
Figure 8.5: Correlation between PM emissions and C/O ratio

The 2022 emissions limits from Table 8.1 show that the future of stove combustion, as is currently the case with other combustion utilities, will be subject to tougher standards. However, there is an over emphasis on stove technology and the progress that can be made because it is evident in this thesis that fuel chemical and physical properties are as influential. Fuel physical properties are also very important and they can be modified by simple changes in the processing operations. The chemical properties are more complex and present a greater challenge when considering future fuels. Pre-treatment has demonstrated many advantages, improving

heat release, combustion efficiency and most emissions by changing the physical and chemical properties, however they are currently underutilised.
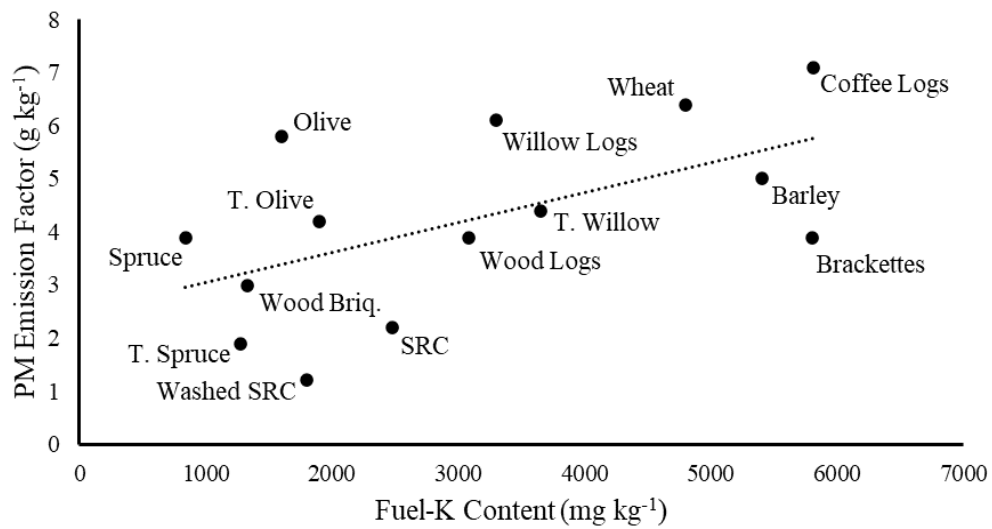
Figure 8.6: Correlation between the fuel-K content and the PM emissions

8.2 How can this Thesis be Applied to the Energy and Fuels Industry?

As the world transitions from fossil fuels the need for diverse sources of biomass is becoming more apparent. The sustainability of expanding the use of wood pellets is being questioned [Gatten, 2021] and energy from biogenic waste is increasing. In this thesis it is apparent that agricultural waste (straws and bracken) and biogenic waste from food and timber residue (olive, coffee and sawdust) have a suitable energy content, between 19-21 MJ kg^{-1}, to be used in various combustion devices. There are some concerns over the fuel-N and S content, however in large scale utilities these can easily be addressed with abatement technology.

This thesis has also demonstrated that pre-treatment can offer many advantages to the energy and fuels industry. Washed fuels can reduce the inorganic and mineral content of biomass and thus reduce emissions of SO_2 and PM. Thermally treated fuels have already demonstrated advantages of increased energy release however from this thesis it can also be connected to reduced emissions of unburnt hydrocarbons, NOx, SO_2 and soot. Pre-treatment is not just limited to its advantages in combustion but also increasing the diversity of biomass sources and homogenising the composition of mixed biomass.

The work in this thesis has been focused on combustion in domestic stoves however producing premium fuels by washing could mitigate problems from ash and so improve plant availability as well as emissions. In both cases fuel users may not be willing to source these more expensive fuels. Policy measures may be necessary to promote this approach, but more evidence is required to make a compelling case.

Stove combustion is an area of research that requires more work. There is significant evidence that suggests the reduction in air quality is from stove systems and there is increasing concern over the long-term impacts to health. This thesis has increased the understanding of how emissions relate to the chemical and physical properties of the fuels. This understanding will aid future decisions on the fuels suitable for application in these systems and start to encourage the use of premium fuels that are pre-treated to protect people's health.

8.3 Future Work

8.3.1 Validation and Refinement of Empirical Correlations

Throughout this thesis there is substantial evidence that connects the chemical composition of fuels to the associated emissions. This data could be expanded further to use the correlations within this thesis and develop equations that could be applied universally to predict the emissions before a fuel is used in a stove type system. These models/equations should focus on the relationship of aromaticity (C/H ratio) to CH_4 emissions, fuel-N content to the NOx emissions, fuel-S and Ca content to the SO_2 emissions or the amount of S converted, and the C/O ratio and ash compositions to the emissions of PM. There are some additional elements of interest and further experimental work is required to establish their impact on these emissions particularly Zn which was measured as the most prominent species in sub-micron PM when the alkali and alkaline metal concentration of the biomass is reduced.

8.3.2 Washing Pre-treatment

Within this work washing was demonstrated to have a significant impact on the mineral content of SRC willow. However, further experimental work on the scalability and robustness of washing operations are required to establish if this is a feasible technological solution to the mineral problems with biomass. This experimental work needs to focus on the different parameters such as temperature,

mechanical action, washing medium and filtration and their impact on the removal efficiency. It is clear from this thesis that an optimal fuel quality could be established for particular combustion devices and therefore how can pre-treatment reproducibly achieve these properties is the ultimate goal of any pre-treatment experiments.

A large body of research would be required to allow full technoeconomic and environmental performance modelling of washing pre-treatment as an approach to help tackle emissions at the smaller scale and also improve plant performance at the larger scale.

8.3.3 Process Integration

Combined cycle operations and increased integration of processes is designed to improve operation efficiency and reduce waste energy and material. Based on the work in this thesis the uptake of pre-treated fuels will help improve operational efficiency and reduce emissions, however there are concerns over the economics of washing, in particular the use of water and the cleaning processes required before it can be discharged, and its effectiveness at large-scale throughputs. By combining torrefaction and washing, the warm organic acids produced from torrefaction could be used to wash the biomass and help remove more stable minerals such as Ca. The leachate produce from washing is high in organic carbon which could be used in anaerobic digestion. Further research into these technologies and the process economics could promote the use of pre-treated fuels.

8.3.4 Alternative Fuels

Novel fuels such as spent coffee and bracken have provided interesting alternatives in stove combustion systems. However, at present these are not suitable for use based on their emissions. Since these fuels are currently exempt from the recent legislation on suitable fuels for use in domestic stoves, further research could be added to the work in this thesis to understand their behaviour and optimise manufacturing to improve their performance. Alternatively, application of these fuels in alternative conversion methods or their use as additives or soil conditioners merits further research.

References

Abanades, S, Flamant, G, Gagnepain, B, and Gauthier, D. 2002. Fate of heavy metals during municipal solid waste incineration. *Waste Management and Research.* **20**, pp. 55-68.

Abelha, P, Janssen, A, Mourão Vilela, C, Nanou, P, Carbo, M. 2018. Low-grade biomass upgrading by washing and torrefaction: lab and pilot-scale results. In: *26th European Biomass Conference and Exhibition*, [Online] 14-17 May, Copenhagen, Denmark (3DV.6.3), pp. 1209-1220.

Abelha, P, Mourão Vilela, C, Nanou, P, Carbo, M, Janssen, A, and Leiser, S. 2019. Combustion improvements of upgraded biomass by washing and torrefaction. *Fuel.* **253**, pp. 1018-1033.

Agency for Toxic Substances and Disease Registry. 2007. *Public Health Statement for Benzene.* [Online]. [Date Accessed: 28/12/2020]. Available from: https://www.atsdr.cdc.gov/phs/phs.

Akinrinola, F.S. 2014. *Torrefaction and Combustion Properties of some Nigerian Biomass.* Ph.D. thesis, University of Leeds

Al Mami, M, Lajili, M, Khiari, B, and Jeguirim, M. 2020. Combustion of raw and densified Tunisian oleic by-products in a fixed bed reactor. *Fuel.* **277**.

An Experimental Assessment of Native and Naturalized Species of Plants as Renewable Sources of Energy in Great Britain, EUR (1985) 10013 EN, final. [Online]. [Accessed: 09/02/2020]. Available From: http://aei.pitt.edu/44135/1/A7028.pdf

Arellano, O, Flores, M, Guerra, J, Hidalgo, A, Rojas, D, and Strubinger, A. 2016. Hydrothermal Carbonization of Corncob and Characterization of the Obtained Hydrochar. *Chemical Engineering Transactions.* **50**, pp. 235-240.

Arnold, T, Harth, C.M, Mühle, J, Manning, A.J, Salameh, P.K, Kim, J, Ivy, D.J, Steele, L.P, Petrenko, V.V, Severinghaus, J.P, Baggenstos, D, Weiss, R.F. 2013. Nitrogen trifluoride global emissions estimated from updated atmospheric measurements. *Earth, Atmospheric and Planetary Sciences.* **110**(6), pp. 2029-2034.

Asif, M. 2009. 2- Sustainability of timber, wood and bamboo in construction. *Sustainability of Construction Materials.* Woodhead Publishing: Cambridge, pp. 31-54. AHDB. 2018. *Barley Growth Guide.* [Online]. AHDB Cereals and Oils: Kenilworth. [Date Accessed: 01/05/2020]. Available from: https://projectblue.blob.core.windows.net/media/Default/Imported%20Publication%20Docs/Barley%20growth%20guide%20130718.pdf

Atiku, F.A, Lea-Langton, A.R, Bartle, K.D, Jones, J.M, Williams, A, Burns, I, and Humphries, G. 2017. Some aspects of the mechanisms of formation of smoke from combustion of wood. *Energy and Fuels.* **31**(2), pp. 1935-1944.

Atiku, F.A, Mitchell, E.J.S, Lea-Langton, A.R, Jones, J.M, Williams, A, and Bartle, K.D. 2016. The impact of fuel properties on the composition of soot produced by the combustion of residential solid fuels in a domestic stove. *Fuel Processing Technology.* **151**, pp. 117-125.

Backman, R. Khalil, R.A. Todorovic, D. Skreiberg, O. Becidan, M. Goile, F. Skreiberg, A. and Sorum, L. 2013. The effect of peat ash addition to demolition wood on the formation of alkali, lead and zinc compounds at staged combustion conditions. *Fuel Processing Technology.* **105**, pp. 20-27.

Backreedy, R.I, Jones, J.M, Pourkashanian, M, and Williams, A. 2002. Modelling the reaction of oxygen with coal and biomass chars. *Proceedings of the Combustion Institute.* **29**(1), pp. 415-421.

Bai, F-W, Yang, S, and Ho, N.W.Y. 2019. 3.05- Fuel ethanol production from lignocellulosic biomass. *Life Sciences: Comprehensive Biotechnology.* **3**(3), pp. 49-65.

Bandara, Y.W, Gamage, P, Gunrathne, D.S. 2020. Hot water washing of rice husks for ash removal: The effect of washing temperature, washing time and particle size. *Renewable Energy.* **153**, pp. 646-652.

Barbosa, B, Boléo, S, Sidella, S, Costa, J, Duarte, M.P, Mendes, B, Cosentino, S.L, and Fernando, A.L. 2015. Phytoremediation of Heavy Metal-Contaminated Soils Using the Perennial Energy Crops *Miscanthus* spp. And *Arundo donax* L. *Bioenergy Research.* **8**, pp. 1500-1511.

Baxter, L.L. 1993. Ash deposition during coal and biomass combustion: A mechanistic approach. *Biomass and Bioenergy.* **4**, pp. 85-102.

Baxter, X.C, Darvell, L.I, Jones, J.M, Barraclough, T, Yates, N.E, and Shield, I. 2012. Study of Miscanthus x giganteus ash composition- Variation with agronomy and assessment method. *Journal of Fuel.* **95**, pp. 50-62.

Berrueco, C, Montané, D, Matas Güell, B, and del Alamo, G. 2014. Effect of temperature and dolomite on tar formation during gasification of torrefied biomass in a pressurized fluidized bed. *Energy.* **66**, pp. 849-859.

Bertrand, A, Stefenelli, G, Bruns, E.A, Pieber, S.M, Temime-Roussel, B, Slowik, J.G, Prévot, A.S.H, Wortham, H, El Haddad, I, and Marchand, N. 2017. Primary emissions and secondary aerosol production potential from woodstoves for residential heating: Influence of the stove technology and combustion efficiency. *Atmospheric Environment.* **169**, pp 65-79.

Birley, R.I, Jones, J.M, Darvell, L.I, Williams, A, Waldron, D.J, Levendis, Y.A, Rokni, E, and Panahi, A. 2019. Fuel flexible power stations: Utilisation of ash co-products as additives for NOx emissions control. *Fuel.* **251**, pp. 800-807.

Blanquet, E, Nahil, M.A, and Williams, P.T. 2019. Enhanced hydrogen-rich gas production from waste biomass using pyrolysis with non-thermal plasma-catalysis. *Catalysis Today.* **337**, pp. 216-224.

Boateng, A, and Mullen, C. 2013. Fast pyrolysis of biomass thermally pretreated by torrefaction. *Analytical and Applied Pyrolysis.* **100**, pp. 95-102.

Bølling, A.K, Pagels, J, Yttri, K.E, Barregard, L, Sallsten, G, Schwarze, P.E, and Boman, C. 2009. Health effects of residential wood smoke particles: the importance of combustion conditions and physicochemical particle properties. *Particle Fibre Toxicology.* **6** (29), pp. 1-20.

Bostrom, D, Skoglund, N, Grimm, A, Boman, C, Öhman, M, Bostrom, M, and Backman, R. 2012. Ash Transformation Chemistry During Combustion of Biomass. *Journal of Energy and Fuels.* **26** (1), pp. 85-93.

Bowe, A. No Date. *All about ferns: A resource guide.* [Leaflet]. Botanical Society: North America. [Date accessed: 01/05/2020]. Available from: https://cpb-us-e1.wpmucdn.com/blogs.cornell.edu/dist/7/3643/files/2013/09/Fern-Guide-27sra8m.pdf

BP. 2019. *BP Statistical Review of World Energy.* [Online]. 68th Edition. BP. [Date Accessed: 23/12/2020]. Available from:
https://www.bp.com/content/dam/bp/business-sites/en/global/corporate/pdfs/energy-economics/statistical-review/bp-stats-review-2019-full-report.pdf

BP. 2020. *BP Statistical Review of World Energy.* [Online]. 69th Edition. BP. [Date Accessed: 23/12/2020]. Available from:
https://www.bp.com/content/dam/bp/business-sites/en/global/corporate/pdfs/energy-economics/statistical-review/bp-stats-review-2020-full-report.pdf

Bradl, H.B. 2005. *Heavy Metals in the Environment: Origin, Interactions and Remediation.* 1st Edition. Cambridge: Academic Press.

Brandt-Talbot, A, Gschwend, F.J.V, Fennell, P.S, Lammens, T.M, Tan, B, Weale, J, and Hallett, J.P. 2017. An economically viable ionic liquid for the fractionation of lignocellulosic biomass. *Green Chemistry.* **19**, pp. 3078-3102.

Breeze, P. 2014. *Power Generation Technologies.* 2nd Edition. Oxford: Elsevier.

Břendová, K, Kubátová, P, Száková, J, and Tlustoš, P. 2018. Trace element leaching from contaminated willow and poplar biomass- A laboratory study of potential risks. *Biomass and Bioenergy*. **112**, pp. 11-18.

Bridgeman, T.G, Jones, J.M, Shield, I, and Williams, P.T. 2008. Torrefaction of reed canary grass, wheat straw and willow to enhance solid fuel qualities and combustion properties. *Fuel*. **87**, pp. 844-856.

Bridgeman, T.G., J.M. Jones, A. Williams, and D.J. Waldron. 2010. An investigation of the grindability of two torrefied energy crops. *Fuel.* **89**(12), pp. 3911-3918.

Bridgewater. A.N. No date. *Neil's Local History and Mining Site: The Renishaw Colliery.* [Online]. [Date Accessed: 06/04/2021]. Available from: https://www.oldminer.co.uk/renishaw.html

British Standards Institute. 2014. BS EN ISO 17225-1:2014. *Solid Biofuels- Fuel specifications and classes; Part 1: General requirements.* Brussels: CEN.

British Standards Institute. 2014. BS EN ISO 17225-2:2014. *Solid Biofuels- Fuel specifications and classes; Part 2: Graded wood pellets.* Brussels: CEN.

British Standards Institute. 2014. BS EN ISO 17225-3:2014. *Solid Biofuels- Fuel specifications and classes; Part 3: Graded wood briquettes.* Brussels: CEN.

British Standards Institute. 2014. BS EN ISO 17225-4:2014. *Solid Biofuels- Fuel specifications and classes; Part 4: Graded wood chips.* Brussels: CEN.

British Standards Institute. 2014. BS EN ISO 17225-5:2014. *Solid Biofuels- Fuel specifications and classes; Part 5: Graded firewood.* Brussels: CEN.

British Standards Institute. 2014. BS EN ISO 17225-6:2014. *Solid Biofuels- Fuel specifications and classes; Part 6: Graded non-woody pellets.* Brussels: CEN.

British Standards Institute. 2014. BS EN ISO 17225-7:2014. *Solid Biofuels- Fuel specifications and classes; Part 7: Graded non-woody briquettes.* Brussels: CEN.

British Standards Institute. 2020. BS EN ISO 21404:2020. *Solid Biofuels: Determination of ash melting behaviour.* Brussels: CEN.

Brown, R.C. 2003. Biorenewable Resources: Engineering New Products from Agriculture. *Ames, Iowa State Press.*

Brunner, G. 2014. Chapter 8- Processing of biomass with hydrothermal and supercritical water. *Supercritical Fluid Science and Technology.* **5**. Elsevier: Amsterdam, pp. 395-509.

Bryers, R.W. 1996. Fireside slagging, fouling, and high-temperature corrosion of heat transfer surfaces due to impurities in steam-raising fuels. *Progress in Energy and Combustion Science*. **22** (1), pp. 29-120.

(Department for) Business, Energy and Industrial Strategy. 2018. *Clean Growth-Transforming Heating.* [Online]. London: Office for National Statistics. Available from: https://assets.publishing.service.gov.uk/government/uploads/system/uploads/attachment_data/file/766109/decarbonising-heating.pdf

(Department for) Business, Energy and Industrial Strategy. 2020. *UK Energy in Brief 2020.* [Online]. London: Office for National Statistics. Available from: https://assets.publishing.service.gov.uk/government/uploads/system/uploads/attachment_data/file/904503/UK_Energy_in_Brief_2020.pdf

Carillo, M.A, Staggenborg, S.A, and Pineda, J.A. 2014. Washing sorghum biomass with water to improve its quality for combustion. *Fuel*. **116**, pp. 427-431.

Callaghan, T.V, Scott, R, and Whittaker, H.A. 1981. *The yield development and chemical composition of some fast growing indigenous and naturalised British plant species in relation to management as energy crops*. [Online]. Report to the UK Department of Energy. Cambridge: Institute of Terrestrial Ecology. [Accessed 11/02/2020]. Available From: http://nora.nerc.ac.uk/id/eprint/8196/1/Project640.pdf

Cao, X.D, Ma, L.Q, Chen, M, Singh, S.P, and Harris, W.G. 2002. Impacts of phosphate amendments on lead biogeochemistry at a contaminated site. *Environmental Science and Technology*. **36**: pp. 5296–5304.

Cao, X.D, Ma, L.Q, Singh, S.P, and Zhou, Q. 2008. Phosphate-induced lead immobilization from different lead minerals in soils under varying pH conditions. *Environmental Pollution*. **152**: pp. 184–192.

Caposciutti, G, Barontini, F, Galletti, C, Antonelli, M, Tognotti, L, and Desideri, U. 2020. Woodchip size effect on combustion temperatures and volatiles in a small-scale fixed bed biomass boiler. *Renewable Energy*. **151**, pp. 161-174.

Caposciutti, G, Baccioli, A, Ferrari, L, and Desideri, U. 2020. Biogas from anaerobic digestion: Power generation or biomethane production? *Energies*. **13**(3), pp. 743-758.

Centre for Disease Control and Prevention. 2019. *Air Quality: Air Pollutants.* [Online]. [Date Accessed: 28/12/2020]. Available from: https://www.cdc.gov/air/pollutants.htm

Chartered Institute for Waste Management (CIWM). 2003. *Agricultural Wastes Survey* [Online]. [Accessed: 11/02/2020]. Available From: https://www.ciwm.co.uk

Chen, H, Chen, X, Qin, Y, Wei, J, and Liu, H. 2017. Effect of torrefaction on the properties of rice straw high temperature pyrolysis char: Pore structure, aromaticity and gasification activity. *Bioresource Technology*. **228**, pp. 241-249.

Chen, L-W. A, Verburg, P, Shackelford, A, Zhu, D, Susfalk, R, Chow, J.C, and Watson, J.G. 2010. Moisture effects on carbon and nitrogen emission from burning of wildland biomass. *Atmospheric Chemistry and Physics.* **10**, pp. 6617-6625.

Chen, W, He, Z.L, Yang, X.E, Mishra, S, and Stoffella, P.J. 2010. Chlorine nutrition of higher plants: Progress and perspectives. *Plant Nutrition.* **33**(7), pp. 943-952.

Chen, W-H, Lin, B-J, Lin, Y-Y, Chu, Y-S, Ubando, A.T, Show, P.L, Ong, H.C, Chang, J-S, Ho, S-H, Culaba, A.B, Pétrissans, A, and Pétrissans, M. 2021. Progress in biomass torrefaction: Principles, applications and challenges. *Progress in energy and combustion science.* **82**.

Chen, Z, Wang, M, Jiang, E, Wang, D, Zhang, K, Ren, Y, and Jiang, Y. 2018. Pyrolysis of torrefied biomass. *Trends in Biotechnology.* **36**(12), pp. 1287-1298.

Chigbo, C, Batty, L, and Bartlett, R. 2013. Interactions of copper and pyrene on phytoremediation potential of *Brassica juncea* in copper-pyrene co-contaminated soil. *Journal of Chemosphere.* **90** (10), pp. 2542-2548.

Chin, Y.S, Darvell, L.I, Lea-Langton, A.R, Jones, J.M, and Williams, A. 2016. Ignition risks of biomass dust on hot surfaces. *Energy and Fuels.* **30**(6), pp. 4398-4404.

Chin, K.L, H'ng, P.S., Paridah, M.T., Szymona, K., Maminski, M., Lee, S.H, Lum, W.C., Nurliyana, M.Y., Chow, M.J., and Go, W.Z. 2015. Reducing ash related operation problems of fast growing timber species and oil palm biomass for combustion applications using leaching techniques. *J. Energy.* **90**: pp. 622-630.

Chio, C, Sain, M, and Qin, W. 2019. Lignin utilization: A review of lignin depolymerization from various aspects. *Renewable and Sustainable Energy Reviews.* **107**, pp. 232-249.

Choi, H, Harrison, R, Komulainen, H, and Delgado Saborit, J.M. 2010. Polycyclic aromatic hydrocarbons. *WHO Guidelines for Indoor Air Quality: Selected Pollutants.* [Online]. Geneva: World Health Organisation. [Date Accessed: 28/12/2020]. Available from: https://www.ncbi.nlm.nih.gov/books/NBK138709/.

Clarke, L.B and Sloss, L.L. 1992. Trace Elements- Emissions from coal combustion and gasification. *IEA Coal Research Report.*

Clean Heat. 2016. *Residential wood burning: Environment impact and sustainable solutions.* [Online]. Deutche Umwelthilfe: Berlin. [Date Accessed: 01/01/2021]. Available from: file:/C:/Users/Downloads/cleanheat_background_paper_english.pdf

Clery, D.S, Mason, P.E, Rayner, C.M, and Jones, J.M. 2018. The effects of an additive on the release of potassium in biomass combustion. *Journal of Fuel.* **214**, pp. 647-655.

Committee on Climate Change. 2019. *Reducing UK emissions: 2019 Progress Report to Parliament.* [Online]. [Date Accessed: 30/12/2020]. Available from: https://www.theccc.org.uk/wp-content/uploads/2019/07/CCC-2019-Progress-in-reducing-UK-emissions.pdf

C2ES. No Date. *Technology Solutions: Electricity: Renewable Energy.* [Online]. C2ES: Arlington County. [Date Accessed: 31/12//2020]. Available from: https://www.c2es.org/content/renewable-energy

Darvell, L.I, Brindley, C, Baxter, X.C, Jones, J.M, and Williams, A. 2012. Nitrogen in biomass char and its fate during combustion: A model compound approach. *Energy and Fuels.* **26**, pp. 6482-6491.

Darvell, L.I, Jones, J.M, Gudka, B, Baxter, X.C, Saddawi, A, Willias, A, and Malmgren, A. 2010. Combustion properties of some power station biomass fuels. *Fuels.* **89**, pp. 2881-2890.

DEFRA. 2014. *Water Framework Directive implementation in England and Wales: new and updated standards to protect the water environment.* [Online]. 1st Edition. London: Open Government License. [Date accessed: 20.11.2020]. Available from: https://www.gov.uk/government/publications

DEFRA. 2019. *Crops grown for bioenergy in the UK: 2018.* [Online]. Government Publishing: London. [Date accessed: 01/05/2020]. Available from: https://assets.publishing.service.gov.uk/government/uploads/system/uploads/attachment_data/file/856695/nonfood-statsnotice2018-08jan20.pdf

DEFRA. 2019. *Farming Statistics Land Use, Livestock Populations and Agricultural Workforce At 1 June 2019 – England.* [Online]. Government Publishing: London. [Date accessed: 01/05/2020]. Available from: https://assets.publishing.service.gov.uk/government/uploads/system/uploads/attachment_data/file/868945/structure-jun19-eng-28feb20.pdf

DEFRA. 2020. *Reducing air pollution from domestic burning.* [Online]. Government Publishing: London. [Date Accessed: /04/2021]. Available from: https://deframedia.blog.gov.uk/2020/02/22/reducing-air-pollution-from-domestic-burning/

Dell'Antonia, D, Gubiani, R, Maroncelli, D, and Pergher, G. 2012. Gaseous emissions from fossil fuels and biomass combustion in small heating appliances. *Agricultural Engineering.* **41**(4), pp. 37-46.

Deng, L, Zhang, T, Che, D. 2013. Effect of water washing on fuel properties, pyrolysis and combustion characteristics, and ash fusibility of biomass. *Fuel Processing Technology.* **106**, pp. 712-720.

Deng, S, Wang, X, Zhang, J, Liu, Z, Mikulčić, H, Vujanović, M, Tan, H, and Duić, N. 2018. A kinetic study on the catalysis of KCl, K_2SO_4 and K_2CO_3 during oxy-biomass combustion. *Environmental Management.* **218**, pp. 50-58.

Department for Business, Energy and Industrial Strategy (BEIS) National Statistics. 2019. *UK Energy Statistics, Q1 2019* [Press Release]. [Accessed: 11/02/2020]. Available From: https://assets.publishing.service.gov.uk

Department for Environment, Food and Rural Affairs. No Date. *Causes of air pollution.* [Online]. [Date Accessed: 28/12/2020]. Available from: https://uk-air.defra.gov.uk/air-pollution/causes

Department for Environment, Food and Rural Affairs. 2007. *The Air Quality Strategy for England, Scotland and Wales: Volume 1 and 2.* [Online]. London: Home Office. [Date Accessed: 30/12/2020]. Available from: https://assets.publishing.service.gov.uk/government/uploads/system/uploads/attachment_data/file/69336/pb12654-air-quality-strategy-vol1-070712.pdf

Department for Environment, Food and Rural Affairs (DEFRA). 2018. *Consultation on cleaner domestic burning of solid fuels and wood.* London: DEFRA.

Department for Environment, Food and Rural Affairs. 2020. *Emissions of air pollutants in the UK, 1970 to 2018 - Summary.* [Online]. London: Home Office. [Date Accessed: 30/12/2020]. Available from: https://www.gov.uk/government/publications/emissions-of-air-pollutants/emissions-of-air-pollutants-in-the-uk-1970-to-2018-summary

Dhaundiyal, A, Singh, S.B, Atsu, D, and Toth, L. 2021. Comprehensive analysis of pre-treated Austrian pine. *Fuel.* **287**.

Dooley, B. 2017. *Combustion characteristics of coal, biomass and their chars in air and oxy-fuel environments*. Ph.D. thesis, University of Leeds.

Donnelly, E, Robertson, J, and Robinson, D. 2002. Potential and historical Uses for bracken (Pteridium aquilinum (L.) Kuhn) in organic agriculture. In. *The UK Organic Research: Proceedings of the COR Conference, 26th-28th March 2002, Aberystwyth.* [Online]. Aberdeen: Aberdeen University Centre for Organic Agriculture, pp. 255-256. [Accessed: 15/02/2020]. Available From: https://orgprints.org/8312/1/Donnelly_Potential_historical_bracken.pdf

Doshi, V, Vuthaluru, H.B, Korbee, R, and Kiel, J.H.A. 2009. Development of a modelling approach to predict ash formation during co-firing of coal and biomass. *Fuel Processing Technology.* **90**, pp. 1148-1156.

Douglas Smoot, L, and Baxter, L.L. 2003. *Fossil Fuel Power Stations- Coal Utilization.* In: Encyclopaedia of Physical Science and Technology. 3rd Edition. Cambridge: Academic Press, pp. 121-144.

Duarte-Davidson, R, Courage, C, Rushton, L, and Levy, L. 2001. Benzene in the environment: An assessment of the potential risks to the health of the population. *Occupational and Environmental Medicine.* **58**(1), pp. 2-13.

EIA. 2013. *EIA projects world energy consumption will increase 56% by 2040.* [Online]. EIA: Washington D.C. [Date Accessed: 30/12/2020]. Available from: https://www.eia.gov/todayinenergy/detail.

EIA. 2015. *Passenger travel accounts for most of world transportation energy use.* [Online]. EIA: Washington D.C. [Date Accessed: 31/12/2020]. Available from: https://www.eia.gov/todayinenergy/detail.

EIA. 2020. *Overview of Energy Markets.* [Online]. EIA: Washington D.C. [Date Accessed: 30/12/2020]. Available from: https://www.eia.gov/outlooks/aeo/pdf/AEO2020

Eleri, A.I and Eleri, E.U. 2009. *Rethinking biomass energy in Sub-Sahara Africa.* [Online]. VENRO: Bonn. [Date Accessed: 30/12/2020]. Available from: https://africa-eu-partnership.org/sites/default/files/documents/091124_afrikas_perspektive_bioenergie studie_final_en_1.pdf

Energy Catapult. 2020. *Decarbonisation of Heat: Why it needs to innovation.* [Online]. [Date Accessed: 04/04/2021]. Available from: https://es.catapult.org.uk/brochures/decarbonisation-heat/

Environment Agency. 2007. *UK Soil and Herbage Pollutant Survey.* [Online]. Bristol: Environment Agency. [Date Accessed: 06/04/2021]. Available from: https://assets.publishing.service.gov.uk/government/uploads

Environmental Protection Agency (US). 2016. *NAAQS Table.* [Online]. [Date Accessed: 30/12/2020]. Available from: https://www.epa.gov/criteria-air-pollutants/naaqs-table

Envirotrain. 2018. *A3.2.8 Toxic Organic Micro-Pollutants TOMPs.* [Online]. [Date Accessed: 28/12/2020]. Available from: http://www.envirotrain.co.uk/module-a/a3-effects-of-releases/a3-2-principal-sources-of-pollutants/a3-2-8toxic-organic-micro-pollutants-tomps.

EPA. 2018. *2018 Edition of the Drinking Water Standards and Health Advisories Tables*. [Online]. Washington D.C.: Office for Water: US Environment Protection Agency. [Date accessed: 20.11.2020]. Available from: https://www.epa.gov/sites/production/files/

European Commission. 2019. *Shot-Term Outlook for E.U. Agricultural Markets in 2018 and 2019.* April 2019. [Date accessed: 01/05/2020]. Available from: https://ec.europa.eu/info/sites/info/files/food-farming-fisheries/farming/documents/short-term-outlook-spring-2019_en.pdf

Fachinger, F, Drewnick, F, Gieré, R, and Borrmann, S. 2017. How the user can influence particulate emissions from residential wood and pellet stoves: Emission factors for different fuels and burning conditions. *Atmospheric Environment.* **158**, pp 216-226.

Fahmi, R, Bridgewater, A.V, Darvell, L.I, Jones, J.M, Yates, N, Thain, S, and Donniston, I.S. 2007. The effect of alkali metals on combustion and pyrolysis of Lolium and Festuca grasses, switchgrass and willow. *Fuel.* **86**, pp. 1560-1569.

Fernández-Bolaños, J. Rodríguez, G. Rodríguez, R. Guillén, R. and Jiménez, A. 2006. Extraction of interesting organic compounds from olive oil waste. *Grasas y Aceites.* **57** (1), pp. 95-106.

Fine, P.M, Cass, G, R, and Simoneit, B.R.T. 2002. Organic compounds in biomass smoke from residential wood combustion: Emissions characterization at a continental scale. *Geophysical Research: Atmospheres.* **107**(D21), pp. 8349.

Finney, K.N, Szuhánszki, A, Darvell, L.I, Booley, B, Milkowski, K, Jones, J.M, and Pourkashanian, M. 2018. Entrained Metal Aerosol Emissions from ai-fired biomass and coal combustion for carbon capture applications. *Materials.*

Fisher, T, Hajaligol, M, Waymack, B, and Kellogg, D. 2002. Pyrolysis behaviour and kinetics of biomass derived materials. *Journal of Analytical and Applied Pyrolysis.* **62** (2), pp. 331-349.

Fitzpatrick, E.M, Jones, J.M, Pourkashanian, M, Ross, A.B, Williams, A, and Bartle, K.D, 2008. Mechanistic aspects of soot formation from the combustion of pine wood. *Journal of Energy and Fuels.* **22** (6), pp. 3771-3778.

Fitzpatrick, E.M, Ross, A.B, Bates, J, Andrews, G, Jones, J.M, Phylaktou, H, Pourkashanian, M, and Williams, A. 2007. Emission of oxygenated species from the combustion of pine wood and its relation to soot formation. *Process Safety and Environmental Protection.* **85**(5), pp. 430-440.

Font, A, and Fuller, G. 2017. *Airborne particulates from wood burning in UK cities.* [Online]. Report to DEFRA. London: Energy Research Group, Kings College London. [Accessed: 08/06/2020]. Available From: https://uk-air.defra.gov.uk/assets/documents/reports/cat05.

Freeman, D.J, and Cattell, F.C.R. 1990. Woodburning as a source of atmospheric polycyclic aromatic hydrocarbon. *Environmental Science and Technology.* **24**(10), pp. 1581-1585.

Friedl, A, Padouvas, E, Rotter, H, and Varmuza, K. 2005. Prediction of heating values of biomass fuel from elemental composition. *Journal of Analytica Chimica Acta.* **544** (1), pp. 191-198.

Garcia-Maraver, A, Mata-Sanchez, J, Carpio, M, Perez-Jimenez, J.A. 2017. Critical review of predictive coefficients for biomass ash deposition tendency. *Journal of the Energy Institute.* **90** (2), pp. 214-228.

Gatten, E. 2021. Mississippi wood pellet plant that supplies UK electricity grid fined $2.5m over air pollution [Online]. *The Telegraph.* 19th February. Available from: https://www.telegraph.co.uk/environment/2021/02/19/mississippi-wood-pellet-plant-supplies-uk-electricity-grid-fined/

Geana, E.I, Iordache, A.M, Voica, C, Culea, M, and Ionete, R.E. 2011. Comparison of three digestion methods for heavy metals determination in soils and sediments materials by ICP-MS technique. Asian *Journal of Chemistry.***23**(12), pp. 5213-5216.

Ghosh, M, and Singh, S.P. 2005. A review on phytoremediation of heavy metals and utilization of it's byproducts. *Energy and Environment*. **6**(4), pp. 18.

Glarborg, P, Jensen, A.D, and Johnsson, J.E. 2003. Fuel nitrogen conversion in solid fuel fired systems. *Progress in Energy and Combustion Science.* **29**, pp. 89-113.

Glarborg, P, Jensen, A.D, and Johnsson, J.E. 2000. Fuel nitrogen conversion in solid fuel fired systems. *Progress in Energy Combustion and Science.* **29**(2), pp. 89-113.

Glassman, I, Yetter, R.A, Glumac, N.G. 2015. Chapter 9- Combustion of nonvolatile fuels. In: *Combustion* (5th Edition), pp. 477-536. Cambrdige: Academic Press.

Glithero, N. J. Wilson, P. and Ramsden, S.J. 2013. Straw use and availability for second generation biofuels in England. *Biomass and Bioenergy.* **55**, pp. 311-321.

González, J.F, González-García, C.M, Ramiro, A, González, J, Sabio, E, Gañán, J, and Rodríguez, M. 2004. Combustion optimisation of biomass residue pellets for domestic heating with a mural boiler. *Journal of Biomass and Bioenergy.* **27**, pp. 145-154.

González, J.F, Román, S, Encinar, J.M, and Martínez, G. 2009. Pyrolysis of various biomass residues and char utilization for the production of activated carbons. *Analytical and Applied Pyrolysis.* **85**, pp. 134-141.

Government of Canada. 2019. *Volatile Organic Compounds.* [Online]. [Date Accessed: 28/12/2020]. Available from: https://www.canada.ca/en/health-canada/services/air-quality/indoor-air-contaminants/volatile-organic-compounds.html.

Granados, D.A, Basu, P, Chejne, F, and Nhuchhen, D.R. 2017. Detailed investigation into torrefaction of wood in a two-stage inclined rotary torrefier. *Energy and Fuels.* **31**, pp. 647-658.

Gregory, A, and Bolwell, G.P. 1999. 3.17- Hemielluloses. *Comprehensive Natural Products Chemistry.* Pergamon Press: Oxford, pp. 599-615.

Gudka, B.A. 2012. *Combustion Characteristics of some Imported Feedstocks and Short Rotation Coppice (SRC) Willow for UK Power Stations.* Ph.D. thesis, University of Leeds.

Gudka, B.A, Baxter, X.C, Darvell, L.I, Jones, J.M, Saddawi, A, Williams, A, Malmgren, A, Kilgallon, P.J, and Simms, N.J. 2010. Combustion of two imported biomass feedstocks for co-firing in the UK. In: *18th European Biomass Conference and Exhibition, 3rd-7th May 2010, Lyon.* Leeds: University of Leeds, pp. 1107-1112.

Gudka, B.A, Jones, J.M, Lea-Langton, A.R, Williams, A, and Saddawi, A. 2016. A review of the mitigation of deposition and emission problems during biomass combustion through washing pre-treatment. *Energy Institute.* **89**(2), pp. 159-171.

Guo, S, Dong, X, Zhu, C, Han, Y, Ma, F, and Wu, T. 2017. Pyrolysis behaviours and thermodynamics properties of hydrochar from bamboo (*Phyllostachys heterocycla* cv. *pubescens*) shoot shells. *Bioresource Technology.* **233**, pp. 92-98.

Guo, C, Tian, W, Wang, Z. Han, F, Su, M, Wu, Y, Li, Z, and Hu, S. 2019. Reduction of Pb availability during surficial leaching in different types of soils with addition of apatite and oxalic acid. *Soils and Sediments.* **19**: pp. 741–749.

Han, J, Choi, Y, and Kim, J. 2020. Development of the Process Model and Optimal Drying Conditions of Biomass Power Plants. *ACS Omega.* **5**, pp. 2811-2818.

Han, K, Gao, J, and Qi, J. 2019. The study of sulphur retention characteristics of biomass briquettes during combustion. *Energy.* **186**, pp. 1-12.

Hasanov, I, Raud, M, and Kikas, T. 2020. The role of ionic liquids in the lignin separation from lignocellulosic biomass. *Energies.* **13**(18), pp. 1-24.

HealthLink British Colombia. 2018. *Indoor Air Quality: Volatile Organic Compounds (VOCs).* [Online]. [Date Accessed: 28/12/2020]. Available from: https://www.healthlinkbc.ca/healthlinkbc-files/air-quality-VOCs

Houshfar, E, Skreiberg, Ø, Glarborg, P and Løvås, T. 2012. Reduced chemical kinetic mechanism for NOx emission prediction in biomass combustion. *Chemical Kinetics.* **44**(4), pp. 219-231.

Horvat,A, Kwapinska,M, Xue, G, Rabou, L.P.L.M, Pandey, D.S, Kwapinski, W, and Leahy, J.J. 2016. Tars from fluidised bed gasification of raw and torrefied miscanthus x giganteus. *Energy and Fuels.* **30**, pp. 5693-5704.

Hoyosa, T, Kawamoto, H, and Saka, S. 2009. Solid/liquid- and vapor-phase interactions between cellulose- and lignin- pyrolysis products. *Analytical and Applied Pyrolysis.* **85**, pp. 237-246.

Ibrahim, R.H.H., L.I. Darvell, J.M. Jones, and A. Williams. 2013. Physicochemical characterisation of torrefied biomass. *Journal of Analytical and Applied Pyrolysis*. **103**(0): p. 21-30.

IEA. 2003. *Municipal Solid Waste and its Role in Sustainability.* [Online]. 2nd Edition. IEA: Paris. [Date Accessed: 31/12/2020]. Available from: https://www.ieabioenergy.com/wpcontent/uploads/2013/10/40_IEAPositionPaperMSW.pdf

IEA. 2019. *Southeast Asia Energy Outlook.* [Online]. IEA: Paris. [Date Accessed: 30/12/2020]. Available from: https://www.iea.org/reports/southeast-asia-energy-outlook-2019

IEA. 2020. *Global Energy Review 2019.* [Online]. 1st Edition. IEA: Paris. [Date accessed: 23/12/2020]. Available from: https://www.iea.org/reports/global-energy-review-2019

IEA. 2020. *System integration of renewables: Decarbonising while meeting growing demand.* [Online]. IEA: Paris. [Date accessed: 31/12/2020]. Available from: https://www.iea.org/topics/system-integration-of-renewables

IEA. 2021. *World energy outlook 2020.* [Online]. IEA: Paris. [Date Accessed: 05/08/2021]. Available from: https://www.iea.org/reports/world-energy-outlook-2020

International Coffee Organisation (ICO). 2018. *Coffee Market Report.* ICO: London: UK. [Date Accessed: 10/08/2020]. Available from: http://www.ico.org/Market-Report-18-19-e.asp.

IRENA. 2018. *Renewable energy policies in a time of transition.* [Online]. IRENA: Abu Dhabi. [Date Accessed: 30/12/2020]. Available from: https://www.irena.org/-/media/Files/IRENA/Agency/Publication/2018/Apr/IRENA_IEA_REN21_Policies_2018.

ITM Power. 2020. *HyDeploy: UK Gas Grid Injection of Hydrogen in Full Operation.* [Online]. [Date Accessed: 04/04/2021]. Available from: https://www.itm-power.com/news/hydeploy-uk-gas-grid-injection-of-hydrogen-in-full-operation

Jenkins, B.M, Bakker, R.R, Baxter, L.L, Gilmer, J.H. Wei, J.B. 1996. Combustion characteristics of leached biomass. *Developments in Thermochemical Biomass Conversion.* **2**, pp. 1319-1330.

Jenkins, B.M, Baxter, L.L, Miles Jr., T.R, and Miles, T.R. 1998. Combustion properties of biomass. *Fuel Processing Technology.* **54**, pp. 17-46.

Jiménez, S, Pérez, M, and Ballester, J. 2008. Vaporisation of trace elements and their emission with submicrometer aerosols in biomass combustion. *Energy and Fuels.* **22**, pp. 2270-2277.

Johansen, J.M, Jakobsen, J.G, Frandsen, F.J, and Glarborg, P. 2011. Release of K, Cl and S during pyrolysis and combustion of high-chlorine biomass. *Journal of Energy and Fuels.* **25**, pp. 4961-4971.

Johansson, L.S, Leckner, B, Gustavsson, L, Cooper, D, Tullin, C, and Potter, A. 2004. Emission characteristics of modern and old-type residential boilers fired with wood logs and wood pellets. *Atmospheric Environment.* **38**, pp. 4183-4195.

Jöller, M, Brunner, T, and Obernberger, I. 2005. Modelling of aerosol formation during biomass combustion in grate furnaces and comparisons with measurements. *Energy and Fuel.* **13**, pp. 311-323.

Jones, J.M, Bridgeman, T.G, Darvell, L.I, Gudka, B, Saddawi, A, and Williams, A. 2012. Combustion properties of torrefied willow compared with bituminous coals. *Fuel Processing Technology.* **101,** pp. 1-9. Jenkins, B.M, Bakker, R.R and Wei, J.B. 1996. On the properties of washed straw. *Biomass and Bioenergy.* **10**, pp. 177-200.

Jones, J.M, Darvell, L.I, Bridgeman, T.G, Pourkashanian, M, and Williams, A. 2007. An investigation of the thermal and catalytic behaviour of potassium in biomass combustion. *Proceedings of the Combustion Institute.* **31**, 1955-1963.

Jones, J.M, Mitchell, E.J.S, Williams, A, Barimah, E.K, Jose, G, Hondow, N, Bartle, K.D, and Lea-Langton, A.R. 2020. Examination of Combustion-Generated Smoke Particles from Biomass at Source: Relation to Atmospheric Light Absorption. *Combustion Science and Technology.* **192**(1), pp. 130-143.

Jones, J.M, Mitchell, E, Williams, A, Kumi-Barimah, E, Jose, G, Bartle, K, Hondow, N and Lea-Langton, A. 2018. Examination of combustion-generated smoke particles from biomass at source: Relation to atmospheric light absorption. *Combustion Science and Technology.* **192**(1), pp. 130-143.

Jones, J.M, Pourkashanian, M, Williams, A, Rowlands, L, Zhu, Q, and Thomas, K.M. 2004. Conversion of char nitrogen to NO during combustion. *Energy Institute.* **77**, pp. 82-89.

Jones, J.M, Saddawi, A, Dooley, B, Mitchell, E.J.S, Werner, J, Waldron, D.J, Weatherstone, S, and Williams, A. 2015. Low Temperature Ignition of Biomass. *Journal of Fuel Processing Technology.* **134**, pp. 372-377.

Kadiyala, A, Kommalapati, R, and Huque, Z. 2016. Evaluation of the Life Cycle Greenhouse Gas Emissions from Different Biomass Feedstock Electricity Generation Systems. *Sustainability.* **8**, pp. 1-12.

Kaliyan, N, and Morey, R.V. 2009. Factors affecting strength and durability of densified biomass products. *Biomass and Bioenergy.* **33**, pp. 337-359.

Kambo, H.S, and Dutta, A. 2015. A comparative review of biochar and hydrochar in terms of production, physico-chemical properties and applications. *Renewable and Sustainable Energy Reviews.* **45**, pp. 359-378.

Kang, S.B, Oh, H.Y, Kim, J.J, and Choi, K.S. 2017. Characteristics of spent coffee ground as a fuel and combustion test in a small boiler (6.5kW). *Renewable Energy.* **113**, pp. 1208-1214.

Karpov, K.A. 2019. Development trends of global energy consumption. *Studies on Russian Economic Development.* **30**(1), pp. 38-41.

Kastanaki, E, and Vamvuka, D. 2006. A comparative reactivity and kinetic study on the combustion of coal-biomass char blends. *Journal of Fuel.* **85** (9), pp. 1186-1193.

Khalil, R.A, Bach, Q-V, Skreiberg, Ø, and Tran, K-Q. 2013. Performance of a residential poeller combustor operating on raw and torrefied spruce and spruce-derived residues. *Energy and Fuels.* **27**, pp. 4760-4769.

Khan, M.I, Zahoor, M, Khan, A, Gulfam, N, and Khisroon, M. 2019. Bioaccumulation of Heavy Metals and their Genotoxic Effect on Freshwater Mussel. *Environmental Contamination and Toxicology.* **102**, pp. 52-58.

Khasraw, D, Spooner, S, Hage, H, Meijer, K, and Li, Z. 2021. Devolatilisation characteristics of coal and biomass with respect to temperature and heating rate for HIsarna alternative ironmaking process. *Fuel.* **284**, pp. 1-11.

Kim, J.Y, and Yeom, S.H. 2020. Optimization of biodiesel production from waste coffee grounds by simultaneous lipid extraction and transesterification. *Biotechnology and Bioprocess Engineering.* **25**, pp. 320-326.

Kleeman, M.J, Schauer, J.J, and Cass, G.R. 1999. Size and Composition Distribution of Fine Particulate Matter Emitted from Wood Burning, Meat Charbroiling, and Cigarettes. *Journal of Environmental Science and Technology.* **33** (2), pp. 3516-3523.

Knudsen, J.N, Jensen, P.A, and Dam-Johansen, K. 2004. Transformation and release to the gas phase of Cl, K and S during combustion of annual biomass. *Energy and Fuels.* **18**, pp. 1385-1399.

Korzeniowska, J, and Stanislawska-Glubiak, E. 2019. Phytoremediation potential of *Phalaris arundinacea, salix viminalis* and *Zea mays* for nickel-contaminated soils. *Internation Journal of Environmental Science and Technology.* **16**, pp. 1999-2008.

Kristensen, E.F, Kristensen, J.K. 2004. Development and test of small-scale batch-fired straw boilers in Denmark. *Journal of Biomass and Bioenergy.* **26**, pp. 561-569.

Ktori, R, Kamaterou, P, and Zabaniotou, A. 2018. Spent coffee grounds valorization through pyrolysis for energy and materials production in the concept of circular economy. In: *11th Panhellenic Scientific Conference of Chemical Engineering, 25th-27th May 2017, Thessaloniki, Greece.* Oxford: Materials Today, pp. 27582-27588.

Kurmshina, N.G, Kuramshin, E.M, Nikolaeva, S.V, and Imashev, Y.B. 2014. The biogeochemical characteristics of the content of heavy metals in soil, plants and animals in different natural areas of Bashkortostan. *Journal of Geochemical Exploration.* **144** (B), pp. 237-240.

Lamberg, H, Tissari, J, Jokiniemi, J, and Sippula, O. 2013. Fine Particle and Gaseous Emissions from a Small-Scale Boiler Fueled by Pellets of Various Raw Materials. *Energy and Fuels*. **27**, pp. 7044-7053.

Lea-Langton, A.R, Baeza-Romero, M.T, Boman, G.V, Brooks, B, Wilson, A.J.M, Atika, F, Bartle, K.D, Jones, J.M, and Williams, A. 2015. A study of smoke formation from wood combustion. *Fuel Processing Technology.* **137**, pp. 327-332.

Lee, B-K. 2010. Sources, distribution and toxicity of polyaromatic hydrocarbons (PAHs) in particulate matter. *Air Pollution.*

Li, C, Ye, K, Mawusi, S, Zhang, W, Xu, Y, Xu, J, Zhou, W, Li, J, Jiao, M, Shrestha, P, Pang, R, Hussein, R, Xue, C, and Liu, G. 2020. A 24-h real-time emissions assessment of 41 uncontrolled household raw coal combustion stoves in four provinces of Northern China. *Atmospheric Environment.* **235**.

Li, H, Ebner, J, Ren, P, Campbell, L, Cizayi, B and Hadavi, S. 2014. Determination of carbon footprint using LCA method for straight used cooking oil as a fuel in HGVs. *Fuels and Lubricants*. **7**(2), pp. 623-630.

Li, J, Biagini, E, Yang, W, Tognotti, L, and Blasiak, W. 2013. Flame characteristics of pulverized torrefied-biomass combusted with high temperature air. *Combustion and Flame.* **160** (11), pp. 2585-2594.

Li, J, Carlson, B.E, and Lacis, A.A. 2014. Application of spectral analysis techniques to the intercomparison of aerosol data- Part 4: Synthesized analysis of multisensor satellite and ground-based AOD measurements using combined maximum covariance analysis. *Atmospheric Measurement Techniques.* **7**, pp. 2531-2549.

Li, T, Wang, L, Ku, X, Güell, B.M, Løvås, T, and Shaddix, C.R. 2015. Eperimental and modelling study of the effect of torrefaction on the rapid devolatilization of biomass. *Energy and Fuels.* **29**, pp. 4328-4338.

Li, X, He, F, Su, X, Behrendt, F, Gao, Z, and Wang, H. 2019. Evaporationrate of potassium chloride in combustion of herbaceous biomass and its calculation. *Fuel.* **257**, pp. 1-7.

Li, Y, Tang, Y, Fan, Z, Zhou, H, and Yang, Z. 2018. Assessment and comparison of three different air quality indices in China. *Environmental Engineering Research.* **23**(1), pp. 21-27.

Liaw, S.B, and Wu, H. 2013. Leaching characteristics of organic and inorganic matter from biomass by water: Differences between batch and semi-continuous operations. *American Chemical Society*. **52**(11), pp. 4280-4289.

Limousy, L, Jeguirim, M, Dutournié, P, Kraiem, N, Lajili, M, and Said, R. 2013. Gaseous products and particulate matter emissions of biomass residential boiler fired with spent coffee grounds pellets. *Fuel*. **107**, pp. 323-329.

Lisandy, K.Y, Kim, G-M, Him, J-H, Kim, G-B, and Jeon, C-H. 2017. Enhanced accuracy of the reaction rate prediction model for carbonaceous solid fuel combustion. *Energy and Fuels.* **31**(5), pp. 5135-5144.

Liu, Y, Liu, Y, Che, D, and Xu, T. 2005. Effects of minerals and sodium addition on nitrogen release during coal combustion. *Proc. CSEE.* **25**(4), pp. 136-141.

Long, J, Deng, L, and Che, D. 2020. Analysis on organic compounds inwater leachate from biomass. *Renewable Energy.* **155**, pp. 1070-1078.

Lu, H, Robert, W, Peirce, G, Ripa, B, and Baxter, L.L. 2008. Comprehensive study of biomass particle combustion. *Energy and Fuels.* **22**, pp. 2826-2839.

Lu, Z, Jian, J, Jensen, P.A, Wu, H, and Glarborg, P. 2016. Influence of torrefaction on single particle combustion of wood. *Energy and Fuels*. **30**, pp. 5772-5778.

Lu, Z, Jian, J, Jensen, P.A, Wu, H, and Glarborg, P. 2017. Impact of KCl impregnation on single particle combustion of wood and torrefied wood. *Fuel.* **206**, pp. 684-689.

Lyme Disease Action. 2011. *Bracken Control Chemical Banned* [Online]. [Accessed 12/02/2020]. Available From: https://www.lymediseaseaction.org.uk

Mączyńska, J, Krzywonos, M, Kupczyk, A, Tucki, K, Sikora, M, Pińkowska, H, Bączyk, A, and Wielewska, A. 2019. Production and use of biofuels for transport in Poland and Brazil: The case of bioethanol. *Fuel.* **241**, pp. 989-996.

Marschner, H. 2012. *Marschner's Mineral Nutrition of Higher Plants.* 3rd Edition. Academic Press: San Diego.

Mason, P.E. 2016.*On the combustion of solid biomass for large scale power generation: Investigations on the combustion behaviour of single particles of pulverised biomass fuel.* Ph.D. thesis, University of Leeds.

Matthews, J.B.R (ed.). 2018. IPCC. *Global Warming of 1.5°C. An IPCC Special Report on the impacts of global warming of 1.5°C above pre-industrial levels and related global greenhouse gas emission pathways, in the context of strengthening the global response to the threat of climate change, sustainable development, and efforts to eradicate poverty.* [Masson-Delmotte, V., P. Zhai, H.-O. Pörtner, D. Roberts, J. Skea, P.R. Shukla, A. Pirani, W. Moufouma-Okia, C. Péan, R. Pidcock, S. Connors,

Matthews, J.A, and Tan, H. 2009. Biofuels and indirect land use change effects: the debate continues. *Biofuels, Bioproducts and Biorefineries.* **3**(3), pp. 305-317.

Maxwell, D, Gudka, B.A, Jones, J.M, and Williams, A. 2020. Emissions from the combustion of torrefied and raw biomass fuels in a domestic heating stove. *Fuel Processing Technology.* **199**.

McNamee, P, Darvell, L.I, Jones, J.M, and Williams, A. 2015. The combustion characteristics of high-heating rate chars from untreated and torrefied biomass fuels. *Biomass and Bioenergy.* **82**, pp. 63-72.

Meng, J, Park, J, Tilotta, D, and Park, S. 2012. The effect of torrefaction on the chemistry of fast-pyrolysis bio-oil. *Bioresource Technology*. **111**, pp. 439-446.

Meng, X, Rokni, E, Zhou, W, Qi, H, Sun, R, and Levendis, Y.A. 2020. Emissions from oxy-combustion of raw and torrefied biomass. *Energy Resources Technology*. **142**.

Miles, T.R, Miles, J.T.R, Baxter, L.L, Bryers, R.W, Jenkins, B.M, and Oden, L.L. 1995. Alklai deposits found in biomass power plants: A preliminary investigation of their extent and nature. Report of the National Renewable Energy Laboratory. Golden, CO, USA.

Miller, S.F, and Miller, B.G. 2007. The occurrence of inorganic elements in various biofuels and its effects on ash chemistry and behaviour and use in combustion products. *Fuel Processing Technology*. **88**(11-12), pp. 1155-1164.

Miranda, T, Esteban, A, Rojas, S, Montero, I, and Ruiz, A. 2008. Combustion analysis of different olive residues. *Molecular Sciences*. **9**, pp. 512-525.

Mitchell, E.J.S, Cottom, J.W, Phillips, D, and Dooley, B. 2019. *A Review of the Impact of Domestic Combustion on UK Air Quality*. [Online]. Leeds: Independent report commissioned for HETAS. Available from: https://www.auldtonstoves.co.uk/wp-content/uploads/2019/12/A-Review-of-the-Impact-of-Domestic-Combustion-on-UK-Air-Quality-1.pdf

Mitchell, E.J.S, Gudka, B, Whittaker, C, Shield, I, Price-Allison, A, Maxwell, D, Jones, J.M, and Williams, A. 2020. The use of agricultural residues, wood briquettes and logs for small-scale domestic heating. *Fuel Processing Technology*. **210**, p.106552

Mitchell, E.J.S, Lea-Langton, A.R, Jones, J.M, Williams, A, Layden, P, and Johnson, R. 2016. The impact of fuel properties on the emissions from the combustion of biomass and other solid fuels in a fixed bed domestic stove. *Fuel Processing Technology*. **142**, pp. 115-123.

Mitchell, E.J.S, Ting, Y, Allan, J, Lea-Langton, A.R, Spracklen, D.V, McFiggins, G, Coe, H, Routledge, M.N, Williams, A, and Jones, J.M. 2019. Pollutant emissions from improved cookstoves of the type used in sub-Saharan Africa. *Combustion Science and Technology*. **122** (1), pp. 1-21.

Mohan, D, Pittman Jr., C.U, and Steele, P.H. 2006. Pyrolysis of wood/biomass for bio-oil: A critical review. *Energy and Fuels.* **20**, pp. 848-889.

Moliere, M. 2005. Expanding fuel flexibility of gas turbines. *Proceedings of the Institution of Mechanical Engineers. Part A, Journal of Power and Energy.* **219**(2), pp. 109-119.

Molina, A, Murphy, J.J, Winter, F, Haynes, B.S, Blevins, L.G, and Shaddix, C.R. 2009. Pathways for conversion of char nitrogen to nitric oxide during pulverised coal combustion. *Combustion and Flame.* **156**(3), pp. 574-587.

Morey, G.W, Kracek, F.C, and Bowen, N.L. 1930. *Journal of the Society of Glass Technology.* **14**, pp. 149-187

Mukhopadhyay, R, Sambandam, S, Pillarisetti, A, Jack, D, Mukhopadhyay, K, Balakrishnan, K, Vaswani, M, Bates, M.N, Kinney, P.L, Arora, N, and Smith, K.R. 2012. Cooking Practices, air quality, and the acceptability of advanced cookstoves in Haryana, India: an exploratory study to inform large-scale interventions. *Journal of Global Health.* **5**, pp. 1-13.

Myat Win, K, and Persson, T. 2014. Emissions from residential wood pellet boilers and stove characterized into start-up, steady operation, and stop emissions. *Energy and Fuels.* **28**, pp. 2496-2505.

Myllyvirta, L, Jones, D, and Buckley, T. 2019. Analysis: Global coal power set for record fall in 2019. *Carbon Brief.* [Date Accessed: 08/06/2020]. Available From: https://www.carbonbrief.org/analysis-global-coal-power-set-for-record-fall-in-2019.

Natural England. 2008. *Bracken.* [Leaflet]. Natural England Species Information Note: York. [Date accessed: 01/05/2020]. Available from: file:///C:/Users/User/Downloads/SIN011[1].pdf

Ndiema, C.K.W, Mpendazoe, F.M, and Williams, A. 1997. Emissions of pollutants from a biomass stove. *Journal of Energy Conservation Management.* **39** (13), pp. 1357-1367.

Neubauer. Y. 2013. 6- *Biomass Gasification.* [Online]. In. Biomass Combustion Science, Technology and Engineering. Woodhead Publishing: Cambridge, pp. 106-129.

New South Wales Government Office for Environmental Health. 2013. *Common air pollutants and their health effects.* [Online]. [Date Accessed: 28/12/2020]. Available from: https://www.health.nsw.gov.au/environment/air/Pages/common-air-pollutants.aspx

Nishimura, M, Iwasaki, S, and Horio, M. 2009. The role of potassium carbonate on cellulose pyrolysis. *Taiwan Institute of Chemical Engineers.* **40**, pp. 630-637.

Niu, S, Gao, L, and Zhao, J. 2015. Risk Analysis of Metals in Soil from a Restored Coal Mining Area. *Bulletin of Environmental Contamination and Toxicology.* **58**, pp. 183-187.

Niu, S, Han, K, and Lu, C. 2011. Release of sulfur dioxide and nitric oxide and characteristics of coal combustion under the effect of calcium based organic compounds. *Chemical Engineering.* **168**, pp. 255-261.

Nizhou, A, and Stanmore, B. 2013. The fate of heavy metals during combustion and gasification of contaminated biomass- A brief review. *Hazardous Materials.* **256-257**, pp. 56-66.

Noor, D. 2020. *The World's First Death Attributed to Air Pollution Could Spark the Change We Need.* [Online]. [Date Accessed: 04/04/2021]. Available from: https://earther.gizmodo.com/the-worlds-first-death-attributed-to-air-pollution-coul-1845897149

Norwegian Ministry of Petroleum and Energy. 2019. *Electricity Production.* [Online]. Energy Facts Norway. [Date Accessed: 31/12/2020]. Available from: https://energifaktanorge.no/en/norsk-energiforsyning/kraftproduksjon

Nosek, R, Tun M.M, and Juchelkova, D. 2020. Energy utilisation of spent coffee grounds in the form of pellets. *Energies.* **13**, pp. 1235-1243.

Nowakowski, D.J, and Jones, J.M. 2008. Uncatalysed and potassium-catalysed pyrolysis of the cell-wall constituents of biomass and their model compounds. *Analytical and Applied Pyrolysis.* **83**, pp. 12-25.

Nunez, C. 2019. *Causes and Effects of Climate Change.* In: National Geographic. [Online]. [Date accessed: 27/12/2020]. Available from: https://www.nationalgeographic.com/environment/global-warming/global-warming-overview/

Núñez, J, Moctezuma-Sánchez, M.F, Fisher, E.M, Berrueta, V.M, Masera, O.R, and Beltrán, A. 2020. Natural-draft flow and heat transfer in a plancha-type biomass cookstove. *Renewable Energy.* **146**, pp. 727-736.

Olungblade, T, Ojo, O, and Mohammed, T. 2019. Influence of Binders on Combustion Properties of Biomass Briquettes: A Recent Review. *BioEnergy Research.* **12**(2), pp. 241-259.

Orasche, J, Schnelle-Kreis, J, Schön, C, Hartmann, H, Ruppert, H, Arteaga-Sala, J.M, and Zimmermann, R. 2013. Comparison of emissions from wood combustion. Part 2: Impact of combustion conditions on emissions factors and characteristics of particle-bound organic species and polycyclic aromatic hydrocarbon (PAH)- related toxicological potential. *Energy and Fuels.* **27**, pp. 1482-1491.

Orasche, J, Seidel, T, Hartmann, H, Schnelle-Kreis, J, Chow, J.C, Ruppert, H, and Zimmermann, R. 2012. Comparison of emissions from wood combustion. Part 1- Emission factors and characteristics from different small-scale residential heating appliances considering particulate matter and polycyclic aromatic hydrocarbon (PAH)-related toxicological potential of particle-bound organic species. *Energy and Fuels.* **26**, pp. 6695-6704.

Ozgen, S, and Caserini, S. 2018. Methane emissions from small residential wood combustion appliances: Experimental emission factors and warming potential. *Atmospheric Environment.* **189**, pp. 164-173.

Ozgen, S, Caserini, S, Galante, S, Giugliano, M, Angelino, E, Marongiu, A, Hugony, F, Migliavacca, G, and Morreale, C. 2014. Emission factors from small scale appliances burning wood and pellets. *Atmospheric Environment.* **94**, pp. 144-153.

Pakeman, R.J, Marrs, R.H, and Jacob, P.J. 1994. A Model of Bracken (Pteridium aquilinum) Growth and the Effects of Control Strategies and Changing Climate. *Journal of Applied Ecology.* **31** (1), pp. 145-154.

Pang, C.H, Hewakandamby, B, Wu, T, and Lester, E. 2013. An automated ash fusion test for characterisation of the behaviour of ashes from biomass and coal at elevated temperatures. *Journal of Fuel.* **103**, pp. 454-466.

Park, Y, and Min, D.J. 2016. Foaming Index of CaO-SiO$_2$-FeO-MgO Slag System. In: *10th International Conference Advances in Molten Slags, Fluxes, and Salts, 22nd-25th May 2016, Seattle.* Seoul: Yonsei University, pp. 607-615.

Pecorini, I, Baldi, F, Bacchi, D, Carnevale, E.A, and Corti, A. 2017. Leaching behaviour of hazardous waste under the impact of different ambient conditions. *Waste Management.* **63**, pp. 96-106.

Pettersson, E, Boman, C, Westerholm, R, Boström, D, and Nordin, A. 2011. Stove performance and emission characteristics in residential wood log and pellet combustion; Part 2: Wood stove. *Energy and Fuels.* **25**, pp. 315-323.

Pfadt-Trilling, A.R, Volk, T.A, and Fortier, M-O, P. 2021. Climate Change Impacts of Electricity Generated at a Waste-to-Energy Facility. *Environmental Science and Technology.* **55**, pp. 1436-1445.

Phillips, D. 2018. *The UK's forest resource and its potential as a sustainable feedstock for bioenergy.* Ph.D. thesis, University of Leeds.

Phillips, D, Mitchell, E.J.S, Lea-Langton, A.R, Parmar, K.R, Jones, J.M, and Williams, A. 2016. The use of conservation biomass feedstocks as potential bioenergy resources in the United Kingdom. *Bioresource Technology.* **212**, pp. 271-279.

Phyllis2 Database. 2020. *Database for the physico-chemical composition of (treated) lignocellulosic biomass, micro- and macroalgae, various feedstocks for biogas production and biochar.* [Date accessed: 20/06/2020]. Available from: https://phyllis.nl/.

Potipa, S, and Wongwuttanasatian, T. 2018. Combustion characteristics of spent coffee ground mixed with crude glycerol briquette fuel. *Combustion Science and Technology.* **190**(11), pp. 2030-2043.

Potter, D.M, and Baird, M.S. 2000. Carcinogenic effects of ptaquiloside in bracken fern and related compounds. *British Journal of Cancer.* **83**(7), pp. 914-920.

Price-Allison, A, Lea-Langton, A.R, Mitchell, E.J.S, Gudka, B.A, Jones, J.M, Mason, P.E, and Williams, A. 2019. Emissions performance of high-moisture wood fuels burned in a residential stove. *Journal of Fuels.* **239**, pp. 1038-1045.

Prins, M.J, Ptasinski, K.J, and Janssen, F.J.J.G. 2006. Torrefaction of wood: Part. 2 analysis of products. *Analytical and Applied Pyrolysis.* **77**, pp. 35-40.

Procrop. 2010. *Barley Growth and Development.* [Online]. NSW Government: Industry and Investment: Sydney. [Date Accessed: 01/05/2020]. Available from: https://www.dpi.nsw.gov.au/__data/assets/pdf_file/0003/516180/Procrop-barley-growth-and-development.pdf

Pronobis, M. 2005. Evaluation of the influence of biomass c-combustion on boiler furnace slagging by means of fusibility correlations. *Journal of Biomass and Bioenergy.* **28** (4), pp. 375-383.

Pulford, I.D, and Watson, C. 2003. Phytoremediation of heavy metal-contaminated land by trees- a review. *Environment International.* **29**, pp. 529-540.

Qiulin, M, Lujia, H and Guangqun, H. 2017. Evaluation of different water-washing treatments effects on wheat straw combustion properties. *Bioresource Technology.* **128** (Part A), pp. 1075-1083.

Ramos-Carmonal, S, Pérez, J.F, Pelaez-Samaniego, M.R, Barrera, R, and Garcia-Perez, M. 2017. Effect of torrefaction temperature on properties of Patula Pine, Maderas. *Ciencia y Tecnología.* **19**, pp. 39-50.

Ranzi, E, Cuoci, A, Faravelli, T, Frassoldati, A, Migliavacca, G, Pierucci, S, and Sommariva, S. 2008. Chemical kinetics of biomass pyrolysis. *Energy and Fuels*. **22**, pp. 4292-4300.

Ravichandran, P, and Corscadden, K. 2014. Comparison of gaseous and particle emissions produced from leached and un-leached agricultural biomass briquettes. *Fuel Processing Technology.* **128**, pp. 359-366.

Reed, T.B.1981. *Biomass gasification: Principles and Technology.* Park Ridge, New Jersey: Noyes Data Corporation.

Ren21. 2019. *Renewables 2019: Global Status Report.* [Online]. Ren21: Paris. [Date Accessed: 31/12/2020]. Available from: https://www.ren21.net/wp-content/uploads/2019/05/gsr_2019_full_report_en.pdf

Ren, Q, Zhao, C, Chen, X, Duan, L, Li, Y, and Ma, C. 2011. NOx and N_2O precursors (NH_3 and HCN) from biomass pyrolysis: Co-pyrolysis of amino acids and cellulose, hemicellulose and lignin. *Proceedings of the Combustion Institute.* **33**, pg. 1715-1722.

Ren, Q, Zhao, C, Wu, X, Liang, C, Chen, X, Shen, J, and Wang, Z. 2010. Formation of NOx precursors during wheat straw pyrolysis and gasification with O_2 and CO_2. *Fuel.* **89**, pp. 1064-1069.

Ren, X, Sun, R, Meng, X, Vorobiev, N, Schiemann, M, and Levendis, Y.A. 2017. Carbon, sulphur and nitrogen oxide emissions from combustion of pulverised raw and torrefied biomass. *Journal of Fuel.* **188**, pp. 310-323.

Riaza, J, Gibbins, J, and Chalmers, H. 2017. Ignition and combustion of single particles of coal and biomass. *Fuel.* **202**, pp. 650-655.

Riaza, J, Mason, P, Jones, J.M, Gibbins, J and Chalmers, H. 2019. High temperature volatile yield and nitrogen partitioning during pyrolysis of coal and biomass fuels. *Fuels.* **248**, pp. 215-220.

Richter, F, and Rein, G. 2018. The Role of Heat Transfer Limitations in Polymer Pyrolysis at the Microscale. *Frontiers in Mechanical Engineering.* **4** (18), pp. 1-13.

Roberts, L.J, Mason, P.E, Jones, J.M, Gale, W.F, Williams, A, Hunt, A, and Ashman, J. 2019. The impact of aluminosilicate-based additives upon the sintering and melting behaviour of biomass ash. *Journal of Biomass and Bioenergy.* **127**, pp. 1-9.

Rokni, E, Liu, Y, Ren, X, and Levendis, Y.A. 2019. Nitrogen-bearing emissions from burning corn straw in a fixed-bed reactor. Effects of fuel moisture, torrefaction and air flowrate. *Energy Resources Technology.* **141**, pp. 1-10.

Ross, A.B, Junyapoon, S, Jones, J.M, Williams, and Bartle, K.D. 2005. A study of different soots using pyrolysis-GC-MS and comparison with solvent extractable material. *Analytical and Applied Pyrolysis.* **74**, pp. 494-501.

Roy, M.M, and Corscadden, K.W. 2012. An experimental study of combustion and emissions of biomass briquettes in a domestic wood stove. *Applied Energy.* **99**, pp. 206-212.

Runge, T., Wipperfurth, P., and Zhang, C. 2013. Improving biomass combustion quality using a liquid hot water treatment. *J. Biofuels.* **4** (1): pp. 73-83.

Rusinowski, S. Krzyak, J. Clifton-Brown, J. Jensen, E. Mos, M. Webster, R. Sitko, K. and Pogrzeba, M. 2019. New Miscanthus hybrids cultivated at a Polish metal-contaminated site demonstrate high stomatal regulation and reduced shoot Pb and Cd concentrations. *Environmental Pollution.* **252**, pp. 1377-1387.

Russo, E, Kuerten, J.G.M, and Geurts, B.J. 2014. Delay of biomass pyrolysis by gas-particle interaction. *J. of Analytical and Applied Pyrolysis.* **110**, pp. 88-99.

Saddawi, A, Jones, J.M, and Williams, A. 2010. Kinetics of the Thermal Decomposition of Biomass and the Influence of Alkali Metals on these Kinetics. In: *18th European Biomass Conference and Exhibition, 3rd-7th May 2010, Lyon.* Leeds: University of Leeds, pp. 1101-1106.

Saddawi, A, Jones, J.M, Williams, A, and Le Coeur, C. 2011. Commodity fuels from biomass through pretreatment and torrefaction: effects of mineral content on torrefied fuel characteristics and quality. *Energy and Fuels.* **26**, pp. 6466-6474.

Sánchez, E.A. 2014. Development of Briquettes from Waste Wood (Sawdust) for Use in Low-income Households in Piura, Peru. In: *Proceedings of the World Congress on Engineering 2014 Volume II, July 2nd-4th 2014, London UK.*

Sánchez, F and San Miguel, G. 2016. Improved fuel properties of whole table olive stones via pyrolytic processing. *Biomass and Bioenergy.* **92**, pp 1-11.

Saqib, N, and Bäckström, M. 2014. Trace element partitioning in ashes from boilers firing pure wood or mixtures of solid waste with respect to the fuel composition, chlorine content and temperature. *Waste Management.* **34**(12), pp. 2505-2519.

Schmidl, C, Luisser, M, Padouvas, E, Lasselsberger, L, Rzaca, M, and Ramirez-Santa Cruz, S. 2011. Particulate and gaseous emissions from manually and automatically fired small scale combustion systems. *Atmospheric Environment.* **45**, pp. 7443-7454.

Schmidt, G, Trouvé, G, Leyssens, G, Schönnenbeck, C, Brillard, A, Olya, M.E, Dewaele, D, and Cazier, F. 2020. Influence and modelling of wood washing on mineral and organic compositions of three woods (beech, fir and oak). *Energy Institute*. **93**, pp. 198-209.

Schmitt, V.E.M, and Kaltschmitt, M. 2013. Effect of straw proportion and Ca- and Al-containing additives on ash composition and sintering of wood-straw pellets. *Fuel.* **109**, pp. 551-558.

Shao, J, Cheng, W, Zhu, Y, Yang, W, Fan, J, Liu, H, Yang, H, and Chen, H. 2019. Effects of combined torrefaction and pelletization on particulate matter emissions from biomass pellet combustion. *Energy and Fuels.* **33**, pp. 8777-8785.

Shen, Z.T, Hou, D.Y, Zhao, B, Xu, W.D, Ok, Y.S, Bolan, N.S, and Alessi, D.S. 2017. Stability of heavy metals in soil washing residue with and without biochar addition under accelerated ageing. *Science of the Total Environment*. **619-620**: pp. 185–193.

Simoneit, B.R.T. 2002. Biomass burning- a review of organic tracers for smoke from incomplete combustion. *Applied Geochemistry*. **17**, pp. 129-162.

Singh, R.N. 2004. Equilibrium moisture content of biomass briquettes. *Biomass and Bioenergy.* **26**(3), pp. 251-253.

Sippula, O, Hokkinen, J, Puustinen, H, Yli-Pirila, P, Jokiniemi, J. 2009. Comparison of particle emissions from small heavy fuel oil and wood-fired boilers. *Atmospheric Environment.* **43** (32), pp. 4855-4864.

Sippula, O, Lamberg, H, Leskinen, J, Tissari, J, and Jokiniemi, J. 20017. Emissions and ash behaviour in a 500kW pellet boiler with various blends of woody biomass and peat. *Fuel*. **202**, pp. 144-153.

Skreiberg, A, Skreiberg, Ø, Sandquist, J, and Sørum, L. 2011. TGA and macro-TGA characteristics of biomass fuels and fuel mixtures. *Journal of Fuel.* **90** (6), pp. 2182-2197.

Solomon, S, Qin, D, Manning, M, Marquis, M, Averyt, K, Tignor, M.M.B, Miller JR., H.L-R. Chen, Z. 2007. *Climate Change 2007: The Physical Science Basis*. IPCC. Cambridge University Press: Cambridge.

Soysa, R, Choi, S.K, Jeong, Y.W, Kim, S.J, and Choi, Y.S. 2015. Pyrolysis of Douglas fir and coffee ground and product biocrude-oil characteristics. *J. of Analytical and Applied Pyrolysis.* **115**, pp. 51-56.

Spracklen, D.V, and Righelato, R. 2016. Carbon storage and sequestration of re-growing montane forests in southern Ecuador. *Forest Ecology and Management.* **364**, pp. 139-144.

Srifa, A, Chaiwat, W, Pitakjakpipop, P, Anutrasakda, W, and Faungnawakij, K. 2019. *Sustainable Bioenergy: Chapter 6- Advances in bio-oil production and upgrading technologies.* Amsterdam: Elsevier.

Staffell, I, Scamman, D, Velazquez Abad, A, Balcombe, P, Dodds, P.E, Ekins, P, Shah, N and Ward, K.R. 2019. The role of hydrogen and fuel cells in the global energy system. *Energy and Environmental Science: Royal Society of Chemistry.* **12**, pp463-491.

Staffell, I. 2017. Measuring the progress and impacts of decarbonising British electricity. *Energy Policy.* **102**, pp. 463-475.

Stals, M, Thijssen, E, Vangronsveld, J, Carleer, R, Schreurs, S, Yperman, J. 2010. Flash pyrolysis of heavy metal contaminated biomass from phytoremediation: influence of temperature, entrained flow and wood/leaves blended pyrolysis on the behaviour of heavy metals. *Analytical and applied pyrolysis.* **87**(1), pp. 1-7.

Sugier, P, and Sugier, D. 2018. Impact of road transport on soil physicochemical characteristics and heavy metal concentrations in the bark of purple willow. *Acta Agrobotanica.* **71**(4), pp. 1753-1764.

Sullivan, H.F, and Glassman, I. 1971. Vapour-phase diffusion flames in the combustion of magnesium, calcium and strontium. *Journal of Combustion Science and Technology.* **4**, pp. 241-256.

Sun, R.C, Salisbury, D, and Tomkinson, J. 2003. Chemical composition of lipophilic extractives released during the hot water treatment of wheat straw. *Bioresource Technology.* **88**, pp. 95-101.

Šyc, M, Pohořelý, M, Kameníková, P, Habart, J, Svoboda, K, and Punčochář, M. 2012. Willow trees from heavy metals phytoextraction as energy crop. *Biomass and Bioenergy.* **37**, pp. 106-113.

Tambe, S.S, Naniwadekar, M, Tiwary, S, Mukherjee, A, and Baran Das, T. 2018. Prediction of coal ash fusion temperatures using computational intelligence based models. *Coal Science and Technology.* **5**, pp. 486-507.

Tanger, P, Field, J.L, Jahn, C.E, DeFoort, M.W, and Leach, J.E. 2013. Biomass for Thermochemical Conversion: Targets and Challenges. *Frontiers in Plant Science.* **4**(218), pp. 1-20.

The British Coffee Association. 2019. *Six Coffee Recycling Myths… Busted.* [Online]. [Date Accessed: 10/08/2020]. Available from: https://www.britishcoffeeassociation.org/blog/six-coffee-recycling-myths-busted.

Thomas, N, Hook, L, and Tighe, C. 2019. How Britain Ended its Coal Addiction. *Financial Times.* 01/10/2019, pp. 6.

Tissari, J, Hytonen, K, Sippula, O, and Jokiniemi, J. 2009. The effects of operating conditions on emissions from masonry heaters and sauna stoves. *Journal of Biomass and Bioenergy.* **33** (3), pp. 513-520.

Tolvik Consulting. 2019. *UK Energy from Waste Statistics 2018.* [Online]. 5th Edition. [Date Accessed: 10/08/2020]. Available from: https://www.tolvik.com/wp-content/uploads/2019/06/Tolvik-EfW-Statistics-2018-Report_July-2019-final-amended-version.pdf.

Torvela, T, Tissari, J, Sippula, O, Kaivosoja, T, Leskinen, J, Virén, A, Lähde, A, and Jokiniemi, J. 2014. Effect of wood combustion conditions on the morphology of freshly emitted fine particulates. *Atmospheric Science.* **87**, pp. 65-76.

Townsend, C.L, and Maynard, R.L. 2002. Effects on health of prolonged exposure to low concentrations of carbon monoxide. *Occupational and Environmental Medicine.* **59**(10), pp. 708-711.

(Department for) Transport. 2021. *Fuelling a greener future: E10 petrol set for September 2021 launch.* [Online]. London: Government Publishing. Available from: https://www.gov.uk/government/news/fuelling-a-greener-future-e10-petrol-set-for-september-2021-launch

(Department for) Transport. 2021. *Jet Zero launches £15 million competition to reduce aviation emissions.* [Online]. London: Government Publishing. Available from:https://www.gov.uk/government/news/jet-zero-launches-15millioncompetition-to-reduce-aviation-emissions

Trubetskaya, A, Beckmann, G, Wadenback, J, Jolm, J.K, Velaga, S.P, and Weber, R. 2017. One way of representing the size and shape of biomass particles in combustion modelling. *Fuel.* **206**, pp. 675-683.

Trubetskaya, A, Leahy, J.J, Yazhenshkikh, E, Müller, M, Layden, P, Johnson, R, Stahl, K, and Monaghan, R.F.D. 2019. Charaterization of woodstove briquettes from torrefied biomass and coal. *Energy.* **171**, pp. 853-865.

U.S. Department for Energy. No Date. *Biomass Resources.* [Online]. [Date Accessed: 31/12/2020]. Available from: https://www.energy.gov/eere/bioenergy/biomass-resources

United States Environment Protection Agency. 2019. *Air Pollution: Nitrogen Dioxide: Particulate Matter: Sulfur Dioxide: Carbon Monoxide: Volatile Organic Compounds.* [Online]. [Date Accessed: 28/12/2020]. Available from: https://www.epa.gov/no2-pollution

Valvanidis, A, Fiotakis, K, and Vlachogianni, T. 2008. Airborne particulate matter and human health: toxicological assessment and importance of size and composition of particles for oxidative damage and carcinogenic mechanisms. *Environmental Science and Health.* **26**, pp. 339-362.

Vamerali, T, Bandiera, M, and Mosca, G. 2010. Field crops for phytoremediation of metal-contaminated land: A review. *Environmental Chemistry Letters.* **8**, pp. 1-17.

Vandepaer, L, Cloutier, J, Bauer, C, and Amor, B. 2019. Integrating batteries in the future Swiss electricity supply system: A consequential environmental assessment. *Industrial Ecology.* **23**(3), pp. 709-725.

Vanholme, R, Demedts, A, Morreel, K, Ralph, J, and Boerjan, W. 2010. Lignin biosynthesis and structure. *Plant Physiology.* **153**, pp. 895.

Van Lith, S.C, Frandsen, F.J, Montgomery, M, Vilhelmsen, T, and Jensen, S.A. 2009. Lab-scale investigation of deposit-indices chlorine corrosion of superheater materials under simulated biomass-firing conditions; Part 1: Exposure at 560°C. *Energy and Fuels.* **23**, pp. 3457-3468.

Vassilev, S.V, Baxter, D, Andersen, L. K, and Vassileva, C.A. 2010. An overview of the chemical composition of biomass. *Fuel.* **89**(5), pp. 913-933.

Vassilev, S.V, and Vassileva, C.A. 2007. Methods for characterisation of coal fly ashes based on their origin, composition, properties and behaviour. *Fuel.* **86**, pp. 1490-1512.

Vassilev, S.V, Vassileva, C.G, Song, Y-C, Li, W-Y, and Feng, J. 2017. Ash contents and ash-forming elements of biomass and their significance for solid biofuel combustion. *Fuel.* **208**, pp. 377-409.

Volpe, M, Fiori, L, Volpe, R, and Messineo, A. 2016. Upgrading of olive tree trimmings residue as biofuel by hydrothermal carbonization and torrefaction: A comparative study. *Italian Association of Chemical Engineering.* **50**, pp. 13-18.

Wang, C, Liu, Y, Jin, X, and Che, D. 2016. Effects of water washing on reactivities and NOx emissions of Zhundong coals. *Energy Institute.* **89**, pp. 636-647.

Wang, L, Skjevrak, G, Hustad, J.E, Grønli, M, and Skreiberg, Ø. 2012. Effects of Additives on Barley Straw and Husk Ashes Sintering Characteristics. *Energy Procedia.* **20**, pp. 30-39.

Wang, W, Wen, C, Li, C, Wang, M, Li, X, Zhou, Y, and Gong, X. 2019. Emission reduction of particulate matter from the combustion of biochar via thermal pre-treatment of torrefaction, slow pyrolysis or hydrothermal carbonisation and its co-combustion with pulverised coal. *Fuel.* **240**, pp. 278-288.

Wang, W, Chang, W, Liu, T, Li, C, Chen, L, Wu, J, Shao, Y, and Liu, E. 2020. Effects of various occurrence modes of inorganics components on the emissions of PM_{10} during torrefied biomass combustion under air and oxy-fuel conditions. *Applied Energy.* **259**, pp. 1-9.

Wang, W, Wen, C, Chen, L, Liu, T, Li, C, Liu, E, and Zhang, Y. 2020. Effect of combining water washing and carbonisation on the emissions of PM_{10} generated by the combustion of typical herbs. *Fuel Processing Technology.* **200**, pp. 1-10.

Wang, W, Wen, C, Liu, T, Li, C, Xu, J, Liu, E, Liu, H, and Yan, K. 2020. Emissions reduction of PM_{10} via pretreatment combining water washing and carbonisation during rice straw combustion: Focus on the effects of pretreatment and combustion conditions. *Fuel Processing Technology.* **205**, pp. 1-9.

Wang, Y, Tan, H, Wang, X, Du, W, Mikulĉić, H, and Duić, N. 2017. Study on extracting available salt from straw/woody biomass ashes and predicting its slagging/fouling tendency. *Journal of Cleaner Production.* **155** (1), pp. 164-171.

Wang, Y, Zhou, Y, Bai, N, and Han, J. 2020. Experimental investigation of the characteristics of NOx emissions with multiple deep air-staged combustion of lean coal. *Fuel.* **280**, pp. 1-10.

Wang, Z, and Xiong, Y. 2020. Simultaneous improvement in qualities of bio-oil and syngas from catalytic pyrolysis of rice husk by demineralization. *Energy Sources, Part A; Recovery, Utilization, and Environmental Effects.* **28**(1), pp. 1-14.

Water Research Centre. No date. *Phosphates in the Environment*. [Online]. [Date accessed: 20.11.2020]. Available from: https://water-research.net/index.php/phosphates

Werkelin, J, Skrifvars, B-J, Zevenhoven, M, Holmbom, B, and Hupa, M. 2010. Chemical forms of ash-forming elements in woody biomass fuels. *Fuel.* **89**(2), pp. 481-493.

Werther, J, Saenger, M, Hartge, E.U, Ogada, T, and Siagi, Z. 2000. Combustion of agricultural residues. *Progress in Energy Combustion and Science.* **26**(1), pp. 1-27.

Wigley, F, Williamson, J, Malmgren, A, and Riley, G. 2007. Ash deposition at higher levels of coal replacement by biomass. *Fuel Processing Technology.* **88**, pp. 1148-1154.

Wigley, T, Yip A.C.K, and Pang, S. 2015. The use of demineralisation and torrefaction to improve the properties of biomass intended as a feedstock for fast pyrolysis. *J. of Analytical and Applied Pyrolysis.* **113**, pp. 296-306.

298

Wiinikka, H, and Gebart, R. 2004. Experimental investigations of the influence from different operating conditions on the particle emissions from a small-scale pellets combustor. *Biomass Bioenergy*. **27**, pp. 645-652.

Williams, A, Jones, J.M, Ma, L, Pourkashanian, M. 2012. Pollutants from the combustion of solid biomass fuels. *Progress in Energy and Combustion Science.* **38**, pp 113-137.

World Health Organisation. 2005. *WHO Air quality guidelines for particulate matter, ozone, nitrogen dioxide and sulfur dioxide: Global update 2005*. [Online]. [Date Accessed: 20/12/2020]. Available from: https://apps.who.int/iris/bitstream/handle/10665/69477/WHO_SDE_PHE_OEH_06.

World Health Organisation. 2007. *Health risks of heavy metals from long-range transboundary air pollution.* [Online]. Geneva: World Health Organisation. [Date Accessed: 28/12/2020]. Available from: https://www.euro.who.int/__data/assets/pdf_file

World Health Organisation. 2017. *Guidelines for Drinking- water Quality.* [Online]. 4th edition. Switzerland: WHO. [Date accessed: 20.11.2020]. Available from: https://www.who.int/publications

Wornat, M.J, Hurt, R.H, Yang, N.Y.C, and Headley, T.J. 1995. Structural and compositional transformations of biomass chars during combustion. *Combustion and Flame.* **100**(1), pp. 131-143.

Yan, Z, Wang, Z, Liu, H, Tu, Y, Yang, W, Zeng, H, and Qui, J. 2015. Decomposition and solid reactions of calcium sulfate doped with SiO_2, Fe_2O_3 and Al_2O_3. *Analytical and Applied Pyrolysis.* **113**, pp. 491-498.

Yang, W, Zhou, J, Liu, M, Zhou, Z, Liu, J, and Cen, K. 2007. Combustion process and nitrogen oxides emission of Shenmu coal added with sodium acetate. *Energy fuel*. **21**(5), pp. 2548-2554.

Yoo. C.G, Li, M, Meng, X, Pu, Y, and Ragauskas, A.J. 2017. Effects of organosolv and ammonia pretreatments on lignin properties and its inhibitions for enzymatic hydrolysis. *Green Chemistry.* **19**, pp. 2006-2016.

Yu, C, Thy, P, Wang, L, Anderson, S.N, Vander Gheynst, J.S, Upadhyaya, S.K, and Jenkins, B.M. 2014. Influence of leaching pretreatment on fuel properties of biomass. *Fuel Processing Technology.* **128**, pp. 43-53.

Zając, G, Szyszlak-Bargłowicz, J, and Szczepanik, M. 2019. Influence of biomass incineration temperature on the content of selected heavy metals in the ash used for fertilizing purposes. *Applied Sciences.* **9**.

Zárubová, P, Hejcman, M, Vondrackova, S, Mrnka, L, Szakova, J, Tlutos, P. 2015. Distribution of P, K, Ca, Mg, Cd, Cu, Fe, Mn, Pb, and Zn in wood and bark age classes of willows and poplars used for phytoextraction on soils contaminated by risk elements. *Environmental Science Pollution.* **22**, pp. 18801-18813.

Zevenhoven-Onderwater, M, Blomquist, J-P, Skrifvars, B-J, Backman, R, and Hupa, M. 2000. The prediction of behaviour of ashes from five different solid fuels in fluidised bed combustion. *Fuel*. **79**, pp. 1353-1361.

Zhang, H, Gong, Z, Liu, L, Wang, Z, and Li, X. 2020. Study on the migration characteristics of sulfur and nitrogen during combustion of oil sludge with CaO additive. *Energy and Fuels.* **34**, pp. 6124-6135.

Zhao, Z.B, Li, W, Qiu, J.S, Wang, X.Z, and Li, B.Q. 2006. Influence of Na and Ca on the emissions of NOx during coal combustion. *Fuel*. **85**(5-6), pp. 601-606.

Zhao, B, Liu, A, Wu, G, Li, D, and Guan, Y. 2017. Characterization of heavy metal desorption from road-deposited sediment under acid rain scenarios. *Environmental Science*. **51**, pp. 284-293.

Zhao, Z.B, Qiu, J.S, Li, W, and Li, B.Q. 2003. Influence of mineral matter in coal on decomposition of NO over coal chars and emissions of NO during char combustion. *Fuel*. **82**(8), pp. 949-957.

Appendix

Appendix A- Data and Information relating to Chapter 4
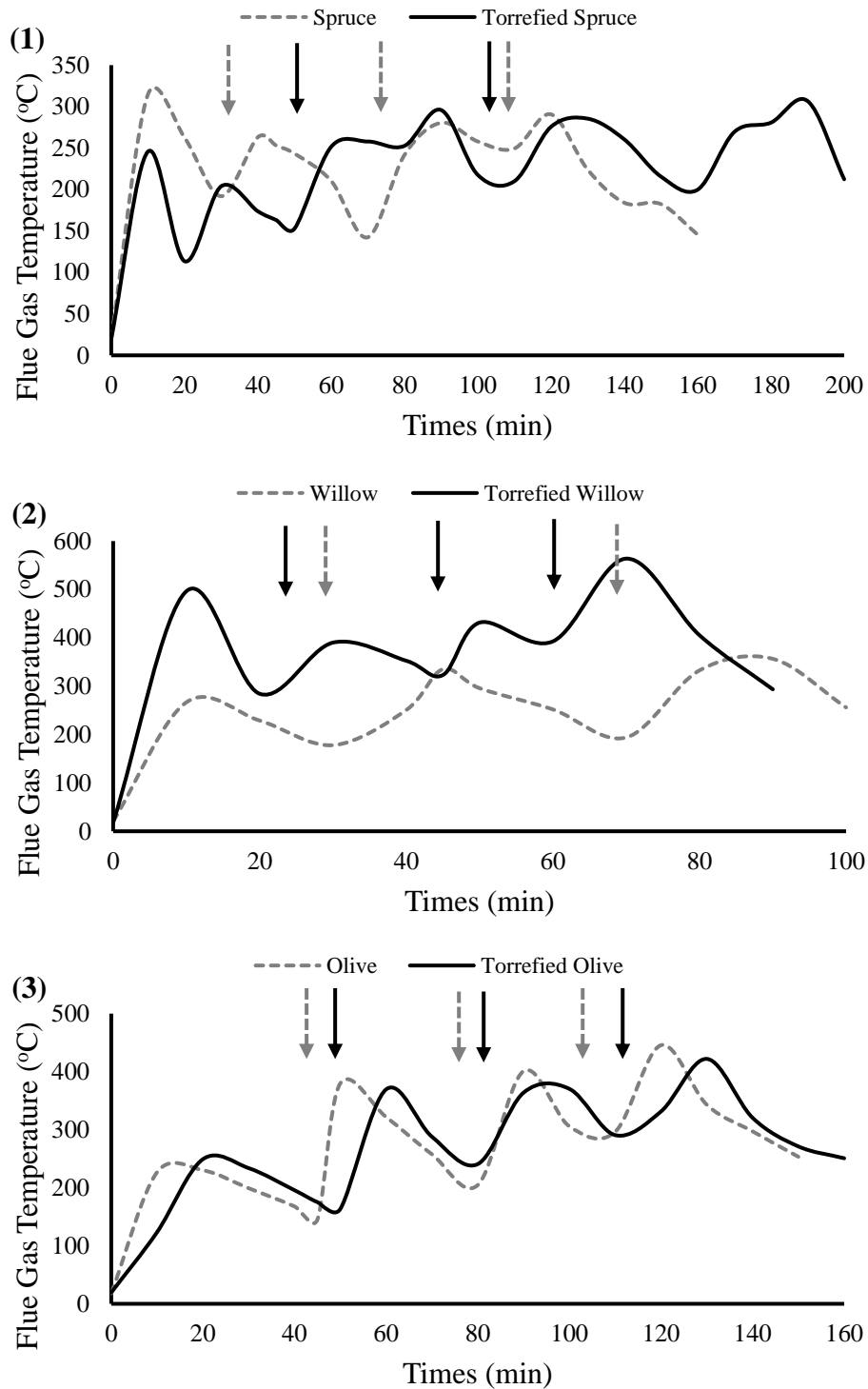
Figures A.1-3: Temperature profiles for (1) Spruce and Torrefied Spruce (2) Willow and Torrefied Willow (3) Olive and Torrefied Olive
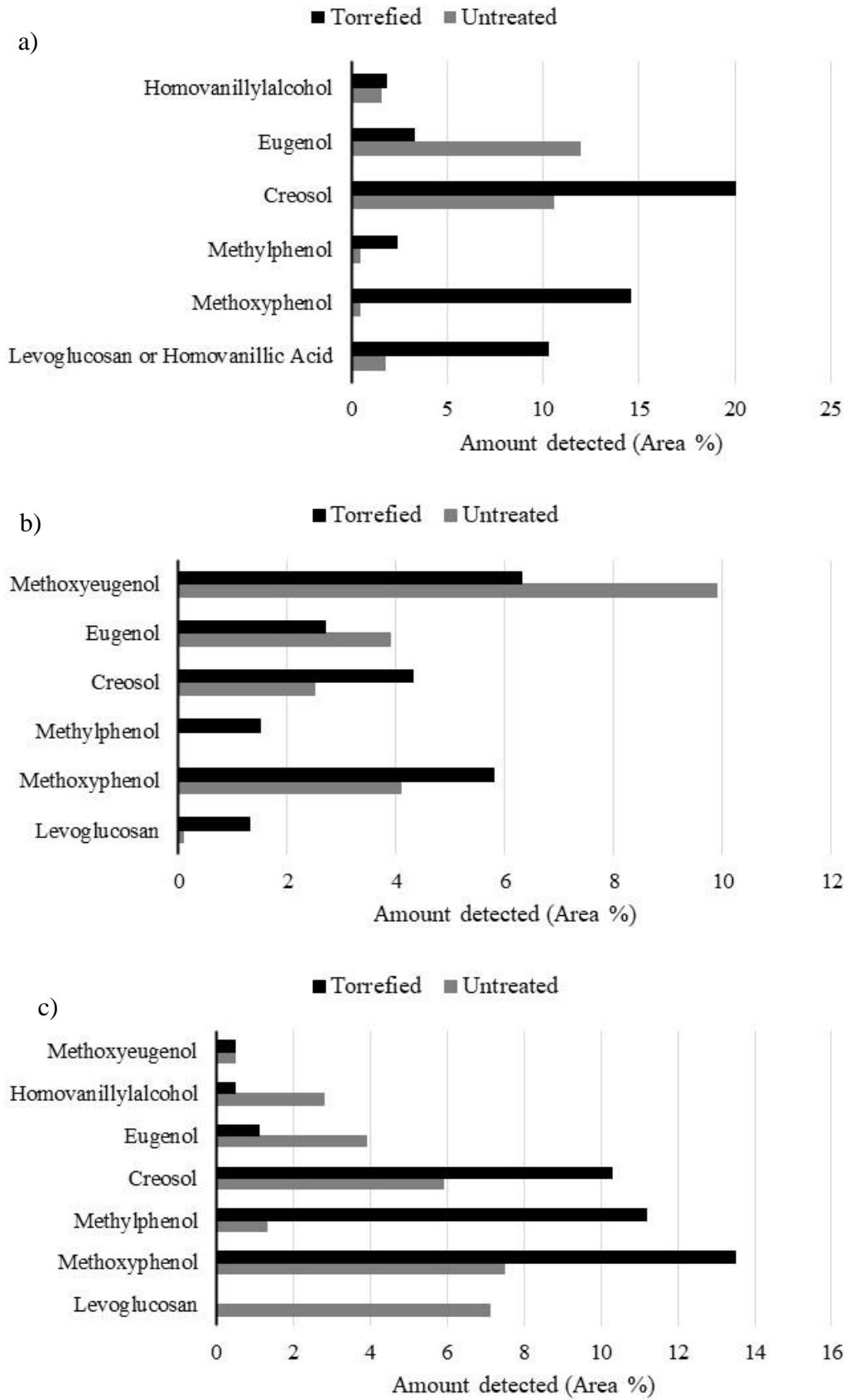
Figure A.4: Comparison of selected detected compounds for fuel pairings a) Spruce b) Willow c) Olive

Appendix B- Data and Information relating to Chapter 5
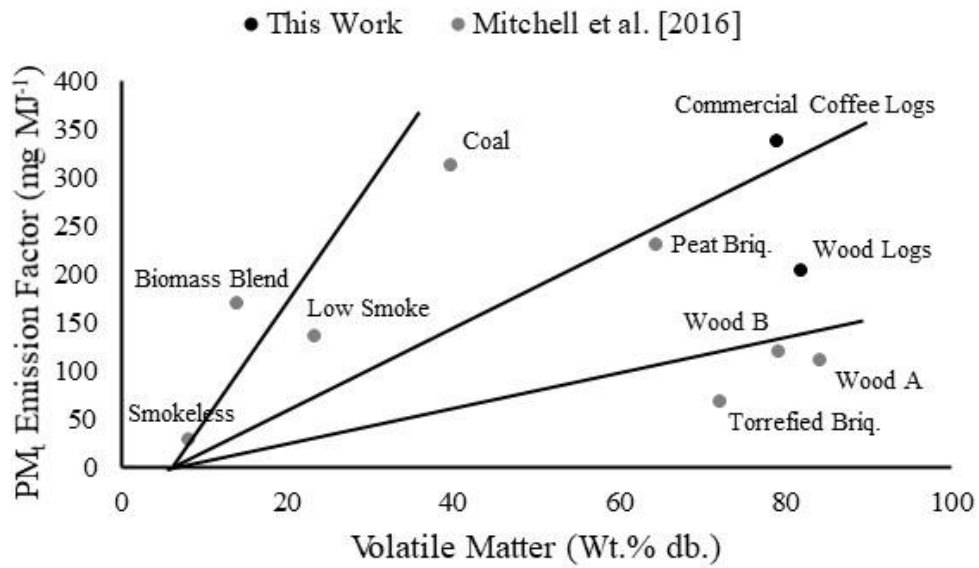
Figure B.1: Total PM emissions against fuel volatile content, data compared with the work of Mitchell et al. [2016]

Figure B.2: Correlation of C/O ratio with PM$_t$, data compared with the work of Roy and Corscadden [2012]

Appendix C- Data and Information relating to Chapter 6

Table C.1: Calculated errors for Table 6.2 from the standard deviation of measured values

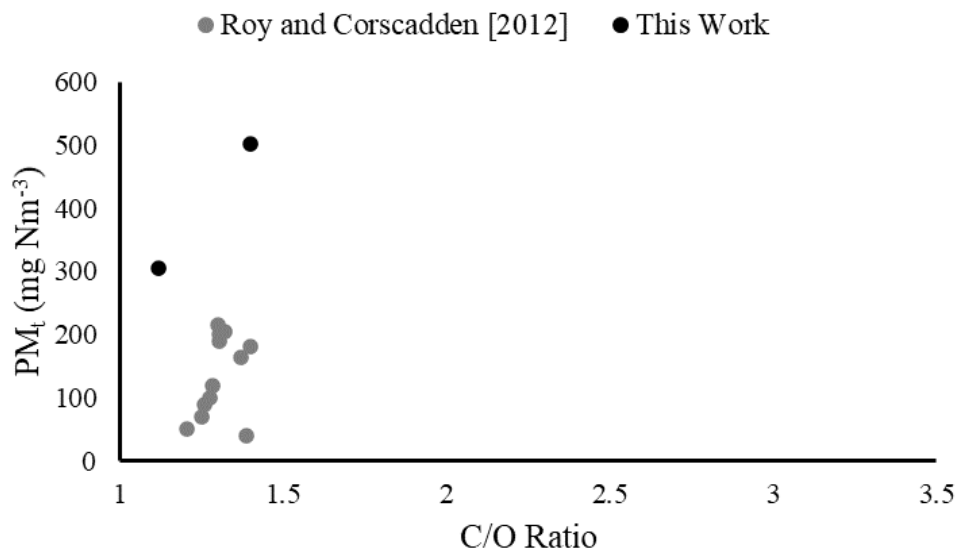| Sample	Site	Sample Period	Moisture (wt.%)^{ar}	Moisture (wt.%)^{ad}	Volatiles (wt.%)^{db}	Ash (wt.%)^{db}
Bracken	1	1	±7.4	±1.1	±3.1	±0.8
		2	±7.2	±1.3	±3.5	±0.8
		3	±6.5	±1.1	±3.0	±0.7
		4	±3.7	±0.8	±2.5	±0.6
	2	1	±10.2	±1.5	±3.7	±0.7
		2	±8.6	±1.3	±3.4	±0.8
		3	±7.9	±1.4	±3.6	±0.8
		4	±5.4	±0.9	±2.9	±0.7
	3	1	±9.8	±1.7	±2.9	±0.6
		2	±7.5	±1.5	±3.2	±0.8
		3	±7.7	±1.4	±3.0	±0.7
		4	±5.1	±1.4	±2.7	±0.5
	4	1	±11.1	±1.2	±4.1	±0.9
		2	±10.2	±0.9	±3.7	±0.9
		3	±7.8	±1.2	±3.6	±0.5
		4	±6.1	±1.0	±3.4	±0.6
	5	1	±8.7	±1.3	±3.7	±0.7
		2	±8.8	±1.6	±4.3	±0.8
		3	±8.5	±1.2	±3.0	±0.6
		4	±4.1	±0.8	±3.1	±0.4

Table C.2: Calculated errors for Table 6.3 from the standard deviation of measured values and propagation of error for the HHV

Sample	Site	Sample Period	C (wt.%)db	H (wt.%)db	N (wt.%)db	S (wt.%)db	HHVb (MJ kg-1)db
Bracken	1	1	±0.15				±0.22
		2	±0.08				±0.13
		3	±0.09				±0.14
		4	±0.04				±0.12
	2	1	±0.10				±0.15
		2	±0.11				±0.16
		3	±0.09				±0.14
		4	±0.05				±0.12
	3	1	±0.06	±0.03	±0.02	n/a	±0.12
		2	±0.13				±0.19
		3	±0.09				±0.14
		4	±0.06				±0.12
	4	1	±0.11				±0.16
		2	±0.07				±0.12
		3	±0.09				±0.14
		4	±0.08				±0.13
	5	1	±0.13				±0.19
		2	±0.14				±0.20
		3	±0.08				±0.13
		4	±0.07				±0.12
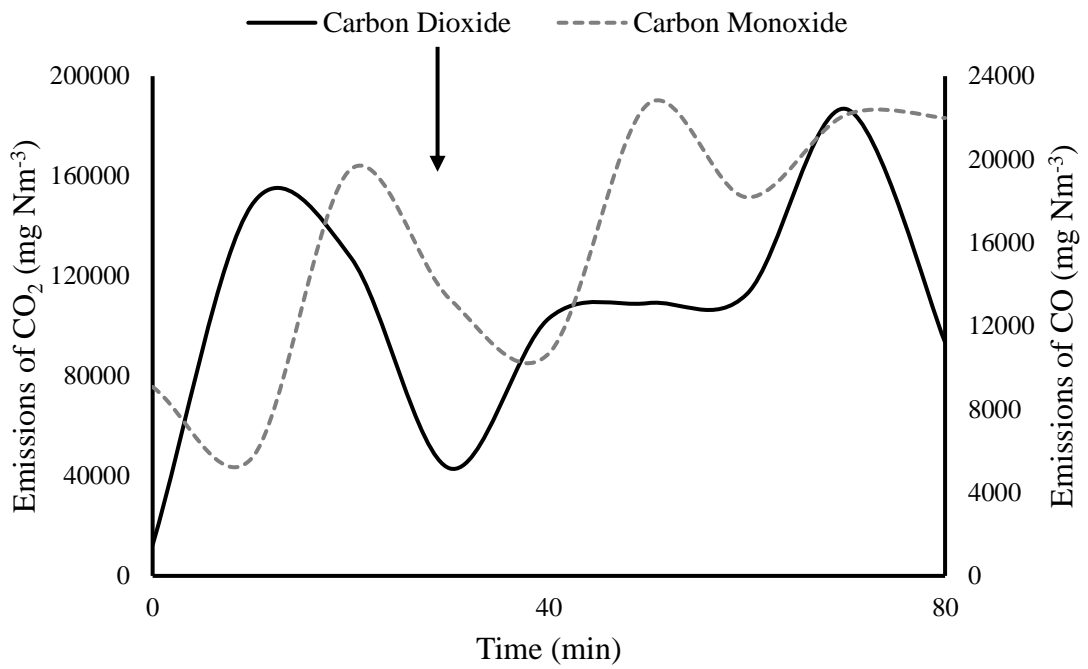
Figure C.1: CO₂ and CO emissions from stove combustion of the miscanthus
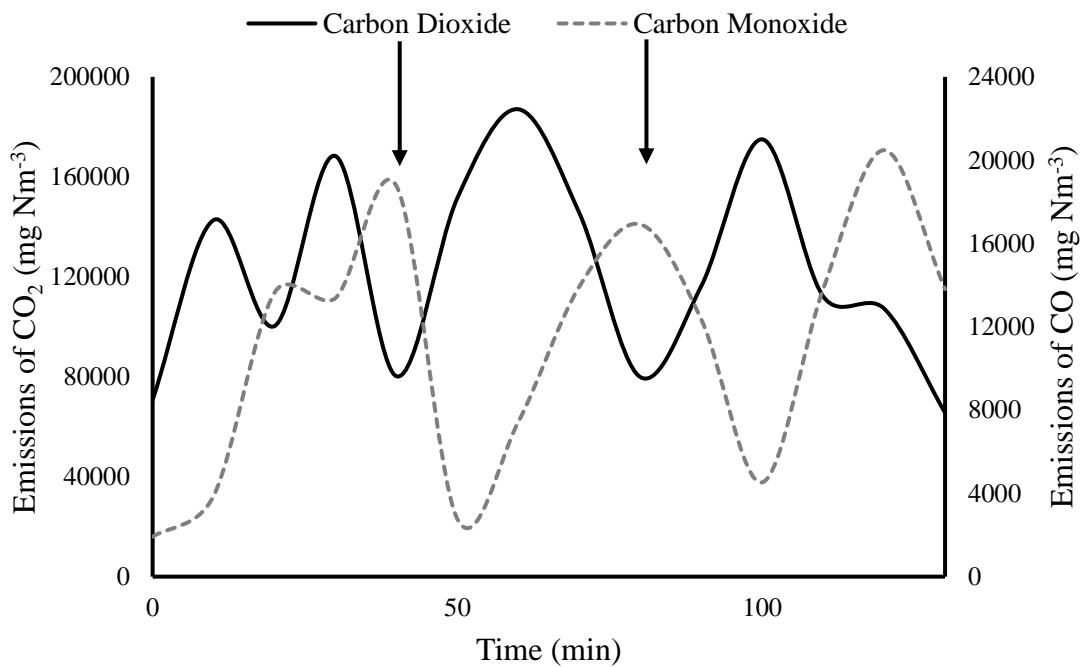
Figure C.2: CO₂ and CO emissions from stove combustion of the barley straw

306
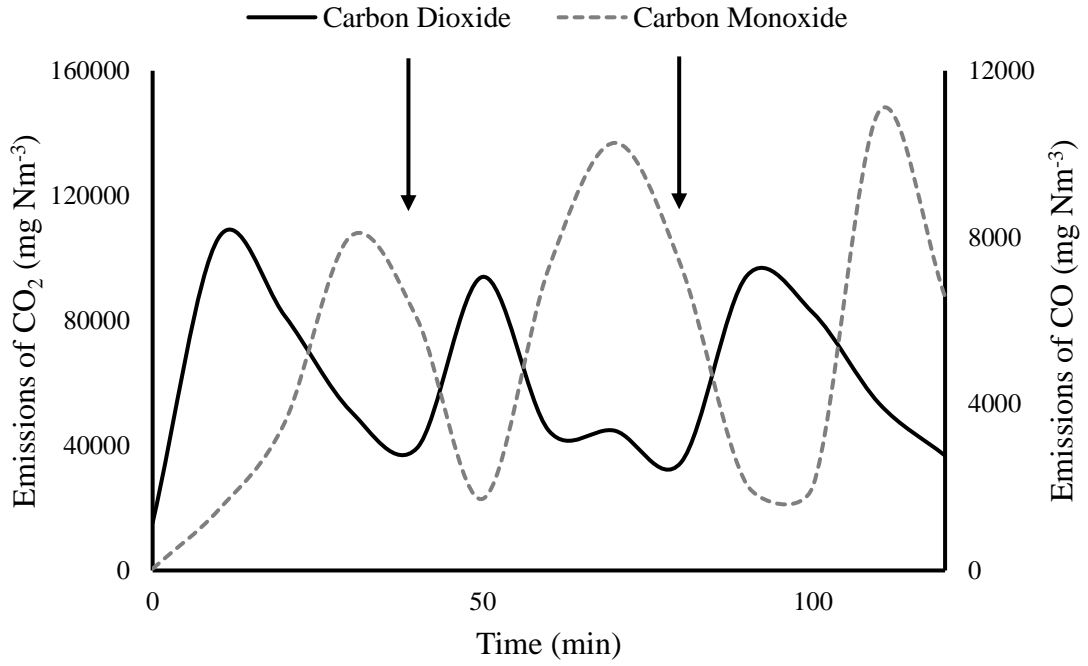
Figure C.3: CO₂ and CO emissions from stove combustion of the wheat straw
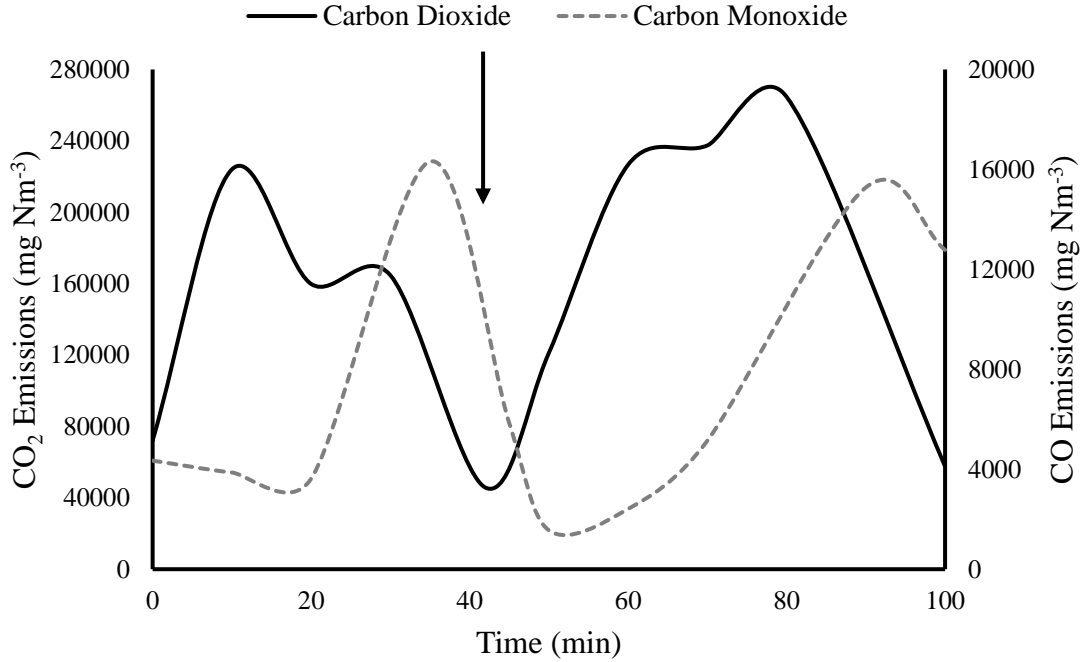
Figure C.4: CO₂ and CO emissions from stove combustion of the wood briquettes

Table C.3: Emissions factor relative errors (%)

	CO$_2$	CO	TOC	NOx	SO$_2$	HCl	PM$_t$
Bracken	±8	±14	±16	±10	±12	±8	±5
Miscanthus	±11	±9	±12	±12	±18	±7	±8
Barley Straw	±13	±12	±22	±11	±14	±8	±6
Wheat Straw	±6	±7	±14	±7	±3	±12	±4
Wood Briquettes	±4	±23	±18	±25	±15	±9	±7

Appendix D- Data and Information relating to Chapter 7

Figure D.1: Renishaw Colliery (a) location (b) early mining operations (c) later operations [Bridgewater, No date]

Table D.1: Soil analysis of the Renishaw site and comparison to the UK urban average [Environment Agency, 2007] [1]

Element	Soil heavy metal concentrations (mg kg⁻¹)		
	Renishaw		UK Average [1]
	Local Agricultural	Open-cast soil	Urban
Cu	10.1	39.8	42.5
Zn	41.6	137.8	95.1
Ni	11.8	31.8	28.5
Pb	17.9	100.5	110
Cd	0.1	0.7	0.44
Cr	19.4	36.5	34.3

Table D.2: Mass balance calculation (a) inputs (b) willow and fines output (c) leachate output (d) overall balance
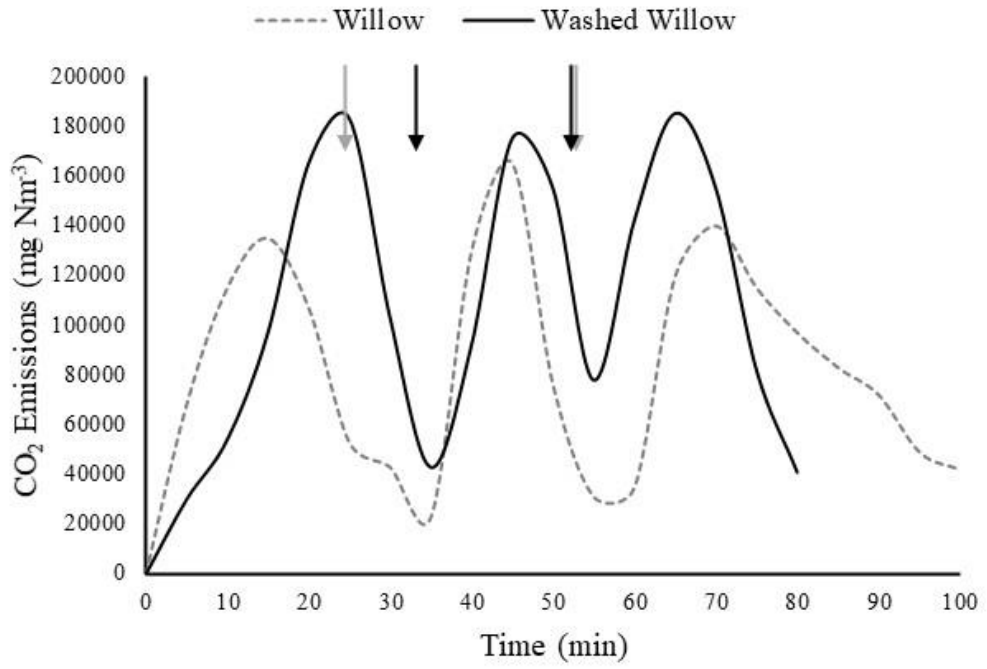
(a)	Input				
	Willow ar. (14.8% M) (g)	Willow Dry (g)	Willow Moisture (g)	Water (g)	Total Water (g)
#	[1]	[2]	[3]	[4]	[5]
Eq.	[1]	[2]=[1]x0.852	[3]=[1]-[2]	[4]	[5]=[4]+[3]
1	519	442	77	1038	1115
2	524	446	78	1048	1126
3	499	425	74	999	1073
4	513	437	76	1025	1101
5	518	441	77	1035	1112
6	521	444	77	1041	1118
7	531	452	79	1061	1140
8	520	443	77	1041	1118
Average	518	441	77	1036	1113
Standard Deviation	9.17	7.81	1.36	18.12	19.48
Error	2	2	2	2	2

| (b)	Willow Output					
	Willow ar. (8% M) (g)	Willow Dry (g)	Willow Moisture (g)	Fines ar. (g)	Fines Dry (g)	Fines Moisture (g)
#	[6]	[7]	[8]	[9]	[10]	[11]
Eq.	[6]	[7]=[6]x0.92	[8]=[6]-[7]	[9]	[10]=[9]x0.965	[11]=[9]-[10]
1	426	392	34.1064	23	22	0.8
2	431	397	34.496	20	20	0.7
3	414	381	33.0896	29	28	1.0
4	418	384	33.412	19	18	0.7
5	423	389	33.8584	12	12	0.4
6	429	395	34.3288	20	19	0.7
7	436	401	34.9064	19	18	0.7
8	429	394	34.3008	8	8	0.3
Average	426	392	34.0623	19	18	0.7
Standard Deviation	7.38	6.79	0.59	6.35	6.12	0.22
Error	2	2	1.7	29	29	28.7

Table D.2 *Cont.*: Mass balance calculation (a) inputs (b) willow and fines output (c) leachate output (d) overall balance

(c)		Leachate Output			
	Leachate (g)	Willow in Leachate (g)	Water in Leachate (g)	Water Lost in Drying (g)	Total Willow (g)
#	[12]	[13]	[14]	[15]	[16]
Eq.	[12]	$[13]=[12] \times [1/\rho \text{Leachate}] \times [\text{Solid Conc}]$	$[14]=[12]-[13]$	$[15]=[5]-[8]-[11]-[14]$	$[16]=[7]+[10]+[13]$
1	658	2.5	655	425	417
2	708	2.7	705	385	419
3	645	2.5	642	397	411
4	650	2.5	648	419	405
5	620	2.4	618	460	404
6	676	2.6	674	409	417
7	696	2.7	694	411	422
8	619	2.4	617	467	405
Average	659	2.5	657	422	412
Standard Deviation	32.66	0.13	32.53	28.63	7.41
Error	5	5.0	5	7	2

(d)	Overall Balance	
	Willow Balance (g)	Unaccounted (%)
#	[17]	[18]
Eq.	$[17]=[2]-[16]$	$[18]=[17]/[2] \times 100$
1	25	6
2	27	6
3	14	3
4	32	7
5	37	8
6	27	6
7	30	7
8	39	9
Average	29	7
Standard Deviation	7.68	1.71

Figure D.2: CO$_2$ emissions from willow and washed willow
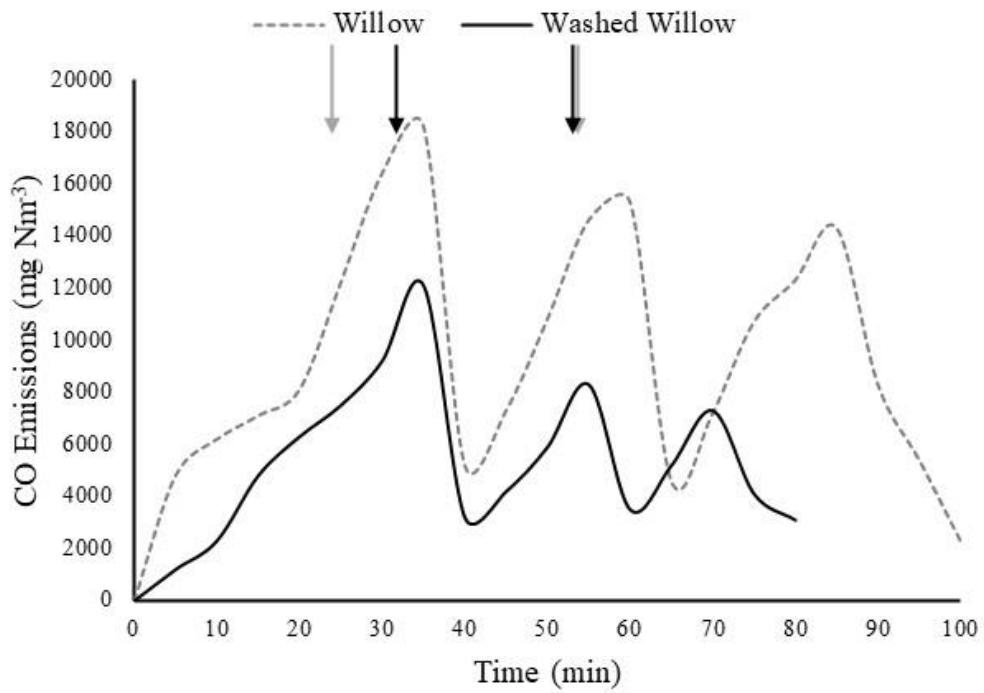
Figure D.3: CO emissions from willow and washed willow
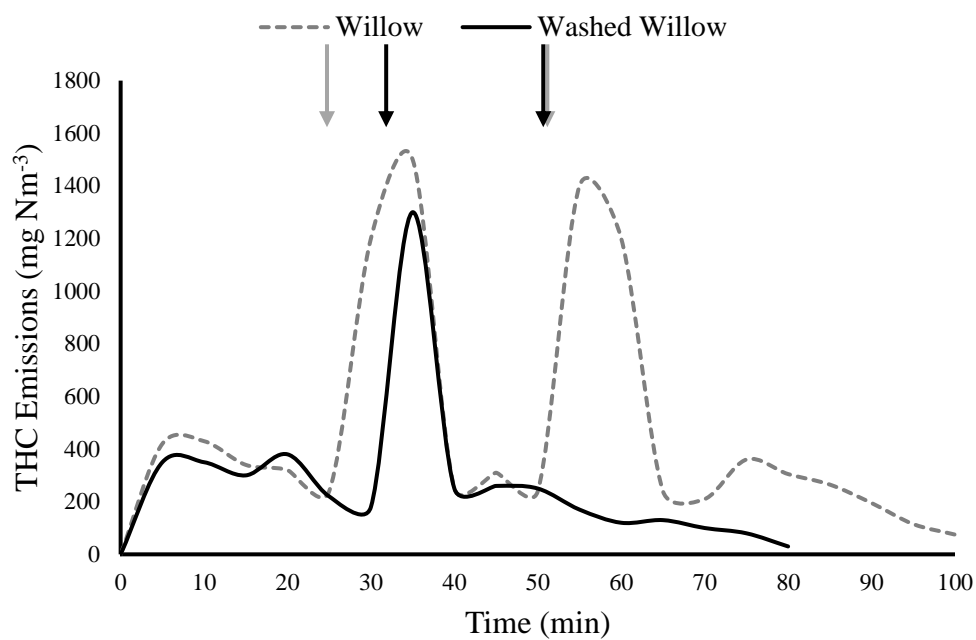
Figure D.4: THC emissions from willow and washed willow

Figure D.5: NOx emissions from willow and washed willow

313

Figure D.6: SO₂ emissions from willow and washed willow

Table D.3(a): Sub-micron PM composition analysis from willow combustion using SEM-EDX

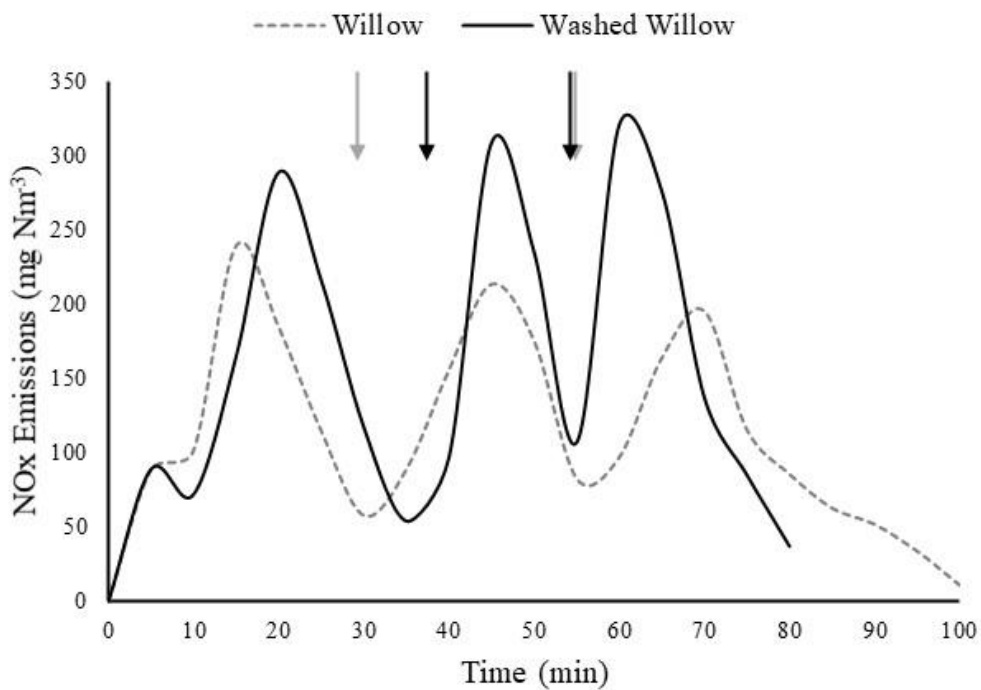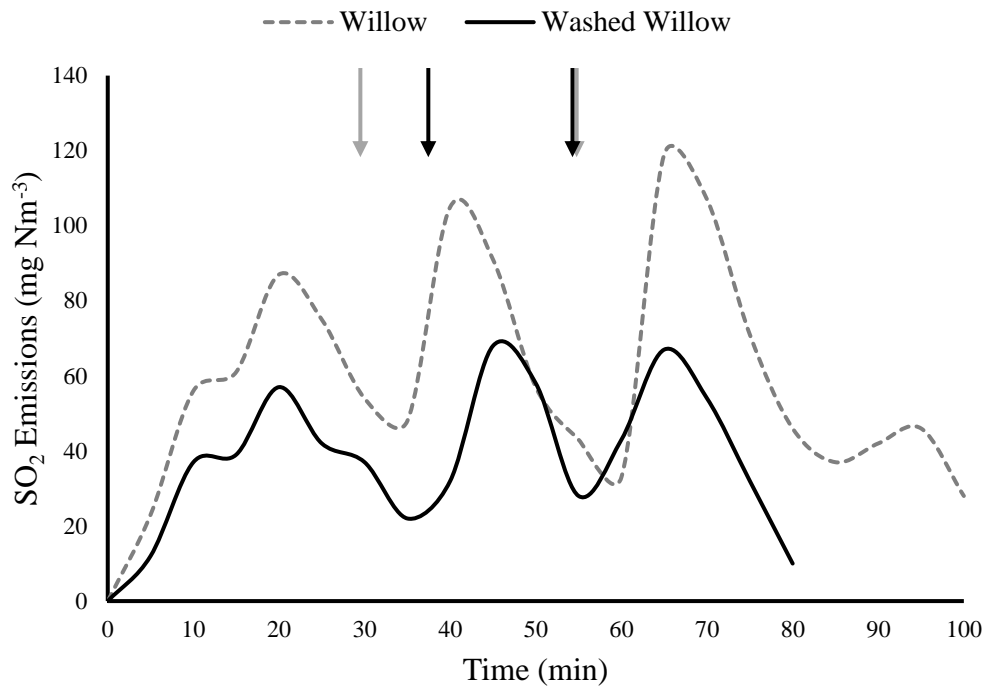| Element	Site																		Average
	1	2	3	4	5	6	7	8	9	10	11	12	13	14	15	16	17	18	
C	51.1	50.9	54.6	55.8	57.3	49.8	46.8	41.4	57.8	52	52.4	55.3	54.8	47.2	61.2	57.4	53.7	55.9	53.08
O	24.5	26.2	19.3	24.6	18.9	22.3	28.9	17.53	24.5	27.4	24.3	20.7	20.5	25.6	28.2	23.46	23.4	25.67	23.66
Ni	0.21	0.37	0	0	0.28	0.08	0	0	0	0	0	0.15	0	0	0	0	0	0.06	0.06
Zn	0	0.24	1.11	0	0.34	0	0.81	2.13	0	0	3.11	0	0	1.32	0.71	0.91	0.74	1.45	0.72
Si	18.22	14.2	17.17	15.61	15.62	23.21	18.52	30.01	8.21	15.7	15.69	17.81	20.35	22.43	5.21	10.64	19.03	9.76	16.52
Al	0.22	0.46	0.85	0.06	2.11	0.09	0.81	0.62	1.23	0.08	0	0	0.36	1.06	1.34	0.98	0.05	0.61	0.61
Fe	0	0.02	0	0	0	0	0.4	0	0	0	0	0.4	0	0	0	0.3	0	0	0.06
Ca	1.87	3.44	4.61	0.57	0.86	1.03	1.49	5.06	0.25	0.61	0.86	2.31	0.45	0.42	0.76	0.65	0.23	0.89	1.46
Na	2.35	0.98	0.79	0.56	1.89	0.84	0	0.93	1.65	2.53	0	1.43	1.89	0.42	2.01	3.61	1.86	1.78	1.42
K	0.89	2.84	0.56	0.34	2.14	1.98	0.94	1.26	0.97	0.79	2.56	0.78	0.89	0.23	0.49	0.67	0.51	1.06	1.11
P	0.15	0	0	1.41	0	0	0	0	4.31	0.44	0.29	0	0	0	0	0	0	1.93	0.47
S	0	0	0.23	0.11	0	0	0.34	0	0	0	0	0.21	0.64	1.09	0	1.32	0	0	0.22
Cl	0.49	0.35	0.78	0.94	0.56	0.67	0.99	1.06	1.08	0.45	0.79	0.91	0.12	0.23	0.08	0.06	0.48	0.89	0.61
Total	100	100	100	100	100	100	100	100	100	100	100	100	100	100	100	100	100	100	100

Table D.3(b): Sub-micron PM composition analysis from washed willow combustion using SEM-EDX

Element	Site 1	2	3	4	5	6	7	8	9	10	11	12	13	14	15	16	Average
C	53.3	47.8	51.1	45.7	54.8	51.3	51.2	56.4	53.7	50.8	46.6	50.1	50.6	52.7	47.6	50.2	50.87
O	18.9	26.9	24.5	23.6	26.5	25.5	19.4	22.1	24.6	25.1	24.3	27.8	26.4	24.7	27.5	26.4	24.64
Ni	0	0	0	0	0	0	0	0	0.1	0	0	0	0	0	0	0	0.01
Zn	1.69	7.91	4.12	3.02	0.94	5.47	1.54	7.89	2.47	0	6.24	5.47	3.48	8.71	6.03	7.46	4.53
Si	18.09	11.22	16.48	20.83	14.8	15.43	18.16	11.24	17.34	15.69	15.73	15.58	15.71	6.25	16.69	8.316	14.85
Al	2.98	0	0	0	1.84	1.61	0	1.99	0	1.77	1.31	0	1.96	1.43	0	0	0.93
Fe	0	0	0.08	0	0	0	0	0	0	0	0.01	0	0	0	0	0	0.01
Ca	0.54	0.78	1.23	1.56	0.21	0.34	1.87	0.38	0.49	0.08	0.75	0.24	0	0.46	0.29	0.664	0.62
Na	0	0	0	0.03	0	0	0	0	0	0	0.02	0	0	0	0	0	0.00
K	3.76	5.31	2.49	4.65	0	0	7.75	0	0.06	5.88	3.47	0.81	0	5.64	1.89	5.78	2.97
P	0	0	0	0	0	0	0.04	0	0	0	0	0	0	0	0	0	0.00
S	0.65	0	0	0.46	0.84	0.24	0	0	0.97	0.46	1.57	0	1.85	0	0	1.18	0.51
Cl	0.09	0.08	0	0.15	0.07	0.11	0.04	0	0.27	0.22	0	0	0	0.11	0	0	0.07
Total	100	100	100	100	100	100	100	100	100	100	100	100	100	100	100	100	100